Blood dendritic cells in chronically HIV-1 infected individuals in South Africa: Phenotype, Function and Immune modulation

by

Dalene de Swardt

Dissertation presented for the degree of Doctor of Philosophy (Medical Virology),
in the Faculty of Medicine and Health Sciences,
at Stellenbosch University

Supervisor: Dr. Richard H. Glashoff

December 2016

Declaration

By submitting this dissertation electronically, I declare that the entirety of the work contained therein is my own, original work, that I am the sole author thereof (save to the extent explicitly otherwise stated), that reproduction and publication thereof by Stellenbosch University will not infringe any third party rights and that I have not previously in its entirety or in part submitted it for obtaining any qualification.

December 2016

Abstract

HIV-1 infection detrimentally affects CD4 T lymphocytes as well as the blood plasmacytoid (pDC) and myeloid dendritic cell (mDC) compartment. DCs act as innate sensors and as initiators and directors of antigen-specific immune responses. Whereas, mDCs have the unique ability to prime naïve T-lymphocytes and activate adaptive immune responses, pDCs are primary producers of type 1 interferons (IFNs), playing a pivotal role in anti-viral immunity. In the current study both pDCs and mDCs from chronically HIV-1 infected South African individuals (on or naïve for ARV therapy) as well as with and without concurrent TB disease, were compared to matched uninfected controls. Similar to CD4 T lymphocytes, bothpDCs and mDCs, were significantly depleted during HIV-1 infection, (reduction of pDC, mDC and CD4 T lymphocyte was 63% ($p \leq 0.001$), 80% ($p \leq 0.001$) and 31% ($p \leq 0.01$), respectively).In parallel, significantly higher levels of generalised immune activation and exhaustion ($CD38^+CD8^+$, $PD\text{-}1^+CD8^+$ and $CD38^+PD\text{-}1^+CD8^+$ T lymphocytes) were observed. ARV treatment (≥ 1 year) did not result in DC number recovery despite a significant increase of CD4 T lymphocytes numbers (CD4 T lymphocyte number gain of 89% ($p \leq 0.01$), it fell short of full recovery).TB co-infection did not exacerbate number loss. Phenotypic characterisation of DC populations in circulation during HIV-1 infection may indicate the underlying reasons for the loss from circulation. Phenotypic profiling by multiparameter flow cytometry included: markers of activation (CD86, CD80 and CD62L), maturation (CD83), apoptosis (TNF-R2, FAS, FASL and TRAIL R1-R4) and chemotaxis (CCR5, CCR7, CCR9 and CXCR6). HIV-infection was associated with a significantly higher percentage of $CD86^+$mDCs which may be indicative of early maturation or transition to secondary lymphoid tissue. The frequency of the $CD86^+$mDCs subset normalised upon ARV therapy. Also, HIV-1 infection influenced the distribution of $TNF\text{-}R2^+$pDCs and $TNF\text{-}R2^+$mDCs. Increased TNF-R2 expression in both subsets, may attest to enhanced survival function. Functionally, DCs of HIV-1 infected individuals were reactive to TLR-L stimulation and in some cases showed enhanced responses compared to uninfected individuals. A significantly higher frequency of $TNF\text{-}R2^+$pDCs, $IFN\text{-}\alpha^+$pDCs, and $TNF\alpha^+$mDCs was observed in whole blood TLR cultures of HIV-1 infected individuals ($TNF\text{-}R2^+$pDCs: LPS ($p = 0.002$) and R848 ($p = 0.01$), $IFN\text{-}\alpha^+$pDCs: R848 ($p = 0.04$), $TNF\alpha^+$mDCs: LPS ($p = 0.003$))s.In addition, whole blood TLR cultures of the ARV treated study group generally showed normalisation of the responses, however; in certain cases ARV therapy reduced responsiveness to levels significantly lower than the control study group (i.e.$TNF\text{-}R2^+$pDCs and $TNF\text{-}R2^+$mDCs in CpG ODN stimulation). In contrast, a significantly lower frequency of $IL12p40^+$mDCs was observed during HIV-1 infection ($p = 0.02$). TLR-L cultures of the ARV treated study groups showed normalisation of $IL12p40^+$mDCsfrequency. Notably, treatment with the immunomodulating peptide VIP induced a decline in $IL12p40^+$mDCs to levels lower than the control study group.The frequency of $TNF\alpha^+$pDCs in TLR-L whole blood cultures was similar between the healthy, untreated and treated HIV-1 infected study groups, however, significantly reduced frequencies were observed in these study groups upon VIP treatment. These data indicate unique phenotypic and functional changes in DC subsets in chronic HIV-1 infection which may provide potential targets for immunotherapeutic intervention.

Opsomming

Die CD4 T limfosiet asook die plasmasitoïede (pDSe) en myeloïede dendritiese selle (mDSe) word nadelig geraak deur `n MIV-1 infeksie. Dendrietiese selle tree op as aangebore sensors en as inisieerders en reguleerders van antigeen-spesifieke immuun reaksies. mDSe het `n besonderse funksie om naïewe T limfosiete teinisieer en so die verworwe immune reaksies te aktiveer. pDSe is primêre produseerders van tipe 1 Interferon wat `n rol speel in anti-virale immuniteit. In die studie is beide die pDSe en mDSe van Suid-Afrikaners met chroniese MIV-1 infeksie (ARV en nie ARV gebruikers) met of sonder TB siekte vergelyk met ooreenstemmende MIV-1 negative kontroles. Soortgelyk aan CD4 T limfosiete, was beide die pDSe en mDSe beduidend verminder tydens `n MIV-1 infeksie (die verlaging in pDSe, mDSe en CD4 T limfosiete was onderskeidelik 63% (p≤ 0.001), 80% (p ≤ 0.001) en 31% (p ≤ 0.01). Terselfdertyd is `n verhoogde vlak van algemene immuun aktivering en uitputting ($CD38^+CD8^+$, $PD\text{-}1^+CD8^+$T en $CD38^+PD\text{-}1^+CD8^+$ T limfosiete) waargeneem. ARV behandeling (≥ 1 jaar) het nie gelei tot die herstel in DSe getalle alhoewel die studie `n beduidende vermeerdering in CD4 T limfosiete waargeneem het (CD4 T limfosiet vermeerdering van 89% (p ≤ 0.01), die verhogingwas nie voldoende nie). TB mede-infeksie het nie die vermindering van DSe vererger nie. Fenotipiese karakterising van die DS populasie in sirkulasie tydens MIV-1 infeksie mag die onderliggende rede vir die verlaging aandui. Fenotipiese profilering deur multi-parametriese vloeisitrometrie het ingesluit merkers van aktivering (CD86, CD80 en CD60L), maturasie (CD83), seldood (TNF-R2, FAS, FASL en TRAIL R1-R4) en chemotaksiese (CCR5, CCR7, CCR9 en CXCR6). MIV-1 infeksie was geassosieer met beduidende hoër persentasie van $CD86^+$mDSe wat moontlik vroeë maturasie of transisie na die sekondêre limfoïedeweefsel aandui. Die frekwensie van die $CD86^+$mDSe subpopulasie normaliseer tydens ARV terapie. MIV-1 infeksie het ook `n invloed op die distribusie van $TNF\text{-}R2^+$pDSe en $TNF\text{-}R2^+$mDSe gehad. Verhoogde TNF-R2 uitdrukking in beide DS populasies mag moontlik getuig van `n verhoogde oorlewings funksie.Op `n funksionele vlak het DSe van MIV-1 geinfekteerde individue reaksie tot TLR-L stimulasie getoon en in sommige gevalle was die reaksie hoër as in MIV-1 negatiewe individue. `n Beduidende hoër frekwensie van $TNF\text{-}R2^+$pDSe, $IFN\text{-}\alpha^+$pDSe, $TNF\alpha^+$mDSe was waargeneem in heel bloed TLR-L kulture van MIV-1 geinfekteerde individue (TNF-R2+pDSe: LPS (p = 0.002) and R848 (p = 0.01), IFN-α+pDSe: R848 (p = 0.04), TNFα+mDSe: LPS (p = 0.003)) terwyl die heel bloed kulture van die ARV studie groep in die algemeen normalisering getoon het. In sekere gevalle het ARV terapie reaksies verlaag tot vlakke beduidend laer as die van die kontrole studie groep (i.e.$TNF\text{-}R2^+$pDSe and $TNF\text{-}R2^+$mDSe met CpG ODN stimulasie). In kontras, `n beduidende laer frekwensie van $IL12p40^+$mDSe is opgemerk gedurende MIV-1 infeksie (p = 0.02). TLR-L kulture van die ARV studie groep het normalisering van die $IL12p40^+$mDSe frekwensie getoon. Behandeling met die immunomodulerende VIP peptied het `n verlaging in $IL12p40^+$mDSe vlakke geinduseer wat laer was as die van die kontrole groep. Normalisering van die $IL12p40^+$mDSe vlakke is waargeeem in die TLR-L kulture van die ARV studie groep. Die frekwensie van $TNF\alpha^+$pDSe in TLR-L heel bloed kulture was soortgelyk tussen die MIV-1 negatiewe, onbehandelde and behandelde MIV-1 geinfekteerde studie groepe. `n Beduidende verlaagde frekwensie was waargeneem in hierdie studie groepe tydens VIP behandeling. Hierdie data wys op unieke fenotipiese en funksionele veranderinge in die DS populasies tydens chroniese MIV-1 infeksie wat`n moontlik potensiele teiken vir immunoterapeutiese intervensie kan wees.

Acknowledgements

I wish to acknowledge the following people and institutions for their support during my studies:

Dr Richard H Glashoff, my study supervisor and promoter, for your continued support in a study that had so many complexities.

Ronell Taylor, research nurse at the Division of Medical Virology, Stellenbosch University, for your professional way of recruiting patients from various HIV and TB clinics, always attending first to the wellness and comfort of patients.

Nursing staff, at the various HIV and TB clinics for supporting our research by allowing us the opportunity to interact with and recruit patients.

Dr Hayley Ipp, Hematologist at the Tygerberg hospital, for your support throughout my studies. Thank you for your willingness to share your ideas and thoughts regarding my research and for the enthusiasm you show and support you give towards scientific research in the field of HIV Immunology.

The medical staff as well as Dr Surita Roux, senior investigator and project leader, for their duties performed at Desmond Tutu Emavundleni Clinic Site. Thank you for the care taken in the recruitment of patients and willingness to assist with all my queries.

The **participants**, by consenting to the collection of specimens your contribution towards expanding the body of knowledge, specifically in medical sciences and HIV, are priceless and greatly appreciated.

Jan de Wit for performing the CD4 T lymphocyte counts and the **diagnostic personnel of the Division of Medical Virology and National Health Laboratory Service** for the viral load testing.

Becton Dickinson Biosciencesfor the opportunity to use the flow cytometers at the Becton Dickinson/Stellenbosch University Flow cytometry Unit(BD-SUFCU) **and a special thanks to Dr Danni Ramduth**, applications specialists supervisor for BD Biosciences. I greatly appreciate your time and patience during the many training session and the willingness to always assist with flow cytometry queries. Thank you for your support as trainer and friend.

My **colleagues and fellow students at the Division of Medical Virology**, Stellenbosch University, for the interest showed in my research, the advice and support given when needed, words of encouragement and creating an extremely pleasant working environment.

Management at Synexa Life Sciences, in supporting me in so many ways to complete my studies and to my **work colleagues,** thank you for your support and words of encouragement.

Armand de Swardt, my husband, I am grateful for your continued support and patience during my study. Thank you for being a great partner in this journey.

David and Marlene Loubser, my parents, thank you for the sacrifices you have made towards providing your children with the gift of education. Your motivation and words of encouragement during our years of study is greatly appreciated. Special thanks to my mom for her keen interest in my project and all the saved newspaper clippings on HIV related matters. **Hanco Loubser**, my brother, thank you for your support and keen interest shown in my studies.

The financial assistance of the following institutions

- **DAAD-NRF(The institutions German Academic Exchange Service/Deutscher Akademischer Austausch Dienst – National Research Foundation)**
- **Poliomyelitis Research Foundation (PRF)**
- **Cape Biotech**
- **South African HIV/AIDS research and innovation platform (SHARP)**
- **Scholarship sponsors of the AIDS Vaccine 2010 conference**

Honoring my commitment to research

- **L'Oréal/UNESCO (United Nation Educational, Scientific and Cultural Organization) Regional Fellowships for Women in Science in Sub-Saharan Africa (2011)**

Publications

- **de Swart D** and Glashoff RH. ARV fails to normalise the reduction of blood plasmacytoid and myeloid dendritic cells in HIV infected South African individuals with active TB. AIDS Research and Human Retroviruses. 2010. 26(10): pA-74.

Presentations

- ***de Swardt D**, Ipp H and Glashoff RH.* Phenotypic characterisation of blood dendritic cells in chronically HIV-infected individuals in South Africa.
  - Virology Africa 2011 conference, Cape Town, South Africa, 29 Nov – 2Dec 2011.

- ***de Swardt D**, Glashoff RH*. ARV fails to normalise the reduction of blood plasmacytoid and myeloid dendritic cells in HIV infected South African individuals with active TB.
  - European Molecular Biology Organisation (EMBO) Global Exchange on HIV/AIDS lecture course, Stellenbosch University, South Africa, 30 Jan - 5 Feb 2011.
  - AIDS Vaccine 2010 conference, Georgia Atlanta, USA, 28 Sept-1 Oct 2010.

- ***de Swardt D**, Glashoff RH.* HIV infection leads to a significant reduction in plasmacytoid and myeloid dendritic cell numbers in South African individuals.
  - Annual Academic day, Faculty of Health Sciences, Cape Town, South Africa, Aug 2010 (updated results).
  - 2nd Symposium on Infectious Diseases in Africa and 3rd African Flow Cytometry Workshop, Johannesburg, NICD, 13-20 Nov 2009.
  - Annual Academic day, Faculty of Health Sciences, Stellenbosch University, Cape Town, South Africa, Aug 2009.

Dedication

In loving memory of my father, D.C.D. Loubser

Contents

List of Tables

List of Figures

List of Abbreviations

7-AAD	7-amino actinomycin D
x g	relative centrifugal force
A	Area
AIDS	Acquired Immunodeficiency Syndrome
APC	Allophycocyanin
APC-Cy7	Allophycocyanin – Cyanine 7
ARV	Antiretroviral
BAL	Bronchoalveolar lavage
BD	Becton, Dickinson and company
BDCA	Blood Dendritic CellAntigen
B lymphocytes	Bone marrow-derived lymphocytes
BP	Band Pass
cAMP	cyclic adenosine monophosphate
CCL	C-C Chemokine Ligand
CCR	C-C Chemokine Receptor
CD	Cluster of Differentiation
COX-2	Cyclooxygenase-2
CpG	Cytosine and Guanine nucleotides on a phosphodiester backbone.
CST	Cytometer setup and tracking beads
CTLA-4	Cytotoxic T-lymphocyte-associated protein 4
CXCR	C-X-C Chemokine Receptor
CXCL	C-X-C Chemokine Ligand
DC	Dendritic cell
DCID	Dendritic Cell identification markers (LIN1, HLA-DR, CD11c and CD123)
DC-SIGN	Dendritic Cell-Specific Intercellular adhesion molecule-3-Grabbing Non-integrin
dsRNA	double stranded Ribonucleic Acid
EDTA	Ethylene Diamine Tetra Acetic Acid
Env	Envelope
FACS	Fluorescent Activated Cell Sorter
FASL	FAS Ligand
FDC	Follicular Dendritic Cell
FITC	Fluorescein isothiocyanate
FL	Fluorescence
FMO	Fluorescence Minus One
FRC	Fibroblastic Reticular Cell
FSC	Forward Scatter
FSC-A	Forward Scatter-Area

FSC-H	Forward Scatter-Height
Gag	Group-specific antigen
GIT	Gastrointestinal tract
GlyCAM-1	Glycosylation-dependent cell adhesion molecule-1
GM-CSF	Granulocyte-macrophage colony-stimulating factor
GM-CSFR	Granulocyte-macrophage colony-stimulating factor receptor
gp	Glycoprotein
H	Height
HBV	Hepatitis B virus
HCV	Hepatitis C virus
HEV	High Endothelial Venules
HHF	Human Immunodeficiency Virus-1 and Host factors
HIV	Human Immunodeficiency Virus
HIV-1	Human Immunodeficiency Virus type 1
HLA-DR	Human Leukocyte Antigen – antigen DRelated
HREC	Health Research Ethics Committee of Stellenbosch University
HSC	Hematopoietic Stem Cell
HUVEC	Human Umbilical Vein Endothelial Cell
IFN	Interferon
IFN-α	Interferon-alpha
IgG	Immunoglobulin G
IgG,κ	Immunoglobulin G, kappa
IKK	IκB kinases
IL	Interleukin
immDC	immature Dendritic Cell
IU	International Units
ITAM	Immunoreceptor tyrosine-based activation motif
LCMV	Lymphocytic choriomeningitis virus
LGL	Large granular lymphocyte leukaemia
LIN1	Lineage 1 (CD3, CD14, CD16, CD19, CD20 and CD56)
LOD	Limit of detection
$\log_{10}$	Logarithm to base 10
LP	Long Pass
LPS	Lipopolysaccharide (TLR4-Ligand)
LTR	Long Terminal Repeat
mAb	monoclonal Antibody
mDC	myeloid Dendritic Cell
mmDC	mature myeloid Dendritic Cell
MFI	Median Fluorescence Intensity
MHC	Major Histocompatibility complex
min	minute(s)

MIP	Macrophage inflammatory protein
MLR	Mixed Leukocyte Reaction
mo-DC	monocyte-derived Dendritic Cell
mRNA	messenger Ribonucleic Acid
n	sample size
NaCl	Sodium Chloride
nef	Negative factor
NEQAS	National External Quality Assessment Service
NF-κB	Nuclear Factor kappa Beta
NHLS	National Health Laboratory Service
NK	Natural Killer
no	number
ODN	Oligodeoxynucleotide (TLR9 ligand)
p	Probability of significance
P	Population
PAMPs	Pathogen-Associated Molecular Patterns
PBS	Phosphate Buffered Saline
PBMC	Peripheral Blood Mononuclear Cell
PCLP	Podocalyxin-like protein
PD-1	Programmed Death-1
pDC	plasmacytoid Dendritic Cell
PE	Phycoerythrin
PE-Cy	Phycoerythrin - Cyanine
PerCP	Peridinin chlorophyll protein
PerCP-Cy 5.5	Peridinin chlorophyll protein – Cyanine 5.5
PGE_2	Prostaglandin E_2
PMTCT	Prevention of Mother to Child Transmission
PNAd	Peripheral-node addressin
Pol	Polymerase
Poly I:C	Polyinosinic-polycytidylic acid
PRRs	Pattern recognition receptors
PT	Pulmonary tissue
Q	Quadrant
r	Correlation coefficient
R848	Resiquimod 848 (TLR7/8 Ligand)
REC	Research Ethics Committee of the University of Cape Town
rev	regulator of viral gene expression
RNA	Ribonucleic Acid
S1P	Sphingosine 1-phosphate
SANAS	South African National Accreditation System
SARS	Severe Acute Respiratory Syndrome

SFV	Simian Foamy Virus
SFTS	Severe Fever with Thrombocytopenia Syndrome
Sgp200	Sialyted glycoproteien of 200kD
SIV	Simian Immunodeficiency Virus
ssRNA	single-stranded Ribonucleic Acid
sTNF-R	soluble Tumor Necrosis Factor Receptor
SSC	Side Scatter
TDF	Tenofovir disoproxil fumarate
T lymphocytes	Thymus-derived lymphocytes
tat	Transcriptional transactivator
TB	Tuberculosis
TLR	Toll-Like Receptor
TLR-L	Toll-Like Receptor – Ligand
$TLR\text{-}L^{-}$	Toll-Like Receptor – Ligand negative
$TLR\text{-}L^{+}$	Toll-Like Receptor-Ligand positive
TNF	Tumor Necrosis Factor
TNF-α	Tumor Necrosis Factor-alpha
TNF-R	Tumor Necrosis Factor Receptor
TRAIL	Tumor Necrosis Factor-related Apoptosis Inducing Ligand
TRAIL-R	Tumor Necrosis Factor-related Apoptosis Inducing Ligand Receptor
UNAIDS	Joint United Nations programme on HIV/AIDS
UCT	University of Cape Town
v	version
vif	viral infectivity factor
VIP	Vasoactive Intestinal Peptide
VPAC	Vasoactive intestinal peptide Pituitary Adenylate Cyclase
vpr	Viral protein r
vpu	Viral protein u
vs	versus
W	Width
WHO	World Health Organization

Glossary

Markers with either “+”, “DIM” or “-”superscriptrefer to their expression as bright positive, intermediate intensity or extremely low/absent, respectively.

ARV^{-}HIV-1 study group	Refer to Table 3.1
ARV^{+}HIV-1 study group	Refer to Table 3.1
ARV^{-}HIV-1/TB study group	Refer to Table 3.1
ARV^{+}HIV-1/TB study group	Refer to Table 3.1

Chapter 1

Introduction

The year 2015 commemorates 32 years since the first published report on the Acquired Immunodeficiency Syndrome (AIDS), a fatal disease caused by the type-1 Human Immunodeficiency Virus (HIV-1). During these three decades, research has immensely advanced our understanding of HIV-1 pathogenesis. However, despite better understanding of disease processes, scientists have not yet been able to develop treatment to completely clear (i.e. cure) or a vaccine to prevent HIV infection. To date, the HIV/AIDS disease has claimed many lives and also disseminated rapidly throughout the world. The global burden of people living with HIV has reached pandemic proportions with an estimated 36.9 million people currently infected. Most concerning is the fact that South Africa is marked as the country with the highest number of HIV-1 infected people in the world.

HIV/AIDS disease is characterised by the gradual deterioration of the immune system and if left untreated, infection ultimately leads to death. Impairment of the immune system is driven by the infectious agent (HIV), which is transmitted via contact with contaminated body fluids (either during sexual intercourse, blood transfusion, trans-placental passage or shared use of syringes/needles during intravenous drug abuse). An important feature of this disease is its high morbidity and mortality rate, mostly brought on by an enhanced susceptibility of HIV infected patients to opportunistic infections due to a compromised immune system. In South Africa, particularly, Tuberculosis (TB) is one of the leading causes of death in HIV-infected individuals.

Treatment options are limited to the chronic use of antiretrovirals (ARVs). Although effective in controlling viral load (in most cases), it has been reported that ARVs only contribute to partial immune reconstitution. This partial recovery is most evident in the T lymphocyte (primarily $CD4^+$) compartment (Almeida M, *et al.* 2006; Finke JS, *et al.* 2004). In addition, the chronic use of ARVs has been associated with an increased risk for the development of cardiovascular diseases and several metabolic syndromes in HIV infected patients (van Wijk JPH and Cabezas MC, 2012; Kotler DP, 2008; Friis-Møller N, *et al*. 2007). Also, drug resistance is another well described problem (most possibly stemming from long term non-compliance) impacting on the use of ARVs (Gupta RK, *et al* 2012; van Zyl GU, *et al*. 2011). These findings suggest that while a cure remains the ultimate goal, advances in current treatment is also a necessity to lessen the burden of side effects associated with ongoing ARV therapy.

In recent years the paradigm “persistent immune activation, driving immune exhaustion” has become a central concept in HIV pathogenesis. A well-described outcome of this phenomenon is the progressive and systemic loss of CD4 T lymphocytes in untreated patients. Cellular deprivation during HIV-1 infection is, however, not limited to the CD4 T lymphocyte compartment. A simultaneous decline in precursor plasmacytoid dendritic cells (pDC) and myeloid DCs (mDC) (also termed conventional DC or cDC) from peripheral blood has been reported by many researchers (Mojumdar K, *et al*. 2010; Sabado RL *et al*. 2010; Lichtner M, *et al.* 2008; Finke JS, *et al*. 2004; Donaghy H, *et al.* 2001; Soumelis V, *et al*. 2001). In view of the central role that these cells play in the surveillance, recognition and elimination of antigens from the microenvironment, it is believed that depletion of these cells from circulation may contribute to major immune

dysfunction during HIV-1 infection. Driven by an interest to know more about the impact of HIV-1 infection on DCs, the current study aimed to characterise the residual DC pool in circulation during HIV-1 infection.

Characteristically, DCs are scarcely distributed in peripheral blood, representing less than 1% of total blood mononuclear cells. However, despite their low frequency they have unique properties (functionally and morphologically) that make them essential role players in effective host immunity. On a functional level, DCs have been referred to as linking innate and adaptive immunity (McKenna K, *et al.* 2005). This is based on the fact that DCs are acknowledged as the primary cell type that recognises and internalises antigen in the periphery, then enters the lymphatic system to transport processed antigen to secondary lymphoid tissue where it primes naïve T-lymphocytes for the initiation of adaptive immune responses. Recognition of antigens is primarily the task of the immature peripheral tissue-resident mDCs and is performed via evolutionary conserved receptors. These include Toll like receptors (TLR) expressed on the cell surface as well as intracellulary within the endosome. Specifically, the processed antigens are presented by the lymphoid tissue-associated mature mDCs to the naïve T lymphocytes in secondary lymphoid tissue. In contrast to mDCs, pDCs are primary producers of type 1 interferons (IFNs), playing a pivotal role in anti-viral immunity. Both immature and mature pDCs primarily populate lymphoid tissues. Furthermore, DCs have unique morphological features, displaying branch-like cellular extensions, aiding in optimally executing the important functions of pathogen surveillance, recognition and capture.

Examination of DCs function *in vitro* is challenging due to the naturally low frequency of these cells in peripheral blood. Previously, studies have relied on culturing monocyte-derived DCs (mo-DCs) to experimentally investigate DCs at a functional level. However, this is a laborious and time-consuming technique of questionable significance and it has been debated whether this method generates responses resembling reactions *in vivo*. Fortunately, advances in modern technology and identification of specific markers allows for the rapid profiling, isolation and manipulation of DCs using freshly isolated whole blood. In the current study DC subsets were collectively distinguished, using flow cytometric applications, within the heterogeneous cell population of whole blood by mutual positive expression of the Human Leucocyte Antigen – antigen D Related (HLA-DR) and low/absent expression of lymphoid markers (CD3, CD14, CD16, CD19, CD 20 and CD56 – collectively referred to as Lineage 1 (LIN1)). Separately defining the pDC and mDC subsets was performed via the differential expression of CD11c and CD123 markers (pDCs: $CD123^{+}CD11c^{-}$; mDC: $CD123^{DIM}CD11c^{+}$).

1.1 Hypothesis and study design

Little has been reported on the effect of HIV-1 infection on DCs in South Africa (a country in which the heterosexual subtype C HIV-1 epidemic predominates). Also, the effect of a TB co-infection (the predominant factor causing HIV-1 related deaths in South Africa) and ARV treatment on blood DCs has also been scantily addressed. Accordingly, the present cross-sectional study focused on investigating changes exerted on blood pDCs and mDCs via HIV-1 infection, HIV-1/TB co-infection (i.e. active TB disease) and ARV therapy.

Altered peripheral blood DC numbers during chronic HIV-1 infection is a well-described phenomenon. It is also well-documented that, in addition to detectable levels of HIV antigens, significantly elevated levels of inflammatory components are present in the plasma/serum of HIV-1 infected patients. Accordingly, the current study hypothesised that the decline of pDCs and mDCs is the net effect of persistent exposure and/or response to a combination of HIV-1 and host factors (HHF). These may include 1) viral elements that may induce a direct cytopathic effect, 2) excessive/persistent production of host inflammatory mediators and/or 3) gut "leakage" components in circulation. It is unclear; however, by which mechanism DCs wane from peripheral blood, whether this phenomenon is permanent (apoptosis) or temporary (enhanced migratory response to HIV-1 associated inflammatory signals) and, in particular, if number loss is also linked to DC dysfunction (e.g. altered cytokine production). The current study proposed the investigation of the residual pool of HHF exposed DCs from HIV-1 infected individuals in current circulation, suggesting these cells to provide "clues" to the cause of the decline of blood DCs and provide information on their functional abilities.

The current study was performed in three parts. **The first part** (Chapter 3) aimed to determine the frequency distribution of 1) pDC, mDC, CD4 T lymphocyte (the primary diagnostic laboratory marker used to monitor disease progression) and CD8 T lymphocyte absolute numbers and 2) CD4 T lymphocyte to CD8 T lymphocyte absolute number ratio (also referred to as CD4:CD8 ratio) in uninfected vs. chronically HIV-1 infected, HIV-1/TB co-infected and ARV-treated HIV-1 infected individuals. Also, the relationship between DC and CD4 T lymphocyte absolute numbers as well as CD8 T lymphocyte counts and HIV-1 viral load within each applicable study group was investigated. Following this it was proposed, in reference to the study hypothesis, that an increase in/alteration of specific physiological mechanisms of cellular waning will result in the net effect of low DC numbers during HIV-1 infection. The study refers to mechanisms suchs as apoptotic cell death, cell activation and/or export/tissue homing (*either due to antigen capture and consequent mobilisation to lymph nodes to present antigen to naïve T lymphocytes (lymphoid directed) or chemotactic movement in response to inflammatory signals generated at sites of infections (tissue directed e.g. gut associated)).* Therefore, **the second part of the study** (Chapter 4) profiled pDCs and mDCs in the peripheral blood of uninfected vs. chronically HIV-1 infected, HIV-1/TB co-infected and ARV-treated individuals using 15 phenotypic markers related to **A)** activation (*CD86, CD80 and CD62L*) and DC maturation (*CD83*), **B)** apoptosis (*both as inducers: FAS Ligand (FASL/CD178) and susceptibility: FAS (CD95), Tumor Necrosis Factor Receptor (TNF-R)-2, TNF- related apoptosis inducing ligand receptor (TRAIL-R) 1 and 2 as well as resistance or avoidance: TRAIL-R3 and -R4*) and **C)** homing (*CCR9 - putative gastrointestinal tract (GIT) homing receptor, CXCR6 - putative pulmonary tissue homing receptor, CCR5 and*

CCR7 - both lymph node homing receptors). We proposed that modification in the expression of these phenotypic markers may direct the fate of DCs during HIV-1 infection. **The third part of the study** (Chapter 5) aimed to 1) define whether the functional abilities of the DCs were altered during HIV-1 infection and if so 2) determine the alleviation potential of ARV therapy. The current study hypothesised that persistent exposure of circulatory pDCs and mDCs to potentially harmful HHF substances affects their functional abilities. Impaired function of DCs during HIV-1 infection has been reported, in particular, the impaired ability of pDCs and mDCs of HIV-1 infected individuals to respond to Toll-like receptor stimulation *in vitro,* attributed to persistent activation, exhaustion and/or general impairment of DCs. However, few studies have addressed the impact of ARV therapy on the functional responses of DCs from HIV-1 infected patients. In this part of the study, TLR responses of DCs in uninfected controls were compared to that of the residual DC pool of HIV infected and ARV treated patients. The response upon *in vitro* whole blood TLR stimulation of pDCs and mDCs were measured by the expression of markers of apoptosis (FAS, TRAIL-R1, TRAIL-R2, TNF-R2) and migration (CCR5, CCR7, CCR9) and production of intracellular cytokines (IFN-α(2b), IL12p40, TNF-α). As a sub-project, the following was also investigated 1) the expression of novel immunemodulatory receptors for the neuropeptide: vasoactive intestinal peptide (VIP), namely VPAC1 and VPAC2, in fresh and cultured whole blood and 2) the immunemodulatory properties of VIP upon *in vitro* whole blood TLR activation of pDCs and mDCs. This sub-study was part of a bigger project aimed at limiting immune activation as a potential treatment option for chronic HIV-1 infection. Various factors (e.g. competent viral reservoirs, host genomic integration) make the development of treatments that aim at the complete elimination of HIV a challenging task. Proposing the development of treatment targeting persistent immune activation with consequent alleviation of immune exhaustion is the first of its kind. The development of treatment that can modulate or “dampen” immune activation via the use of a natural peptide (with the prospects of limited side effects) might possibly increase the life expectancy of HIV-infected patients. **The final part of the study** (Chapter 6) aimed to investigate the relationship of the DC subsets positively expressing phenotypic markers of activation, apoptosis and migration (characterised in Chapter 4) to markers of immune activation and exhaustion commonly associated with HIV-1 infection. The latter factors were profiled via the expression of CD38 and the Programmed death – 1 (PD-1) receptor on CD8 T lymphocytes, respectively. In this chapter the immune activation and exhaustion profile of the control, untreated and treated HIV-1 and HIV-1/TB co-infected study groups was firstly examined. This entailed determining the 1) frequency distribution of the $CD8^+CD38^+$ and $CD8^+PD\text{-}1^+$ subsets as well as the $CD38^+PD\text{-}1^+$ dual expressing CD8 T lymphocyte subsets in peripheral blood and 2) relationship of the CD8 T lymphocyte subsets to CD4 T lymphocyte counts and viral load (as applicable). Following this, the DC relationship to the CD8 T lymphocyte subsets for each study group was examined.

In an attempt to streamline the reporting of information, each chapter commences with a brief literature review, specific study aim and objectives on the related topic. Chapter 2 serves as an introductory overview and survey of the literature on HIV and DCs, particularly their role in HIV pathogenesis.

Chapter 2

Literature Review

2.1 The HIV-1 pandemic

Since, the first published report on HIV/AIDS, a mere 32 years ago, the disease rapidly transformed into a worldwide pandemic. This is evident from the 2015 HIV global statistics report on people living with HIV, showing that the total number of HIV-infected adults (15 years and older) and children (0-14 years) amounts to 36.9 million individuals globally (The Joint United Nations Program on HIV/AIDS (UNAIDS) global statistics fact sheet, 2015). Furthermore, approximately 70% of the global HIV-infected population resides in Sub-Saharan Africa, marking South Africa part of a region with the highest number of HIV infections in the world.

The worldwide attempt to resolve the problem of HIV/AIDS should not solely focus on finding a cure or a vaccine but should also undertake the challenge of preventing the spread of the disease. Successful eradication of HIV/AIDS would be dependent on a significant decrease in mortality numbers and also, in particular, the rate of new infections. Although, a decline of 35.5% in new infections was apparent in comparing data collected from the 2000 to the 2014 survey, new infections during 2014 were estimated at 2 million individuals (UNAIDS 2015 Global statistics facts sheet). It was/has been proposed that lack of adherence to ARV therapy, society's misinterpretation of the disease and continued high risk sexual behaviour are some factors still playing a significant role in the current spread of the virus. In South Africa, particularly, a major complicating factor in the HIV epidemic is sexual violence against women (Jewkes RK, *et al.* 2010.)

Currently, no cure or vaccine is available for HIV/AIDS treatment is restricted to the chronic use of ARVs. It has proven to be effective in controlling viral replication by decreasing the plasma viral load to undetectable levels (in most cases) and also contributed to a reduction in morbidity and mortality associated with the disease (WHO guidelines 2015; Palella FJ Jr, *et al*. 1998). However, there are other factors that mark ARVs as suboptimal in treating an HIV infection. One important finding is that it contributes minimally in a) reducing generalised immune activation, a hallmark of an HIV infection (Boasso and Shearer GM. 2008; Silvestri G and Feinberg MB. 2003) and b) immune reconstitution (Almeida M, *et al.* 2006; Guadalupe M, *et al.* 2003). Furthermore, long term ARVs have also been implicated in causing cardiovascular disease, several metabolic syndromes and hypertriglyceridemia in HIV infected patients (van Wijk JPH and Cabezas MC, 2012; Kotler DP, 2008; Friis-Møller N, *et al*. 2007). Drug resistance is another well described problem impacting on the use of ARVs (Gupta RK, *et al*, 2012; van Zyl GU, *et al*. 2011).

Although an immense volume of published data on the pathogenesis of HIV infection exists, we still do not clearly understand the disease process. Also, in the absence of individuals who have spontaneously recovered, the natural correlates of protection remain unknown. These factors are the main reasons for the lack of available treatment targeting the complete eradication of the virus. In view of this, perhaps a cure for the HIV/AIDS disease entails a radically different approach than the current vaccine/treatment approaches. Nonetheless, it is imperative that scientists persevere in defining host responses to obtain better insight into

HIV pathogenesis. Unravelling the disease process might aid in reaching the ultimate goal of developing a remedy that would alleviate the detrimental effects that HIV infection inflicts on mankind.

2.2 Society's misconceptions on HIV infection

The HIV/AIDS problem is a multi-faceted challenge for all health sectors worldwide. Not only is finding a cure or an effective vaccine for the disease crucial, also society's misconceptions regarding the origin of the disease should be addressed as it might play a role in high rate of new infections recorded yearly. In particular, certain groups believe that its ontogeny is politically driven. In a study conducted by Ross and colleagues in 2006, it was found that most of the sample subjects, which included both genders of four different racial groups (African American, Latino, non-Hispanic whites, Asian) living in Houston, Texas, believed that HIV's development was part of a genocidal conspiracy by the federal government. This view was seemingly associated with reduced condom use in especially African American men. As hypothesised by Bogart LM and Thorburn S (2005), this action might be based on mistrust and suspicious belief in government. These men believed that those allegedly "responsible" for HIV's creation are now suddenly proclaiming the use of condoms to prevent HIV infection. The opinion of black inhabitants from San Bernardino, California, was that the HIV was "man-made", targeting the extermination of this ethnic group specifically (Klonoff EA and Landrine H, 1999).

Other studies have reported on the myth that condoms cause HIV/AIDS. Some people in rural Northern Namibia believe that the virus is contained in the lubricant. As expected, this view was also associated with reduced condom use (Mufune P, 2005). Similarly, the view of a group of Zimbabwean individuals transpired to "virus-containing condoms produced by racist Whites/Americans" (Rödlach A, 2006). Locally, in addition to genocidal beliefs, a cultural practice such as witchcraft is contemplated by young black South Africans as cause of the HIV/AIDS disease. They also believed that HIV can be cured simply by consuming fresh fruits and vegetables. Also, these views were associated with lack of condom use during intercourse (Bogart LM, *et al.* 2011). These misconceptions undoubtedly result in continuous sexual risk behavior within a community, having a profound effect on the global spread of the disease. Addressing misconceptions regarding the HIV/AIDS disease is as important as finding a cure and/or effective treatment for eradicating and preventing the spread of the HIV.

2.3 So from where did the HIV actually originate?

Zoonotic transmission is accepted as the main introductory path into the human population. Phylogenetic analyses have shown that the virus was introduced into the human species via transmission from African primates including Sooty Mangabeys (*Cercocebus atys*), African Green monkeys (*Chlorocebus sabaeus)*, Mandrills (*Mandrillus sphinx)* as well as chimpanzees (*Pan troglodytes*). Notably, these animals are regarded as natural hosts of SIV (simian immunodeficiency virus) - HIV's counterpart -as it, in contrast to HIV infection in humans, does not cause a life-threatening pathogenic effect. SIV refers to simian "immunodeficiency" virus but unlike its name, given in reference to the primary discovered HIV, the natural host rarely progress to the associated disease. Primate non-natural hosts to SIV infection include Rhesus Macaque monkeys (*Macaca mulatta)*. The sooty mangabey SIV specific strain is related to the HIV-2 subtype (Hirsch VM, *et al*. 1989) whereas the origin of HIV-1 subtype have been traced to a SIV specific strain that naturally infect

chimpanzees (Gao F, *et al.* 1999). Recently, it was reported that zoonotic transmission could also have occurred via the western lowland gorillas (*Gorilla gorilla gorilla)* from west-central Africa (D'arc M, *et al.* 2015).

The mechanism of zoonotic transfer of the virus to humans has been linked to bushmeat trading, which refers to the hunting and sale of wild animals including above-mentioned non-human primates. Cross-species transmission may have occurred upon contact with meat of SIV-infected animals during handling and/or butchery (Hahn BH, 2005). Apetrei C, *et al*. (2005) conducted a study on Sooty Mangabey bushmeat sold at markets of rural Sierra Leone in West Africa. They obtained twelve subjects and found that seven of these were positive for the SIV. In fact, they characterised seven new sooty mangabey SIV specific strains. Also, SIV infected bushmeat has been reported in a study conducted in Cameroon, and most alarming is that researchers also detected SIV infection in monkeys owned as pets (Ndembi N, *et al.* 2009; Peeters M, *et al.* 2002).

In addition to possibly contracting SIV (genus: lentivirus) infection from bushmeat hunting and consumption, there is also the risk of becoming infected with other viruses. In two separate studies conducted in Cameroon, serological and molecular testing of blood samples from human volunteers who have had exposure to blood and other body fluids of non-human primates during bushmeat practices, tested positive for simian foamy virus (SFV) infection (genus: retroviruses) (Calattini S, *et al*, 2007; Wolfe ND, *et al*. 2004). SFV has also been detected in employees working at the zoo and research institutions in Northern America (injury and non-injury related), with no evidence of horizontal transmission when tests were extended to include spouses (Calattini S, *et al*. 2007; Switzer WM, *et al.* 2004). Similar results were observed in wives and children of men exposed to non-human primates in the natural setting (Betsem E, *et al.* 2011). Notably, SFV infection does not manifest with clear disease symptoms in both humans and non-human primates even after years of infection (Boneva RS, *et al.* 2007; Switzer WM, *et al.* 2005), whereas *in vitro* assays have shown this virus to exert a cytopathic effect. It is presumed that certain host factors are suppressing disease progression during SFV infection (Murray SM, *et al.* 2006; Meiering CD and Linial ML, 2001). Interestingly, higher SFV messenger ribonucleic acid (mRNA) levels have been observed in the small intestine of SIV infected than in uninfected Rhesus Macaques monkeys. This finding seems to indicate the reduced level of immune control in an immune-compromised system (Murray SM, *et al.* 2006).

2.4 SIV and HIV: cousin viruses with opposing pathogenic effect in the natural and non-natural host

The underlying mechanism preventing transition to AIDS in the natural host have not been elucidated. It is believed that upon accurately identifying the immune correlates of protection that prevents pathogenic SIV infection in the natural host, it might aid in clarifying the reason(s) for the opposing effect of SIV/HIV infection in the non-natural host. This may also pave the way for the development of effective treatment or a cure for HIV infection. Nevertheless, researchers have acquired much knowledge on HIV pathogenesis from studies of SIV infection in the natural and non-natural host. In HIV/SIV infection of the non-natural host, disease progression is characterised by a) loss of peripheral and mucosal CD4 T lymphocytes, b) chronic immune activation and inflammatory responses and c) microbial leakage from the lumen of the GIT into circulation. In contrast, SIV infection of the natural host shows a) CD4 T lymphocytes maintained at levels similar to that of

the uninfected natural host, b) limited immune activation and c) no microbial translocation (as reviewed by Paiardini M, *et al*. 2009). Added to these key features is the finding of disrupted fibroblastic reticular cell network (FRC) (important for the livelihood of the naïve T lymphocytes) during HIV/SIV infection of the non-natural host, which remains intact during SIV infection of the natural host (Zeng M, *et al*. 2012). Figure 2.1 depicts, in relation to viral load, HIV-associated changes of specific host immune parameters (CD4 from peripheral blood, CD4 from mucosa-associated lymphoid tissue and immune activation) involved in the development of AIDS from primary infection in the non-natural vs. natural host (Figure 2.1a and 2.1b, respectively). In acute infection the profile of these parameters in HIV/SIV infection of the non-natural host seem similar to that of SIV infection in the natural host with a peak increase in viral load accompanied by an increase in immune activation and parallel decline of Peripheral blood and mucosa-associated lymphoid tissue CD4. However, during chronic infection these parameters profile differently in the non-natural vs. natural host. In chronic SIV infection of the natural host immune control is evident, displaying recovery in peripheral blood and mucosa-associated lymphoid tissue CD4 (recovery in African green monkeys more significant than in sooty mangabeys) and a decline in viral load (although the latter is not completely cleared from the host) and immune activation. In the early phase of chronic infection of the non-natural host, a slight decline in immune activation levels and increase of peripheral blood CD4 was observed. However, this changes as the disease progresses as evidenced by declining numbers of the mucosa-associated lymphoid tissue CD4 and a steady viral load. The status of these parameters persists with transition to AIDS/death, except for viral load that increases in the non-natural host. In contrast, in the natural host these parameters are maintained and the host, rarely, develops AIDS (as reviewed by Paiardini M, *et al.* 2009).

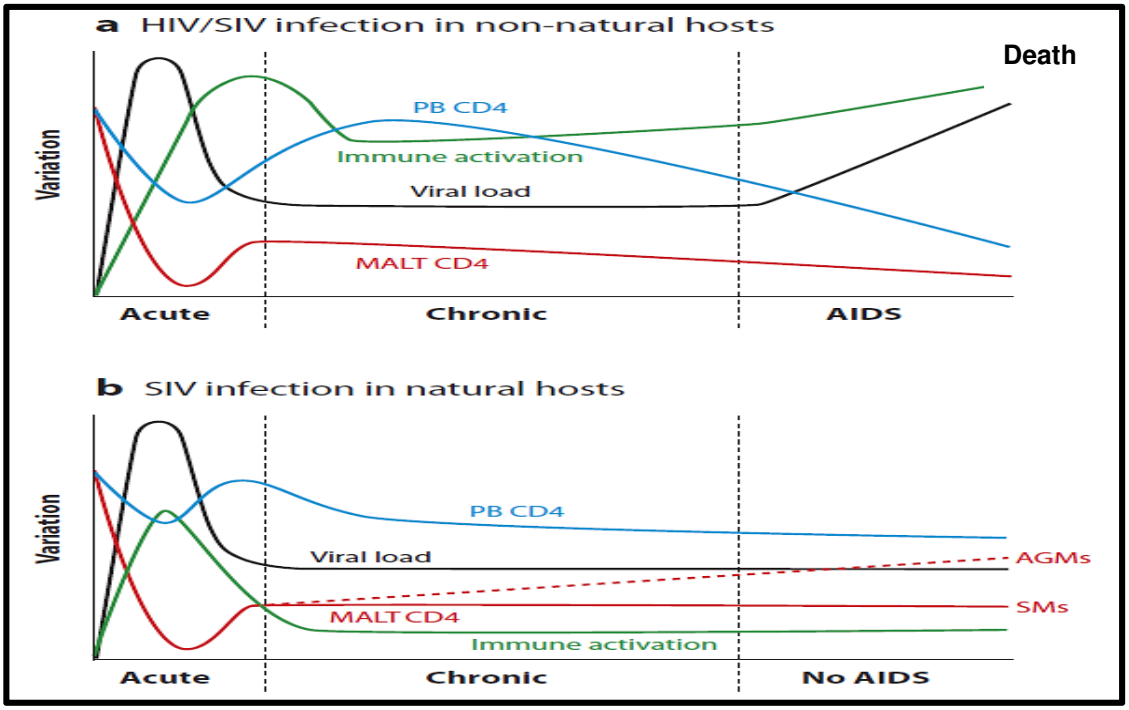

Figure 2.1: Kinetics on the changes of specific host immune parameters, in relation to viral load, during HIV/SIV infection of the natural and non-natural host.

The line graph compares viral load to specific host immune parameters (CD4 from peripheral blood, CD4 in mucosa-associated lymphoid tissue and immune activation) to illustrate the changes of these parameters between HIV/SIV infection of the non-natural hosts: human and rhesus macaque monkeys (A) and SIV infection of the natural hosts: sooty mangabeys and african green monkeys (B) (as reviewed by Paiardini M, et al. 2009).

2.5 Biological characteristics of the HIV

The HIV is taxonomically within the Lentivirus group (*lentus*-, Latin for "*slow*") and is a member of the Retroviridae family. Two types of HIVs have been identified namely HIV-1 (previously termed Lymphotropic Adeno Virus or Human T-lymphotropic virus Type III) and HIV-2 (Wain-Hobson S, *et al.* 1985). The latter type is a less virulent form of the virus and is primarily localised to West Africa. Morphologically, the HIV virion has a spherical structure and measures approximately 120 nm in diameter. The inner core or capsid of the virus is enclosed by a coat of viral encoded proteins (p24) containing the genome (9.2kb) of the virus which consists of two identical positive sense, single-stranded RNA strands as well as the enzymes: reverse transcriptase, protease and integrase. These essential components are protected from the external environment by a phospholipid bilayer membrane envelope derived from the infected host cell. The envelope membrane contains approximately 70 copies of a trans-membrane trimeric complex consisting of glycoproteins gp41, which anchors the outer external unit, gp120, in the envelope membrane itself (Figure 2.2) (Abbas AK, *et al.* 2012).

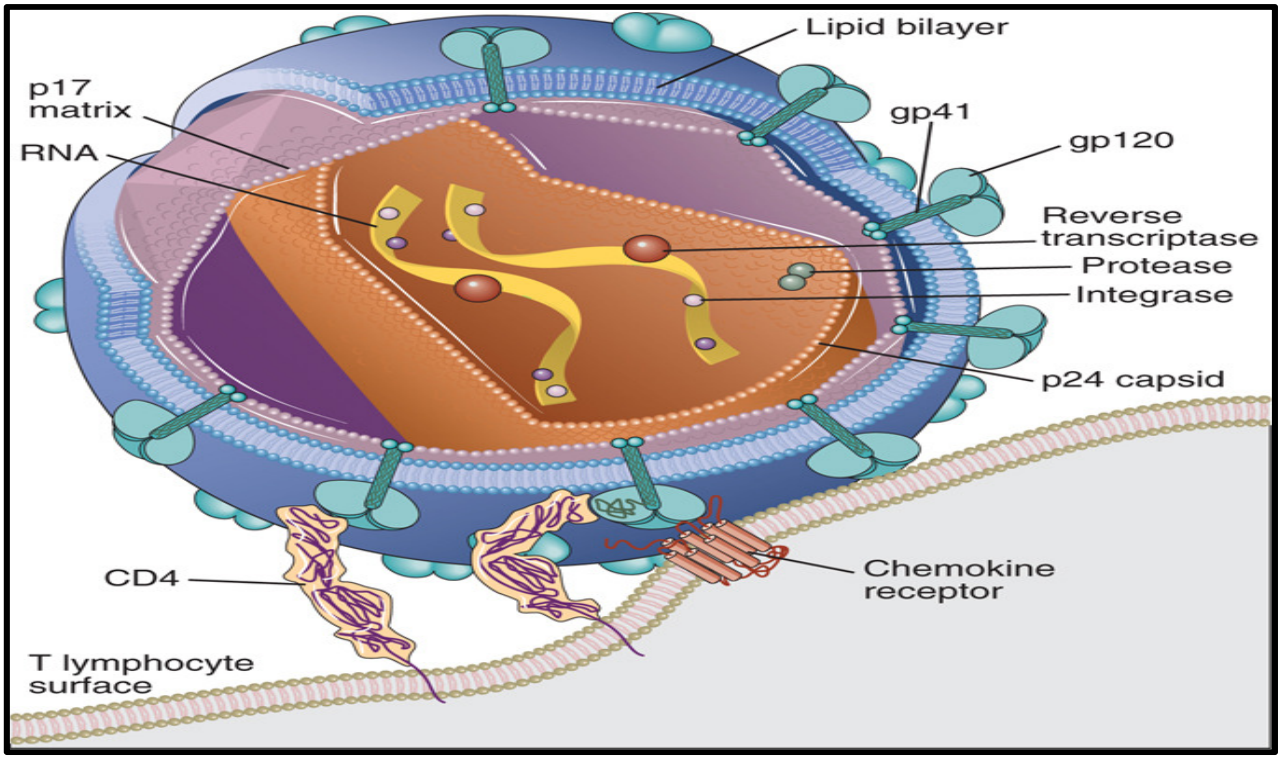

Figure 2.2: An illustration of the HIV virion

The figure shows the constituents of the internal core and envelope membrane of the HIV virion (Abbas AK, et al. 2012)

2.6 Replication in the host cell: HIV viral entry, integration and budding of new virions

The gp120/gp41 complex plays a distinct role in the attachment and consequent entry of the virus into the host cell. The gp120 subunit binds to the CD4 receptor and chemokine co-receptors (the most important co-receptors are CCR5 and CXCR4, however, others have also been defined which include CCR2, CCR3, CCR4, CCR2b, CCR8 and CXCR6) promoting the insertion of the fusion peptide gp41 into the cell membrane of the host. This allows for the viral envelope membrane to merge with the membrane of the target cell (Figure 2.3). Fusion results in the subsequent release and disassembly of the HIV capsid into the target cell and activation of the core enzymes: reverse transcriptase and integrase. The reverse transcriptase enzyme transcribes the viral single stranded RNA (ssRNA) into double stranded complimentaryDNA in the cytoplasm which is transported to the nucleus where the integrase enzyme promotes integration of viral DNA, i.e. provirus, into the host cell genome (Figure 2.4). The integrated provirus either remains in a dormant phase or produces new virions under appropriate conditions (Abbas AK, *et al*. 2012).

Host and other physiological factors (e.g. cytokines, stimuli) that normally induce the activation of T lymphocytes are major role players in the initiation of HIV replication. Activation of T lymphocytes results in the up-regulation of host transcriptional factors, especially, Nuclear Factor kappa Beta (NF-κB). The Long Terminal Repeat (LTR) endpoints of the HIV genome contain binding sites for NF-κB and subsequent interaction triggers the transcription of HIV integrated proviral genes and production of multiple new RNA copies. Proteins are translated from full length mRNA transcripts which are appropriately spliced to produce regulatory (Tat, Rev, Nef, Vif, Vpr, Vpu) and structural proteins (Pol, Gag, Env). Fully spliced mRNA transcripts of the regulatory proteins and at a later stage incompletely spliced structural proteins are transported from the nucleus to the cytoplasm of the host cell. Further processing includes the generation of the enzymes: reverse transcriptase, protease and integrase from the Pol precursor protein; p24 (capsid), p17 (matrix surrounding capsid) and p15 (nucleocapsid) polypeptides from the Gag precursor protein and gp120 and gp41 proteins from the Env precursor protein. In the final phase of virion formation, the full length RNA transcripts of the proviral genome together with the Gag and Pol proteins are packaged within the nucleoprotein capsid and this buds from the surface of the host together with the membrane-associated Env proteins (Figures 2.4 and 2.5) (Abbas AK, *et al*. 2012)

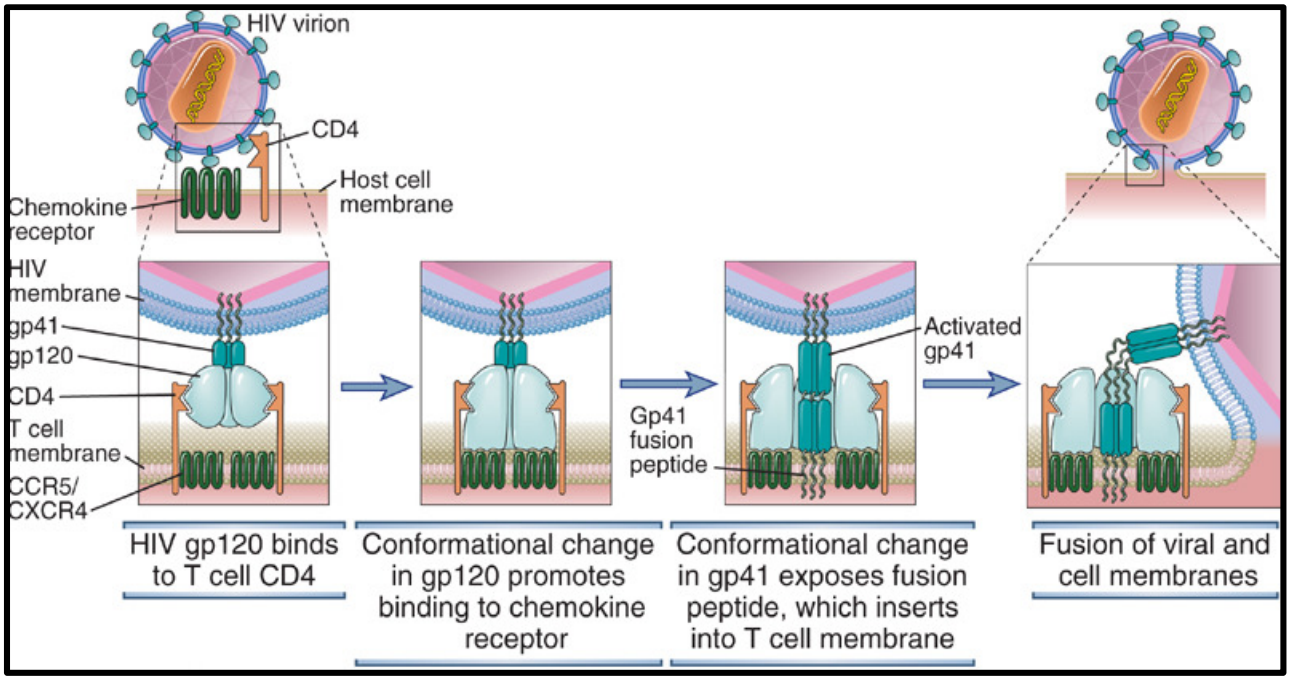

Figure 2.3: HIV membrane fusion with the viral host membrane

Viral entry entails binding of the gp120/gp41 complex to the CD4 and chemokine receptors (CCR5/CXCR4) of the host cell and the consequent fusion of the viral and host membrane (Abbas AK, et al. 2012)

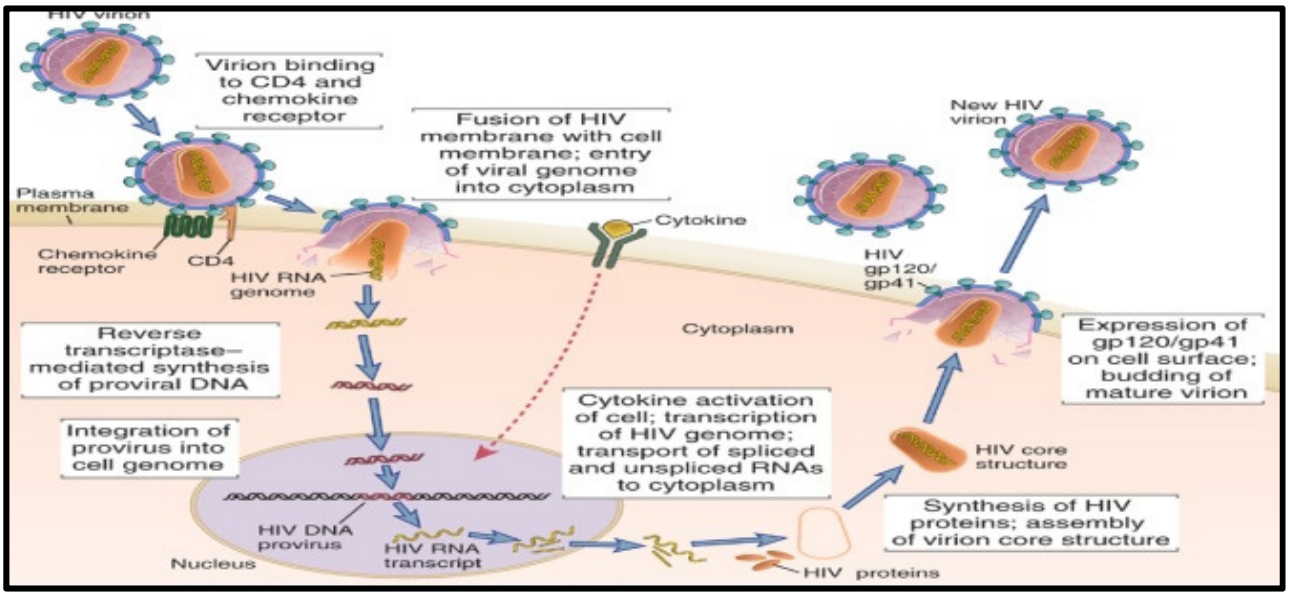

Figure 2.4: HIV viral entry, genomic integration and budding from host cell.

The HIV enters the cell via membrane fusion and enzymatic activity allows for the integration of proviral DNA into the host genome. Host cell activation results in the up-regulation of proviral genes and the subsequent formation and release of new virions (Abbas AK, et al. 2012)

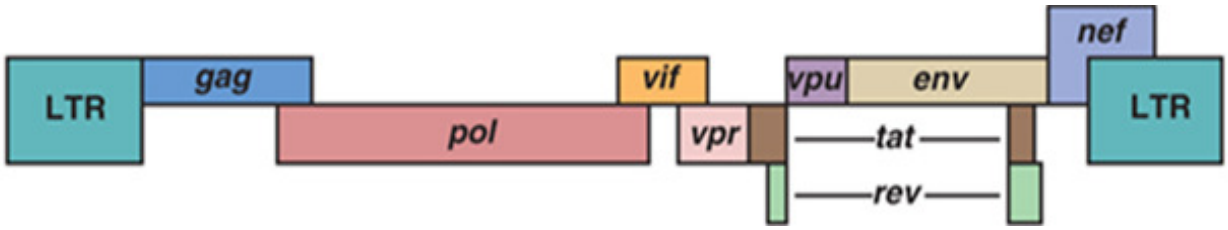

	Genome	Function
	Long terminal repeats (LTR)	Found at the endpoints of HIV RNA genome, controls viral gene expression, replication and integration into the genome of the host
Structural Genes	Group-specific antigen *(gag)*	p55 protein is cleaved into p24, p17, p6 and p7proteins. Encodes for structural proteins
	Envelope *(env)*	Encodes for gp160 which is processed by cellular protease to form the subunits gp120 and gp41, involved in binding to the host cell
	Polymerase *(pol)*	Encodes for the enzymes reverse transcriptase (p50), protease (p10), RNaseH (p15) and integrase (p31), required for viral replication
Regulatory Genes	Viral infectivity factor *(vif)*	Interferes with the function of APOBEC3G (host factor that interferes with reverse transcription)
	Viral protein r *(vpr)*	Apprehends cell division at G2/M cell cycle stage
	Viral protein u *(vpu)*	Release of newly formed virions from infected cell
	Negative factor *(nef)*	Downregulates CD4, Major histocompatibility complex (MHC) class I and II
	Transcriptional transactivator *(tat)*	Amplifies the production of complete viral mRNA transcripts
	Regulator of viral gene expression *(rev)*	Mobilisation of structural unspliced mRNA from the nucleus to cytoplasm

Figure 2.5: Layout and function of the 9 genes and LTR of the HIV *(Abbas AK, et al. 2012).*

2.7 Clinical hallmarks of HIV infection: loss of CD4 T lymphocytes and dendritic cells

The progressive loss of CD4 T lymphocytes from various compartments of the human body is one of the hallmarks of HIV infection, which persists to some extent even after ARV suppression of viral replication. In addition, the numbers of blood pDCs and mDCs (as well as other cell types) are also detrimentally affected. (Sabado RL, *et al.* 2010;Hosmalin, A *et al.* 2008;Lichtner M, *et al.* 2008; Brown KN, *et al.* 2007; Donaghy H, *et al.* 2001). It is proposed that DC loss may impact on the unique role that that these cells play in immune responses. Specifically, DCs are central to the initiation of effective immunity (mDC stimulation of naïve T lymphocytes) and in mounting of effective innate antiviral defenses (pDC production of interferon-α) (as reviewed by Banchereau J, *et al.* 2000).

2.8 Discovery of DCs - the 'one of a kind' blood cell

The 2011 Nobel Prize winner Ralph M. Steinman and his colleague Zanvil A. Cohn from the Rockefeller University, New York were the first to report on a novel adherent cell type, they termed dendritic cell. According to their original published work (1973), while investigating cells of mouse spleen that adhere to plastic and glass they noticed a large stellate cell with distinctive morphological features different from other adherent cells such as mononuclear phagocytes (macrophages), and to a lesser extent granulocytes and lymphocytes. To date, two major types of DCs have been described, mDCs and pDCs, both naturally present in very low numbers in peripheral blood. mDC constitute less than 1% of peripheral blood mononuclear cells (Upham J, *et al*. 2000) and pDCs have been quantified at levels to half that of mDCs (as reviewed by Reizis, *et al.* 2011). These cells are described as "one of a kind" as no other blood cell has the same morphological and mobility characteristics (Banchereau J and Steinman RM, *et al*. 1998). During certain stages of maturation they develop branch-like structures, key to the amplification of their specific function in the immune response (Figure 2.6 A and B). Cella M, *et al.* (1999) has reported on the different level of branch formation observed between pDCs and mDCs. In culturing these cells with Granulocyte-macrophage colony-stimulating factor (GM-CSF) and Interleukin (IL)-4 (or solely culturing pDCs with IL-3) the formation of branch-like structures in pDCs was minimal compared to the abundance observed in mDCs (Figure 2.6 C and D). Also, *in vitro* culturing revealed that pDCs had a more dispersed and mDCs a more clustered distribution pattern (Figure 2.6 E and F).

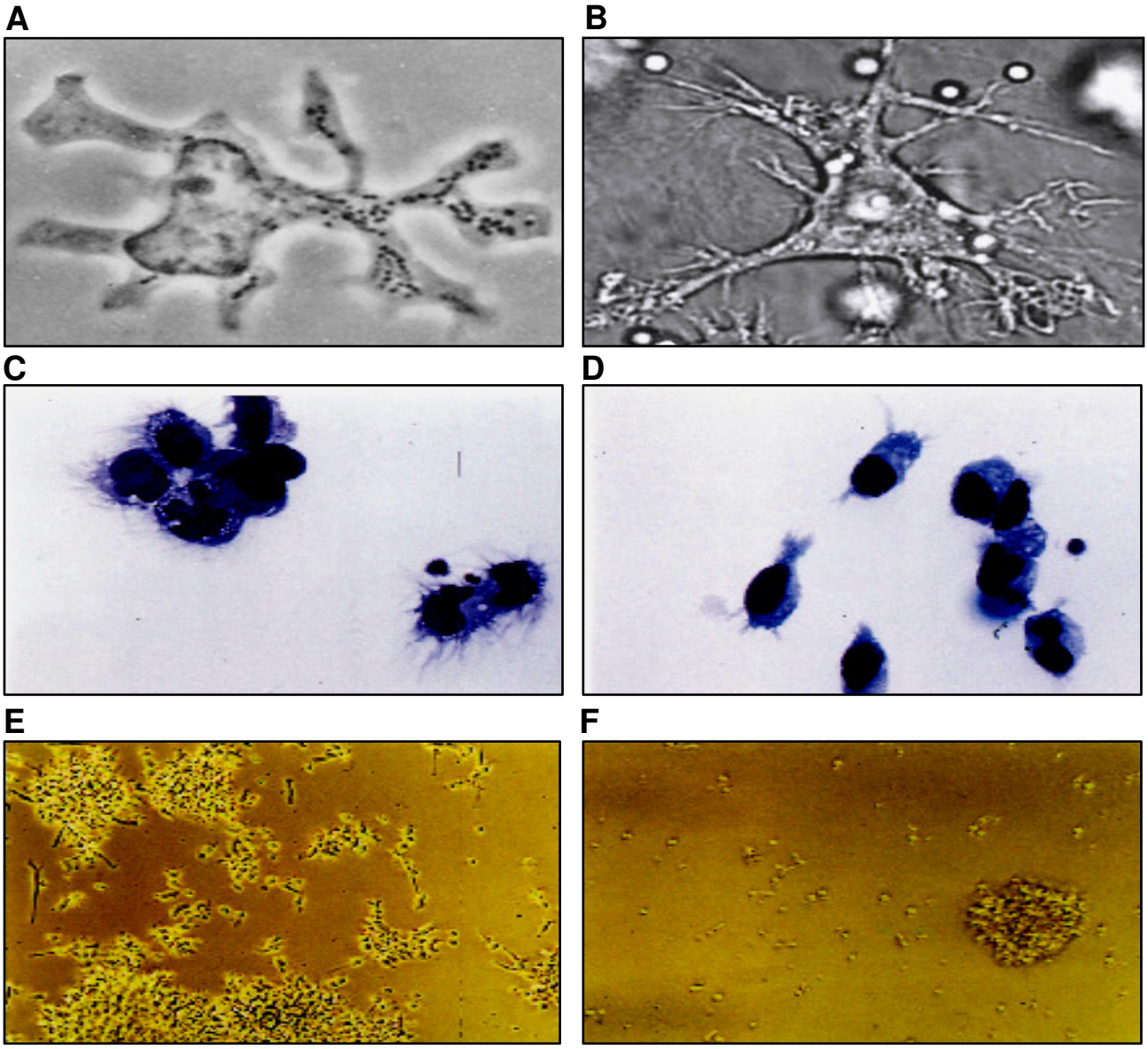

Figure 2.6: Microscopic images of DCs

Graph A represents a phase-contrast micrograph of a single DC isolated from the spleen of mouse. This is the first image of a DCs published by the cofounders Steinman RM and Cohn ZA in 1973. Graph B represent a 3-D micrograph of a single DC, clearly showing the dendrite-like structures unique to this cell type (Behnsen J, et al. 2007). pDCs and mDCs differ morphologically. Micrograph C and D represents May-Grünwald Giemsa staining of DCs, showing the high and low levels of dendrite-like structures of mDCs and pDCs, respectively (Cella M, et al. 1999).Micrograph E shows the multiple formations of mDC aggregates in comparison to the less clustered and more dispersed appearance of pDCs as presented in micrograph F (Cella M, et al. 1999).

2.9 Origin of DCs

DCs, like all other blood cell types, originate from a pluripotent CD34 expressing hematopoietic stem cell (HSC) in the bone marrow. During the process of haematopoiesis, the $CD34^+$HSC differentiates into myeloid and lymphoid progenitors, giving rise to the myeloid and lymphoid lineages of blood cells, respectively. The myeloid lineage of cells refers to the development of thrombocytes, erythrocytes, mast cells, basophils, eosinophils and monocytes/macrophages whereas the lymphoid lineage of blood cells refers to development of the lymphocytes viz. Natural Killer cells, T and B lymphocytes. mDCs derive from the myeloid lineage but it is still unclear from which of the two described lineages pDCs originate. The controversy regarding the line of descent of pDCs lead to these cells being given various titles and before the accepted term of "plasmacytoid" DCs they were also referred to as "plasmacytoid monocytes" or "plasmacytoid T cells". They were given the general term plasmacytoid due to their morphology resembling that of a plasma cells (antibody producing B cells), but as they lack B cell markers and were abundant in the T cell zone of human lymphoid tissue they were then designated as plasmacytoid T cells. However, in the late 1980s, studies showed that these cells lacked most lymphocytic markers (although expressing low levels of CD4) but expressed markers associated with monocytes (CD31, CD36, CD68), hence, their name changed to plasmacytoid monocytes (as reviewed by Galibert L, *et al*. 2001). Being referred to as a DC, came from a study by Grouard G, *et al.* (1997) who observed the formation of DC specific branch-like structures (and rescue from apoptosis) upon *in vitro* culturing of these "plasmacytoid T cells" with IL-3 and CD40L.

Research on the origin of pDCs has been controversial as some studies seem to assign pDC development to the lymphoid lineage and others to the myeloid lineage. One study investigated pDCs origin via ectopic expression of two specific genes (Id2 and Id3 - Inhibitor of DNA binding proteins), reported to be involved in hindering lymphoid T and B cell development, in $CD34^+CD38^-$ progenitor cells. The authors found that enforced expression of Id2 and Id3 genes inhibited development of precursor pDCs, but had no effect on the development of the myeloid lineage derived mDC precursors, hence promoting lymphoid lineage of origin (Spits H, *et al*. 2000). In contrast, a myeloid lineage of origin was proposed by Olweus J and colleagues (1997) based on 1) pDC's expression of a marker restricted to $CD34^+$ cells of the myeloid lineage, namely GM-CSF receptor (GM-CSFR) and 2) the parallel expression of CD123 (IL-3) receptor) by pDCs and $CD34^+$ myeloid cells. Stemming from experiments showing that within a subset of cultured CD34 progenitor cells up-regulation of CD123 coincided with a down-regulation of GM-CSFR during *in vitro* culturing, the authors suggest that $CD34^+$GM-$CSFR^+CD123^+$ cells defined a pDC precursor of myeloid lineage. However, recent molecular studies might have shed some light on the controversy regarding the origin of pDCs and proposed the development of these cells from a lymphoid rather than a myeloid progenitor. This was assumed on the basis that the same transcription factor (E protein transcription factor E2-2) involved in T lymphocyte development also controls pDC gene transcription (Reizis B, 2010).

2.10 DC: Markers of identification, subtypes and their respective locations

The conventional method for detecting pDCs and mDCs from the heterogeneous cell population in blood or lymphoid tissue requires the use of a combination of markers. The expression pattern of these markers profile pDCs and mDCs as follows: 1) differential expression of CD11c (αX subunit of the integrin CR4) and CD123 markers - pDCs: $CD11c^-$ $CD123^+$, mDC: $CD11c^+CD123^{DIM}$ and 2) mutual positive expression of

HLA-DR and dim expression of lymphocytic lineage markers: collectively refer to as LIN1 which includes CD3 (expressed by T lymphocytes), CD14 (expressed by monocytes, macrophages, neutrophils and eosinophils), CD16 (expressed by NK cells, macrophages, monocytes and neutrophils), CD19 and CD20 (B lymphocyte marker) and CD56 (expressed on activated and resting NK cells). This method of detection was used in this study although single marker detection of pDCs and mDCs can also be performed via the blood DC antigen (BDCA) markers: BDCA-1 (also referred to as CD1c), BDCA-2 (CD303), BDCA-3 (CD141) and BDCA-4 (CD304) (Dzionek A, *et al.* 2000). BDCA-1 detects the $LIN1^{-}HLA\text{-}DR^{+}CD11c^{+}CD123^{DIM}$ subset or mDCs. A smaller mDC subset defined as $LIN1^{-}HLA\text{-}DR^{+}CD11c^{+}CD123^{-}$ express BDCA-3 and differs from the BDCA-1 subset by the expression of CLEC9A, a C-type lectin with immunoreceptor tyrosine-based activation motif (ITAM)-like motifs. Dual expression of BDCA-2 and BDCA-4 identifies the $LIN^{-}HLA\text{-}DR^{+}CD11c^{-}CD123^{+}$ subset or pDCs. To date, two pDC subsets have been identified namely, $CD2^{HIGH}$ and $CD2^{LOW}$, and these showed, via Mixed Leukocyte Reaction (MLR), to play a role in the stimulation of allogeneic T lymphocytes. The latter subtype, however, shows a weaker T cell stimulation ability (Ueno H, *et al.* 2010; Dzionek A, *et al*. 2000).

DCs in different stages of development are found in different compartments of the body also having different function. Precursor mDC circulate in blood while immature (immDC) and mature mDC (mmDC) phenotypes are found in peripheral tissue and secondary lymphoid tissue, respectively. immDCs from skin, also known as the Langerhans cells, contains Birbeck granules and expresses CD1a and CD207 (langerin). They are found predominantly in the epidermis, while the dermis hosts a DC population with a $CD1a^{+}CD14^{+}$ phenotype (dermal DCs). In contrast to mDCs, pDCs are not peripheral tissue resident cells - both the immature and mature pDC phenotypes are found in secondary lymphoid tissue, while precursor pDC circulate in the blood (Gessani S and Filippo B, 2007)

2.11 *In vitro* research: the mo-DC model vs. blood DCs

The naturally scarce distribution of DCs together with the (prior) limited availability of DC-specific research tools made exploring these subsets complex. Previously, to overcome this obstacle the mo-DC model was used. Briefly, this entailed *in vitro* culturing of purified peripheral blood $CD14^{+}$ monocytes with various supplementary agents which included GM-CSF, IL-4 and Tumor Necrosis Factor (TNF)-α for seven days (Van Brussel I, *et al*. 2012). However, it has been debated whether mo-DCs are a true representation of the CD11c blood DC counterpart as these cells differ morphologically and functionally. Osugi Y, *et al*. (2002) reported that freshly isolated CD11c DCs were smaller than mo-DCs, also the nucleus of the CD11c DC had lobule-like features, while that of the mo-DCs was large, rounded and located eccentrically. Furthermore, the expression of the Dendritic Cell-Specific Intercellular adhesion molecule-3-Grabbing Non-integrin (DC-SIGN/CD209), a DC specific marker playing a role as HIV attachment receptor, was found expressed by mo-DCs but not blood CD11c DCs. Nonetheless, similar expression of HLA-DR, CD40, CD86 and CD83 has been detected in both phenotypes. On a functional level, higher proliferation responses of T lymphocyte were observed with mo-DCs than blood CD11c DCs in allostimulatory MLRs. However, the latter induced higher antigen specific T lymphocyte proliferation responses and, in particular, induced higher IFN-γ production than mo-DCs (Osugi Y, *et al*. 2002). Advances in modern technology have mostly eliminated the

need to use laborious and time-consuming preparations of mo-DCs, allowing for the direct analyses of DCs in whole blood or *in vitro.*

2.12 The imperative role of DCs in the initiation of primary adaptive immune responses

Primary adaptive immune responses are essential for the elimination of harmful pathogens and fundamental to the activation and priming of effector cells is a series of events primarily performed by DCs, in particular, mDCs. These include recognition and capture of pathogens at peripheral sites of preferential pathogen entry (gastrointestinal-, respiratory- and genital tracts), processing of antigen in a "readable" format, delivery and presentation to the naïve CD4 and CD8 T lymphocytes in secondary lymphoid tissue. Specifically, recognition, internalisation and processing are performed by the immDCs that circulate in peripheral tissue. Upon differentiation into the mature phenotype, mmDCs migrate to secondary lymphoid tissue and present processed peptide antigen via the MHC molecule to naïve T lymphocytes (as reviewed by Banchereau J, *et al.* 2000). Also, essential to this interaction is communication between the co-stimulatory/activation ligands CD86 and CD80 expressed on mmDCs and the CD28 receptor expressed on CD4 and CD8 T lymphocytes. Conventionally, the outcome of these events is 1) the activation and clonal expansion of antigen-specific T lymphocytes, 2) antigen clearance and 3) establishment of antigen-specific central and effector memory T cells. The latter cells are situated primarily in lymphoid and peripheral non-lymphoid tissue and mount a rapid and vigorous immune response upon re-entry of the pathogen.

2.13 "Tools" for the recognition of pathogens

Initiation of immune responses is greatly dependent on the ability of the immune system to distinguish between self and non-self antigens. This recognition process is central to the innate immune system, the first line of defense against antigen, involving among other innate immune cells also pDCs and mDCs. Recognition of microbial pathogens within the host's microenvironment is an important "cognitive" function and is performed via molecular structures referred to as pattern recognition receptors (PRRs). These receptors are found in different locations of the cell and accordingly differ in antigen specificity (Refer to Figure 2.7). The best described class of PRRs is the TLRs. *Toll* refers to the gene which was first identified to be involved in the development of the dorsal-ventral axis of the *Drosophila Melanogaster* fruit fly during embryogenesis. The anti-fungal properties of the receptor were only later discovered (Lemaitre B, *et al.* 1996). In general 10-15 TLRs, labeled as TLR 1, TLR 2 etc., have been identified in mammalian species (as reviewed by Iwasaki A and Medzhitov R, 2004). In humans 10 TLRs have been described (Barreiro LB, *et al.* 2009). PRRs function by recognizing evolutionary conserved pathogen-associated molecular patterns (PAMPs). PAMPs can be divided in two groups: microbe specific and microbe non - specific. The **microbe specific PAMPs** are molecular structures unique to microbes and not characteristic of the host. These microbe-specific PAMPs are recognised by TLRs located on the surface of cells. Examples include PAMPs of mostly a structural nature such as the lipopolysaccharide (LPS) and lipoteichoic acid, the major structural components of the cell wall of gram-negative and gram-positive bacteria, respectively (Abbas AK, *et al.* 2012). The latter PAMPs are recognised by TLR 4 (Beutler B, 2000) and TLR 2 (Schwandner R, *et al.*1999), respectively. The protein flagellin, the major constitute of the structural component of bacteria involved in the motility, namely the flagellum, is recognised by TLR5 (Hayashi F, *et al.* 2001).

The **microbe non-specific PAMPs** refer to the recognition of molecular structures generally found in both the host and microbe species and includes various types of nucleic acids. Differentiation between self and non - self is in this case location-specific and not entirely performed on the basis of molecular structure. Microbial nucleic acids are captured and trapped in endosomes, a compartment within eukaryotic cells that does not normally internalise nucleic acids of the host. Examples of microbe non-specific PAMPs include unmethylated CpG DNA sequences of bacterial origin that is recognised by TLR9 and ssRNA and double stranded RNA (dsRNA) of viral origin recognised by TLR7 and TLR8, respectively. TLR 7, 8 and 9 is expressed on the endosome (Abbas AK, *et al*. 2012).

TLRs are membrane constituents of both pDCs and mDCs, specifically, pDCs express TLR's 1, 6, 7 and 9 and mDCs express TLR 1 - 6 and 8 (Liu K-J, 2006; Gorden KB, *et al.* 2005; Iwasaki A and Medzhitov R, 2004;Kadowaki, *et al*. 2001). TLRs are also found expressed on macrophages, neutrophils and epithelial cells. Other members of the PRRs include NOD-like and RIG-like receptors which are expressed in the cytoplasm and sense bacterial cell wall peptidoglycans and viral nucleic acid (ssRNA and dsRNA), respectively.

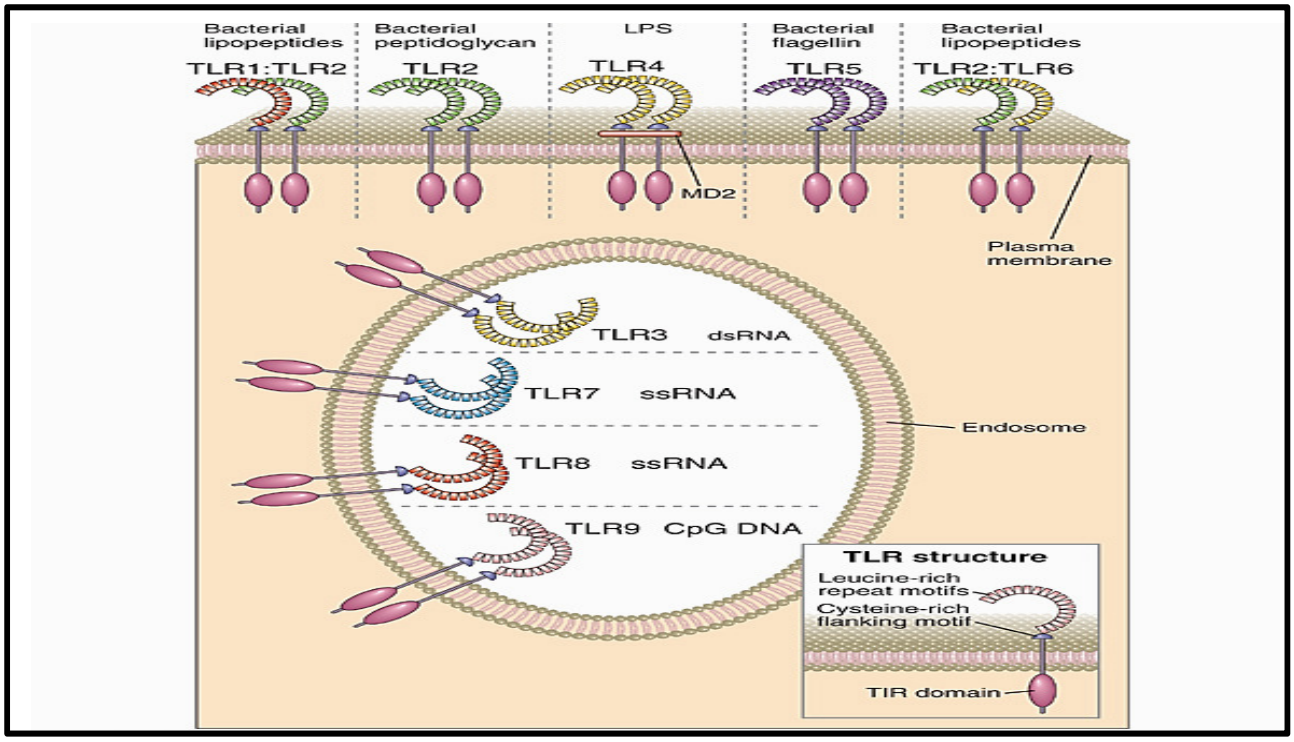

Figure 2.7: Cell surface and Intra-vesicular TLRs

TLR 1, 2, 4, 5 and 6 are located on the cell surface and senses PAMPs of a structural nature in the external milieu while TLRs 3, 7, 8 and 9 are located intra-vesicularly and senses PAMPs of genomic origin. (Abbas AK, *et al*. 2012)

Interaction between PAMPs and the PRRs, such as TLRs, initiates signal transduction pathways culminating in transcription factor activation and production of pro-inflammatory mediators (e.g. cytokines and chemokines) which initiate cell responses that promote the elimination of pathogens and enforce healing. Specifically, these inflammatory mediators function as activators of intracellular cell signaling (initiated upon binding to its cognate cell surface receptor) which subsequently leads to the activation of additional genes and the production of other cytokines and proteins involved in inflammation (e.g. IL-6), inhibition of viral

replication (IFN), proliferation (IL-2), apoptosis (FASL), etc. However, crucial to the activation of the immune system is subsequent "deactivation" upon clearance of the pathogen as components produced during inflammation, although beneficial in eliminating pathogens, are harmful in excessive quantities and can cause pathological damage. In HIV infection the inability of immune activity status to return to a basal state (homeostasis) is a well-described and problematic feature.

2.14 The transmission role of DCs in HIV pathogenesis

DCs are problematic in HIV pathogenesis in that they paradoxically both function in initiating effective immunity, and also play a central role in disseminating of HIV-1 within the host. DCs can carry viral particles to lymph nodes via the lymphatics and then expose the virus to its primary target cells (activated CD4 T cells).It is also proposed that these cells are the first to make contact with the virus. In horizontal transmission of HIV, which is mainly via sexual intercourse (vaginal or anal) with semen being the main transmitting source from male to female/male, the deposition of semen from HIV-infected males transfers infectious virus either as free virus, spermatozoa-associated or via host infected leukocytes. Micro-abrasions in the epithelial layer at the vaginal mucosal surfaces and/or trauma to the single cell epithelium of the rectal mucosa lining provide easy entry to HIV. However, an intact epithelial lining effectively hinders transmigration of HIV virions and viral entry via transcytosis has proven insufficient in cellular transmigration during HIV infection (Bobardt MD, *et al.* 2007). In view of this, it has been suggested that viral entry may involve DCs, believed to be facilitated by the branch-like structures of these cells. As these projections can cross the mucosal epithelial surface and enter the lumen of the vagina/rectum, it is possible that the HIV virions can latch on and be transported across. Refer to Figure 2.8 for an illustration of this proposed process.

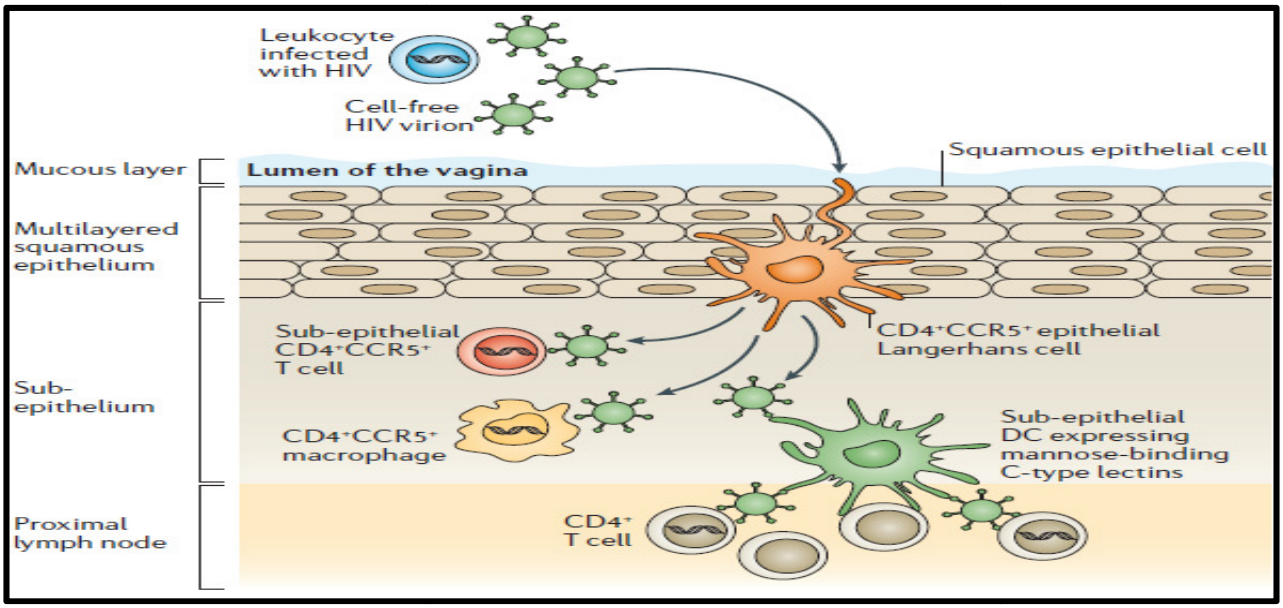

Figure 2.8: The proposed role of DCs in the mobilisation of HIV virions from the lumen of the vagina into circulation.

Semen deposited during intercourse can cross the mucosa epithelial layer of the vagina via attachment to the DC projections that extend into the lumen of the vagina (Lederman MM, et al. 2006).

Attachment receptors expressed on DCs and involved in facilitating transport of HIV virions across the vaginal epithelial barrier have been linked to Syndecan-3. The latter is a DC-specific heparin sulfate proteoglycan, found abundantly expressed on the projections of cervical DCs. Its interaction with the HIV has been linked to the gp120 envelope glycoprotein. Another DC specific receptor, well described in literature to play a role in HIV binding and dissemination, is DC-SIGN. DC-SIGN is a C-type lectin receptor which localises mostly at the center rather than the dendrite compartment of the cells. Interestingly, dual blocking of these HIV attachment receptors completely abolished viral capture and transmission, while blocking of Syndecan-3 alone elicited only partial blocking (de Witte L, *et al.* 2007). Notably, heparin sulfate expression on spermatozoa has been implicated in facilitating virus binding and transport of HIV into the lumen of the vagina. Other well-described HIV attachment receptors, namely, CD4, chemokine receptors and mannose, seemed not to play a role. Accordingly, it was determined that spermatozoa lack CD4 expression and that binding of HIV to spermatozoa was preserved despite blocking/cleaving of mannose receptors (Ceballos A, *et al.* (2009).

2.15 References

Books

Abbas AK, Lichtman AH, Pillai S. Cellular and Molecular Immunology. 7th ed. USA: Elsevier Saunders. 2012. P55-88.

Gessani S and Filippo B.The biology of dendritic cells and HIV infection. US: Springer; 2007. p406-433.

Hosmalin A, Lichtner M, Louis S. Clinical analysis of dendritic cell subsets The Dendritogram. In: Ewbank J, Vivier E, editors. Methods in Molecular Biology™ 415. New Jersey: Humana Press Inc; 2008.p.273-290.

Rödlach A. Witches, Westerners, and HIV: AIDS and cultures of blame in Africa Walnut Creek, California: Left Coast Press; 2006. p1-247.

Journals

Almeida, M., Cordero, M., Almeida, J., and Orfao, A. (2006).Persistent abnormalities in peripheral blood dendritic cells and monocytes from HIV-1 positive patients after 1 year of antiretroviral therapy. J. Acquir. Immune Defic.Syndr.*41*, 405–415.

Apetrei, C., Metzger, M.J., Richardson, D., Ling, B., Telfer, P.T., Reed, P., Robertson, D.L., and Marx, P.A. (2005). Detection and partial characterization of Simian Immunodeficiency Virus SIVsm strains from bush meat samples from rural Sierra Leone. J. Virol. *79*, 2631–2636.

Banchereau, J., and Steinman, R.M. (1998).Dendritic cells and the control of immunity. Nature *392*, 245–252.

Banchereau, J., Briere, F., Caux, C., Davoust, J., Lebecque, S., Liu, Y., Pulendran, B., and Palucka, K. (2000). Immunobiology of dendritic cells.Annu. Rev. Immunol. *18*, 767–811.

Barreiro, L.B., Ben-Ali, M., Quach, H., Laval, G., Patin, E., Pickrell, J.K., Bouchier, C., Tichit, M., Neyrolles, O., Gicquel, B., *et al*. (2009).Evolutionary dynamics of human Toll-like receptors and their different contributions to host defense. PLoS Genet. *5*, 1–18.

Behnsen, J., Narang, P., Hasenberg, M., Gunzer, F., Bilitewski, U., Klippel, N., Rohde, M., Brock, M., Brakhage, A.A., and Gunzer, M. (2007). Environmental dimensionality controls the interaction of phagocytes with the pathogenic fungi *Aspergillus fumigatus* and *Candida albicans*. PLoS Pathog. 3, 138–151.

Betsem, E., Rua, R., Tortevoye, P., Froment, A., and Gessain, A. (2011).Frequent and recent human acquisition of simian foamy viruses through apes' bites in central Africa. PLoS Pathog. *7*, 1–15.

Beutler, B. (2000). TLR4: central component of the sole mammalian LPS sensor. Curr.Opin.Immunol.*12*, 20–26.

Boasso, A., and Shearer, G.M. (2008).Chronic innate immune activation as a cause of HIV-1 immunopathogenesis.Clin.Immunol.*126*, 235–242.

Bobardt, M.D., Chatterji, U., Selvarajah, S., Van der Schueren, B., David, G., Kahn, B., and Gallay, P.A. (2007). Cell-free Human Immunodeficiency Virus type 1 transcytosis through primary genital epithelial cells. J. Virol. *81*, 395–405.

Bogart, L.M., and Thorburn, S. (2005). Are HIV/AIDS conspiracy beliefs a barrier to HIV prevention among African Americans? J. Acquir. Immune Defic.Syndr.*38*, 213–218.

Bogart, L.M., Skinner, D., Weinhardt, L.S., Glasman, L., Sitzler, C., Toefy, Y., and Kalichman, S.C. (2011). HIV misconceptions associated with condom use among black South Africans: an exploratory study. African J. AIDS Res. *10*, 181–187.

Boneva, R.S., Switzer, W.M., Spira, T.J., Bhullar, V.B., Shanmugam, V., Cong, M.-E., Lam, L., Heneine, W., Folks, T.M., and Chapman, L.E. (2007). Clinical and virological characterization of persistent human infection with Simian Foamy Viruses.AIDS Res. Hum. Retroviruses *23*, 1330–1337.

Brown, K.N., Trichel, A., and Barratt-boyes, S.M. (2007).Parallel loss of myeloid and plasmacytoid dendritic cells from blood and lymphoid tissue in simian AIDS. J. Immunol. 6958–6967.

Calattini, S., Betsem, E.B.A., Froment, A., Mauclère, P., Tortevoye, P., Schmitt, C., Njouom, R., Saib, A., and Gessain, A. (2007).Simian Foamy Virus Transmission from Apes to Humans, Rural Cameroon.Emerg. Infect. Dis. *13*, 1314–1320.

Ceballos, A., Lenicov, F.R., Sabatté, J., Rodrígues, C.R., Cabrini, M., Jancic, C., Raiden, S., Donaldson, M., Agustín, R., Pasqualini Jr, R.A., *et al*. (2009). Spermatozoa capture HIV-1 through heparan sulfate and efficiently transmit the virus to dendritic cells. J. Exp. Med. *206*, 2717–2733.

Cella, M., Jarrossay, D., Facchetti, F., Alebardi, O., Nakajima, H., Lanzavecchia, A., and Colonna, M. (1999). Plasmacytoid monocytes migrate to inflamed lymph nodes and produce large amounts of type I interferon. Nat. Med. *5*, 919–923.

D'arc, M., Ayouba, A., Esteban, A., Learn, G.H., Boué, V., Liegeois, F., Etienne, L., Tagg, N., Leendertz, F.H., Boesch, C., *et al.* (2015). Origin of the HIV-1 group O epidemic in Western Lowland gorillas.Proc. Natl. Acad. Sci. 112, E1343–E1352.

de Witte, L., Bobardt, M., Chatterji, U., Degeest, G., David, G., Geijtenbeek, T.B.H., and Gallay, P. (2007). Syndecan-3 is a dendritic cell-specific attachment receptor for HIV-1. Proc. Natl. Acad. Sci. U. S. A. *104*, 19464–19469.

Donaghy, H., Pozniak, A., Gazzard, B., Qazi, N., Gilmour, J., Gotch, F., and Patterson, S. (2001). Loss of blood CD11c+ myeloid and CD11c- plasmacytoid dendritic cells in patients with HIV-1 infection correlates with HIV-1 RNA virus load. Blood *98*, 2574–2576.

Dzionek, A., Fuchs, A., Schmidt, P., Cremer, S., Zysk, M., Miltenyi, S., Buck, D.W., and Schmitz, J. (2000). BDCA-2, BDCA-3, and BDCA-4: three markers for distinct subsets of dendritic cells in human peripheral blood. J. Immunol. *165*, 6037–6046.

Finke, J.S., Shodell, M., Shah, K., Siegal, F.P., and Steinman, R.M. (2004). Dendritic cell numbers in the blood of HIV-1 infected patients before and after changes in antiretroviral therapy. J. Clin. Immunol.*24*, 647–652.

Friis-Møller, N., Reiss, P., Sabin, C.A., Weber, R., Monforte, A. d'Arminio, El-Sadr, W., Thiébaut, R., De Wit, S., Kirk, O., Fontas, E., *et al*. (2007). Class of antiretroviral drugs and the risk of myocardial infarction. N. Engl. J. Med. *356*, 1723–1735.

Galibert, L., Maliszewski, C.R., and Vandenabeele, S. (2001). Plasmacytoid monocytes/T cells: a dendritic cell lineage? Semin.Imunol.*13*, 283–289.

Gao, F., Bailes, E., Robertson, D.L., Chen, Y., Rodenburg, C.M., Michael, S.F., Cummins, L.B., Arthur, L.O., Peeters, M., Shaw, G.M., *et al*. (1999). Origin of HIV-1 in the chimpanzee *Pan troglodytes troglodytes*. Nature *397*, 436–441.

Gorden, K.B., Gorski, K.S., Gibson, S.J., Kedl, R.M., Kieper, W.C., Qiu, X., Tomai, M.A., Alkan, S.S., and Vasilakos, J.P. (2005). Synthetic TLR agonists reveal functional differences between human TLR7 and TLR8. J. Immunol. *174*, 1259–1268.

Grouard, G., Rissoan, M., Filgueira, L., Durand, I., Banchereau, J., and Liu, Y. (1997). The enigmatic plasmacytoid T cells develop into dendritic cells with Interleukin (IL)-3 and CD40-Ligand. J. Exp. Med. *185*, 1101–1111.

Guadalupe, M., Reay, E., Sankaran, S., Prindiville, T., Flamm, J., Mcneil, A., and Dandekar, S. (2003). Severe CD4+ T-cell depletion in gut lymphoid tissue during primary Human Immunodeficiency Virus type 1 infection and substantial delay in restoration following Highly Active Antiretroviral Therapy. J. Virol. *77*, 11708–11717.

Gupta, R.K., Jordan, M.R., Sultan, B.J., Hill, A., Davis, D.H.J., Gregson, J., Sawyer, A.W., Hamers, R.L., Ndembi, N., Pillay, D., *et al*. (2012). Global trends in antiretroviral resistance in treatment-naive individuals with HIV after rollout of antiretroviral treatment in resource-limited settings: a global collaborative study and meta-regression analysis. Lancet *380*, 1250–1258.

Hahn, B.H. (2005). Tracing the Origin of the AIDS Pandemic.PRN Noteb.*10*, 4–8.

Hayashi, F., Smith, K.D., Ozinsky, A., Hawn, T.R., Yi, E.C., Goodlett, D.R., Eng, J.K., Akira, S., Underhill, D.M., and Aderem, A. (2001). The innate immune response to bacterial flagellin is mediated by Toll-like receptor 5. Nature *410*, 1099–1103.

Hirsch, V., Olmsted, R., Murphey-Corb, M., Purcell, R., and Johnson, P. (1989). An African primate lentivirus (SIVsm) closely related to HIV-2. Nature 339, 389–392.

Iwasaki, A., and Medzhitov, R. (2004).Toll-like receptor control of the adaptive immune responses. Nat. Immunol. *5*, 987–995.

Jewkes, R.K., Dunkle, K., Nduna, M., and Shai, N. (2010). Intimate partner violence, relationship power inequity, and incidence of HIV infection in young women in South Africa: A cohort study. Lancet *376*, 41–48.

Kadowaki, N., Ho, S., Antonenko, S., de Waal Malefyt, R., Kastelein, R.A., Bazan, F., and Liu, Y.J. (2001). Subsets of human dendritic cell precursors express different toll-like receptors and respond to different microbial antigens. J. Exp. Med. *194*, 863–869.

Klonoff, E.A., and Landrine, H. (1999). Do Blacks believe that HIV/AIDS is a government conspiracy against them? Prev. Med. *28*, 451–457.

Kotler, D.P. (2008). HIV and antiretroviral therapy: lipid abnormalities and associated cardiovascular risk in HIV-infected patients. J. Acquir. Immune Defic.Syndr.*49*, S79–S85.

Lederman, M.M., Offord, R.E., and Hartley, O. (2006).Microbicides and other topical strategies to prevent vaginal transmission of HIV. Nat. Rev. Immunol. *6*, 371–382.

Lemaitre, B., Nicolas, E., Michaut, L., Reichhart, J.M., and Hoffmann, J. A.(1996). The dorsoventral regulatory gene cassette spätzle/Toll/cactus controls the potent antifungal response in Drosophila adults. Cell *86*, 973–983.

Lichtner, M., Rossi, R., Rizza, M.C., Mengoni, F., Sauzullo, I., Massetti, A.P., Luzi, G., Hosmalin, A., Mastroianni, C.M., and Vullo, V. (2008). Plasmacytoid dendritic cells count in antiretroviral-treated patients is predictive of HIV load control independent of CD4+ T-cell count. Curr. HIV Res. *6*, 19–27.

Liu, K.-J.(2006). Dendritic cell, Toll-like receptor and the immune system. J. Cancer Mol. *2*, 213–215.

McKenna, K., Beignon, A.-S., and Bhardwaj, N. (2005). Plasmacytoid dendritic cells: Linking innate and adaptive immunity. J. Virol. *79*, 17–27.

Meiering, C.D., and Linial, M.L. (2001).Historical perspective of Foamy virus epidemiology and infection.Clin.Microbiol. Rev. *14*, 165–176.

Mojumdar, K., Vajpayee, M., Chauhan, N.K., Mendiratta, S., and Wig, N. (2010). Defects in blood dendritic cell subsets in HIV-1 subtype C infected Indians. Indian J. Med. Res. *132*, 318–327.

Mufune, P. (2005). Myths about condoms and HIV/AIDS in rural northern Namibia. Int. Soc. Sci. J. *57*, 675–686.

Murray, S.M., Picker, L.J., Axthelm, M.K., and Linial, M.L. (2006). Expanded tissue targets for foamy virus replication with Simian Immunodeficiency Virus-induced immunosuppression. J. Virol. *80*, 663–670.

Ndembi, N., Kaptue, L., and Ido, E. (2009). Exposure to SIVmnd-2 in Southern Cameroon: Public health implications. AIDS Rev. *11*, 135–139.

Olweus, J., BitMansour, A., Warnke, R., Thompson, P.A., Carballido, J., Picker, L.J., and Lund-Johansen, F. (1997). Dendritic cell ontogeny: a human dendritic cell lineage of myeloid origin. Proc. Natl. Acad. Sci. U. S. A. *94*, 12551–12556.

Osugi, Y., Vuckovic, S., and Hart, D.N.J. (2002). Myeloid blood CD11c(+) dendritic cells and monocyte-derived dendritic cells differ in their ability to stimulate T lymphocytes. Blood *100*, 2858–2866.

Paiardini, M., Pandrea, I., Apetrei, C., and Silvestri, G. (2009). Lessons learned from the natural hosts of HIV-related viruses. Annu. Rev. Med. *60*, 485–495.

Palella, F.J. Jr., Delaney, K., Moorman, A., Loveless, M.., Fuhrer, J., Satten, G., Aschman, D., and Holmberg, S. (1998). Declining morbidity and mortality among patients with advanced Human Immunodeficiency Virus infection. N. Engl. J. Med. *338*, 853–860.

Peeters, M., Courgnaud, V., Abela, B., Auzel, P., Pourrut, X., Bibollet-Ruche, F., Loul, S., Liegeois, F., Butel, C., Koulagna, D., *et al*. (2002).Risk to human health from a plethora of Simian Immunodeficiency Viruses in primate bushmeat.Emerg. Infect. Dis. *8*, 451–457.

Reizis, B. (2010). Regulation of plasmacytoid dendritic cell development.Curr.Opin.Immunol.*22*, 206–211.

Reizis, B., Bunin, A., Ghosh, H.S., Lewis, K.L., and Sisirak, V. (2011). Plasmacytoid dendritic cells: recent progress and open questions. Annu. Rev. Immunol. *29*, 163–183.

Ross, M.W., Essien, E.J., and Torres, I. (2006).Conspiracy beliefs about the origin of HIV/AIDS in four racial ethnic groups. J. Acquir. Immune Defic.Syndr.*41*, 342–344.

Sabado, R.L., O'Brien, M., Subedi, A., Qin, L., Hu, N., Taylor, E., Dibben, O., Stacey, A., Fellay, J., Shianna, K. V, *et al*. (2010).Evidence of dysregulation of dendritic cells in primary HIV infection.Blood *116*, 3839–3852.

Schwandner, R., Dziarski, R., Wesche, H., Rothe, M., and Kirschning, C.J. (1999). Peptidoglycan- and lipoteichoic acid-induced cell activation is mediated by toll-like receptor 2. J. Biol. Chem. *274*, 17406–17409.

Silvestri, G., and Feinberg, M.B. (2003).Turnover of lymphocytes and conceptual paradigms in HIV infection. J. Clin. Invest. *112*, 821–824.

Soumelis, V., Scott, I., Gheyas, F., Bouhour, D., Cozon, G., Cotte, L., Huang, L., Levy, J.A., and Liu, Y.-J.(2001). Depletion of circulating natural type 1 interferon-producing cells in HIV-infected AIDS patients. Blood *98*, 906–912.

Spits, H., Couwenberg, F., Bakker, A.Q., Weijer, K., and Uittenbogaart, C.H. (2000). Id2 and Id3 inhibit development of CD34(+) stem cells into predendritic cell (pre-DC)2 but not into pre-DC1. Evidence for a lymphoid origin of pre-DC2. J. Exp. Med. *192*, 1775–1783.

Steinman, R.M., and Cohn, Z.A. (1973).Identification of a novel cell type in peripheral lymphoid organs of mice. J. Exp. Med. *137*, 1142–1162.

Switzer, W.M., Bhullar, V., Shanmugam, V., Cong, M., Parekh, B., Lerche, N.W., Yee, Joann, L., Ely, J.J., Boneva, R., Chapman, L.E., *et al*. (2004). Frequent Simian Foamy Virus infection in persons occupationally exposed to nonhuman primates. J. Virol. *78*, 2780–2789.

Switzer, W.M., Salemi, M., Shanmugam, V., Gao, F., Cong, M., Kuiken, C., Bhullar, V., Beer, B.E., Vallet, D., Gautier-hion, A., *et al.* (2005). Ancient co-speciation of simian foamy viruses and primates. Nature *434*, 376–380.

The Joint United Nations Program on HIV/AIDS (UNAIDS) (2015). Global statistics facts sheet.Geneva, Switzerland.1–8.

Ueno, H., Schmitt, N., Klechevsky, E., Pedroza-Gonzales, A., Matsui, T., Zurawski, G., Oh, S., Fay, J., Pascual, V., Banchereau, J., *et al.* (2010). Harnessing human dendritic cell subsets for medicine.Immunol. Rev. *234*, 199–212.

Upham, J.W., Lundahl, J., Liang, H., Denburg, J.A., O'Byrne, P.M., and Snider, D.P. (2000).Simplified quantitation of myeloid dendritic cells in peripheral blood using flow cytometry. Cytometry *40*, 50–59.

Van Brussel, I., Berneman, Z.N., and Cools, N. (2012). Optimizing dendritic cell-based immunotherapy: tackling the complexity of different arms of the immune system. Mediators Inflamm.1–14.

Van Wijk, J.P.H., and Cabezas, M.C. (2012). Hypertriglyceridemia, Metabolic Syndrome, and Cardiovascular disease in HIV-Infected patients: effects of antiretroviral therapy and adipose tissue distribution. Int. J. Vasc. Med. 1–13.

Van Zyl, G.U., Merwe, L. Van Der, Claassen, M., Zeier, M., and Preiser, W. (2011). Antiretroviral resistance patterns and factors associated with resistance in adult patients failing NNRTI-based regimens in the Western Cape, South Africa. J. Med. Virol. *83*, 1764–1769.

Wain-Hobson, S., Sonigo, P., Danos, O., Cole, S., Alizon, M. (1985).Nucleotide sequence of the AIDS virus, LAV. Cell *40*, 9-17.

World Health Organisation (WHO) (2015).Guideline on when to start antiretroviral therapy and on pre-exposure prophylaxis for HIV.1–76.

Wolfe, N.D., Switzer, W.M., Carr, J.K., Bhullar, V.B., Shanmugam, V., Tamoufe, U., Prosser, A.T., Torimiro, J.N., Wright, A., Mpoudi-Ngole, E., *et al*. (2004). Naturally acquired simian retrovirus infections in central African hunters. Lancet *363*, 932–937.

Zeng, M., Paiardini, M., Engram, J.C., Beilman, G.J., Chipman, J.G., Schacker, T.W., Silvestri, G., and Haase, A.T. (2012). Critical role of CD4 T cells in maintaining lymphoid tissue structure for immune cell homeostasis and reconstitution. Blood *120*, 1856–1867.

Chapter 3

Impact of HIV-1 infection on absolute pDC and mDC numbers in peripheral whole blood: relationship to standard clinical markers of disease progression

3.1 Introduction

The systemic loss of CD4 T lymphocytes is a distinctive characteristic of an HIV-1 infection. In clinical practice in South Africa, enumeration of absolute number of CD4 T lymphocytes in peripheral blood is used as the primary immunological marker to assess HIV-1 disease progression and eligibility for ARV treatment. Recently, the value of the CD4:CD8 ratio as an important marker to evaluate immunological status during long term ARV therapy has been reviewed (Lu W, *et al.* 2015). The current CD4 T lymphocyte threshold for initiation of ARV therapy in South Africa is ≤500 cells/µl, which has been newly implemented since January 2015 (Green A and Skosana I, 2014; Department of Health, South Africa, 2014).Previously, a threshold CD4 T lymphocyte count of ≤350 cells/µl provided admissibility to ARV therapy. This scale raise was recommended by the WHO and reported in their revised guidelines of 2013. It was based on studies showing that earlier initiation of ARV therapy, in particular, improved the clinical outcome of HIV-1 infected individuals and reduced the risk of HIV transmission to the HIV negative partner in discordant infected couples. Notably, WHO has recently (September 2015) released revised guidelines recommending the administration of ARV therapy to HIV-infected individuals regardless of their CD4 count.

Similar to the loss of CD4 T lymphocytes, a decline in pDC and mDC numbers in peripheral blood during acute and chronic HIV-1 infection has been reported (Mojumdar K, *et al*. 2010; Sabado RL *et al*. 2010; Lichtner M, *et al.* 2008; Finke JS, *et al*. 2004; Donaghy H, *et al.* 2001; Soumelis V, *et al*. 2001). DC depletion has also been observed in peripheral blood of SIV infected macaque monkeys (*Macaca mulatta)* (Wijewardana V, *et al*. 2010; Malleret B, *et al.* 2008; Brown KN, *et al.* 2007; Reeves RK and Futz PN, *et al.* 2007). In one particular SIV study the loss of blood pDCs during infection was mirrored by the loss of these cells from axillary lymph nodes (Brown KN, *et al*. 2009). This finding contradicted the hypothesis that DC loss from peripheral blood is due to increased migration to and accumulation in lymph nodes. Brown KN, *et al*. (2009) initially proposed that the systemic decline of pDCs might be due to arrested development of these cells in the bone marrow but no association was found. However, apoptosis was seemingly involved as higher expression of Annexin V and 7-AAD (markers for early and late stage apoptosis, respectively) was observed in lymph node pDCs. Also, up-regulation of the FAS receptor was detected (other cell death associated markers, TRAIL-R2, FASL and TNF-related apoptosis inducing ligand (TRAIL), showed no change in expression). These findings might explain why Brown KN *et al*. in a previous study (2007) observed a significantly higher degree of spontaneous apoptosis by lymph node harvested pDCs and mDCs of SIV infected macaque monkeys compared to their uninfected counterparts in 24h cultures. Wijewardana V, *et al.* (2013) also confirmed the role of apoptosis in the loss of mDCs during SIV infection and illuminated the role of these cells in contributing to immune activation during HIV-1 infection. In contrast to the findings in SIV infected macaque monkeys, DC number loss in peripheral blood of chronically HIV-1 infected humans were analogous to DC number increase in lymph nodes (Dillon SM, *et al.* 2008). This finding was supported by a study conducted by Dave B and colleagues (2012) who also reasoned that the contrasting reports

regarding DC numbers in the lymph nodes versus peripheral blood of the non-natural human and monkey hosts during HIV/SIV infection may be due to the extraction of DCs at inconsistent time points during infection.

Main research focus

The loss of DCs from peripheral blood during HIV-1 infection has been reported, however, little is known regarding the distribution of pDCs and mDCs in peripheral blood of chronically HIV-1 infected patients from South Africa. Also, not much has been reported on the impact of active TB co-infection (the major death-causing co-infection among HIV-1-infected South African) and combination ARV treatment (the standard treatment approach) on DC numbers.

The study aim

The aim of the present study was to gain an understanding of the whole blood distribution of absolute pDC and mDC numbers of South African HIV-1 mono, HIV-1/TB co-infected and ARV treated individuals compared to uninfected matched controls.

The objectives of the study were

- ***to describe the absolute number distribution of pDCs and mDCs as well CD4 and CD8 T lymphocytes in peripheral blood during HIV-1 infection***
- ***to determine the impact of a TB co-infection and ARV treatment on the pDC and mDCs number as well as CD4 and CD8 T lymphocyte numbers in peripheral blood***
- ***to evaluate the CD4:CD8 ratio between the control study group and HIV-1 related study groups***
- ***to determine whether pDC and mDC numbers correlates with CD4 and CD8 T lymphocytes as well as viral load***

3.2 Outline of the study

Refer to sections 3.3.1 - 3.3.8 for a detailed description on the collection and processing of samples and data

SAMPLE COLLECTION
Patient recruitment, blood collection by venesection at various clinics in the Western Cape, South Africa

↓

STUDY GROUPS
5 Study groups: Control, ARV$^-$HIV-1, ARV$^-$HIV-1/TB, ARV$^+$HIV-1 and ARV$^+$HIV-1/TB

↓

WHOLE BLOOD (EDTA)			**PLASMA (EDTA)**
50µl	100µl	100µl	1ml
↓	↓	↓	↓
4-COLOUR FLOW CYTOMETRIC QUANTIFICATION OF			**REAL TIME PCR QUANTIFICATION OF**
CD4 and CD8 T cells **ASSAY:** Staining with BD MultiTEST™ mAbs: CD3 FITC, CD8 PE, CD45 PerCP, CD4 APC in BD TruCOUNT^{TM} tube	**pDCs** **ASSAY:** Staining with mAbs: HLA-DR APC, CD45 PerCP, LIN1 FITC, CD123 PE in BD TruCOUNT^{TM} tube	**mDCs** **ASSAY:** Staining with mAbs: HLA-DR APC, CD45 PerCP, LIN1 FITC, CD11c PE in BD TruCOUNT^{TM} tube	**Viral load** **ASSAY:** ABBOTT Real Time HIV-1 PCR assay (ABBOTTm 2000rt)/ bioMérieux NucliSens EasyQ® HIV-1, v1.2 test
↓	↓	↓	↓
DATA COLLECTED			
CD4 and CD8 T cells - cells/µl - % of CD45$^+$CD3$^+$ cells	**pDCs** - cells/ml - % of HLA-DR_LIN1^{DIM} events	**mDCs** - cells/ml - % of HLA-DR_LIN1^{DIM} events	**Viral load** - RNA copies/ml

3.3 Materials and Methods

3.3.1 Study groups and clinical data

A total of five study groups were included in this first part of the study which included the Control (n=24), ARV^-HIV-1 (n=21), ARV^-HIV-1/TB (n=20), ARV^+HIV-1 (n=22) and ARV^+HIV-1/TB (n=17) study groups. The selection criteria for participant enrolment for each study group is summarised in Table 3.1. Participants were enrolled from February to October 2009 and were of black African or mixed race origin. The enrolled individuals were also of similar socio-economic status. The majority of patients on ARV therapy (61%) were following the Stavudine, Lamivudine and Efavirenz (EFV) regimen, 20% were using the Stavudine, Lamivudine and Nevirapine (NVP) regimen, 5% were on the Prevention of Mother-to-Child Transmission (PMTCT) regimen and 2-4% was using one of five different ARV regimens. At the time of enrolment, HIV-1/TB co-infected patients were primarily using either Pyridoxine and/or Rifafour (combination of four agents Rifampicin, Isoniazid, Pyrazinamide and Ethambutol) drugs. Participants of each study group were recruited from the following state clinics in a peri-urban area of Cape Town, South Africa, which included Stellenbosch (47% of total recruits), Idasvalley (12%), Kuils River (2%), Tygerberg (13%), Eerste River (23%) as well as the Carl Bremer Hospital in Parow (2%).

Informed consent was obtained from all the study participants. The study was reviewed and approved by the Health Research Ethics committee (HREC) of the Faculty of Medicine and Health Sciences of Stellenbosch University and was assigned the Ethics reference number N08/02/057. Demographic and clinical data of the study participants are shown in Table 3.2.

Table 3.1: Description of study groups for the whole blood analysis of pDCs and mDCs

Study groups		Description of study group
Control		At the time of blood collection participants had a) a negative HIV-1 serology[a] test result, b) showed no clinical symptoms of other infections.
ARV$^-$	HIV-1	HIV-1 diagnoses of participants of this study group were confirmed with a positive HIV-1 serology[a] test. At the time of blood collection, enlistees a) were not receiving ARV therapy, b) had no clinical symptoms of a current TB co-infection.
	HIV-1/TB[b]	HIV-1 diagnoses of participants of this study group were confirmed with a positive HIV-1 serology[a] test. Diagnosis of active TB co-infection (cough, night sweats, weight loss) was confirmed with sputum culture and/or chest X-ray evidence. At the time of blood collection, enlistees were a) not on ARV treatment, b) using anti-TB[c] medication.
ARV$^+$	HIV-1	HIV-1 diagnoses of participants of this study group were confirmed with a positive HIV-1 serology[a] test. At the time of blood collection, enlistees a) were receiving ARV[c] treatment, b) showed no clinical symptoms of a current TB co-infection.
	HIV-1/TB[b]	At the time of diagnoses, HIV-1 infection was confirmed by an HIV-1 serology test[a] and active TB infection was confirmed with sputum culture/chest X rays. At the time of blood collection the enlistees were a) on ARV[c] treatment, b) using anti-TB[c] medication.

[a] *Combination antibody and antigen*
[b] *TB co-infection being either a primary/secondary infection or reactivation*
[c] *Specific time on treatment was not a defining criteria for this study*

Table 3.2: Demographic and clinical data of participants in the study groups analysed for the whole blood enumeration of pDCs and mDCs

	Study groups				
	Control	ARV$^-$		ARV$^+$	
		HIV-1	HIV-1/TB	HIV-1	HIV-1/TB
Total (n)	24	21	20	22	17
Male: Female					
Nr	11:13	11:10	14:6	9:13	9:8
%	46:54	52:48	70:30	41:59	53:47
Age[a]					
Median	35	37	37	34	35
Range	18 - 62	21 - 53	24 - 53	19 - 53	24 - 53
Time on ARV therapy[b]					
Median	N/A	N/A	N/A	9	15
Range				<1 - 43	<1 - 44
Time on anti-TB therapy[b]					
Median	N/A	N/A	1	N/A	3
Range			<1 - 5		<1 - 8

[a] *Age median and range expressed in years*
[b] *Time on treatment median and range expressed in months*

3.3.2 General specimen processing

Each of the participants enrolled in the study was allocated a patient number and all laboratory procedures were performed in reference to this number. Whole blood from participants was obtained aseptically by venisection into 5 ml Ethylene diamine tetra acetic acid (EDTA) vacutainer tubes (Becton, Dickinson and Company (BD) Biosciences, San Jose, CA) of which 500µl was aliquoted into screw cap tubes for the whole blood CD4 and CD8 T lymphocyte count assay. A volume of 200µl of the remainder blood volume was collected for the whole blood procedure used to determine the absolute number of pDCs and mDCs. The remaining blood volume was used for plasma collection to determine the viral load (refer to section 3.3.7) and/or storage at -80°C.Processing of samples was at all times performed in a biosafety cabinet (NUAIRE biological class II safety cabinet).

3.3.3 Monoclonal antibodies (mAbs) used for the detection of pDCs and mDCs in peripheral whole blood

In identifying the general DC population in whole blood, the following mouse anti-human monoclonal antibodies, all obtained from BD Biosciences (San Jose, CA), were used: HLA-DR APC, CD45 PerCP, CD123 PE, CD11c PE and LIN 1. The latter contains a combination of 6 mAb clones against several leukocyte subsets all conjugated to the same fluorochrome, namely FITC. It is also labeled as the "dump channel" as it is used to identify the majority of "unwanted" cells. The mAb clones of the LIN1 cocktail includes CD3 (expressed on all T lymphocytes), CD16 (expressed on resting NK cells, and certain macrophages, monocytes and neutrophils), CD19 and CD20 (expressed on B lymphocytes), CD14 (expressed on monocytes, macrophages, neutrophils and eosinophils) and CD56 (expressed on activated and resting NK cells). For the purpose of the study the target markers HLA-DR, LIN1, CD123 and CD11c were collectively given the term, DCID (DC identification) markers. Refer to Table 3.3 for mAb clone and isotype information.

Table 3.3: Clone, isotype and reactivity information on the mAbs used to detect pDCs and mDCs

mAb	Clone	Isotype	Reactivity
LIN1 FITC:CD3 CD16 CD19 CD20 CD14 CD56	SK7 3G8 SJ25C1 L27 MΦP9 NCAM16.2	Mouse IgG_1, κ Mouse IgG_1, κ Mouse IgG_1, κ Mouse IgG_1, κ Mouse IgG_{2b}, κ Mouse IgG_{2b}, κ	Human
CD45 PerCP	2D1	Mouse IgG_1, κ	Human
HLA-DR APC	L243	Mouse IgG_{2a}, κ	Human
CD123 PE	9F5	Mouse IgG_1, κ	Human
CD11c PE	S-HCL-3	Mouse IgG_{2b}, κ	Human

3.3.4 Whole blood staining procedure for the detection of pDCs and mDCs

The whole blood staining procedure to detect and enumerate the pDC and mDC population was performed in BD TruCOUNT™ tubes (BD Biosciences, San Jose, CA) usually used for absolute CD4 and CD8 count procedures. The BD TruCOUNT™ tube contains a lyophilised pellet with fluorescent beads situated beneath a stainless steel retainer at the base of the tube. Once the specimen and the mixture of fluorochrome-conjugated antibodies have been added, the bead pellet dissolves, resulting in the release of a fixed number of beads. The absolute number of cells is then determined by comparing bead events to cellular events.

Two sets of cocktails were separately prepared in Eppendorf tubes (Hamburg, Germany) labeled as cocktail 1 (pDC) and 2 (mDC). Both of these contained the mAbs HLA-DR Allophycocyanin (APC), CD45 Peridinin Chlorophyll Protein (PerCP) and LIN1 Fluorescein isothiocyanate (FITC), while the CD123 Phycoerythrin (PE) and CD11c PE mAbs was added to cocktail 1 and cocktail 2, respectively. All antibodies were used according to the manufacturers' recommendations (during the course of the study titration of mAbs was introduced which aids in determining the optimal volume to use in an assay as the manufacturer

recommended volume may be an overestimate. mAb titrations were applied to the assays performed in chapters 4 and 5). Whole blood (100 µl), followed by cocktail 1, was carefully and without touching the bead pellet, aspirated above the metal retainer of a BD TruCOUNT™ tube (BD Biosciences, San Jose, CA). The sample was gently vortexed and incubated for 15 min in the dark at room temperature. Afterwards, the red blood cells were lysed and leukocytes fixed with 900 µl of 1x BD FACS Lysing solution (BD Biosciences, San Jose, CA) for 10 min at room temperature. The same staining procedure was followed for cocktail 2. Experimental staining controls such as Fluorescence Minus One (FMO), which aids in defining true positive events from a complex marker staining profile (cases where positive and negative marker expression cannot be clearly defined), was not required as the populations of interest were clearly identifiable upon analyses post staining. The samples were immediately acquired on a BD FACSCalibur™ 4-colour flow cytometer (BD Biosciences, San Jose, CA). Approximately 100 000 total events were acquired with a specific threshold set on the FL3 (PerCP) detector to exclude negative events and debris. Refer to Appendix A for the configuration of the BD FACSCalibur™ 4-colour flow cytometer (BD Biosciences, San Jose, CA) utilised in this part of the study.

3.3.5 Flow cytometric analyses: Gating strategy to identify DC subset and bead events

The identification of beads, pDC and mDC events was performed via a specific gating strategy designed using the BD CellQuest™ Pro software (BD Biosciences, San Jose, CA). The graphical representation of events as seen in Figures 3.1 and 3.2 was generated using the BD FACSDiva™ software v6.1.3 (BD Biosciences, San Jose, CA) utilised for its automated hierarchical gating function which is not a defined option of the BD CellQuest™ Pro software. Bead events were identified and gated from a PE Fluorescence (FL) 2 vs. FITC FL1 density plot in which all events were displayed (Figure 3.1). In identification of the blood DCs, firstly, a polygon gate, designated as population (P)1, was drawn to include the monocyte and lymphocyte population in a Side Scatter (SSC) vs. CD45 density plot (Figure 3.2: A1 (pDCs), B1 (mDCs)). This broad gate was drawn to ensure maximum collection of the DC population which granular properties places it in the region between that of the monocyte and lymphocyte events on a SSC scale. The P1 population was then displayed in a HLA-DR vs. LIN1 density plot and a P2 gate collected $LIN1^{DIM}$ as well as both $HLA\text{-}DR^{+}$ and $HLA\text{-}DR^{-}$ events (referred to as $HLA\text{-}DR\_LIN1^{DIM}$ events) (Figure 3.2: A2 (pDCs), B2 (mDCs)) (markers with either "+", "DIM" or "-"superscriptrefers to their expression as bright positive, intermediate intensity or extremely low/absent, respectively). In effect, DCs are characteristically positive for HLA-DR expression and the reason for the broad P2 gate was to ensure that DCs with a lower range of HLA-DR expression was also included during gating of events. Events in the P2 gate was displayed in HLA-DR vs.CD123 density plot and the pDC population identified as $HLA\text{-}DR^{+}CD123^{+}$ and collected in a P3 gate. Similarly, mDC events were identified as $HLA\text{-}DR^{+}CD11c^{+}$ upon analysis of P2 events in a HLA-DR vs.CD11c density plot and collected in a P4 gate (Figure 3.2: A3 (pDCs) and B3 (mDCs)). The absolute count, cells/µl, of pDCs and mDCs was determined using the following mathematical formula:

$$\frac{\text{nr of gated pDC or mDC events}}{\text{nr of gated bead events}} \times \frac{\text{nr of beads in lyophilised pellet as provided}}{\text{test volume}}$$

Both the absolute number and percentage of gated events, as per standard flow cytometric analysis, for the pDCs and mDCs were determined. Percentage of gated events refers to the fraction of pDCs and mDCs within the $CD45^{+}HLA\text{-}DR\_LIN1^{DIM}$ events and fraction of CD4 and CD8 T lymphocytes within the $CD45^{+}CD3^{+}$ population.

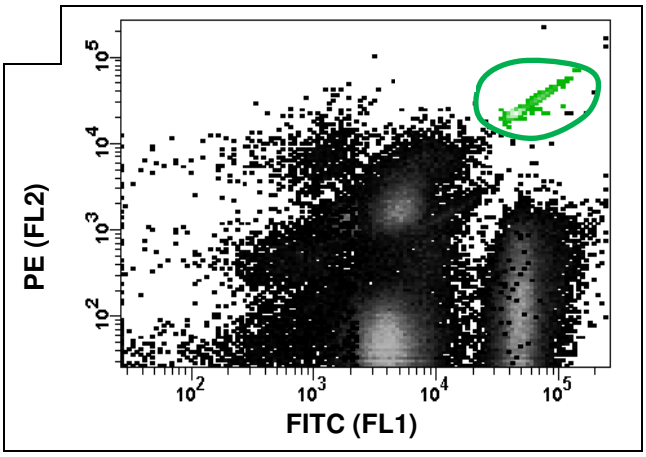

Figure 3.1: Collecting bead events to determine absolute cell counts

Bead events (green-coloured events) required to determine absolute pDC and mDC events in cells/µl were collected from a PE (FL2) vs. FITC (FL1) density plot displaying all events

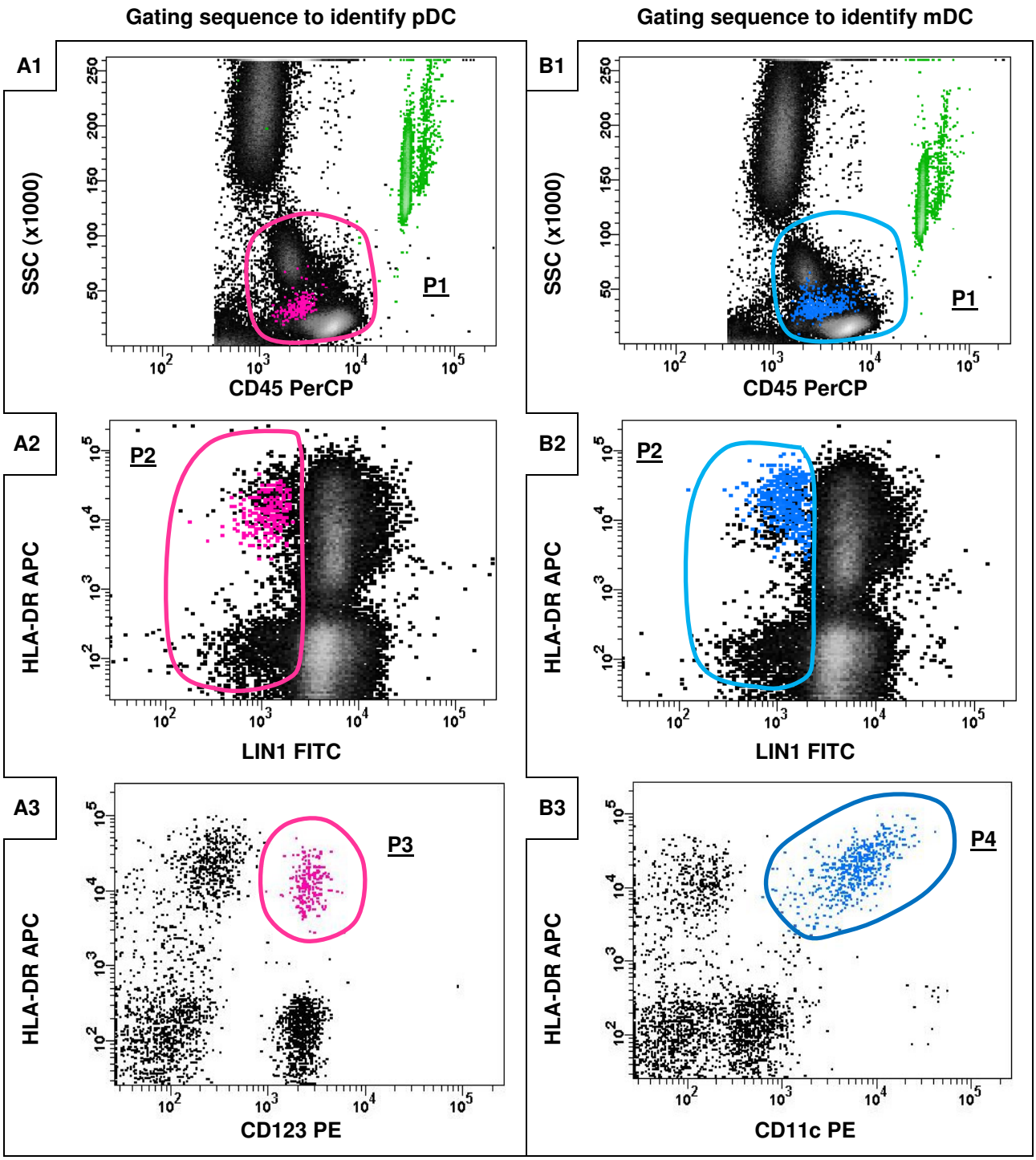

Figure 3.2: Gating strategy to identify DCs from total acquired flow cytometric events

A broad gate (P1) was used to select the lymphocyte and monocyte events in a SSC vs. CD45 density plot (A1: pDCs, B1: mDCs).The broad gate ensured maximum collection of pDCs (pink-coloured events) and mDCs (blue-coloured events) located, based on their unique granular properties, between the lymphocyte and monocyte events on a SSC scale. P1 events were displayed in a HLA-DR vs. LIN1 density plot and a P2 polygon gate collected the HLA-DR_LIN1^{DIM}events (A2: pDCs, B2: mDCs). P2 events were then analysed in HLA-DR vs. CD123 (A3: pDCs) and CD11c (B3: mDCs) density plot to collect the pDC (P3) and mDC (P4) events, respectively.

3.3.6 Procedure for determining CD4 and CD8 T lymphocyte counts from whole blood

The absolute numbers of CD4 and CD8 T lymphocytes were determined by staining 50µl whole blood with the BD MultiTEST™ CD3 FITC, CD8 PE, CD45 PerCP, CD4 APC mAb cocktail in BD TruCOUNT™ tubes according to the manufacturer's recommendations (BD Biosciences, San Jose, CA). Red blood cells were then lysed for 10 minutes (min) with 450µl of BD FACS lysing solution (BD Biosciences, San Jose, CA). The sample was immediately acquired using a BD FACSCalibur™ 4 colour flow cytometer (BD Biosciences, San Jose, CA) and analyzed using the BD MultiSET™ V1.1.2 software (BD Biosciences, San Jose, CA) which automatically determines the absolute number of CD4 and CD8 T lymphocyte in the sample. In addition, the software also defines the CD4:CD8 ratio as well as CD4 and CD8 T lymphocytes as a percentage of the $CD45^{+}CD3^{+}$ population. Routine quality control included daily preparation of a standardised blood sample of LymphoSure (Synexa Life Sciences, South Africa) and quarterly use of an external control (National External Quality Assessment Service (NEQAS)) from the NHLS. The CD4 and CD8 T lymphocyte count assay performed has been accredited by the South African National Accreditation System (SANAS).

3.3.7 Assay for viral load quantification

Viral load testing is performed as a routine assay by the SANAS accredited diagnostic laboratories of the Division of Medical Virology, Stellenbosch University and National Health Laboratory Services (NHLS). Plasma samples from HIV-1 infected patients were prepared by centrifuging whole blood, obtained in EDTA vacutainer tubes (BD Biosciences, San Jose, CA), for 10 min at 800 x g (Hettich Rotanta 460R benchtop centrifuge, Massachussets, USA). A volume of 1ml plasma was collected for viral load testing and the remaining plasma stored in labeled cryovials at -80°C. Multiple platforms were involved in detecting the viral load during the study. Initially, the bioMérieux NucliSens EasyQ® HIV-1 v1.2 test, which expressed the viral load as IU/ml (IU-international units), was used and later the updated v2.0 version, which expressed the viral load as RNA copies/ml. Conversion of 1 copy = 1 IU was confirmed by the supplier's memorandum (Scott LE, *et al*. 2009). Limit of detection (LOD) for this assay using 1 ml plasma input was estimated at 25 RNA copies/ml. This viral load detection system was later replaced by the ABBOTT Real Time HIV-1 PCR assay (ABBOTT m2000rt) which also expressed the viral load as RNA copies/ml. TheLOD for this assay using 1ml plasma input was estimated at 40 RNA copies/ml.

3.3.8 Statistical analyses

Comparative analyses of the absolute number of CD4 and CD8 T lymphocytes, pDCs and mDCs were performed as follows:

- **to assess HIV-1 infection (mono and TB dual infection),** the ARV^-HIV-1 and ARV^-HIV-1/TB study groups were compared to the control study group. The one-way ANOVA non-parametric Kruskal-Wallis test with pairwise comparison to the control group using the Dunns multiple comparison post-test was applied;
- **to assess probable immune reconstitution during HIV-1 infection (mono and TB dual infection):** the ARV^+HIV-1 and ARV^+HIV-1/TB study groups were compared to the control study group. The one-way ANOVA non-parametric Kruskal-Wallis test with pairwise comparison to the control group using the Dunns multiple comparison post-test was applied;
- **to assess the impact of ARV treatment:** the ARV^+HIV-1 and ARV^+HIV-1/TB study groups were compared to the ARV^-HIV-1 and ARV^-HIV-1/TB study groups, respectively. The non-parametric two tailed Mann-Whitney t test was applied;
- **to assess the impact of TB co-infection:** the ARV^-HIV-1/TB study group was compared to the ARV^-HIV-1 study group. The non-parametric two tailed Mann-Whitney t test was applied.

Similar data analyses were performed with data representing CD4 and CD8 T lymphocytes as a percentage of $CD45^+CD3^+$ cells and pDCs and mDCs as a percentage of $CD45^+$HLA-DR_$LIN1^{DIM}$events. This was performed to determine whether the frequency distribution as determined by absolute count is comparable to percentage data.

Correlation analyses were performed as follows:

- **to assess disease severity and progression:** the relationship of pDC and mDC counts to CD4 and CD8 T lymphocyte counts was determined for the control, combined ARV^-HIV-1 study group (ARV^-HIV-1 and ARV^-HIV-1/TB study groups) and combined ARV^+HIV-1 study group (ARV^+HIV-1 and ARV^+HIV-1/TB study groups). Also, the relationship of DCs to viral load was determined for the combined ARV^-HIV-1 study groups. Correlation measurements were performed using the non-parametric Spearman test in which the correlation coefficient (r) was used to determine the type of relationship (direct, indirect or none) and t-statistics (p) the significance thereof.

These tests were performed using the Graphpad Prism version 5.00 software (San Diego, California, USA). Refer to Table 3. 4 for the summary of the method used to report significant and non-significant data as well as the corresponding p value range.

Table 3.4: Summary of the method used to report significant and non-significant data as well as the corresponding p value range

The software used to determine statistical significance report p value from the ANOVA test as indicated in the table below while the t-test reports exact numbers.

Method	Definition	p value
***	Extremely significant	≤ 0.001
**	Very significant	≤ 0.01
*	Significant	≤ 0.05
ns	Not significant	>0.05

3.4 Results and Discussion

3.4.1 Frequency distribution of CD4 and CD8 T lymphocytes, pDCs and mDCs in the peripheral blood of the control and HIV-1 related study groups

Number of pDCs, mDCs and CD4 T lymphocytes in peripheral blood is similar between HIV-1 untreated and HIV-1/TB co-infected patients, but reduced in comparison with uninfected patients

Similar to the reports of others, we found a significant decline in CD4 T lymphocyte, pDC and mDC numbers in peripheral blood during chronic HIV-1 infection. Compared to the control study group, the ARV^{-}HIV-1 study group showed a reduction (determined as the percentage change in absolute number from the reference study group) of 80% ($p \leq 0.001$), 63% ($p \leq 0.001$) and 31% ($p \leq 0.01$) in the median CD4 T lymphocyte, pDC and mDC numbers, respectively. A similar profile was observed with the ARV^{+}HIV-1 study group with a reduction of 80% ($p \leq 0.001$), 66% ($p \leq 0.001$) and 35% ($p \leq 0.01$) in the median CD4 T lymphocyte, pDC and mDC numbers when compared to the control study group, respectively.(Refer to Table 3.5; Figure 3.3 A, C and D, respectively). The blood cell number data of the ARV^{-}HIV-1 and ARV^{-}HIV-1/TB study groups was comparable even though the study participants of the latter group were on TB treatment at the time of blood collection. Notably, the TB participants enrolled were within the first term of anti-TB treatment with a strong likelihood of a TB infection persisting (median time on anti-TB therapy: 1 month (Table 3.2)). Hence, the data suggested that a TB dual infection does not significantly exacerbate cell number loss during HIV-1 infection.

The literature also reports on the loss of blood DCs during HIV-1 infection. Both pDC and mDC median numbers during HIV-1 infection, as determined by Barron MA, *et al.* (2003), were found to circulate at a reduced rate of 50% compared to the control. According to numbers defined by Donaghy H, *et al.* (2001), the median number loss of pDCs and mDCs was estimated at 67% and 82%, respectively. Similarly, the median pDC and mDC numbers reported by Mojumdar K, *et al.* (2010) showed a decline of 69% and 79%, respectively. The level of signature CD4 T lymphocyte decline during HIV-1 infection as reported by Messele T, *et al.* (1999) accounted for a median loss of 43%. The reported data of Moir S, *et al.* (2010) revealed a 47% and 71% decline in median CD4 T lymphocytes during acute and chronic HIV-1 infection, respectively. The median CD4 T lymphocyte numbers as reported by Rodriques DSS, *et al.* (2003) converted to a loss of greater than 80% in both the HIV-1 and HIV-1/TB co-infected study groups investigated. As with the current study, the authors did not observe a statistical difference between these study groups. In contrast, another study observed that the level of decline in CD4 T lymphocytes between the HIV-1 and HIV-1/TB study group was significant. However, the HIV-1/TB cohort of this study comprised of a very small number of participants (n=6) which may have affected the statistical estimates (Pitabut N, *et al.* 2013).

Notably, a decline in the number of pDCs and mDCs in peripheral blood has also been observed in other viral infections such as Hepatitis C (Longman RS, *et al.* 2005; Kanto T, *et al.* 2004) and dengue virus (De Carvalho Bittencourt M, *et al.* 2012) as well as parasitic associated infections such as Malaria (Pinzon-Charry A, *et al.* 2013). This may be suggestive of DC decline not being HIV-1 specific but rather a normal consequence of infection.

Number of CD8 T lymphocytes in peripheral blood is similar between HIV-1 untreated and HIV-1/TB co-infected patients, but significantly higher in comparison with uninfected patients

Parallel to the number loss of CD4 T lymphocytes, pDCs and mDCs during HIV-1 infection, significantly higher CD8 T lymphocyte numbers were observed in the ARV$^-$HIV-1 and ARV$^-$HIV-1/TB study groups. Notably, the absolute CD8 T lymphocyte numbers in peripheral blood during HIV-1 infection was not as severely altered as the CD4 T lymphocyte numbers. Compared to the control, a significant 46**%** ($p \leq 0.05$) and 40% ($p \leq 0.01$) higher median CD8 T lymphocyte number was observed in the ARV$^-$HIV-1 and the ARV$^-$ HIV-1/TB study group, respectively (Table 3.5; Figure 3.3 B). Higher numbers of CD8 T lymphocytes during HIV-1 infection have also been reported by others. The absolute numbers as reported by Messele T, *et al.* (1999) showed a 57% increase in the CD8 T lymphocyte subset whereas the data of Moir S, *et al.* (2010) showed a 64% increase in both early and chronic HIV-1 infection. As with CD4 T lymphocytes, pDCs and mDCs, a significant change in CD8 T lymphocyte number between the ARV$^-$HIV-1 and ARV$^-$HIV-1/TB study groups was also not observed which may indicate that HIV-1/TB co-infection does not affect CD8 T cell numbers more profoundly than an HIV-1 mono infection.

ARV associated recovery/restoration of CD4 T lymphocytes in peripheral blood was not mirrored by DC subsets

Although ARVs are effective at controlling viral replication and are largely reparative (at the CD4 T lymphocyte level) they do not fully restore the immune status to pre-infection levels. Comparing the CD4 T lymphocyte number distribution between the control and ARV$^-$HIV-1 study group, for treatment to effectively restore CD4 T lymphocyte numbers (in other words replenish the reported 80% loss observed in the ARV$^-$ HIV-1 study group), an approximate 4 fold gain in median CD4 T lymphocyte count would be required. Nonetheless, by comparing the CD4 T lymphocyte count of the ARV$^+$HIV-1 to ARV$^-$HIV-1 and ARV$^+$HIV-1/TB to ARV$^-$HIV-1/TB study groups we observed that current ARV therapy was able to induce a 89% ($p \leq 0.01$) and 63% ($p \leq 0.01$) gain in median CD4 T lymphocyte numbers, respectively. Although, the increase in CD4 T lymphocyte number was statistically significant, the gain was nowhere sufficient to completely restore the CD4 T lymphocyte compartment during HIV-1 infection and, compared to the control study group, adjusted median numbers were still 61**%** ($p \leq 0.001$) and 67**%** ($p \leq 0.001$) lower in the ARV$^+$HIV-1 and ARV$^+$HIV-1/TB study group, respectively (refer to Table 3.5; Figure 3.3 A). Notably, the median time on ARV therapy for the ARV$^+$HIV-1 and ARV$^+$HIV-1/TB study groups was 9 and 15 months, respectively (refer to Table 3.2). This finding showed that an approximate 1 year ARV treatment period seemed insufficient for the complete restoration of the immune system. It was also proposed that the observed slow rate/level of restoration may also be dependent on the CD4 T lymphocyte number at time of initiation of therapy - with low CD4 T lymphocyte numbers associated with slow rate of restoration.

Despite relatively successful CD4 restoration on ARVs, no significant recovery of pDC and mDC numbers was detected in the ARV$^+$HIV-1 and ARV$^+$HIV-1/TB study groups. Similar to the ARV untreated groups and compared to the control there were 51**%** ($p \leq 0.01$) and 70**%** ($p \leq 0.001$) lower median pDC numbers and 22**%** ($p \leq 0.05$) and 36**%** ($p \leq 0.01$) lower median mDC numbers in ARV$^+$HIV-1 and ARV$^+$HIV-1/TB study groups, respectively. Although pDC and mDC numbers did not normalise during ARV therapy, we did observe a slightly higher (although not statistically significant) number of pDCs and mDCs in the ARV$^+$HIV-1

compared to the ARV$^-$HIV-1 study group, but not in the ARV$^+$HIV-1/TB compared to the ARV$^-$HIV-1/TB study group (refer to Table 3.5; Figure 3.3 C and D, respectively).

Collectively, these cross-sectional findings indicated that short-term (<15 months) ARV treatment contributes to a partial but significant recovery in CD4 T lymphocyte and a low insignificant (ARV$^+$HIV-1 study group) or absent (ARV$^+$HIV-1/TB study group) recovery of the blood DC population during ARV$^+$HIV-1 and ARV$^+$HIV-1/TB infection, respectively. Although we observed recovery in CD4 T lymphocyte numbers during ARV therapy, the lack of recovery in DC numbers seem to indicate the sensitivity of these cells to HIV-1 associated changes such as persistent immune activation. If this should be the case then in view of a report by Vinikoor MJ, *et al.* (2013) showing that immune activation persists even during ARV therapy, it was proposed that peripheral blood number recovery of DCs rather than CD4 T lymphocytes might be a better predictor of effective treatment regimens. In clear contrast to the cell number changes, ARV therapy was, as expected, effective in controlling the viral load. The median ARV treatment period of participants in the ARV$^+$HIV-1 and ARV$^+$HIV-1/TB study group was 9 and 15 months (refer to Table 3.2), respectively, and most participants had a very low or undetectable HIV-1 viral load reading (refer to Table 3.5). In agreement with the ARV associated findings of the current study, Barron MA, *et al.* (2003) and Pacanowski J, *et al.* (2001) also showed that 6-12 months of HAART leads to an increase in CD4 T lymphocytes numbers and a decline in viral load which is accompanied by lack of recovery of both DC subsets. Another study showed also no recovery in blood DC numbers after 1-2 years of HAART (Lichtner M, *et al.* 2008).

ARV therapy was more efficient in normalizing the CD8 than CD4 T lymphocyte numbers. The CD8 T lymphocyte numbers in the ARV$^+$HIV-1 and ARV$^+$HIV-1/TB study groups were reduced to levels similar to that of the control (median time on ARV treatment 9 and 15 months, respectively (refer to Table 3.2)). Hence, ARV therapy seemingly contributes towards restoring the CD8 T lymphocyte numbers observed during HIV-1 infection (refer to Table 3.5; Figure 3.3 B). As CD8 T lymphocytes are pivotal in the control of viral infections, including HIV-1, it is anticipated that controlling viral replication via ARV therapy would/should lead to decreased CD8 numbers, if no other infection or condition is present. Jiao Y, *et al.* (2011) observed a decline in CD8 T lymphocyte count already 3 months after the initiation of ARV therapy, however, Almeida M, *et al.* (2006) reported on the lack of CD8 T lymphocytes number recovery after 1 year of therapy.

Table 3.5: Summary of the CD4 T and CD8 T lymphocytes, pDCs and mDCs absolute numbers; CD4:CD8 ratio and viral load (as applicable) of the control, HIV-1 and HIV-1-related study groups.

Study groups						
		Control	**ARV$^-$ HIV-1**	**ARV$^-$HIV-1/TB**	**ARV$^+$HIV-1**	**ARV$^+$HIV-1/TB**
CD4 T cells	**Me^a**	830	169	166	320	271
	R^a	392 – 1534	11 – 387	7 - 304	131 - 786	56 - 703
	Me^b	41	12	10	22.5	17
	R^b	29 - 53	2 - 22	1 - 15	9 - 38	5 - 31
CD8 T cells	**Me^a**	580	848	814	657	748
	R^a	125 - 1141	378 - 1535	289 - 2135	300 - 2194	236 - 2767
	Me^b	29.50	60	64	48	49
	R^b	12 - 46	43 - 84	55 - 81	25 - 78	38 - 85
CD4:CD8 ratio	**Me^c**	1.48	0.19	0.17	0.47	0.35
	R^c	0.76-4.45	0.02-0.49	0.01-0.25	0.11-1.52	0.06-0.75
pDC	**Me^d**	8.84	3.25	2.99	4.34	2.63
	R^d	2.83 - 14.39	0.92 - 7.51	0.65 - 8.39	1.44 - 10.13	1.36 - 13.18
	Me^e	3.64	1.3	1.04	1.19	1.05
	R^e	0.68 - 10.15	0.14 - 6.9	0.19 - 6.24	0.12 - 4.82	0.23 - 2.47
mDC	**Me^d**	14.78	10.19	9.61	11.47	9.52
	R^d	8.3 - 34.19	5.21 -17.74	1.38 - 23.12	4.97 - 23.71	3.76 - 24.07
	Me^e	7.47	4.53	4.96	4.25	3.62
	R^e	3.63 - 14.97	0.97 - 10.84	0.66 - 14.51	1.05 - 16.19	0.9 - 7.89
Viral load	**Me^f**	NA	3.4 x10^4	4,1 x10^4	LOD	LOD
	R^f		230 – 4 x10^6	240 – 7 x10^5	LOD – 1.7 x10^3	LOD - 1.6 x10^3

Data indicated as

Me^a *= Median cells/µl,*

R^a *= Range cells/µl,*

Me^b *= Median % of CD45$^+$CD3$^+$ events,*

R^b *=Range % of CD45$^+$CD3$^+$ events,*

Me^c *= Median ratio of CD4 Lymphocyte absolute number to CD8 T lymphocyte absolute number*

R^c *=Range of CD4:CD8 ratio*

Me^d *= Median x10^3cells/ml,*

R^d *=Range x10^3cells/ml,*

Me^e *= Median % of CD45$^+$HLA-DR_LIN1^{DIM}events,*

R^e *=Range % of CD45$^+$HLA-DR_LIN1^{DIM}events,*

Me^f *= Median RNA copies/ml,*

R^f *= Range RNA copies/ml*

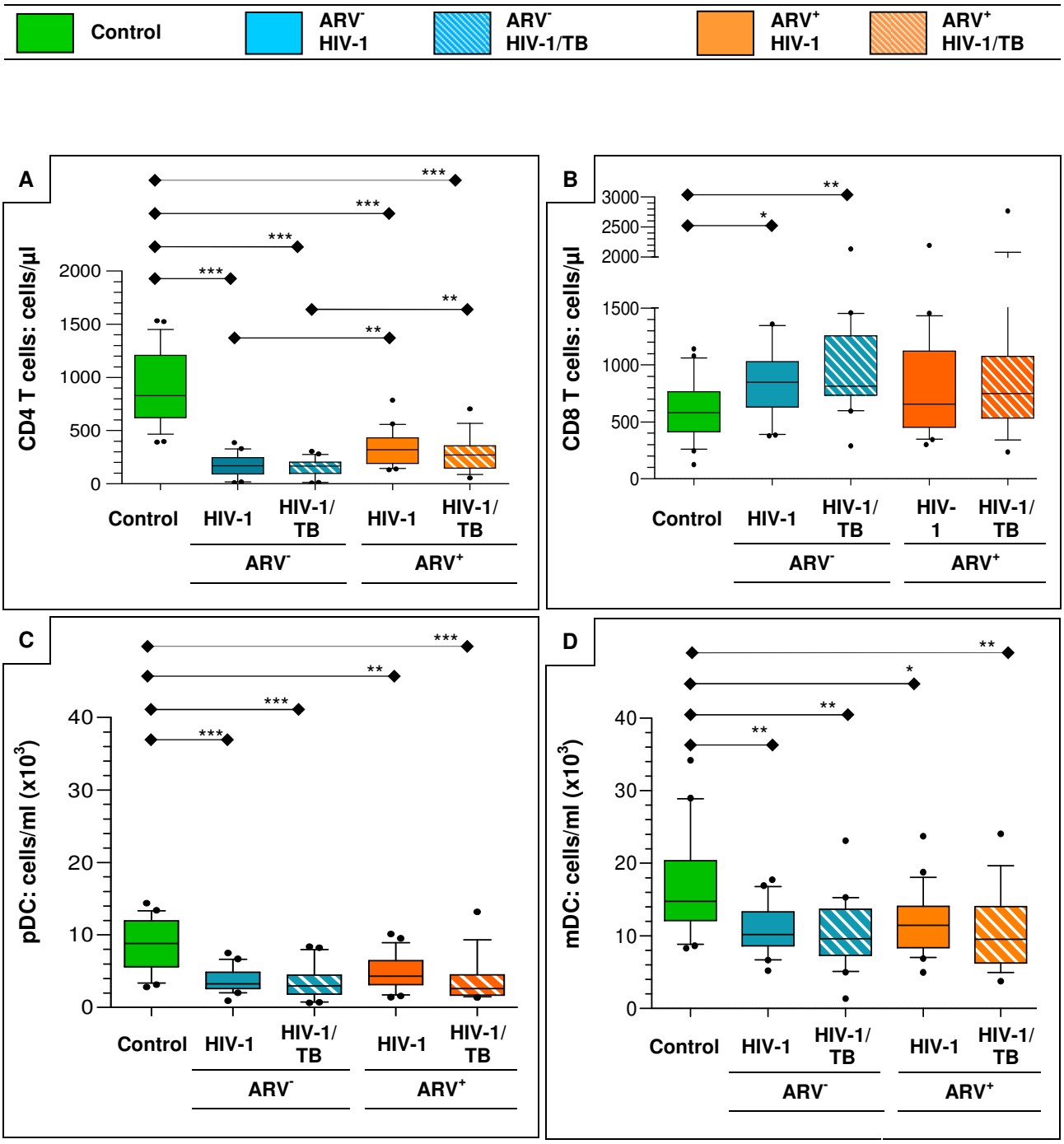

Figure 3.3: Changes in absolute number of CD4 and CD8 T lymphocytes, pDCs and mDCs during ARV untreated and treated HIV-1 mono and HIV-1/TB co-infection

Peripheral whole blood was stained with the BD MultiTEST™ reagent (CD3, CD8, CD45 and CD4 mAb cocktail) to determine the absolute count (cells/µl) of CD4 and CD8 T lymphocytes. Similarly, staining with DCID markers (HLA-DR, LIN1, CD123/CD11c mAb cocktail) aided in determining the absolute count (cells/ml) of pDCs and mDCs. Analyses were performed using the BD TruCOUNT™ assay and 4-colour flow cytometry. The box and whiskers graph represents the absolute number of CD4 T lymphocytes (A), CD8 T lymphocytes (B), pDCs (C) and mDCs (D), respectively, of the control, ARV⁻ HIV-1, ARV⁻ HIV-1/TB, ARV⁺ HIV-1 and ARV⁺ HIV-1/TB study groups.Each boxplot shows the 10-90 percentile range of data and the horizontal line represents the median value. Outliers are represented by black enclosed circles. Horizontal lines with diamond arrows indicate the specific study group comparison of interest and an asterisk(s) the significance. Refer to Table 3.4 for a description of the method used to indicate the level of statistical significance.

Absolute number vs. percentage data output

Comparative analysis of the absolute number of CD4 T lymphocytes, pDCs and mDCs revealed very similar trends to the percentage data. Both HIV-1 infection (CD4 and CD8 T lymphocytes and DC subsets) and ARV therapy (CD4 T lymphocytes) significantly altered absolute numbers which also reflected in the percentage data (refer to Figures 3.3 A-D vs. 3.4 A-D). However, assessing immune recovery and the impact of ARV therapy and TB co-infection on CD8 T lymphocytes we found no significant difference in comparing relevant study groups using absolute CD8 T lymphocyte number data, while a different profile was observed with percentage data. Median cell number data indicated a trend towards normalisation of CD8 T lymphocytes whereas lack of immune recovery was observed with percentage data (ARV^{+}HIV-1 ($p \leq 0.001$) and ARV^{+}HIV-1/TB ($p \leq 0.001$) study group vs. control study group) (Figures 3.3 B vs. 3.4 B). More specifically, ARV therapy did show a significant reduction in the percentage CD8 T lymphocytes but it was not sufficient to induce full restoration (ARV^{+}HIV-1 vs. ARV^{-}HIV-1 ($p \leq 0.01$) and ARV^{+}HIV-1/TB vs. ARV^{-}HIV-1/TB ($p \leq 0.01$)). TB co-infection seemed to induce a significantly higher percentage of CD8 T lymphocytes in peripheral blood compared to HIV-1 mono infection (HIV-1/TB vs. HIV-1; $p \leq 0.05$; refer to Table 3.5; Figure 3.4 B).

The distribution pattern of the percentage pDC and mDC data was similar to that of the absolute number of pDCs and mDCs during HIV-1 infection. Expressed as a fraction of $CD45^{+}$HLA-DR_$LIN1^{DIM}$ events, percentage pDCs and mDCs was found significantly lower in the ARV^{-}HIV-1 study groups (pDCs: $p \leq 0.01$, mDCs: $p \leq 0.05$), ARV^{-}HIV-1/TB study groups (pDCs: $p \leq 0.001$, mDCs: $p \leq 0.05$) as well as the ARV^{+}HIV-1 study groups (pDCs: $p \leq 0.01$, mDCs: $p \leq 0.01$) and ARV^{+}HIV-1/TB study groups (pDCs: $p \leq 0.001$, mDCs $p \leq 0.001$) when compared to the control study group. The lack of recovery during ARV therapy was also observed as similar pDC and mDC percentages between the ARV^{+}HIV-1 study group and ARV^{-}HIV-1 study group as well as the ARV^{+}HIV-1/TB study group and ARV^{-}HIV-1/TB study group was observed (Figure 3.4 C (pDCs) and D (mDCs)).

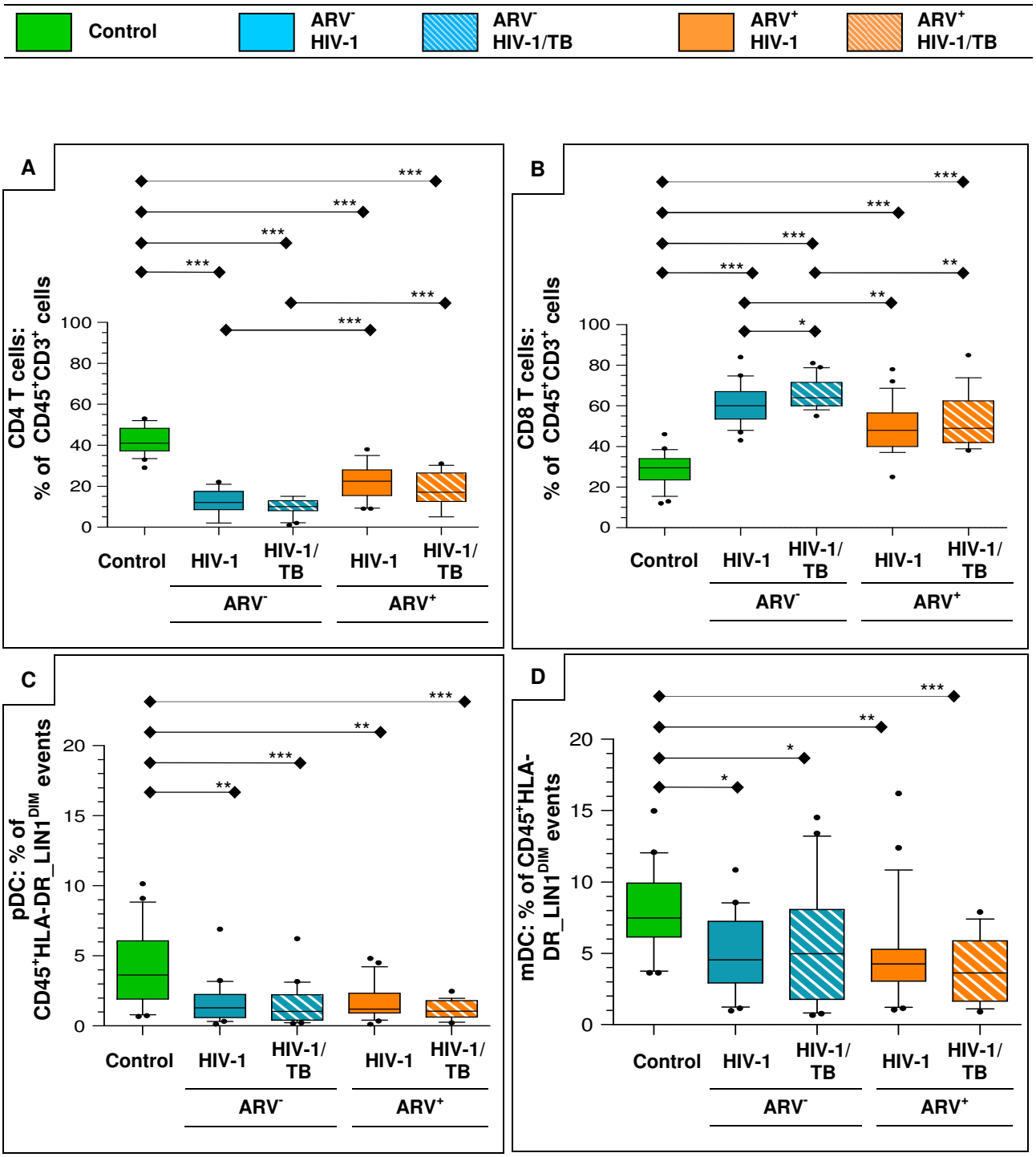

Figure 3.4: Changes in percentage CD4 T and CD8 T lymphocyte, pDCs and mDCs during ARV untreated and treated HIV-1 mono and HIV-1/TB co-infection

Peripheral whole blood was stained with the BD MultiTEST™ reagent (CD3, CD8, CD45, CD4 mAb cocktail) and analysed using 4-colour flow cytometry to determine CD4 and CD8 T lymphocytes as a percentage of $CD45^+CD3^+$cells. Similarly, staining with DCID markers (HLA-DR, LIN1, CD123 or CD11c mAb cocktail) was performed to determining pDCs and mDCs as a percentage of $CD45^+$ HLA-DR_$LIN1^{DIM}$events. The box and whiskers graph represents the percentage of CD4 T lymphocytes (A), CD8 T lymphocytes (B), pDCs (C) and mDCs (C) of the control, ARV HIV-1, ARV HIV-1/TB, ARV^+HIV-1 and ARV^+HIV-1/TB study groups. Each boxplot shows the 10-90 percentile range of data and the horizontal line represents the median value. Outliers are represented by black enclosed circles. Horizontal lines with diamond arrows indicate the specific study group comparison of interest and an asterisk(s) the significance. Refer to Table 3.4 for a description of the method used to indicate the level of statistical significance.

CD4:CD8 ratio

The median CD4:CD8 ratio was significantly lower in both the ARV$^-$HIV-1 study group ($p \leq 0.001$) and ARV$^-$ HIV-1/TB study group ($p \leq 0.001$) when compared to that of the control study group. As the CD4:CD8 ratio is a marker of efficient immune status, the observed change during infection is indicative of the poor immunological state of HIV-1 infected individuals. A similar profile was observed when the median CD4:CD8 ratio of the ARV$^+$HIV-1 ($p \leq 0.001$) and ARV$^+$HIV-1/TB ($p \leq 0.001$) study groups were compared to that of the control study group. This was indicative of the lack of immune recovery during ARV therapy. In evaluating the effect of TB co-infection, the study observed a tendency ($p = 0.12$) of lower median CD4:CD8 ratio in the ARV$^-$HIV-1/TB study group when compared to the ARV$^-$HIV-1 study group. The median CD4:CD8 ratio was significantly higher in the ARV treated vs. untreated study groups, however, recovery did not reach a level comparable to the control study group (ARV$^+$HIV-1 study group vs. ARV$^-$HIV-1 study group: $p = 0.001$; ARV$^+$HIV-1/TB study group vs. ARV$^-$HIV-1/TB study group; $p = 0.004$) (Figure 3.5).

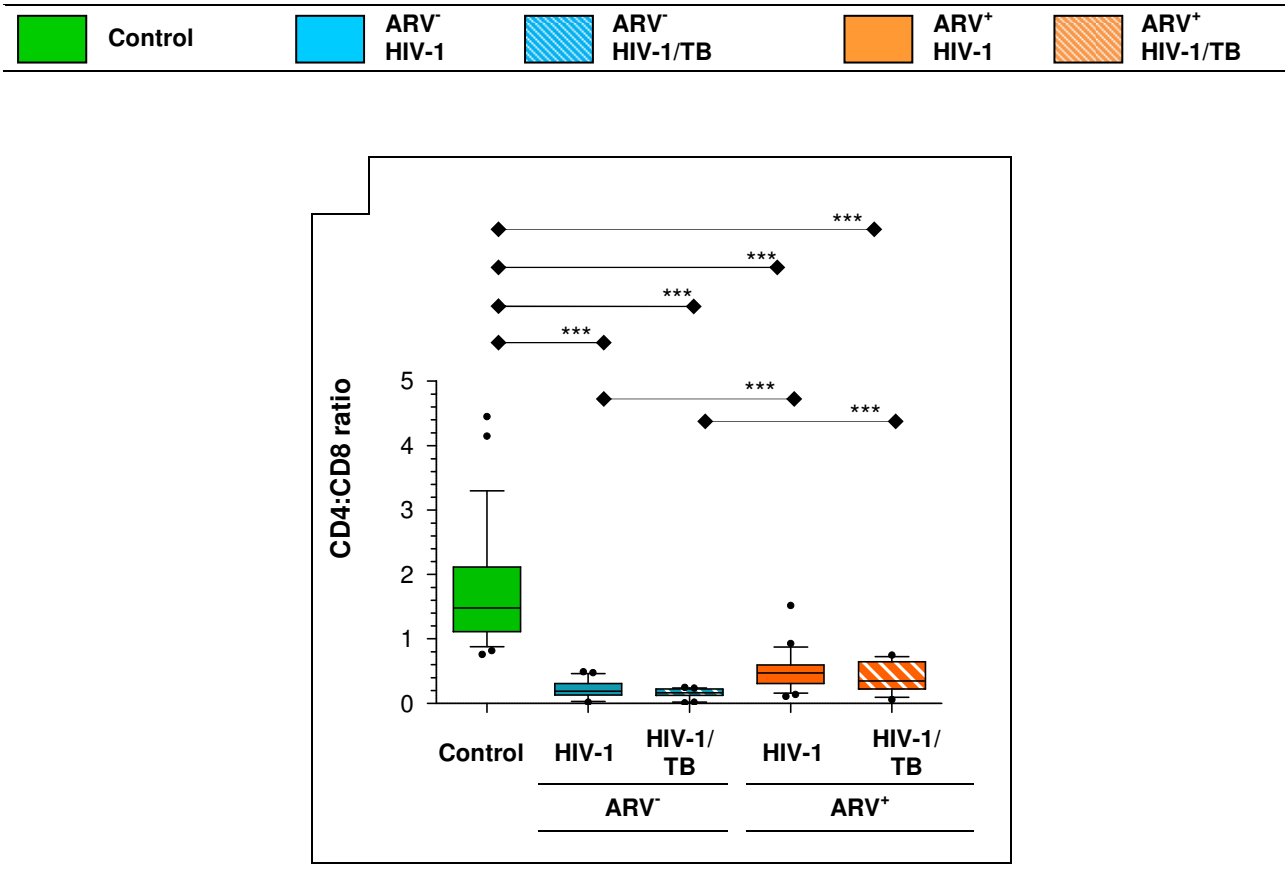

Figure 3.5: Changes in CD4:CD8 ratio during ARV untreated and treated HIV-1 mono and HIV-1/TB co-infection

Peripheral whole blood was stained with the BD MultiTEST™ reagent (CD3, CD8, CD45 and CD4 mAb cocktail) to determine the absolute count (cells/µl) of CD4 and CD8 T lymphocytes. Analyses were performed using the BD TruCOUNT™ assay and 4-colour flow cytometry. The ratio of CD4 T lymphocyte to CD8 T lymphocyte absolute number was determined. The box and whiskers graph represents the CD4:CD8 ratio of the control, ARV$^-$HIV-1, ARV$^-$HIV-1/TB, ARV$^+$HIV-1 and ARV$^+$HIV-1/TB study groups. Each boxplot shows the 10-90 percentile range of data and the horizontal line represents the median value. Outliers are represented by black enclosed circles. Horizontal lines with diamond arrows indicate the specific study group comparison of interest and an asterisk(s) the significance. Refer to Table 3.4 for a description of the method used to indicate the level of statistical significance.

The signature loss of CD4 T lymphocytes

To date, research has not been able to fully elucidate the underlying cause(s)/mechanism(s) of CD4 T lymphocyte depletion. Notably, literature contains an immense amount of data on apoptosis and its association with the depletion of CD4 T lymphocytes during HIV-1 infection. Apoptosis is a controlled form of cell death, crucial for maintaining homeostatic balance in the host. It directs the elimination of activated cells upon clearance of an infection to prevent inflammation associated tissue damage. Furthermore, apoptosis is a "safe" form of cell death as apoptotic cells are phagocytosed – typically, "sealed off" cellular degradation occurs so to limit harmful inflammation. In view of this, it was questioned in which way a highly controlled process seemed to reach a stage of "instability". It has been reported that the aberrant apoptotic events observed during HIV-1 infection appear to be steered by the virus itself. It seems that the virus has the ability to hijack the host's apoptotic machinery, resulting in the uncontrolled demise of CD4 T lymphocytes. Specifically, the apoptotic properties of the HIV proteins Tat, Vpr, Nef, Vpu as well as protease have been defined (as reviewed by Mbita Z, *et al.* 2014). The reason for the virus initiated destruction of its primary "habitat" remains a mystery; though, it has been proposed a tactic of the virus to detain immune effectors (Gougeon ML, 2003).

Adding to the apoptosis-associated decline of CD4 T lymphocytes is the reported disparity between number of productively infected cells and cell number loss. In view of the excessive decline of CD4 T lymphocytes during HIV-1 infection one would assume that it is driven by apoptosis of infected cells – cell suicide to eliminate the virus. However, as the level of productively infected CD4 T lymphocytes (0.1-1%) does not nearly "tally up" to the level of declining CD4 T lymphocyte numbers during HIV-1 infection (Brenchley JM, *et al.*2006; Finkel TH, *et al*. 1995), another mechanism steering the loss of CD4 T lymphocyte is implicated. Notably, numerous studies have shown that HIV pathogenesis was rather driven by the death of non-productively infected CD4 T lymphocyte also referred to as bystander cells (as reviewed by Garg H, *et al.*2012; Finkel TH, *et al*. 1995). Some of these cells, as reported by Doitsh G, *et al.* (2010), are associated with abortive HIV-1 infection, a phenomenon which results in incomplete viral DNA transcripts present in the intracellular matrix. These antigens cause an innate immune response and the activation of death associated proteins. An additional mechanism of CD4 T lymphocyte loss is virus-independent deletion via activation-induced cell death, either intrinsically or extrinsically (death receptor) regulated. These processes are linked to immune activation, which is both a direct and indirect consequence of viral replication. In an attractive report by Doitsh G, *et al.* (2013) it was shown that the demise of bystander CD4 T lymphocytes during HIV-1 infection is particularly steered by a form of cell death referred to as pyroptosis. Notably, this form of cell death is associated with inflammation, and is believed to play a major part in promoting chronic inflammation associated with HIV-1 infection. Specifically, pyroptosis is a programmed cell executioner pathway associated with caspase 1 activity and the release of intracellular contents as well as pro-inflammatory cytokines (such as IL-1β). In contrast, apoptosis is associated with caspase 3 activity and is an immune "silent" form of cell death. By examining tonsil tissue from HIV-1 infected patients Doitsh G, *et al.* (2013) found active caspase 3 in productively infected CD4 T lymphocytes, while caspase 1 was predominantly found in bystander non-productively infected CD4 T lymphocytes. This finding, along with the previous report from this group (2010) in which they showed that bystander CD4 T lymphocytes constituted 95% of the CD4 T lymphocyte population of tonsil tissue of HIV-1 infected patients, illuminated the dominant and destructive role (high rate of cell death and inflammation) of pyroptosis during HIV-1 infection. Furthermore, it greatly

supports the paradigm of inflammation (in addition to cell death) being a strong driving force of HIV-1 disease. In view of their findings Doitsh G and colleagues (2013) proposed a treatment strategy of targeting host-specific events rather than elimination of the virus to treat HIV-1 infection and showed that blocking of pyroptosis could be initiated by caspase 1 inhibitors.

Another mechanism involved in bystander cell death during HIV-1 infection involves the *env* glycoprotein. It is expressed on the surface of infected cell and interacts with CD4 and the co-receptor CXCR4/CCR5 of bystander cells. Receptor/co-receptor binding are the initials steps for the induction of apoptosis, however, bystander apoptosis is also dependant on the process of hemifusion (joining of the outer membrane leaflets of two membranes with no merging of the inner membranes or development of a fusion pore (Chernomordik LV and Kozlov MM, 2005)) driven by the gp41 domain of Env glycoprotein. Joshi A, *et al.* (2011) showed that the degree of CCR5 expression also has an impact and found that with low level of CCR5 expression virus continues with absent bystander cell apoptosis.

As mentioned, chronic immune activation also plays a role in the decline of CD4 T lymphocytes. Chapter 6 describes the significant increase in the percentage $CD8^+$ T lymphocyte subsets expressing the T lymphocyte activation associated antigen, CD38, during HIV-1 infection and also show the significant inverse relationship between the CD4 T lymphocyte counts and percentage $CD8^+CD38^+$ subset.

The lack of cell number recovery during HIV-1 infection

The lack of complete recovery of pDCs, mDCs and CD4 T lymphocytes during ARV therapy could indicate ongoing infection/inflammation which impacts on the cells. This may include 1) persistent viral replication in compartments where the HIV-1 escapes the suppressive effect of ARVs (i.e. reservoirs), 2) ongoing immune activation, 3) gut leakage and/or 4) other secondary infections. In addition, hindrance in revival of pDC, mDC and CD4 T cell numbers in the peripheral blood could be due to a slow rate of replenishment from the bone marrow (DCs) or thymus (T lymphocytes) or irreversible damage caused by the HIV-1 infection. In a study by Zeng M, *et al*. (2012) it was observed that the loss of naïve CD4 T lymphocytes ($CD4^+CD45^+$) correlated with the destruction of the 1) FRC network in the T lymphocyte zone and 2) follicular dendritic cell (FDC) network in the B cell follicle in the lymph nodes of pathogenic SIV infected Rhesus Macaque monkeys. In contrast, intact FDC networks were observed in the non-pathogenic SIV infected sooty mangabeys while having detectable SIV viral load and a stable CD4 T lymphocyte numbers. It should be noted that the maintenance of the FRC and FDC network is reliant on the production of lymphotoxin-β, produced by naïve T lymphocytes (Ngo VN, *et al.* 1999). In return, the survival of naïve T lymphocytes is dependent on the production of IL-7 by the FRC (Link A, *et al*, 2007; Tan JT, *et al*. 2001). Hence, loss of the lymphotoxin-β source results in a dysregulation of FRC and FDC events. This phenomenon may illuminate why immune abnormalities still persist during HIV-1 infection regardless of undetectable viral load. The FRC and FDC damage caused by the HIV-1 may explain the slow rate of CD4 T lymphocytes replenishment in the lymph nodes during ARV therapy. Further research is required to determine whether applicable therapy that aims to recover the FRC and FDC network, would also aid in CD4 T lymphocyte and DC subset number reconstitution.

3.4.2 Relationship of the absolute number of pDCs and mDCs to CD4 and CD8 T lymphocyte count and HIV-1 viral load

Other studies investigating the decline of pDCs and mDCs in peripheral blood of HIV-1 infected patients have found a significant relationship between DC subsets, CD4 T lymphocyte count and viral load. pDCs and mDCs tend to directly correlate with CD4 T lymphocyte numbers while viral load inversely correlated with low CD4 T lymphocyte, pDC and mDC numbers (Mojumdar K, *et al*. 2010; Lichtner M, *et al.* 2008; Finke JS, *et al*. 2004). In the current study, similar to some other studies (Sabado RL, *et al.* 2010; Fontaine J, *et al*. 2009; Diop OM, *et al.* 2008) a significant relationship between the DC numbers, CD4 T lymphocyte counts and viral load during HIV-1 infection and ARV therapy was not observed. We proposed that the overall contrasting findings might be due to the small sample size of the study groups (refer to Table 3.2). As we observed similar frequencies (median and range, Table 3.2) of pDC and mDC counts, CD4 and CD8 T lymphocyte counts and viral load between the ARV^-HIV-1 and ARV^-HIV-1/TB as well as the ARV^+HIV-1 and ARV^+HIV-1/TB study groups, we combined relevant data sets so to increase sample size for correlation statistical analyses. In re-evaluation of the correlation measurements between DC subsets and 1) CD4 T lymphocytes (Figure 3.6A), CD8 T lymphocytes (Figure 3.6B) and viral load (Figure 3.7A) of the combined ARV^-HIV-1 study group (ARV^-HIV-1 and ARV^-HIV-1/TB study groups) and 2) CD4 T lymphocytes (Figure 3.6C) and CD8 T lymphocytes (Figure 3.6D) of the combined ARV^+HIV-1 study group (ARV^+HIV-1 and ARV^+HIV-1/TB study groups), we observed a relationship not much different to what was obtained upon comparing individual study groups. Also, the relationship of CD4 and CD8 T lymphocytes to viral load in the combined ARV^-HIV-1 study group was similar to what was observed in the individual study groups (Figure 3.7B). The lack of significant association may be due to 1) difference in the stage of HIV-1 infection and/or 2) rate of disease progression of individuals comprising the study cohorts investigated. As our study had no specific inclusion/exclusion criteria on disease staging and CD4 T lymphocyte count of HIV-1 infected volunteers at the time of blood collection, the random selection of untreated HIV-1 infected patients (for both HIV-1 mono and TB co-infected) resulted in a cohort with median CD4 T lymphocyte count of less than 200 cells/µl. Therefore patients in later stages of chronic HIV-1 infection were predominant. A longitudinal study, monitoring participants from acute to early and late stage of chronic HIV-1 infection, would provide more clarity on the relationship of the DC subsets to CD4 and CD8 T lymphocyte numbers as well as HIV-1 viral load during HIV-1 infection.

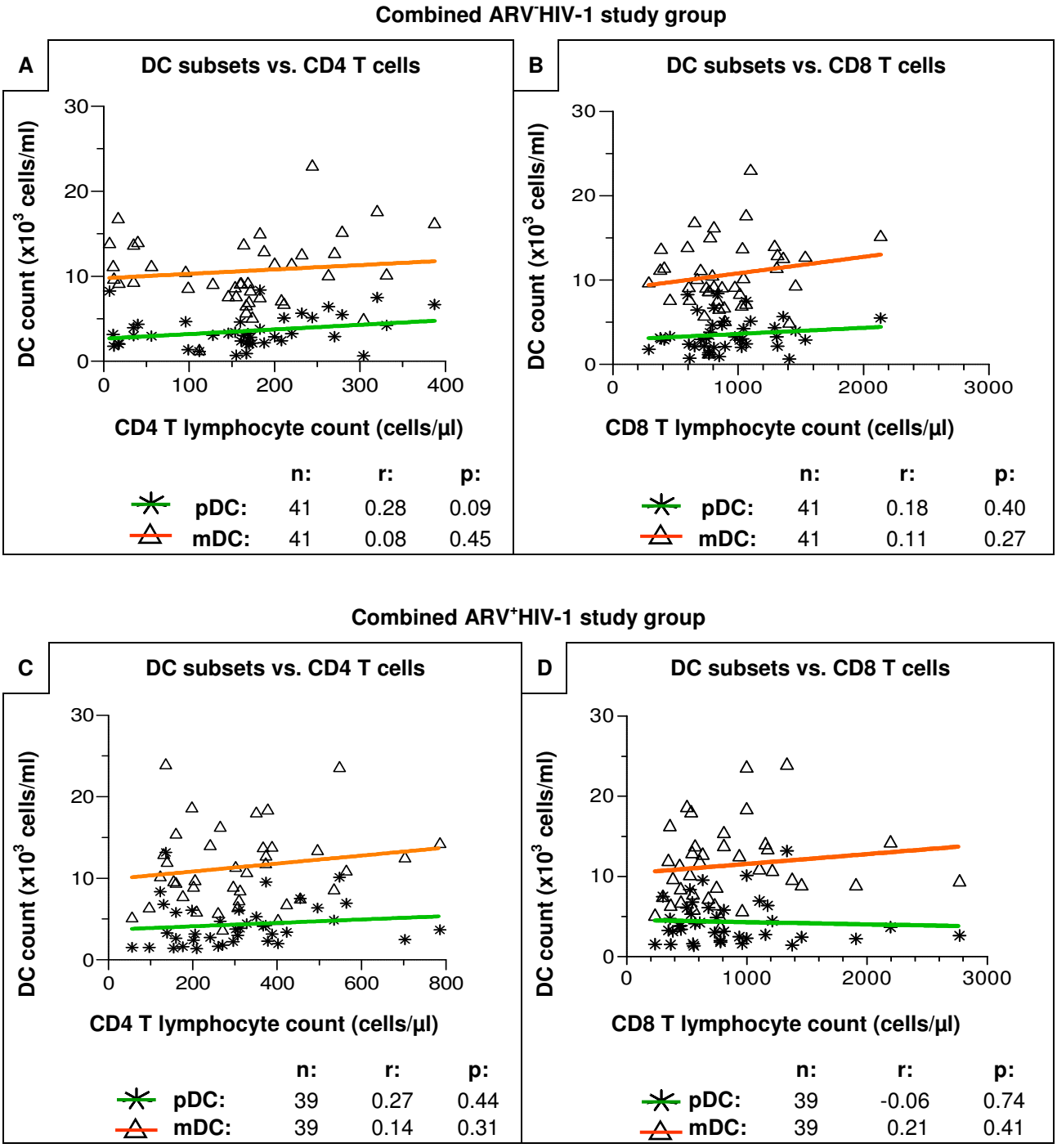

Figure 3.6: Correlating DC numbers to CD4 and CD8 T lymphocyte numbers of the combined ARV⁻ HIV-1 and ARV⁺HIV-1 study groups.

The absolute number of pDCs and mDCs was determined for each of the participants of the combined ARV⁻ *HIV-1 (*ARV⁻*HIV-1 and* ARV⁻*HIV-1/TB) and combined ARV⁺HIV-1 (ARV⁺HIV-1 and ARV⁺HIV-1/TB) study groups and plotted together with its corresponding CD4 and CD8 T lymphocyte counts. The pDC and mDC counts were 1) represented by the symbols ✳ and △, and 2) their relationship to CD4 (A,C) and CD8 T lymphocyte count (B,D) indicated by a green and orange coloured linear regression lines, respectively. The non-parametric Spearman test was use to correlate the absolute number of the DC subsets to that of CD4 and CD8 T lymphocytes.*

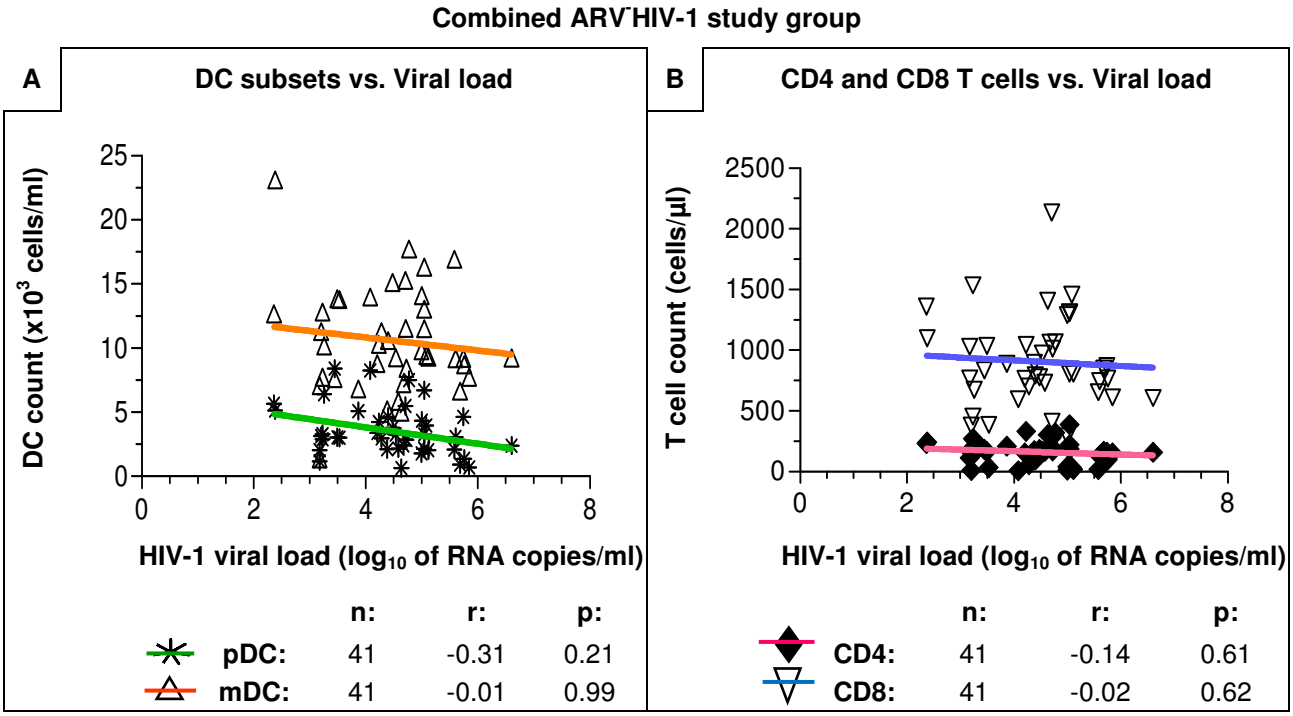

Figure 3.7: Correlating pDC, mDC, CD4 and CD8 T lymphocyte numbers to HIV-1 viral load of the combined ARV⁻HIV-1 study group.

The absolute number of pDCs, mDCs, CD4 and CD8 T lymphocytes was determined for each of the participants of the combined ARV⁻*HIV-1 study group (*ARV⁻*HIV-1 and* ARV⁻*HIV-1/TB) and plotted together with its corresponding viral load. The pDC and mDC numbers were 1) represented by the symbols ✳ and △, and 2) their relationship to viral load indicated by green and orange coloured linear regression lines, respectively (A). The CD4 and CD8 T lymphocyte counts were 1) represented by the symbols ◆ and ▽ and 2) their relationship to HIV-1 viral load indicated by pink and blue coloured linear regression lines, respectively (B). The non-parametric Spearman test was use to correlate the absolute number of CD4 and CD8 T lymphocytes, pDCs and mDCs to viral load.*

However, what was evident from the current study is the disruption in the relationship of mDCs to CD4 and CD8 T lymphocytes during HIV-1 infection. Upon comparing the correlation data of the combined ARV⁻HIV-1 study group to that of the control study group the latter study group showed a direct correlation between mDC and both the CD4 ($p = 0.01$, $r = 0.47$, Figure 3.8A) and CD8 T lymphocytes ($p = 0.004$, $r = 0.67$, Figure 3.8B) which was absent in the combined ARV⁻HIV-1 study group (mDC vs.CD4 T lymphocytes: $p = 0.45$, $r = 0.08$, Figure 3.6A; mDC vs.CD8 T lymphocytes: $p = 0.27$, $r = 0.11$ Figure 3.6B). We also found that the relationship was not restored during ARV therapy as there was no correlation between the mDC and both the CD4 and CD8 T lymphocytes in the combined ARV⁺HIV-1 study group (mDC vs.CD4 T lymphocytes: $p = 0.31$, $r = 0.14$, Figure 3.6C; mDC vs.CD8 T lymphocytes: $p = 0.41$, $r = 0.21$, Figure 3.6D). In contrast to mDCs, there was no relationship between pDCs and both the CD4 and CD8 T lymphocytes of the control study group (pDCs vs CD4 T lymphocytes: $p = 0.69$, $r = 0.1$; pDCs vs. CD8 T lymphocytes $p = 0.28$, $r = 0.3$, Figure 3.8 A and B, respectively). However, a trend towards direct correlation of pDCs to CD4 T lymphocytes was observed in the combined ARV⁻HIV-1 study group (pDCs vs CD4 T lymphocytes: $p = 0.09$, $r = 0.28$, Figure 3.6 A). pDCs showed further no correlation with the CD8 T lymphocyte count of the combined ARV⁻ HIV-1 study group (pDC vs.CD8 T lymphocytes: $p = 0.18$, $r = 0.4$, Figure 3.6B) as well as no correlation with

the CD4 and CD8 T lymphocytes of the combined ARV^{+}HIV-1 study group (pDC vs.CD4 T lymphocytes: p = 0.44, r = 0.27, Figure 3.6C; pDC vs.CD8 T lymphocytes: p = 0.74, r = -0.06, Figure 3.6D).

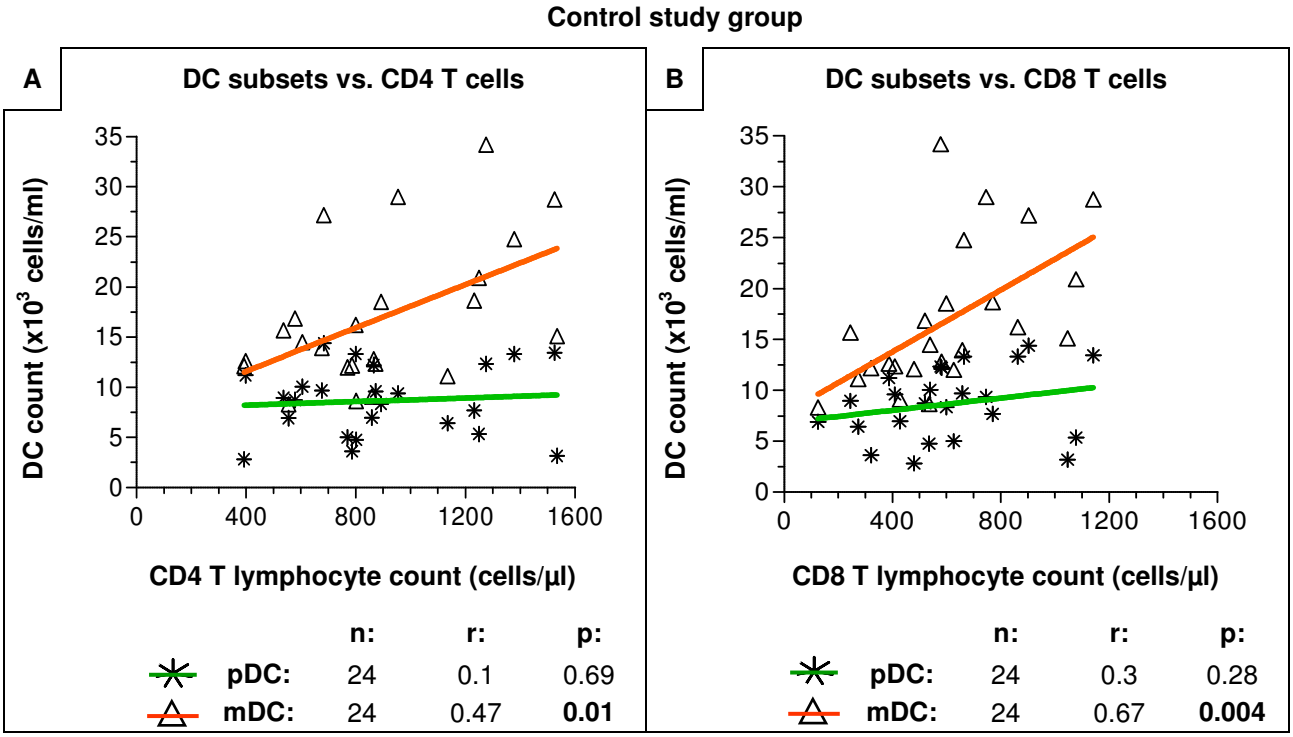

Figure 3.8: Correlating DC numbers to CD4 and CD8 T lymphocyte numbers of the control study group.

The absolute number of pDCs and mDCs was determined for each of the participants of the control study groups and plotted together with its corresponding CD4 and CD8 T lymphocyte count. The pDC and mDC counts were 1) represented by the symbols ✳ and △, and 2) their relationship to CD4 (A) and CD8 T lymphocyte counts (B) indicated by a green and orange coloured linear regression lines, respectively. The non-parametric Spearman test was used to correlate the absolute number of the DC subsets to that of CD4 and CD8 T lymphocytes.

3.5. Conclusion

The decline of CD4 T lymphocyte from the peripheral blood of chronically HIV-1 infected patients is a well described phenomenon, as is the reduction of pDC and mDC numbers (Mojumdar K, *et al*. 2010; Sabado RL *et al*, 2010; Lichtner M, *et* al. 2008; Finke JS, et al. 2004; Soumelis V, et al. 2001). In the current study, enumeration of pDC and mDC numbers in peripheral blood was performed in South African cohorts of uninfected as well as chronically HIV-1 infected and HIV-1/TB co-infected patients on or naïve for ARV therapy. Changes in pDC, mDC, CD4 and CD8 T lymphocyte absolute number as well as CD4:CD8 ratios across the study groups were investigated. In addition, the study also examined the relationship of blood pDCs and mDCs numbers to CD4 and CD8 T lymphocytes counts and viral load. In summary the following was found

1) A significant decrease in both the blood pDC and mDC subsets, with the loss of pDCs being more severe than mDCs during HIV-1 infection.
2) Similar DC cell number distribution during HIV-1 and HIV-1/TB infection, showing that TB co-infection does not *per se* exacerbate depletion of these cells.
3) After 1 year of ARV therapy we found
   3.1) a significant reduction in plasma viral load
   3.2) a significant but partial recovery in CD4 T lymphocyte counts and CD4:CD8 ratio,
   3.3) minimal (insignificant) increase of DC subsets during chronic HIV-1 infection,
   3.4) no recovery in DC subsets during HIV-1/TB co-infection
4) mDCs, but not pDCs, directly correlating with CD4 and CD8 T lymphocytes in healthy controls. However, this relationship was majorly altered in the untreated HIV-1 study group, where the mDCs no longer correlated with CD4 and CD8 T lymphocytes but now pDCs tended to directly correlate with CD4 T lymphocytes. No correlation was observed between both DC subsets and HIV-1 viral load.
5) Frequency distribution of pDCs and mDCs in HIV-1 infection can also be determined with the use percentage gated events as the statistical significance profile obtained was similar to that of the absolute count.

It is clear from this cross-sectional study that the DC compartment is detrimentally affected during HIV-1 infection and it is proposed that the broader effect might relate to reduced immune responses. As mDCs are key role players in the initiation of adaptive immunity and pDCs are the principal produces of IFN-α, reduced numbers may result in the down-regulation of these immune activities. The lack of recovery whilst under reduced viral load are also concerning and the reason needs to be established (e.g. due to physical damage caused by the HIV-1 infection or hindrance in development form the bone marrow) so to develop a treatment strategy for alleviating DC numbers to accordingly strengthen the immune system.

As we were interested in gaining more insight into the decline of blood DCs during HIV-1 infection, it was proposed to phenotypically investigate the pool of pDCs and mDCs in current circulation. We theorised that the loss of pDCs and mDCs from peripheral blood of HIV-1 infected patients could be due to increased or altered physiological activities characteristic of cellular waning such as activation, apoptosis and migration. Therefore, the second part of the study focused on examining cell surface markers related to these processes in an attempt to better define DC cell losses and HIV pathogenesis

3.6. References

Almeida, M., Cordero, M., Almeida, J., and Orfao, A. (2006). Persistent abnormalities in peripheral blood dendritic cells and monocytes from HIV-1 positive patients after 1 year of antiretroviral therapy. J. Acquir. Immune Defic. Syndr. *41*, 405–415.

Barron, M.A., Blyveis, N., Palmer, B.E., Mawhinney, S., and Wilson, C.C. (2003). Influence of plasma vireamia on defects in number and immunophenotype of blood dendritic cell subsets in Human Immunodeficieny. J. Infect. Dis. *187*, 26–37.

Brenchley, J.M., Price, D.A., and Douek, D.C. (2006). HIV disease: fallout from a mucosal catastrophe? Nat. Immunol. *7*, 235–239.

Brown, K.N., Trichel, A., and Barratt-boyes, S.M. (2007). Parallel loss of myeloid and plasmacytoid dendritic cells from blood and lymphoid tissue in simian AIDS. J. Immunol. 6958–6967.

Brown, K.N., Wijewardana, V., Liu, X., and Barratt-boyes, S.M. (2009). Rapid influx and death of Plasmacytoid dendritic cells in lymph nodes mediate depletion in acute Simian Immunodeficiency Virus infection. PLoS Pathog. *5*, 1–13.

Chernomordik, L. V., and Kozlov, M.M. (2005). Membrane hemifusion: Crossing a chasm in two leaps. Cell *123*, 375–382.

De Carvalho Bittencourt, M., Martial, J., Cabié, A., Thomas, L., and Césaire, R. (2012). Decreased peripheral dendritic cell numbers in dengue virus infection. J. Clin. Immunol. *32*, 161–172.

Dave, B., Kaplan, J., Gautam, S., and Bhargava, P. (2012). Plasmacytoid dendritic cells in lymph nodes of patients with Human Immunodeficiency Virus. Appl. Immunohistochem. Mol. Morphol. *20*, 566–572.

Department of Health South Africa (2014). National consolidated guidelines for the prevention of mother-to-child transmission of HIV (PMTCT) and the management of HIV in children, adolescents and adults. pp. 1–119.

Dillon, S.M., Robertson, K.B., Pan, S.C., Mawhinney, S., Meditz, A.L., Folkvord, J.M., Connick, E., McCarter, M.D., and Wilson, C.C. (2008). Plasmacytoid and myeloid dendritic cells with a partial activation phenotype accumulate in lymphoid tissue during asymptomatic chronic HIV-1 infection. J. Acquir. Immune Defic. Syndr. *48*, 1–12.

Diop, O.M., Ploquin, M.J.-Y., Mortara, L., Faye, A., Jacquelin, B., Kunkel, D., Lebon, P., Butor, C., Hosmalin, A., Barré-Sinoussi, F., *et al.* (2008). Plasmacytoid dendritic cell dynamics and alpha interferon production during Simian immunodeficiency virus infection with a nonpathogenic outcome. J. Virol. *82*, 5145–5152.

Doitsh, G., Cavrois, M., Lassen, K.G., Zepeda, O., Yang, Z., Santiago, M.L., Hebbeler, A.M., and Greene, W.C. (2010). Abortive HIV infection mediates CD4 T cell depletion and inflammation in human lymphoid tissue. Cell *143*, 789–801.

Doitsh, G., Galloway, N.L.K., Geng, X., Yang, Z., Monroe, K.M., Zepeda, O., Hunt, P.W., Hatano, H., Sowinski, S., Muñoz-Arias, I., *et al.* (2013). Cell death by pyroptosis drives CD4 T-cell depletion in HIV-1 infection. Nature 1–19.

Donaghy, H., Pozniak, A., Gazzard, B., Qazi, N., Gilmour, J., Gotch, F., and Patterson, S. (2001). Loss of blood CD11c+ myeloid and CD11c- plasmacytoid dendritic cells in patients with HIV-1 infection correlates with HIV-1 RNA virus load. Blood *98*, 2574–2576.

Finke, J.S., Shodell, M., Shah, K., Siegal, F.P., and Steinman, R.M. (2004). Dendritic cell numbers in the blood of HIV-1 infected patients before and after changes in antiretroviral therapy. J. Clin. Immunol. *24*, 647–652.

Finkel, T.H., Tudor-Williams, G., Banda, N.K., Cotton, M.F., Curiel, T., Monks, C., Baba, T.W., Ruprecht, R.M., and Kupfer, A. (1995). Apoptosis occurs predominantly in bystander cells and not in productively infected cells of HIV- and SIV-infected lymph nodes. Nat. Med. *1*, 129–134.

Fontaine, J., Coutlée, F., Tremblay, C., Routy, J.-P., Poudrier, J., and Roger, M. (2009). HIV infection affects blood myeloid dendritic cells after successful therapy and despite nonprogressing clinical disease. J. Infect. Dis. *199*, 1007–1018.

Garg, H., Mohl, J., and Joshi, A. (2012). HIV-1 induced bystander apoptosis. Viruses *4*, 3020–3043.

Gougeon, M.-L. (2003). Apoptosis as an HIV strategy to escape immune attack. Nat. Rev. Immunol. *3*, 392–404.

Green, A., and Skosana, I. Motsoaledi reveals “progressive” HIV treatment plans. Mail Guard. 2014–2015.

Jiao, Y., Hua, W., Zhang, T., Zhang, Y., Ji, Y., Zhang, H., and Wu, H. (2011). Characteristics of $CD8^+$ T cell subsets in Chinese patients with chronic HIV infection during initial ART. AIDS Res. Ther. *8*, 1–7.

Joshi, A., Nyakeriga, A.M., Ravi, R., and Gargs, H. (2011). HIV ENV glycoprotein-mediated bystander apoptosis depends on expression of the CCR5 co-receptor at the cell surface and ENV fusogenic activity. J. Biol. Chem. *286*, 36404–36413.

Kanto, T., Inoue, M., Miyatake, H., Sato, A., Sakakibara, M., Yakushijin, T., Oki, C., Itose, I., Hiramatsu, N., Takehara, T., *et al*. (2004). Reduced numbers and impaired ability of myeloid and plasmacytoid dendritic cells to polarize T helper cells in chronic hepatitis C virus infection. J. Infect. Dis. *190*, 1919–1926.

Lichtner, M., Rossi, R., Rizza, M.C., Mengoni, F., Sauzullo, I., Massetti, A.P., Luzi, G., Hosmalin, A., Mastroianni, C.M., and Vullo, V. (2008). Plasmacytoid dendritic cells count in antiretroviral-treated patients is predictive of HIV load control independent of CD4 + T-cell count. Curr. HIV Res. *6*, 19–27.

Link, A., Vogt, T.K., Favre, S., Britschgi, M.R., Acha-Orbea, H., Hinz, B., Cyster, J.G., and Luther, S.A. (2007). Fibroblastic reticular cells in lymph nodes regulate the homeostasis of naive T cells. Nat. Immunol. *8*, 1255–1265.

Longman, R.S., Talal, A.H., Jacobson, I.M., Rice, C.M., and Albert, M.L. (2005). Normal functional capacity in circulating myeloid and plasmacytoid dendritic cells in patients with chronic hepatitis C. J. Infect. Dis. *192*, 497–503.

Lu, W., Mehraj, V., Vyboh, K., Cao, W., Li, T., and Routy, J.-P. (2015). CD4:CD8 ratio as a frontier marker for clinical outcome, immune dysfunction and viral reservoir size in virologically suppressed HIV-positive patients. J. Int. AIDS Soc. *18*, 1–9.

Malleret, B., Manéglier, B., Karlsson, I., Lebon, P., Nascimbeni, M., Perié, L., Brochard, P., Delache, B., Calvo, J., Andrieu, T., *et al*. (2008). Primary infection with simian immunodeficiency virus: plasmacytoid dendritic cell homing to lymph nodes, type I interferon, and immune suppression. Blood *112*, 4598–4608.

Mbita, Z., Hull, R., and Dlamini, Z. (2014). Human immunodeficiency virus-1 (HIV-1)-mediated apoptosis: new therapeutic targets. Viruses *6*, 3181–3227.

Messele, T., Abdulkadir, M., Fontanet, A.L., Petros, B., Hamann, D., Koot, M., Roos, M., Schellekens, P., Miedema, F., and Rinke de Wit, T. (1999). Reduced naive and increased activated CD4 and CD8 cells in healthy adult Ethiopians compared with their Dutch counterparts. Clin. Exp. Immunol. *115*, 443–450.

Moir, S., Buckner, C.M., Ho, J., Wang, W., Chen, J., Waldner, A.J., Posada, J.G., Kardava, L., O’Shea, M.A., Kottilil, S., *et al*. (2010). B cells in early and chronic HIV infection : evidence for preservation of immune function associated with early initiation of antiretroviral therapy. Blood *116*, 5571–5579.

Mojumdar, K., Vajpayee, M., Chauhan, N.K., Mendiratta, S., and Wig, N. (2010). Defects in blood dendritic cell subsets in HIV-1 subtype C infected Indians. Indian J. Med. Res. *132*, 318–327.

Ngo, V.N., Korner, H., Gunn, M.D., Schmidt, K.N., Riminton, D.S., Cooper, M.D., Browning, J.L., Sedgwick, J.D., and Cyster, J.G. (1999). Lymphotoxin α/B and Tumor Necrosis Factor are required for stromal cell expression of homing chemokines in B and T Cell areas of the spleen. J. Exp. Med. *189*, 403–412.

Pacanowski, J., Kahi, Sandrine, Bailet, M., Lebon, P., Deveau, C., Goujard, C., Meyer, L., Oksenhendler, E., Sinet, M., and Hosmalin, A. (2001). Reduced blood CD123+ (lymphoid) and CD11c+ (myeloid) dendritic cell numbers in primary HIV-1 infection. Blood *98*, 3016–3021.

Pinzon-Charry, A., Woodberry, T., Kienzle, V., McPhun, V., Minigo, G., Lampah, D.A., Kenangalem, E., Engwerda, C., López, J.A., Anstey, N.M., *et al.* (2013). Apoptosis and dysfunction of blood dendritic cells in patients with falciparum and vivax malaria.J. Exp. Med. *210*, 1635–1646.

Pitabut, N., Sakurada, S., Tanaka, T., Ridruechai, C., Tanuma, J., Aoki, T., Kantipong, P., Piyaworawong, S., Kobayashi, N., Dhepakson, P., *et al.* (2013). Potential function of granulysin, other related effector molecules and lymphocyte subsets in patients with TB and HIV/TB coinfection. Int. J. Med. Sci. 1003–1014.

Reeves, R.K., and Fultz, P.N. (2007). Disparate effects of acute and chronic infection with SIVmac239 or SHIV-89.6P on macaque plasmacytoid dendritic cells. Virology *365*, 356–368.

Rodrigues, D.D.S.,Cunha, R.M., Kallas, E.G., Salomao, R. (2003). Distribution of Naive and Memory/Effector CD4+ T Lymphocytes and expression of CD38 on CD8+ T Lymphocytes in AIDS patients with Tuberculosis. Brazillian J. Infect. Dis.*7*, 161–165.

Sabado, R.L., O'Brien, M., Subedi, A., Qin, L., Hu, N., Taylor, E., Dibben, O., Stacey, A., Fellay, J., Shianna, K. V, *et al.* (2010). Evidence of dysregulation of dendritic cells in primary HIV infection. Blood *116*, 3839–3852.

Scott, L.E., Noble, L.D., Moloi, J., Erasmus, L., Venter, W.D.F., and Stevens, W. (2009). Evaluation of the Abbott m2000 RealTime human immunodeficiency virus type 1 (HIV-1) assay for HIV load monitoring in South Africa compared to the Roche Cobas AmpliPrep-Cobas Amplicor, Roche Cobas AmpliPrep-Cobas TaqMan HIV-1 and BioMerieux NucliSENS. J. Clin. Microbiol. *47*, 2209–2217.

Soumelis, V., Scott, I., Gheyas, F., Bouhour, D., Cozon, G., Cotte, L., Huang, L., Levy, J.A., and Liu, Y.I. (2001). Depletion of circulating natural type 1 interferon-producing cells in HIV-infected AIDS patients. Blood *98*, 906–912.

Tan, J.T., Dudl, E., LeRoy, E., Murray, R., Sprent, J., Weinberg, K.I., and Surh, C.D. (2001). IL-7 is critical for homeostatic proliferation and survival of naive T cells. Proc. Natl. Acad. Sci. U. S. A. *98*, 8732–8737.

Vinikoor, M.J., Cope, A., Gay, C.L., Ferrari, G., McGee, K.S., Kuruc, J.D., Lennox, J.L., Margolis, D.M., Hicks, C.B., and Eron, J.J. (2013). Antiretroviral therapy initiated during acute HIV infection fails to prevent persistent T-cell activation. J. Acquir. Immune Defic. Syndr. *62*, 505–508.

Wijewardana, V., Kristoff, J., Xu, C., Ma, D., Haret-Richter, G., Stock, J.L., Policicchio, B.B., Mobley, A.D., Nusbaum, R., Aamer, H., *et al.* (2013). Kinetics of myeloid dendritic cell trafficking and activation: impact on progressive, nonprogressive and controlled SIV infections. PLoS Pathog. *9*, 1–18.

Wijewardana, V., Soloff, A.C., Liu, X., Brown, K.N., and Barratt-Boyes, S.M. (2010). Early myeloid dendritic cell dysregulation is predictive of disease progression in simian immunodeficiency virus infection. PLoS Pathog. *6*, 1–13.

World Health Organization (WHO) (2013). Consolidated guidelines of the use of antiretroviral drugs for treating and preventing HIV infection: Recommendation for a public health approach. 1–269.

World Health Organisation (WHO) (2015).Guideline on when to start antiretroviral therapy and on pre-exposure prophylaxis for HIV. 1–76.

Zeng, M., Paiardini, M., Engram, J.C., Beilman, G.J., Chipman, J.G., Schacker, T.W., Silvestri, G., and Haase, A.T. (2012). Critical role of CD4 T cells in maintaining lymphoid tissue structure for immune cell homeostasis and reconstitution. Blood *120*, 1856–1867.

Chapter 4

Ex vivo phenotypic properties of pDCs and mDCs in the peripheral whole blood of HIV-1 mono-infected and HIV-1/TB co-infected individuals

4.1 Introduction

Declining numbers of pDCs and mDCs in the peripheral blood of HIV-1 infected patients (reported by others and supported by the findings of the current study (chapter 3)) prompted investigation into possible underlying reason(s) for their loss from circulation. The current study hypothesised that this decline (as well other related DC changes) is due to chronic exposure/response to the HHF cocktail in circulation. This hypothesis was based on published *in vitro* studies demonstrating a level of reduced "fitness" in blood pDCs and mDCs isolated from HIV-1/SIV infected individuals/primates. In particular, these cells showed a higher susceptibility to undergo spontaneous apoptosis in culture (Dillon SM, *et al.* 2011; Brown KN, *et al.* 2007). In evaluating viability (amine fluorescent staining assay) of DCs during SIV infection, Brown KN, *et al.* (2007) showed that the frequency of lymphoid tissue-associated viable pDCs (isolated from spleen) and mDCs (isolated from spleen and peripheral lymph nodes) of SIV naïve rhesus macaque monkeys were similar to animals with AIDS at the onset of culture. However, after 24h incubation, viable pDCs and mDCs of the SIV uninfected monkeys were reduced by 10-20% while a significant reduction of 40-45% in viable pDCs and mDCs was observed in monkeys with AIDS. Similarly, Dillon SM, *et al.* (2011) examined spontaneous apoptosis of DCs from HIV-1 infected patients by evaluating the viability of these cells 24h post-collection via the expression of the apoptotic markers 7-amino-actinomycin D (7-AAD) (apoptotic DNA-binding marker, indicative of late stage of apoptosis), Annexin V (apoptotic cell surface binding marker, indicative of early stage of apoptosis) and anti-apoptotic Bcl-2 (mitochondrial associated anti-apoptotic marker). The authors showed, compared to healthy controls, mDCs of HIV-1 infected individuals having a high tendency to be undergoing late stage of apoptosis. Furthermore, the level of anti-apoptotic Bcl-2 was significantly lower in mDCs from HIV-1 infected individuals. These studies have demonstrated the adverse effect of an HIV-1/SIV infection on blood and lymphoid tissue DCs. In view of these results, viral and host related factors that may contribute to the altered DC phenotype in circulation during HIV-1 infection was investigated.

Viral elements contributing to DC apoptosis

A viral associated factor that might predispose DCs of HIV-1 infected individuals to apoptosis are gp120 immune complexes found in plasma. These represent shed particles of maturing HIV-1 virions (Gelderblom H.R, *et al.* 1985) which, upon binding with antibodies of the host, form immune complexes (Liu P, *et al.* 2011). Chen Y, *et al.* (2013) reported on the significant increase in apoptotic activity of mo-DCs, treated with gp120 immune complex preparations (formed by cross-linking recombinant gp120 and anti-HIS tag mAb), upon interaction with autologous activated CD4 T lymphocytes. The authors established that the apoptotic activity was related to the interaction of the DC-SIGN molecule on DC with gp120 and activated via CD40/CD40L interaction. Similarly, the *in vitro* pulsing of purified blood DC-SIGN$^+$CD40$^+$ DC subset from healthy individuals cross-linked with gp120 immune complexes also showed elevated levels of apoptosis upon culture with CD40L transfected cells. Also, in the *in vivo* setting the DC-SIGN$^+$CD40$^+$ DC subset of HIV-1 infected patients, naturally exposed to gp120 immune complexes, showed significantly higher fractions of

apoptotic cells when incubated with CD40L transfected cells compared to unexposed DC-SIGN$^+$CD40$^+$ DC subset of healthy controls.

The gp120/antibody immune complex phenomenon may represent one mechanism justifying the loss of DCs from peripheral blood during untreated HIV-1 infection. Accordingly, the current study questioned in which way this phenomenon relates to the lack of DC number recovery during ARV therapy when accompanied with undetectable plasma viral load (presumably with parallel reduction of gp120 levels) as reported in Chapter 3. Some clarity came from a study conducted by Rychert J and colleagues (2010) who showed that the level of plasma gp120 detected during acute HIV-1 infection remained unchanged regardless of a decline in plasma viral load over prolonged use of ARV therapy. Hence, in view of this report it was proposed that 1) the continuous presence of viral antigens may have the potential of steadily draining DCs from circulation, 2) inhibition of viral replication may not be sufficient for the control of an HIV-1 infection and 3) removal of total viral products from circulation produced in acute (and during chronic) HIV-1 infection might be required for recovery of DC numbers (and other affected parts of the immune system) in circulation.

Host elements contributing to DC apoptosis

In studying host-specific elements produced during chronic HIV-1 infection with the aim of identifying those which could detrimentally impact blood DCs, an extensive array of publications reporting on changes in pro- and anti-inflammatory biomarkers during chronic HIV-1 infection was found. In view of this, it was proposed that the term “immunodeficient” might not give full “credit” to the state of the immune system during HIV-1 infection. The increased cytokine plasma level is supportive evidence for the continuous attempt of the immune system to counteract the infection. Paradoxically, it is the chronic production of these factors that is presumed to be one of the driving forces of the HIV-1/AIDS disease and resulting mortality. Accordingly, it is proposed that the term “immunocompromised” better describes an HIV-1 exposed immune system triggered to aberrantly produce host factors. The destructive effect of persistent cytokine production has also been reported in other infectious diseases. Referred to as a cytokine storm (hypercytokinemia), this phenomenon has, specifically, been implicated as a contributing factor to the death of many people that have been infected with the phlebovirus (causing Severe Fever with Thrombocytopenia Syndrome (SFTS)), Ebolavirus (species *Zaire)* or H1N1 influenza strain (Sun Y, *et al.* 2012; Monsalvo AC, *et al*. 2011, Wauquier N, *et al.* 2010). Also, the severe acute respiratory syndrome (SARS) outbreak of 2002 has been associated with an IFN-γ related cytokine storm (Huang KJ, *et al.* 2005). It should be noted that in HIV-1 infection the cytokine storm phenomenon is limited to the acute phase of the disease, which declines as a certain level of control is gained over the infection. This is followed by a steady increase in immune activation upon transition from the acute to the chronic disease phase. (Refer to Figure 2.1). Moreover, aberrant cytokine production is not infectious disease-specific as aberrant production of inflammatory cytokines has proven deleterious also in autoimmune diseases such as rheumatoid arthritis, atherosclerosis, psoriasis, periodontitis, Crohn’s disease, ulcerative colitis and systemic lupus erythematosus (Kaur S, *et al.* 2013; Su DL, *et al.* 2012; Ozbalkan Z, *et al.* 2010; Strober W, *et al.* 2010; Nishimura M, *et al.* 2009; Arican O, *et al.*2005).

Among several changes in the cytokine milieu observed during HIV-1 infection, altered plasma levels of the IL-10 anti-inflammatory cytokine was interesting (Brockman MA, *et al.* 2009; Orsilles MA, *et al.* 2006; as

reviewed by Breen EC. 2002). A former study by Ludewig B, *et al.* (1995) showed that this anti-inflammatory cytokine induced apoptosis of DCs and a more recent study determined that IL-10 functions via suppressing the transcription of the three anti-apoptotic genes *bcl-2, bcl-x and bfl-1* (Chang WLW, *et al.* 2007). Hence, it was proposed that aberrant production of IL-10 during chronic HIV-1 infection may contribute to the apoptotic-associated loss of DCs from circulation. Elevated plasma levels of IL-10 with associated apoptosis of DCs have also been reported in *Plasmodium falciparum* (*Pf*) and *P. vivax* (*Pv*) infected patients suffering from malaria. Interestingly, the authors showed reduced apoptosis of DCs upon *in vitro* IL-10 blocking. Despite the beneficial prospects of anti-IL10 treatment, employing IL-10 antagonists with the purpose to hinder apoptotic death of DCs so to re-establish the DC compartment should be approached with caution in HIV-1 infection as it has the potential to introduce adverse effects. This was reasoned on the basis of the following: IL-10 plays an immune-regulatory role by promoting intestine health, apparent from studies that showed IL-10 deficient mice developing intestine–related diseases (such as chronic colitis) due to an inappropriate immune responses to naturally occurring microflora/gut antigens (Gomes-Santos AC, *et al*. 2011; Madsen KL, *et al*. 1999; Kühn R, *et al.* 1993). Also, colitis in IL-10 deficient mice coincided with increased intestinal permeability (Liu Z, *et al.* 2011; Arrieta MC, *et al.* 2009; Kennedy RJ, *et al*. 2000; Madsen KL, *et al*. 1999) which results in the sifting through of toxic gut antigens (e.g. LPS). This phenomenon is referred to as leaky gut. Notably, leaky gut is also a well-defined trademark of HIV-1 pathogenesis, believed to be a major contributory factor driving chronic inflammatory responses (Brenchley JM, *et al*. 2006a, 2006b). Accordingly, anti-IL-10 therapy in HIV-1 infection might worsen the disease.

The viral and host entities discussed here that may trigger DC cell death during HIV-1 infection represent a few possible apoptotic related factors that may contribute to low cell number distribution. In addition, it is proposed that these HHF entities may also drive DC loss in a non-apoptotic manner viz. chemotactic mobilisation and activation-induced export. Accordingly, the current study proposed that DC responses to HHF elements may reflect as modified marker expression with regard to *ex vivo* markers related to apoptosis, chemotaxis, activation and maturation when compared to the marker profile obtained from an uninfected system. This concept marks the principal aim of the study and the specific markers of interests investigated linked to these processes are discussed in sections 4.1.1 to 4.1.3.

4.1.1 Investigating *ex vivo* apoptotic marker expression on blood mDCs and pDCs

This part of the study aimed to determine whether blood DCs of HIV-1 infected individuals circulate with altered death-associated marker expression. The markers of interest included FAS and its ligand (FASL), TNF-R2, TRAIL-R1 and –R2 (both pro-apoptotic markers). In addition, the study was also interested in examining subsets of DCs expressing TRAIL-R3 and -R4, markers of decoy/anti-apoptotic receptor expression, so to assess the inter-relationship between pro- and anti-apoptotic marker expressions during HIV-1 infection. Notably, in HIV-1 infection significantly raised plasma levels of the cognate ligands to these apoptotic markers namely: FASL (cognate receptor FAS), TNF-α (TNF-R2) and TRAIL (TRAIL R1, -R2, -R3 and –R4) have been reported (Piddubna AI, *et al.* 2013; Gasper-Smith N, *et al.* 2008; Herbeuval JP, *et al.* 2005). As an HIV-1 infection is not cleared, it was proposed that these raised levels persist throughout the course of the disease. This may result in a progressive rate of cell death, leading to the steady drainage of

affected immune cells from circulation and weakening of the immune system. A brief description on the apoptotic markers investigated follows.

FAS and its cognate ligand, FASL, are both transmembrane proteins with an atomic mass of 48-kDa and 40-kDa, respectively. Their interaction activates an apoptotic pathway in the cell that expresses the FAS receptor. The latter is moderately expressed on resting T lymphocytes, while functional expression of FASL is only found in activated T lymphocytes. This may be indicative of FASL expression being a more stringently controlled process. Notably, constitutive expression of FASL is restricted to immune privilege sites where it directs cell death in FAS bearing immune cells that enter these sites in response to infection/inflammation. This form of FASL expression has been associated with the eyes (Ferguson TA and Griffith TS, 2006; Gregory MS, *et al.* 2002), central nervous system (as reviewed by Gimsa U, *et al.*2013) and placenta (Stenqvist AC, *et al.* 2013). In contrast, constitutive FASL expression is also significant of certain pathological conditions. Fang L, *et al.* (2013) and Das SN, *et al.* (2011) reported that in contrast to normal squamous epithelia of the oral cavity, malignant tissue expresses FASL. Upon interaction with FAS expressing cytotoxic T lymphocytes, the very cell responsible for the destruction of cancer cells is destroyed which may lead to persistent tumour growth.

Two circulating formats of the FASL molecule have been identified, namely, membrane-bound (mFASL) and soluble FASL (sFASL) which were found to play opposing roles with regard to cell death. It has been reported that the former promotes while the latter blocks cell death (O' Reilly LA, *et al.* 2009; Suda T, *et al.* 1997). In glaucoma, an autoimmune/neurodegenerative disease of the eyes, sFASL was found to protect while mFASL enhanced death of retinal ganglion cells (Gregory MS, *et al.* (2011). This "protective role" of sFASL, however, has been found to play to host's disadvantage in certain cases. In large granular lymphocyte (LGL) leukaemia, a lymphoproliferative disorder associated with apoptosis resistance, sFASL were found as the central role player in blocking cell death of malignant cells regardless of the high FAS expression by LGLs (Liu JH, *et al.* 2002).

In HIV infection, increased plasma level of sFASL as well as another apoptosis blocker, sFAS (functions by inhibiting the binding of FAS and FASL), has been observed (Ikomey GM, *et al.* 2012; de Milito A, *et al.* 2000; Hosaka N, *et al.* 1998). However, in view of the extensive cellular loss reported during HIV infection the protective actions of these seemed to be overpowered by an HIV infection. It was proposed that sFAS-sFASL aggregates form in the plasma of HIV-1 infection patients, leading to a deficient restrain in aberrant apoptotic events associated with HIV-1 infection. However, intensive literature search could not elaborate on this suggested concept.

TRAIL-R1 and TRAIL-R2 (the former known as DR4, Apo-2 or CD261 and the latter known asDR5, TRIC2, KILLRT or CD262) engage with their natural ligand, TRAIL, to initiate TRAIL-mediated apoptosis (Pan G, *et al.* 1997; Walczak H, *et al.* 1997). Conversely, TRAIL's interaction with **TRAIL-R3** (also known as DcR1, TRID, LIT and CD263) or **TRAIL-R4** (DcR2, TRUNDD and CD 264), collectively referred to as TRAIL decoy receptors (DcR), promotes anti-apoptotic signalling (i.e. survival) (Degli-Esposti MA, *et al.* 1997a, 1997b). The anti-apoptotic function of these receptors has been ascribed to an absent (TRAIL-R3) or truncated

(TRAIL-R4) intracellular death domain (as reviewed by de Vries EGE, *et al.* 2006). TRAIL, also known as CD253, is a type II membrane protein of which the C terminal in the extracellular domain are homologous to members of the TNF-R family of death proteins. It was cloned and characterised by Wiley SR and colleagues (1995) who also determined that both the cell surface and soluble forms induced rapid apoptosis in several cell lines. The TRAIL receptor family share a sequence homology of > 50% with regard to their cysteine-rich extracellular domain. Specifically, TRAIL-R1 and TRAIL-R2 share an overall sequence homology of 58% (as reviewed by Falschlehner C, *et al.* 2007) and these share a sequence identity of 58% and 54% with TRAIL R3, respectively (Degli-Esposti MA, *et al.* 1997a). TRAIL-R4 shares an identity of 58%, 57% and 70% to TRAIL-R1, TRAIL-R2 and TRAIL-R3, respectively (Degli-Esposti MA, *et al.* 1997b).

TRAIL-mediated apoptosis have recently gained much attention as a therapeutic agent in cancer therapy (as reviewed by Holland PM, 2014). TRAIL seems to selectively target apoptosis of transformed cells such as tumour cells. Zhang XD, *et al.* (2000) investigated TRAIL mediated apoptosis in the TRAIL-R2$^+$ cancerous/transformed T cell line (Jurkat cells) and TRAIL-R2$^+$ non-cancerous cell line (human umbilical vein endothelial cells (HUVECs)). Significant apoptotic activity upon *in vitro* TRAIL treatment was only observed with the transformed Jurkat cell line. It became apparent that HUVEC cells were protected from apoptosis via its intrinsic decoy receptor, TRAIL-R3, as chemical removal of this receptor resulted in increased apoptosis of HUVECs. Jurkat cells characteristically lack decoy receptors, justifying their sensitivity to TRAIL mediated apoptosis (Sprick MR, *et al.* 2000; Zhang XD, *et al.*2000).

In contrast to the beneficial effect of TRAIL-mediated killing of “unwanted or distressed” cells, it has been shown to play a role in the obstruction of, particularly, antiviral immune responses. Hosts bearing hepatitis B (HBV) or hepatitis C (HCV) virus infection exhibits dysfunctional HBV/HCV-specific CD8 T lymphocyte responses (Boni C, *et al.* 2007; as reviewed by Rehermann B, 2009). This is due to the killing of TRAIL-R2$^+$ HBV-specific CD8 T lymphocytes upon interaction with TRAIL$^+$ NK cells. HBV chronically infected individuals have a significantly higher frequency of TRAIL-R2$^+$ HBV-specific CD8 T lymphocytes (Peppa D, *et. al.*2013) and their NK cells upregulate expression of TRAIL as a result of the cytokine milieu (significantly higher concentrations of IFN-α and IL-8) induced during HBV infection (Dunn C, *et al.* 2007). Accordingly, TRAIL$^+$ NK cells kill TRAIL-R2$^+$ HBV-specific CD8 T lymphocyte upon ligand-receptor contact.

TNF-R2, similar to TRAIL-R3 and –R4, does not bear an intracytoplasmic death domain (as reviewed by Faustman DL and Davis M, 2013; as reviewed by Pfeffer K, 2003). The TNF-R2pathway activation is dependent on interaction with its cognate ligand, TNF-α. This cytokine plays an important role in host defence and inflammation as a pluripotent mediator. However, if TNF-α levels are not sufficiently moderated, it has the ability to cause major tissue/organ damage. It is well documented that HIV-1 infection is characterised by persistent levels of inflammatory agents, which includes TNF-α. The effects thereof have been investigated in the HIV-1 transgenic mouse line, Tg 26. The latter, in contrast to the non-transgenic mouse line, manifest with a 50-fold increase in TNF-α serum levels (De SK, *et al.* 2002). Also, these animals exhibit severe pathologic conditions related to disorders of the kidneys (proteinuria, glomerulosclerosis (Dickie P, *et al.* 1991)) and skin (e.g. epidermal papillomas and diffuse hyperkeratosis (Kopp JB, *et al.*1993)) which is accompanied by a high mortality rate. Interventions (treatment with TNF-α antibody) targeting the

TNF-α storm in Tg26 showed profound suppression of HIV-1 induced conditions. A major decrease in the serum levels and mRNA transcripts of TNF-α as well gp120 in the skin was observed, promoting the survival of the host. In parallel, employing cytokine blockers in autoimmune disease seem promising in hindering host tissue damage. Prospective studies that addressed aberrant production of TNF-α in autoimmune disease in humans have proved promising in alleviating the harmful effects associated with the disease. Reimold AM, (2003) employed TNF-α blockers in treating rheumatoid arthritis (a disease driven by aberrant levels of TNF-α and characterised by inflammation of the joints causing damage to cartilage and bones) and reported on a significant reduction in the symptoms associated with the disease with limited side effects. Crohn's disease is another inflammatory condition that have benefitted from the use of anti-inflammatory agents. Accordingly, it was debated, whether the use of antagonist would translate beneficial when applied to chronic inflammation caused by infectious disease. The question was raised whether inhibition of the cytokine response during infectious disease would give the infectious agent a greater upper hand during antagonist treatment. Most intervention strategies employed to combat infectious diseases focus on elimination of the pathogen as it is, plausibly, safer and "easier" to target the sole non-host-inherent infectious particle (HIV-1) than suppressing any one or selected few of the array of post-stimulatory host-inherent molecules produced via stringently controlled and interlinked processes.

4.1.2 Investigating *ex vivo* chemotactic marker expression on blood mDCs and pDCs

As HIV-1 infection is driven by chronic inflammation, it was proposed that inflammatory signals may drive chemotactic export of blood DCs to sites of infection. It was further suggested that continuous export could reach a stage where it overtakes the rate of replenishment from the bone marrow, hence, maintaining significantly low DC numbers in circulation. Accordingly, the aim of investigating markers of cellular migration was so to ascertain whether the decline of blood DCs during HIV-1 infection may be due to *amplified* export of these cells from peripheral blood. Specifically, the study hypothesised that infection/inflammatory signals (either aberrant levels of host elements and/or whole or products of pathogens (viral/other)) associated with HIV-1 infection are recognised by blood DCs and in response induces a change in specific homing markers expressed on these cells. It was proposed that these signals would initiate two principal routes of migration namely 1) to the sites of infection and/or 2) lymphoid tissue, ensuring that antigen captured DCs interact with naïve T lymphocytes in the lymph nodes, the primary site for the initiation of adaptive immune responses.

Acknowledging that a compromised immune system may have multiple sites of ongoing infection, the study focused on examining chemokine markers reported to direct homing to, specifically, the GIT and pulmonary tissue. Homing of DCs to the GIT may be related to the leaky gut phenomenon associated with HIV-1 infection. This refers to the translocation of microbial products from the lumen of the gut to the portal blood stream due to a breach in the integrity of the mucosal barrier initiated during acute HIV-1 infection. The breach is the result of excessive loss of intestinal CD4 T lymphocytes (Guadalupe M, *et al*. 2003). It is believed that the continuous sifting through of bacteria and bacterial products from the intestinal lumen to the blood stream subsequently induces and fuels chronic immune activation and inflammatory responses during HIV-1 infection (Brenchley JM, *et al.* 2006a, 2006b*).* In addition, the current study also aimed to investigate blood DC depletion via homing to pulmonary tissue. Defining blood DC loss via chemokine markers that direct leukocyte homing to pulmonary tissue was of particular interest for the HIV-1/TB co-infection arm of

the study. This was performed in view of the fact that the majority of South African HIV-1 infected individuals succumb to a TB co-infection. For this part of the study chemotactic markers associated with migration to the GIT and pulmonary tissue needed to be sourced. Accordingly, it was decided to investigate the expression of chemokine receptors CCR9 and CXCR6, as putative homing markers to GIT and lungs, respectively. ***CCR9***, also known as CD199, has been identified as a putative GIT chemokine marker in view of reports linking this chemokine receptor to the mobilisation of CD4 T lymphocyte and pDC to the small intestine (Wendland M, *et al.* 2007; Stenstad H, *et al.* 2006). The role of this chemokine marker in directing cell mobilisation to, specifically, the intestines was also supported by studies showing that its natural ligand, CCL 25 (referred to as the thymus expressed chemokine), is preferentially expressed by the epithelia of the small intestine (Papadakis KA, *et al.* 2000). In view of the localised expression of CCL25 and given that aberrant plasma levels of other localised enteric-associated host factors such as intestinal fatty acid binding protein (a molecule expressed by enterocytes and released in circulation upon damage to the intestine (as reviewed by Pelsers MMAL, *et al.* 2005) have been observed during HIV-1 infection (Mavigner M, *et al.* 2012), it was proposed that the components leaking from the gut might also introduce aberrant CCL25 into circulation. This may induce enhanced blood DC export from circulation by gradient attraction to the GIT site of infection. ***CXCR6***, also known by alternate names Bonzo/STRL33/TYMSTR/CD186, has been characterised as a putative pulmonary tissue chemokine marker. A study investigating the expression of several chemokine receptors on T lymphocytes from bronchoalveolar lavage (BAL) and peripheral blood in patients with the respiratory disease, Sarcoidosis, found a significant increase in the expression of CXCR6 in T lymphocytes from BAL fluid compared to those in blood. Similar results were also found with interstitial lung disease. Furthermore, the authors determined that alveolar macrophages are the prime source of its natural ligand, the transmembrane CXCL16 chemokine and also identified two soluble isoforms (60kDa and 35kDa) in BAL fluid (Agostini C, *et al.* 2005; Morgan AJ, *et al.* 2005).

In addition to investigating putative chemokine marker expression related to tissue mobilisation, this study also aimed at profiling blood DCs on chemotactic receptors known to respond to chemotactic gradient that directs mobilisation of leukocytes to secondary lymphoid tissue. The latter is the primary site for the initiation of adaptive immune responses which is greatly reliant on the interaction of DCs that have captured antigen at sites of infection and migrated to present processed antigen to naïve T lymphocyte. In this part of the study *ex vivo* profiling of chemokine receptors, CCR5 and CCR7, on blood DCs was of interest. In view of publications that have reported on significantly increased serum levels of natural ligands to CCR5 and CCR7 during HIV-1 infection, the study proposed 1) this to result in a heightened migration of DCs to secondary lymphoid tissue and 2) signified by altered CCR5 and/or CCR7 *ex vivo* marker expression (Damås JK, *et al.* 2009; Montes de Oca Arjona M, *et al.* 2005; Ye P, *et al.* 2004). ***CCR5*** is a chemokine marker that binds to RANTES, macrophage inflammatory protein-1 (MIP-1α) (also known as CCL-3) and MIP-β (CCL4). It is closely related to CCR2b (71% identity) and shares an amino acid sequence homology of 55, 49 and 48% to the CCR1, CCR3 and CCR4 chemokine receptors. Sequence homology seems to involve the intracellular structure as the divergent sequences are found in the amino-terminal extracellular domains which are the sites associated with ligand binding (Raport CJ, *et al.* 1996).CCR5 and its ligands are major role players during inflammation. In a rat model that investigated colitis (induced with trinitrobenzene sulfonic acid) increasing RANTES levels and macrophages and monocytes numbers were observed in colonic tissue over

a period of 2 weeks. Treatment with a CCR5 antagonist (Met-RANTES) showed recuperation of colonic tissue and a reduction in mast cells and monocyte numbers (Ajuebor MN, *et al.* 2001). In HIV-1 infection CCR5 also acts as a co-receptor for viral entry. The discovery of a 32-base pair deletion (refer to CCR5 delta-32 (Δ32)) resulting in a non-functional CCR5 receptor that hinders viral-host membrane fusion (refer to the HIV life cycle as described in Chapter 2) confers protection against infection. In one particular case, resistance to HIV infection was seemingly introduced in an HIV infected individual who received a bone marrow transplant from an individual homozygous for the CCR5 Δ32 mutation. The bone marrow recipient remained cleared from the virus even after ARV therapy was discontinued (Hütter G, *et al.* 2009).

CCR7 is a lymphoid homing marker that interacts with the chemokines, CCL19 and CCL21, which are expressed by high endothelial venules (HEV) on lymph nodes in a constitutive manner. This persistent CCR7 ligand gradient sustains immune cell immigration to and retention in secondary lymphoid tissue (the central congregating point of processed antigens captured at diverse sites of the host) where these cells are "educated" by DCs on the antigen milieu present in the host. In HIV-1 infection it has been shown that gp120 plays a role in enhancing the response of CD4 T lymphocyte to CCL21, while hindering CD4 T lymphocyte responses to the sphingosine 1-phosphate (S1P) receptor. The latter plays a role in overriding the CCR7 signal to endorse cellular emigration from secondary lymphoid tissue (Pham THM, *et al.* 2008; Matloubian M, *et al.* 2004). Accordingly, the enhanced migration to and declining emigration from lymphoid tissue results in cellular accumulation in the lymph nodes which may contribute to the manifestation of lymphadenopathy, a clinical condition significant of abnormal enlargement of the lymph nodes and characteristic of HIV-1 infection (Green DS, *et al.* 2009). Furthermore, CCR7 receptor expression is one of various factors that differ between pathogenic and non-pathogenic SIV infection. Mandl JN, *et al.* (2008) observed no significant change in CCR7 expression by blood pDCs and mDCs of the natural host, sooty mangabeys, infected with SIV. In contrast, SIV infection of the non-natural host, rhesus macaque, showed upregulated expression of CCR7 on both, pDCs and mDCs. It seemed, from these findings, that stable CCR7 expression on DCs play a role in the immune control over SIV infection. Accordingly, it was deliberated whether SIV-associated immune control can be mimicked in HIV-1 infection by, for one, antagonizing the CCR7 receptor. According studies in CCR7 deficient mice have shown paradoxical immune control in viral vs. bacterial/fungus infection. In viral infection arrested immune response in CCR7-deficient mice was observed (Kocks JR, *et al.* 2009; Junt T, *et al.* 2004) whereas these subjects were able to clear bacterial infection more efficiently than the wild type (Eppert BL, *et al.* 2010). Accordingly, increased cytokine levels of IL-12/23p40, IFN-γ and IL-1α in BAL fluid of CCR7 deficient mice infected with *Pseudomonas aeruginosa* (causative agent of hospital acquired respiratory infection) was observed (Eppert BL, *et al.* 2010). Also, lung tissue showed a significant decline in bacterial load at 16h post infection, a significant increase in neutrophilic respiratory burst activity and higher numbers of mDCs (with greater upregulated CD80 and CD86 expression) and T lymphocytes compared to the wild type. The "control over infection" in CCR7 deficient mouse has also been reported in studies investigating invasive *Aspergillus fumigatus (*fungus infection affecting pulmonary tissue and known to cause fatality in bone marrow transplant) (Hartigan AJ, *et al.*2009) as well as *M. tuberculosis* (Kahnert A, *et al.*2007). Possibly, the enhanced immune control observed in CCR7 deficient mice may be due to atypical cellular containment at the site of infection, resulting in higher phagocytic activity and levels of pro-inflammatory cytokines. Although, these findings may stimulate anti-CCR7 immuno-therapy approaches; a

yet undefined level of risk is involved as other studies have observed the development of autoimmunity in CCR7 deficient mice (Winter S, *et al.* 2011; Davalos-Misslitz ACM, *et al.* 2007). Nevertheless, it would be interesting to investigate the effect of transient blocking of CCR7 receptors during viral infection of the human host.

4.1.3 Investigating *ex vivo* activation and maturation marker expression on mDCs and pDCs

In the final part of the study focus was placed on *ex vivo* profiling of DC specific markers associated with activation and maturation during HIV-1 infection. The aim was to determine whether blood DCs of HIV-1 infected individuals circulate with altered expression of these markers. This change may be indicative of 1) response to host and/or viral associated signals, 2) antigen encounter and capture and/or 3) activation-induced export of DCs from peripheral blood to transport captured antigen to secondary lymphoid tissue for presentation to naïve T lymphocytes. The latter concept builds on the study's hypothesis of persistent signal (in this case viral antigens) leading to persistent export that in time overtakes the rate of DC replenishment resulting in low DC numbers in circulation. Profiling the residual pool of blood DCs of HIV-1 infected patients, exposed to HHF, might provide clues to whether the decline of blood DCs may be due to activation-induced export steered by the altered matrix created by an HIV-1 infection. The DC specific markers investigated that is associated with activation included CD80 and CD86. Also, the expression of the activation associated marker, CD62L, on blood DCs was investigated. CD83 was the DC specific maturation marker examined.

CD80 (also known as B7-1), CD86 (B7-2) and CD83 are ligands expressed by DCs which play an interactive role in the formation of the immunological synapse (the interface between antigen primed (activated) DC and naïve T lymphocytes) involved in the "dual signal" initiation of adaptive immune responses in secondary lymphoid tissue. This entails the interaction of 1) the peptide-MHC composite **on activated DCs** with the T lymphocyte receptor and 2) CD80 and CD86 ligands, also referred to as co-stimulatory ligands, **on activated DCs** with the CD28 receptor on T lymphocytes. The outcome of these interactions is the establishment of a systemic response to eliminate the pathogen which includes 1) the production of cytokines and up-regulation of cognate receptors, 2) generation of antibodies and 3) the clonal expansion of antigen-specific lymphocytes from which vital effector T lymphocytes (short lived cells that undergo apoptosis upon clearance of the antigen) and memory T lymphocytes (remain in circulation to protect and respond more rapidly in the event of a secondary infection) differentiates (Abbas AK, *et al.* 2012).

CD62L, also referred to as L-selectin, together with E- and P-selectin are members of the selectin family of adhesion molecules (as reviewed by Rosen SD. 2004). CD62L is found constitutively expressed by circulating T lymphocytes (Klinger A, *et al.* 2009) and E- and P-selectin are found on activated epithelial cells with P – selectin also expressed by activated platelets (as reviewed by Ivetic A and Ridley AJ. 2004). CD62L has been described to facilitate immune surveillance - directing the transitional circulation of lymphocytes between blood and lymphoid tissue at the level of cellular transmigration also referred to as diapedesis. Briefly, this process entails interaction between CD62L and its ligands (CD34, Glycosylation-dependent cell adhesion molecule-1(GlyCAM-1), sialylated glycoprotein of 200 kD (Sgp200) or podocalyxin-like protein (PCLP) (collectively referred to as peripheral-node addressin (PNAd) adhesion molecules) expressed on

endothelia which stimulates deceleration of cellular flow. The low affinity binding between CD62L and its ligand results in the rolling or tethering of lymphocytes, which in combination with other immune markers, eventually leads to steady adhesion of these cells to the cell wall and subsequent transmigration (Raffler NA, *et al.* 2005; as reviewed by Rosen SD, 2004). CD62L driven diapedesis allows lymphocyte mobilisation across the HEV and entry into lymph nodes, the primary site where these immune cells can “browse” the array of antigens presented by mature DCs. Hence, it is a molecule of major importance as immune response cannot be initiated without the extravasation of leucocytes across the venule barrier (as stated by Muller WA. 2013). In the absence of interacting with their cognate antigen, lymphocytes exit the lymph node via the efferent lymphatics and return to circulation to continue with immune surveillance.

In addition to its role as immune surveyor, CD62L has also been categorised as a marker of immune activation. This is related to the characteristic shedding of CD62L upon cellular activation. The phenomenon was recently reported to be associated with the acquisition of CD107a, a marker of lytic activity, by CD4 T lymphocytes (Yang S, *et al.* 2011). Notably, higher levels of soluble CD62L have been reported during disseminated *Cryptococcus Neoformans* and respiratory infection (Jackson LA, *et al.* 2005; Malaponte G, *et al.* 2004). This phenomenon has also been reported during HIV-1 infection (Kourtis AP, *et al.* 2000).

Most interestingly, CD62L has been implicated in the transmission of virus to T lymphocytes during HIV-1 infection. Thibault S, *et al.* (2007) reported on the ability of the HIV-1to integrate host associated and functional CD62L into its envelope membrane. This phenomenon on adsorption of host factors during infection has been observed in several virus species. These include Ebstein Barr virus (incorporates HLA-DR) and human cytomegalovirus (CD55 and CD59) (as reviewed by Cantin R, *et al.* 2005). The adsorption of host associated CD62L is proposed as an adapted/expanded tactic of the virus - by acquiring this molecule the virus gains the ability to bind to the same cognate ligands on endothelia that lymphocytes specifically use to perform their immune surveillance function. This ensures maximum contact with lymphocytes, the virus’s preferential target of infection, and sets a supreme platform for trans-infecting lymphocyte. Thibault S, *et al.* (2007), also suggested that trans-infection of lymphocytes might be intensified by the inflammatory state during HIV-1 infection as some dormant CD62L ligands become functional in the presence of inflammatory molecules.

Main research interest

In view of the declining blood DC numbers during HIV-1 mono infection and HIV-1/TB dual infection and lack of restoration on short term ARV therapy, the current study proposed that this phenomenon stems from an anomaly in activity related to apoptosis, cellular activation and/or chemotactic export in response to signals generated at sites of infection/inflammation. The study proposed that further phenotypic analysis of the circulating pool of blood pDCs and mDCs during HIV-1 infection may provide "clues" to the underlying reason for their loss from/lack of recovery in peripheral blood.

The study aim:

The aim of the current study was to phenotypically characterise the (HHF exposed) pool of blood pDCs and mDCs of chronically HIV-1 mono, HIV-1/TB dual infected as well as ARV treated individuals.

The study objectives:

to examine pDC and mDC subsets in relation to their expression the phenotypic markers associated with

- ***apoptosis, which included FAS and its natural ligand (FASL), pro-apoptotic TRAIL-R1 and -R2, anti-apoptotic (survival) TRAIL-R3 and -R4 and TNF-R2 (implicated as death or survival receptor),***
- ***migration, which included CCR9 (a putative GIT homing chemokine maker), CXCR6 (a putative PT homing chemokine marker), CCR5 (lymphoid homing chemokine marker), CCR7 (implicated in lymph node migration) and***
- ***activation/maturation, which included CD86, CD80 (both characterised as markers of DC activation), CD83 (marker of DC maturation) and CD62L (immune activation marker).***

In addition, the cell surface expression of immunemodulatory neuropeptide receptors VPAC1 and VPAC2 was also examine of which the outcome was further discussed in Chapter 5.

The current study proposed that a significant change in frequency distribution (% output) of blood pDCs and mDCs, analysed for the expression of the selected apoptotic, migratory and activation cell surface markers, in current circulation in HIV-1 and HIV-1-related study groups may correlate with underlying loss of DCs from peripheral blood and thus establish any underlying mechanistic link.

4.2 Outline of the study

Refer to sections 4.3.1 - 4.3.11 for a detailed description on sample collection and processing

<table>
<tr><th colspan="9">SAMPLE COLLECTION</th></tr>
<tr><td colspan="9">Patient recruitment, blood collection by venesection at various clinics in the Western Cape, South Africa</td></tr>
<tr><td colspan="9">5 Study groups: Control, ARV$^-$HIV-1, ARV$^-$HIV-1/TB, ARV$^+$HIV-1 and ARV$^+$HIV-1/TB</td></tr>
<tr><td colspan="9">↓</td></tr>
<tr><th colspan="8">WHOLE BLOOD</th><th>PLASMA</th></tr>
<tr><td>50µl</td><td colspan="7">7 x 200 µl</td><td>1ml</td></tr>
<tr><td>↓</td><td colspan="7">↓</td><td>↓</td></tr>
<tr><th>4-COLOUR FLOW CYTOMETRIC QUANTIFICATION</th><th colspan="7">8-COLOUR FLOW CYTOMETRIC PROFILING</th><th>REAL TIME PCR QUANTIFICATION ASSAY</th></tr>
<tr><td rowspan="2">CD4 and CD8 T cells

ASSAY: Staining with BD MultiTEST™ mAbs: CD3 FITC, CD8 PE, CD45 PerCP, CD4 APC in BD TruCOUNT™ tube</td><td colspan="7">pDCs and mDCs

ASSAY: Staining with DCID markers and marker specific mAbs set out in the table below</td><td rowspan="2">Viral load

ASSAY: ABBOTT Real Time HIV-1 PCR assay (ABBOTT m2000rt)/ bioMérieux NucliSens EasyQ® HIV-1, v1.2 test)</td></tr>
<tr><td>Panel A</td><td>Panel B</td><td>Panel C</td><td>Panel D</td><td>Panel E</td><td>Panel F</td><td>Panel G</td></tr>
<tr><td>↓</td><td colspan="7">↓</td><td>↓</td></tr>
<tr><td></td><td colspan="7">DATA COLLECTED</td><td></td></tr>
<tr><td>CD4 and CD8 T cells
- cells/µl</td><td colspan="7">pDC and mDCs
- % of pDCs/mDCs positively expressing cell surface markers of interest</td><td>Viral load
- RNA copies/ml</td></tr>
</table>

**Refer to Chapter 5*

4.3 Material and Methods

4.3.1 Study groups and clinical data

A new cohort of patients were recruited and similar to the previous chapter also five different study groups, (Control (n=38), ARV^-HIV-1 (n=62), ARV^-HIV-1/TB (n=14), ARV^+HIV-1 (n=40) and ARV^+HIV-1/TB (n=25) study groups) were included for this second part of study. Table 3.1 defines the criteria used for the enrolment of candidates for the different study groups employed in this part of the study. Recruited patients on ARVs were using one of the following treatment regimens: Tenofovirdisoproxil fumarate(TDF), Lamivudine, EFV (39% of the total ARV users); Stavudine, Lamivudine, EFV (32%); Stavudine, Lamivudine, NVP (11%); TDF, Lamivudine, NVP (7%) and less than 11% were using different combination of ARV therapy. TB co-infected patients were either using Pyridoxine or Rifafour (Combination of four agents: Rifampicin, Isoniazid, Pyrazinamide and Ethambutol) drugs. Participants were recruited (May 2010 – Mar 2012) from state clinics in a peri-urban area of Cape Town, South Africa, which included Tygerberg (2% of the total recruits), Idasvalley (17%), Durbanville (29%), Kuilsriver (2%) and Kraaifontein (8%) as well as the Desmond Tutu Emavundleni Clinic Site in Khayelitsha (41%). Participants from the latter site were predominantly enlistees of the and ARV^-HIV-1 study groups. Demographic and clinical data of the participants in each study group are shown in Table 4.1.

Informed consent was obtained from all the study participants. The study was reviewed and approved by the HREC of the Faculty of Medicine and Health Sciences of Stellenbosch University (Ethics reference number N08/02/057). Ethical approval for the collection and analysis of blood samples from participants recruited at the Desmond Tutu Emavundleni Clinic Site in Khayelitsha was initially obtained from the Research Ethics Committee (REC) of the Health Sciences Faculty of the University of Cape Town (UCT) (Ethics reference number 417/2006) with subsequent amendments to the project approved by the HREC of US.

Table 4.1: Demographic and clinical data of participants in the study groups analysed for the phenotypic profiling of pDCs and mDCs

	Study Groups				
	Control	ARV$^-$		ARV$^+$	
		HIV-1	HIV-1/TB	HIV-1	HIV-1/TB
Total (n)	38	62	14	40	25
Male: Female nr %	17:21 45:55	9:53 15:85	7:7 50:50	17:23 42:58	12:13 48:52
Age[a] Median Range	29 19 - 58	31 18 - 50	34 23 - 69	37 13 - 56	37 25 - 50
Time on ARV therapy[b] Median (m) Range	N/A	N/A	N/A	18 <1 - 75	5.5 <1 - 76
Time on anti-TB therapy[b] Median Range	N/A	N/A	0.5 <1 - 8	N/A	3 <1 - 8

[a] *Age median and range expressed in years*
[b] *Time on treatment median and range expressed in months*

4.3.2 General specimen processing

Each of the participants enrolled in the study was allocated a patient number and all laboratory procedures were performed in reference to this number. Whole blood was collected aseptically by venisection into either EDTA or Lithium Heparin vacutainer tubes. Blood specimens from the Desmond Tutu Emavundleni Clinic Site were provided in (1x10 ml) Lithium Heparin vacutainer tubes (BD Biosciences, San Jose, CA) of which a volume of 1.4 ml was allocated for phenotyping blood pDC and mDC (The remaining blood volume was used in other ethically permitted studies). Additionally, blood (1x5 ml) collected in the EDTA vacutainer tubes (BD Biosciences, San Jose, CA) were provided for CD4 and CD8 T lymphocyte count (refer to section 3.3.6) and plasma collection for viral load quantification (refer to section 3.3.7) and/or storage at -80℃. Whole blood specimens from other clinics (refer to section 4.3.1) were collected in (1x10 ml) EDTA vacutainer tubes (BD Biosciences, San Jose, CA) of which 500µl were aliquoted into screw cap tubes for the CD4 and CD8 T lymphocyte count application (refer to section 3.3.6) and 1.4 ml used for profiling blood pDC and mDC. The remaining blood volume was used for plasma collection to determine the viral load (refer to section 3.3.7) and/or storage at -80℃. Processing of samples was at all times performed in a biosafety cabinet (NUAIRE biological class II safety cabinet).

4.3.3 mAbs used for the phenotypic profiling of pDCs and mDCs

A total of 15 different mouse anti-human mAbs were included in the study which aided in investigating specific phenotypic properties of pDCs and mDCs during HIV-1 infection. These were grouped into seven panels, labeled A to G, and were used in conjunction with the DCID mAbs to directly stain whole blood. Refer to Table 4.2 for a summary on these panels and corresponding markers as well as details on the clone and isotype of the mAbs. The mAbs were obtained from Biolegend[1] (San Diego, CA), BD Biosciences[2] (San Jose, CA) and R&D systems[3] (Minneapolis, MN).

In reference to the sub-project of the larger study, which aimed at examining the effect of the immunemodulatory protein VIP upon TLR activated pDCs and mDCs (refer to Chapter 5), mAbs for the VIP receptors, VPAC1 and VPAC2, were included in the phenotypic staining panel. These mAbs were purchased as unlabeled antibodies from MerckMillipore (Temecula, CA) and R&D systems (Minneapolis, MN), respectively (refer to Table 4.2 for clone and isotype information). The Lightning-Link™ fluorochrome conjugation kit from Innova Biosciences (Babraham, Cambridge, UK) was used to label VPAC1 to the fluorochrome PE and VPAC2 to PerCP according to the manufacturer's instructions. A VPAC1 PE and VPAC2 PerCP stock concentration of 50µg/ml was prepared in 1 x Phosphate buffer saline (PBS) pH 7.4 (Gibco® Carlsbad, CA, USA). To simplify data reporting, the staining profile of these receptors on pDCs and mDCs in fresh whole blood was discussed in Chapter 5.

Table 4.2: mAb panels used for the phenotypic profiling of pDCs and mDCs.

Panels	mAb	Clone	Isotype	Alternate names
DCID	HLA-DR APC-Cy[a]™7 [1] CD123 PE-Cy™7 [1] CD11c Pacific blue™ [1] LIN1 FITC [2]	L243 6H6 Bu15 Refer to chapter 3	mouse IgG_{2a}, κ mouse IgG_1, κ mouse IgG_1, κ Refer to chapter 3	- - - -
Panel A	CCR5 APC [2] CCR7 PerCP [3] CD80 PE [1]	3A9 150503 2D10	mouse IgG_{2a}, κ mouse IgG_{2a} mouse IgG_1, κ	CD195 CD197 -
Panel B	CXCR6 APC [3] CCR9 PE [3] CD83 PerCP-Cy™5.5 [1]	56811 112509 HB15e	mouse IgG_{2b} mouse IgG_{2a} mouse IgG_1, κ	CD186 CD199 -
Panel C	TRAIL-R1 APC [1] TRAIL-R3 PE [1]	DJR1 DJR3	mouse IgG_1, κ mouse IgG_1, κ	CD261/DR4 CD263/DcR1
Panel D	TRAIL-R2 APC [1] TRAIL-R4 PE [3]	DJR2-4 (7-8) 104918	mouse IgG_1, κ mouse IgG_1	CD262/DR5 CD264/DcR2
Panel E	TNF-R2 PE[3]	22235	mouse IgG_{2a}	CD120b
Panel F	CD86 PerCP-Cy™5.5 [1] FASL PE [1] FAS Alexa Fluor®647 [1]	IT2.2 NOK-1 DX2	mouse IgG_{2b}, κ mouse IgG_1, κ mouse IgG_1, κ	- CD178/CD95L CD95
Panel G	CD62L APC [2] VPAC1[b] PE VPAC2[b] PerCP	DREG-56 - 476031	mouse IgG_1, κ mouse IgG_{2a} mouse IgG_1	- VIP R1 VIP R2

[a]*Cy refers to Cyanine*

[b]*Refer to Chapter 5*

4.3.4 Optimization of mAb volume for multi-parameter flow cytometry (mAb titration)

The minimum volume of mAb that would produce the greatest signal- to- background ratio was determined for all the mAbs used in this study. Each of the mAbs listed in Table 4.2 were serially diluted (2-fold) in staining buffer with the highest titer representing a volume equal to the manufacturer's recommendation and the lowest titer equal to a 1:256 dilution. Whole blood (EDTA, 200µl/titration) was separately stained with each of the titrated mAbs (dilution series prepared in staining buffer (0.4% heat-inactivated foetal calf serum in 1 x PBS pH 7.4 (Gibco® Carlsbad, CA, USA) in a 50µl total volume) following the procedure described in section 4.3.5. The samples were acquired uncompensated on the BD FACSCanto™ II 8-colour flow cytometer (BD Biosciences, San Jose, CA). In determining the optimal volume of mAb one requires the median fluorescent intensity (MFI) value of both positive (marker bound) and negative (marker unbound) fluorescent signals generated by the populations of interest, therefore, an unstained sample was also prepared. Furthermore, as this procedure entailed the use of single marker stains, identification of rare DC-related events was required in the absence of the four DCID surface markers. This was performed by targeting events in the relative position in which DCs are found in a SSC – Area (A) vs. Forward Scatter (FSC) - A density plot. Recall that in this platform, due to the morphological properties (granularity and size) of the DCs, these cells are scaled between the monocyte and lymphocyte population. Accordingly, DC-related events were collected using a tight polygon gate and displayed in a SSC - A vs. titrated marker density plot. Interval gates were used to collect negative and positively stained DC events for each of the titer points of the titrated mAb and to obtain the according MFI values. The ratio of positive to negative MFI for each titration point was plotted on a line graph, with the antibody concentrations on the x-axis and the MFI ratio on the y-axis. The corresponding titrated value at the point where the curve reached a plateau was selected as optimal.

4.3.5 Whole blood staining procedure for the phenotypic profiling of pDCs and mDCs

Staining of whole blood was performed in 12 x 75 mm, 5 ml polystyrene round bottom capped Falcon™ tube (BD Biosciences, San Jose, CA). For each patient, seven of these tubes were prepared and appropriately labeled with the patient number and name of the specific staining panel. Whole blood (200µl) was added to each of these test tubes followed by 50µl of the relevant freshly prepared mAb cocktail. These cocktails were prepared in seven appropriately labeled Eppendorf tubes (Hamburg, Germany) each consisting of staining buffer (0.4% heat-inactivated foetal calf serum in 1 x PBS pH 7.4 (Gibco® Carlsbad, CA, USA)), DCID mAbs and the relevant mAbs defined for each of the staining panels A-G (refer to Table 4.2). The volume of the mAbs (predetermined via titration) was as follows: a volume of 2µl was used for mAbs CCR5 APC, CD80 PE, TRAIL-R1 APC, TRAIL-R3 PE, TRAIL-R2 APC, FASL PE, CD62L APC, VPAC1 PE and VPAC2 PerCP; a volume of 1µl was used for mAbs CCR7 PerCP, CXCR6 APC, CCR9 PE, TRAIL-R4 PE and TNF-R2 PE; and a volume of 0.5µl was used for mAbs CD83 PerCP-Cy™5.5, FAS Alexa Fluor®647 and CD86 PerCP-Cy™5.5. The predetermined titrated volumes for the DCID surface markers were as follows, 2µl for the LIN1 FITC, HLA-DR APC-Cy™7 and CD123 PE-Cy™7 mAbs and 0.5 µl for CD11c Pacific blue™ mAb.

Whole blood was incubated with the prepared cocktails for 30 min at room temperature in the dark. Red blood cell lysing and cell fixation was performed with 1.8 ml of 1x BD FACS Lysing solution (BD Biosciences, San Jose, CA) and incubated for 10 min at room temperature in the dark. Centrifugation at 400 x g (Hettich

Rotanta 460R, Massachussets, USA) for 5 min allowed for the collection of the leukocyte pellet and after discarding the supernatant, 2 ml staining buffer (0.4% heat-inactivated foetal calf serum in 1x PBS pH 7.4 (Gibco® Carlsbad, CA, USA)) was added. The wash step was repeated and the supernatant discarded by inverting the tube and blotting the inverted tube dry on absorbent paper. The sample was resuspended in 500µl staining buffer and immediately acquired on a BD FACSCanto™ II 8-colour flow cytometer (BD Biosciences, San Jose, CA). Debris was excluded from the acquired data by placing a threshold value of 0 - 50 000 on the FSC - A scale. A total of 750 000 total events were acquired per sample. Data on the height (H), area (A) and width (W) of the fluorescence pulse generated in the different channels was collected.

4.3.6 Instrument controls: Daily set up and performance monitoring of the flow cytometer

Optimal performance of the 8-colour BD FACSCanto™II digital flow cytometer was monitored by the use of BD Cytometer Setup and Tracking beads. These beads, stained by the manufacturer with a mixture of specific fluorochromes, are excited by the lasers of the flow cytometer and emits in all the detectors. Accordingly, several automated measurements were taken to establish optimal baseline photomultiplier tube voltages to maximise population resolution in each detector. The application of CST beads allowed for monitoring cytometer performance on a daily basis.

4.3.7 Assay controls for the analysis of marker expression by pDCs and mDCs

4.3.7.1 Assay control 1: fluorochrome single stains to assess bead-based compensation settings

Compensation in flow cytometry refers to the mathematical “removal” of the fluorescent spillover occurring when the emission spectra of a specific fluorochrome overlaps into an unassigned (secondary) detector. Corrected compensation results in the detection of fluorescence only in the assigned (primary) detector and in multi-color flow cytometry this is calculated with the use of BD™ CompBeads (BD Biosciences, San Jose, CA). Single stains of these polystyrene micro-particles are prepared, according to the manufacturer’s instructions, using the same fluorochrome conjugated antibodies intended to stain samples in a proposed multi-color experiment. Two sets of these beads are simultaneously stained; one set binds to any anti-mouse κ light chain antibody while the other set lacks binding properties. This allows for the detection of distinct positive and negative fluorescence signals required for calculating compensation settings. In the current study these settings were determined by BD FACSDiva™ software v6.1.3 (BD Biosciences, San Jose, CA).

Next, single stain controls were again applied but in this case they were used to determine whether the bead-based compensation settings sufficiently withdrew the spectral overlap from unassigned detectors when applied to cell analysis. These single stain controls were prepared by staining aliquots of whole blood (as outlined in section 4.3.5) individually with the pre-determined optimal volume of mAbs for the DCID and markers of Panels A-G (this was also performed for Panel 5 and 6 (refer to Table 5.4)). These samples were acquired on the BD FACSCanto™ II 8-colour flow cytometer (BD Biosciences, San Jose, CA) with the pre-determined bead-based compensated settings applied. The gating strategy as described in section 4.3.4 was employed to identify the DC population from total acquired events, which was then displayed in a combination of 6 density plots, assigning the specific single stain control to the x-axis and the parameters of the remainder detectors to the y-axis. Detection of spillover entailed evaluating the signal produced by the

single stain in each of the detectors employed in a specific staining panel. A positive signal produced in detectors other than that of the single stain control was identified spillover and required manual adjustment of the bead-based compensation value. A (false) positive signal in an unassigned detector defines the overlap as under-compensated. In addition, single stains can also be used to identify over-compensation which can also be rectified manually.

In the current study, bead-based compensation, in most cases, was optimal for the analysis of cells. However, the calculated value was not sufficient to correct the overlap of APC-Cy™7 fluorescence into APC/Alexa Fluor®647 detectors and further adjustment was required (*in the current study this fluorochrome was used conjugated to the antibody HLA-DR, one of the DCID surface markers. As DCs positively expressed this marker, the positive fluorescent signal generated in the APC-Cy™7 channel overlapped into APC/Alexa Fluor®647 detectors. Hence, the correct removal of the overlap was essential as APC/ Fluor®647 was used conjugated to mAbs directed towards the analyses of the phenotypic markers of interest).* Accordingly, manually correcting compensation entailed tweaking (using BD FACSDiva™ software v6.1.3 (BD Biosciences, San Jose, CA) the initial bead-based compensation value for removal of overlapping primary fluorescence, APC-Cy™7, from the unassigned secondary detector, APC/Alexa Fluor®647, so that the median APC/Alexa Fluor®647 fluorescence of the APC-Cy™7 positive population is similar to that of the APC-Cy™7 negative population (Hulspas R, *et al.* 2009; Herzenberg LA, *et al.* 2006). This procedure of adjusting compensation values required the specific use of unstained and APC-Cy™7 single stained DC events, to obtain a negative and positive APC-Cy™7 signal for manually adjusting compensation. This preparation would then entail identifying DCs upon morphological properties (as described in section 4.3.4). However, as it was later found that this procedure does not maximally identify DCs (gating DCs using this method results in DC events contaminated with monocytes and lymphocytes) and foreseeing that this method of collecting DCs might become more complex upon daily compensation checks, especially with samples from HIV-1 infected patients being limited in number due to HIV-1 induced cellular changes, the current study sought for an alternative method to correct and check compensation on DC events, specifically.

In analyses of FMO staining controls, the influence of overlapping fluorescence in DC specific events could be clearly observed and corrected. The purposes of these controls in multi-parameter flow cytometry are discussed in more detail in section 4.3.7.2. Briefly, it entails staining cells with all the markers in a specific multi-color panel with the simple exclusion of one marker at a time. However, in the current study these controls were prepared by staining whole blood with all the DCID markers, but applying FMO staining only to the markers of interest in each panel. Hence, the influence of e.g. overlapping APC-Cy™7 fluorescence in the APC/Alexa Fluor®647 channel, when the latter fluorochrome was omitted from the staining assay, could be detected with DC events, specifically. Attempting to adjust the abovementioned overlap observed in the DC events using randomly selected events negatively stained with APC-Cy™7 (recall that a negative and positive signal are required to adjust compensation) was not optimal (observing mostly an overcompensation profile in the DC subsets), presumably due to differential autofluorescence properties of events. In view of this, the study approached several strategies similar and different to the conventional method to correct compensation and found the following most optimal. In analyses of FMO controls of the APC/Alexa

Fluor®647 fluorochrome the study observed that in addition to the high intensity of APC-Cy™7 positive DC events overlapping into the unassigned secondary APC detector (refer to Figure 4.1: green-coloured events A1 (pDCs) and B1 (mDCs), a portion of these events showed minor to zero frequency of overlapping events (pink and blue events, Figure 4.1 A1 and B1, respectively). Consequently, and as expected, the APC fluorescence intensity of these opposing events was very different. Conversely, amongst fluorochrome combinations with non-overlapping properties or where bead-based compensation sufficiently corrected overlapping fluorescence, e.g. PE and APC-Cy™7, it was observed that the signal generated in the secondary unassigned detector (e.g. PE), when comparing 50% of events lower to 50% of events higher than the fluorescence peak of the positive events generated from the primary assigned detector (APC-Cy™7), had similar fluorescence signal intensities. (Figure 4.1 A2 and B2, comparing the MFI of green events to pink and blue events, respectively). Accordingly, using a histogram to display APC-Cy™7 positive pDC and mDC events an interval gate was used to collect 50% of APC-Cy™7 positive pDC and mDC events lower than peak APC-Cy™7 fluorescence, which mostly included the non to minimal overlapping and lower fluorescent intensity portion of events. Similarly, events that included the higher fluorescing and, subsequently, greater overlapping APC-Cy™7 events (Figure 4.1 A3 and B3) were also collected. The compensation value was adjusted using BD FACSDiva™ software v6.1.3 (BD Biosciences, San Jose, CA) so that the APC MFI value of these events closely matched (Figure 4.1 A4 and B4). This technique was effective for correcting compensation and removing overlapping events, yet proved to be time-consuming as gates to collect 50% of lower and higher than APC-Cy™7 fluorescent peak events had to be slightly adjusted for every sample. However, further analyses confirmed that equalizing the APC MFI value of total pDC or mDC events to that of the relevant lower intensity fluorescent peak events was also effective and a more rapid technique for correcting overlapping fluorescence.

In addition to the removal of the APC-Cy™7 fluorescence overlap from the APC detector, certain batches of antibodies required removal of overlapping PE-Cy™7 and PerCP/PerCP-Cy™5.5 fluorescence from the PE channel. Similar adjustments, as described above, were performed to correct compensation.

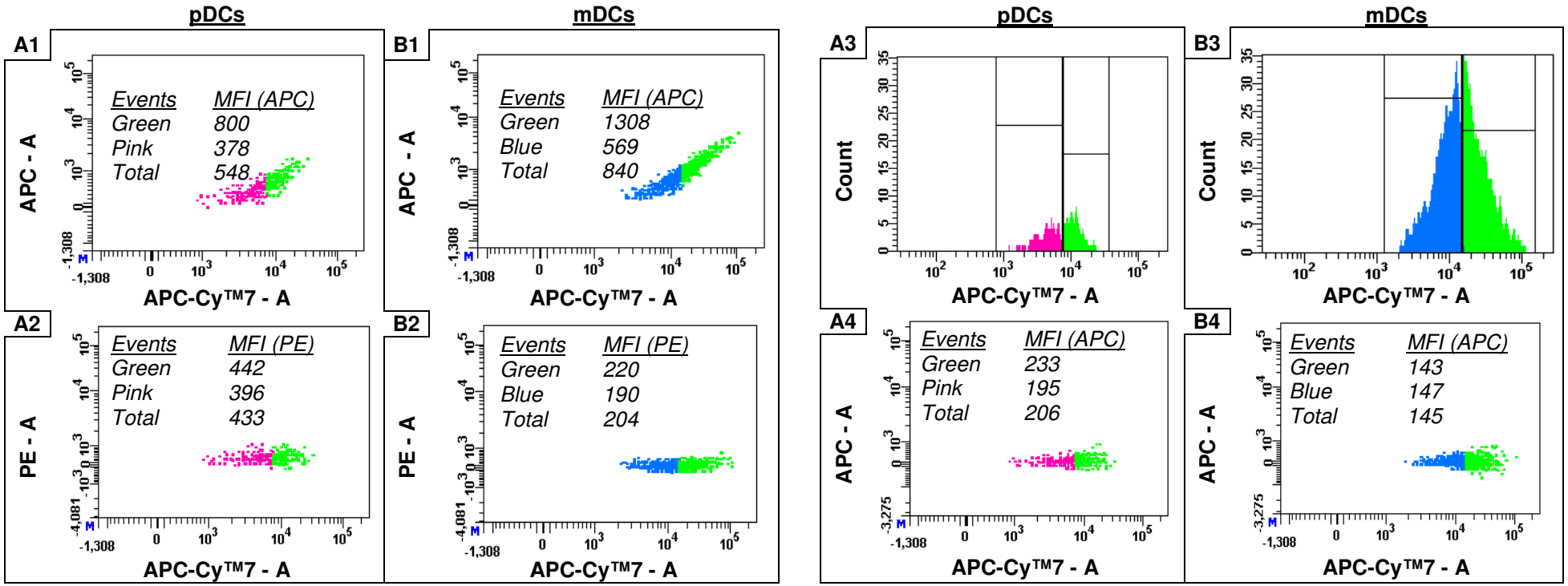

Figure 4.1: Compensating the fluorescence overlap of APC-Cy™7 into APC.

A1 and B1 show the profile of the influence of overlapping (green-coloured) and non-overlapping fluorescence (pDCs: pink-coloured; mDC: blue-coloured) from the primary detector, APC-Cy™7, into the secondary unassigned detector, APC, upon DC events specifically. Refer to the MFI (APC) values, which show the different APC MFI values between the overlapping and non-overlapping fluorescence. A2 and B2 show the profile of non-overlapping events between e.g. primary APC-Cy™7 and secondary PE detector with corresponding APC MFI when comparing green to pink and blue events. A3 and B3 illustrate the method used to collect the overlapping green (corresponding to 50% higher than peak pDC and mDC events) and non-overlapping pink/blue events (corresponding to 50% lower than peak pDC and mDC events, respectively) so to compare and equate APC MFI values and eliminate false positive data. A4 and B4 show the resulting profile of pDCs and mDCs events upon removal of the overlapping fluorescence.

4.3.7.2 Assay control 2: The role of Fluorescence Minus One (FMO)

Prior to the analysis of expression of marker of interest by pDCs and mDCs (or any other cell type), background or artefact fluorescence in relevant detectors must be defined as this could lead to false positive results. Recognition of these artefacts is mainly important where marker expression is negative and is characteristic of events having slightly higher fluorescent intensity than negative expressing events. Specifically, the tandem dyes (Cy™5, Cy™7, Texas red®) have been implicated as contributors of either direct (Forman MA or Gupta RK, 2007) or indirect (Maecker HT, *et al*. 2004) background fluorescence. Note that tandem dyes, in contrast to the conventional fluorochromes, consist of two fluorescent molecules, namely the donor (i.e. APC) and acceptor (i.e.Cy™7). This combined fluorochrome has the excitation properties of the donor but the emission properties of the acceptor.Forman MA and Gupta RK (2007) showed in staining leukocytes with CD3 PE-Cy™5, atypical CD3 positive expression by monocyte was observed, a cell type characteristic of negative CD3 expression. It was concluded to be the result of non-specific binding of the CD3 conjugated tandem dye to monocytes. A detailed report by Maecker HT, *et al*. (2004) showed how false positive events observed in the APC and PE detectors were dependent on cells positively stained with APC-Cy™7 andPE-Cy™7, respectively. They proposed that this phenomenon might be due to a break in the bond between the donor (APC or PE) and acceptor dye (Cy™7) with resulting fluorescence in the donor detector. It should also be noted that 1) background staining may differ between new batches of tandem dye conjugated antibodies and 2) these dyes are sensitive to unfavourable conditions. Excessive exposure to light and fluctuating temperature can cause a break in their chemical structure resulting in enhanced non-specific binding. This is a specific problem with tandem dyes.

The procedure performed to detect for possible false positive events entails the application of FMO controls. These controls, in contrast to single stain controls, were prepared by staining cells with all the markers in a specific multi-color panel with the simple exclusion of one marker at a time. In doing so total background fluorescence, contributed either directly or indirectly (as described above), can be detected in the channel in which the corresponding fluorochrome was omitted. In the current study FMO staining controls were prepared for the markers of interest but not for the DCID markers as 1) exclusion of any one of the 4 DCID markers would hinder the identifications of DCs per se from total events and 2) primarily, detection/evaluation of <u>total</u> background fluorescence, contributed by the fluorescence from the DCID markers and/or other positively expressed markers, in the FMO applied channel of the markers of interest was of relevance. Recognizing which fluorochrome(s) specifically contributed towards background fluorescence in the channels dedicated to examine expression of the markers of interest was not important. The main aim of this procedure was to monitor background fluorescence and guide placement of the gates so to exclude false positive events generated by background fluorescence.

In addition to FMO controls serving to identify background fluorescence, this technique (reported more accurate than isotype controls) also aids in defining the staining boundary of negative expressing events and are most valuable in cases were positive events do not separate well from negative events (Herzenberg LA, *et al*. 2006; Perfetto SP, *et al.* 2004). Also, in drawing combination two-parameter density plots using the FMO control stain vs. the other markers of a relevant panel, enabled detection and examination of

fluorescence overlap specific to the DC events which was adjusted following the method as discussed in section 4.3.7.1.

In the current study, FMO controls were prepared following the procedure on whole blood staining and sample acquisitions as described in section 4.3.5. Whole blood from an HIV-1 seronegative individual was used. Post-staining sample analyses required 1) defining the pDCs and mDCs from the total acquired events using the gating strategy as shown in section 4.3.9 (Figure 4.20) followed by 2) examining DC events for possible background fluorescence caused by non-specific binding (especially were marker expression is found negative (FMO vs. marker stain) and 3) setting gates on the negative staining boundary. Density plots with gates were created for each of the FMO staining controls prepared for the 15 phenotypic and 2 immunemodulatory markers of interest (Table 4.2) and the profile obtained compared to staining profile of marker stained samples. Accordingly, events of marker stained samples displayed outside the staining boundary of these gates and displaying strong increased signal intensity were regarded as positively expressing the marker of interest. Marker expression that displayed the same profile as the relevant FMO control was regarded as evidence for the lack of expression of marker of interest. Events collected via the gate of marker stained samples were used for statistical analyses.

Certain literature (Baumgarth N& Roederer M, 2000) recommends performing single stains (refer to section 4.3.7.1) and FMO controls with daily experiments. Notwithstanding the fact that preparation of these controls is labour intensive and time-consuming it is also a prohibitively expensive routine. In an attempt to preserve resources, single stain and FMO controls were performed once after bead-based compensation setting was established to take note of the 1) markers with potential risk of overlapping into unassigned secondary detectors, 2) approximate staining boundary of positive and negative events and 3) channels prone to background staining. Upon exclusion of FMO controls from the assays, internal controls were sought to aid in accurately distinguishing between negative and positive events for the marker of interest in daily experiments. These internal controls were required to have a data spread profile (related to autofluorescence and/or compensation-induced) similar to that of the DCs upon FMO staining of markers of interest. It was determined that basophils and negative events collected from a $LIN1^{-}HLA\text{-}DR^{-}$ gate as well as events from a $LIN1^{+}HLA\text{-}DR^{+}$ gate were suitable to employ as internal controls. Specifically, it was found that the data spread of negative events collected from a $LIN1^{-}HLA\text{-}DR^{-}$ gate were similar to the event distribution of both DCs in the PE channel and mDC events in the PerCP and PerCP-Cy™5.5 channel. The data spread of basophils in the latter two channels corresponded to that of pDCs. Furthermore, the data spread of events within the $LIN1^{+}HLA\text{-}DR^{+}$ population was similar to that of pDC and mDC events in the APC and Alexa Fluor®647 channel (refer to Figure 4.2 in which the data spread in the APC/Alexa Fluor®647, PerCP/PerCP-Cy™5.5 and PE channels are displayed: the basophil and negative population captured from the $LIN1^{-}HLA\text{-}DR^{-}$ gate are shown as grey and black coloured events, respectively, and the control population from the $LIN1^{+}HLA\text{-}DR^{+}$ gate are represented as brown-coloured events). In cases were the data spread of the internal control coincided with that of the DC events, marker expression was regarded as negative and where a shift in the distribution of pDC and/or mDC events (accompanied by increase in MFI) in relation to the control occurred, marker expression was determined as positive.

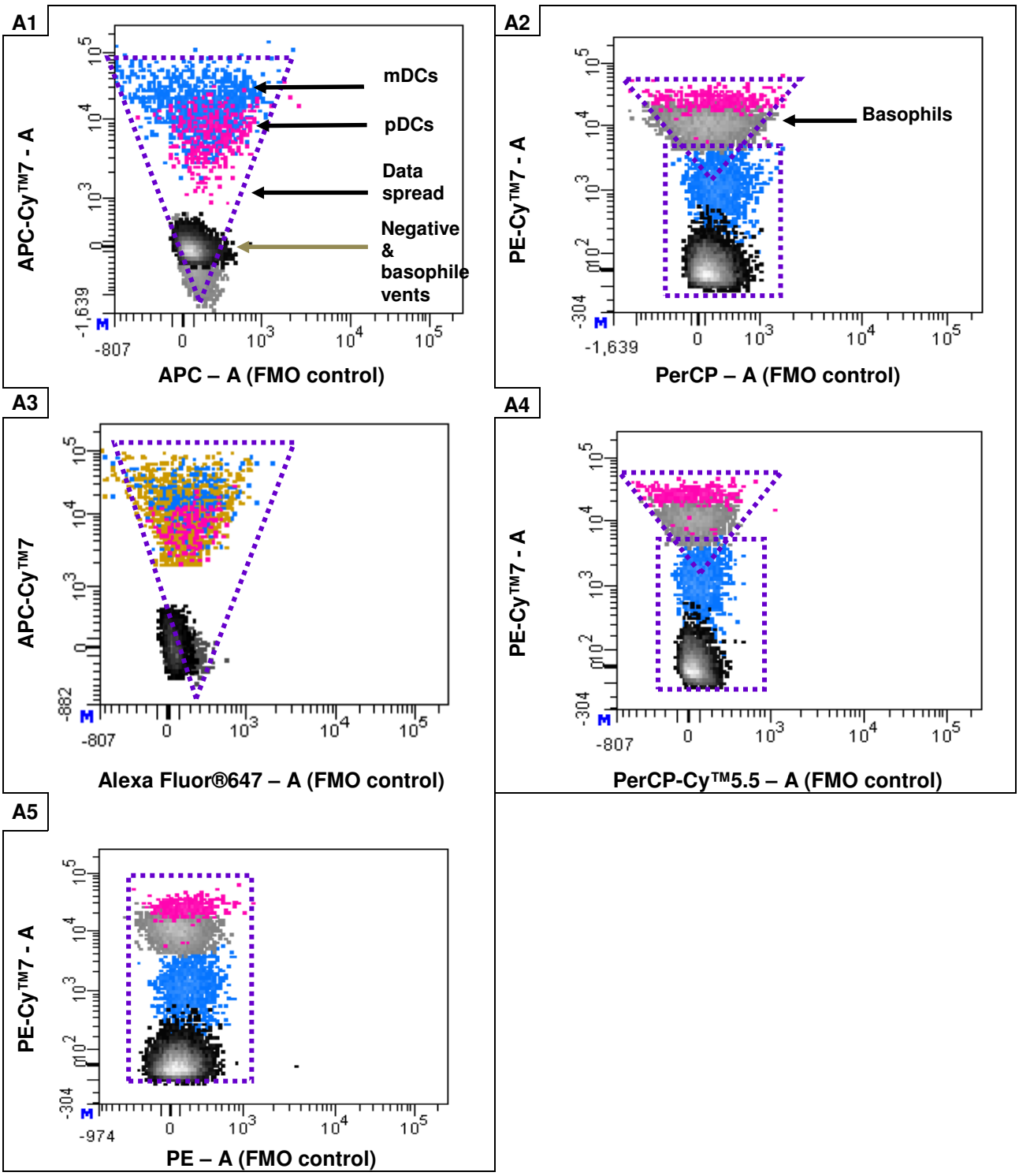

Figure 4.2: Data spread profile of FMO control stains related to the APC/Alexa Fluor®647, PerCP/PerCP-Cy™5.5 and PE channels

The graph shows the data spread (purple-coloured dotted line) of pDC (pink-coloured) and mDC (blue-coloured) events in the APC (A1), PerCP (A2), Alexa Fluor®647 (A3), PerCP-Cy™5.5 (A4) and PE (A5) channel in relation to negative stained (black-coloured), basophil (grey-coloured)and LIN1$^+$HLA-DR$^+$ events (brown-coloured).

4.3.8 Analysis method of acquired events

In analysis of the FMO control and marker stained samples, the use of two-parameter density plot and Height (H) vs. Area (A) parameters of the fluorescent signal related to the marker of interest, e.g. TNF-R2 PE – H vs. TNF-R2 PE – A, were found to give better resolution in characterizing negative/positive events than the conventional marker X - Area vs. marker Y - Area (e.g. HLA-DR APC-Cy™7 - A vs. TNF R2 PE – A) assessment. Latter analyses produced a dispersed profile (due to characteristic rare number distribution) of DC events, while the former analysis method produced a profile of condensed events simplifying, to a degree, event analyses. Also, by employing two entities of the fluorescent signal, height and area, negative and positive events with a more distinct discrimination profile was obtained. Refer to Figure 4.13 for an illustration on mDC events in a TNF-R2 PE – H vs. TNF-R2 PE – A density plot with (marker stain) or without (FMO control stain) TNF-R2 PE staining to observe the different event profile of negative and positive TNF-R2 marker staining on mDCs using this platform of analyses. This method was also found optimal in analysis of samples when slight shifts in fluorescence occurred due to instrument related changes or upon staining with new batches of antibodies. Furthermore, in analyses of events two gates, solid and dashed line parallelograms, were used to identify the staining boundary and collect positive events, respectively. Refer to Figures 4.3 – 4.19 which illustrate the marker and FMO control stain for the 17 markers investigate. Graphs A1, B1 and C1 display the internal control, pDC and mDC events as per FMO control stain, respectively. Graphs A2, B2, C2 display the internal control, pDC and mDC events as per marker stained sample, respectively.

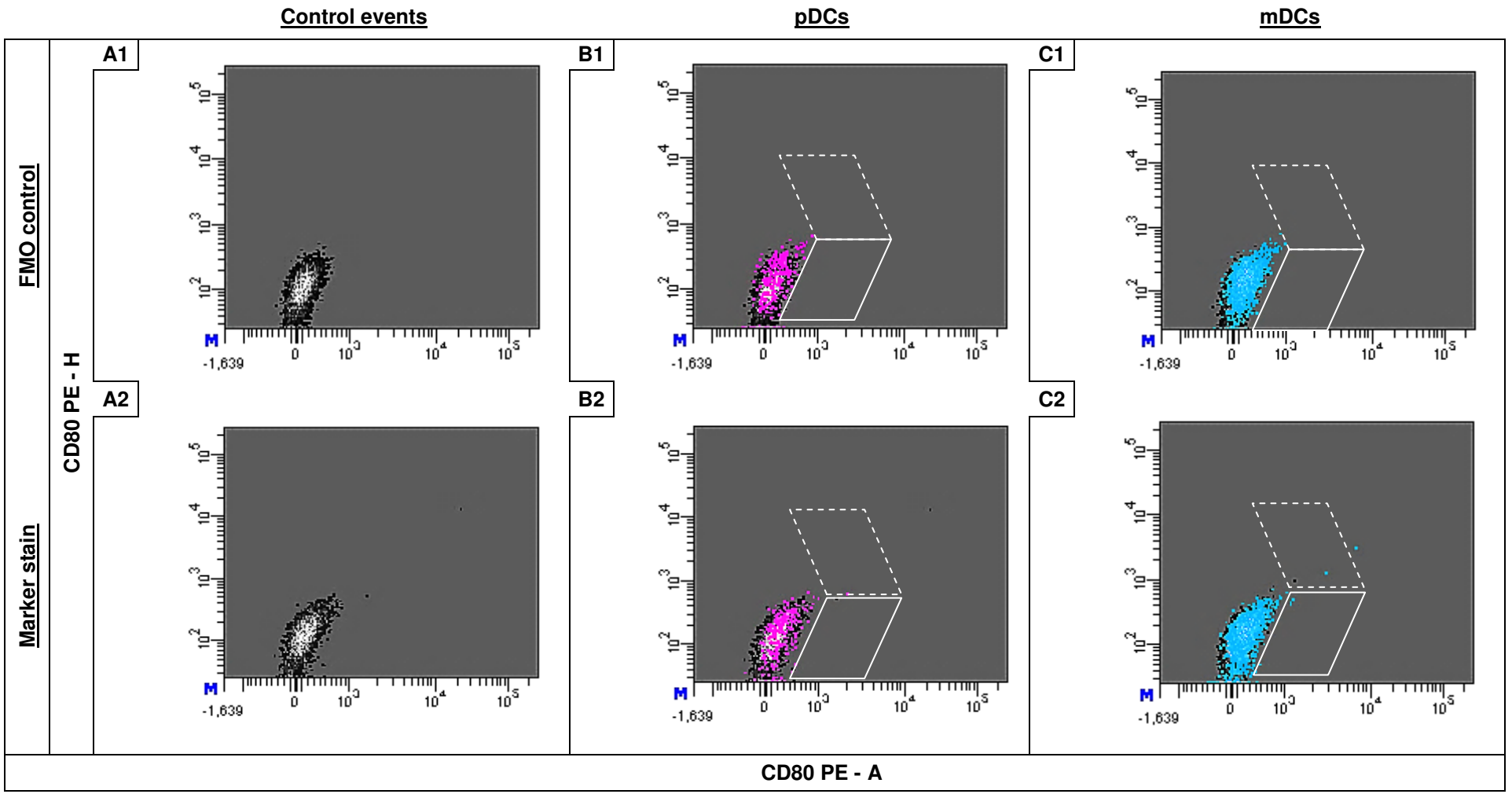

Figure 4.3: pDC and mDC staining profile of CD80 and relevant FMO control

Graph A1-C1 and A2-C2 represents the control, pDC (pink-coloured) and mDC (blue-coloured) events upon CD80 FMO control and marker staining, respectively. B1-2 and C1-2contains DC (to the front) and control events (black-coloured and displayed to the back of the DC population) to show the relationship of pDCs and mDCs to control events. The white dash border gate was used to capture positive events for statistical analysis. Events within the solid gate were not regarded as positive.

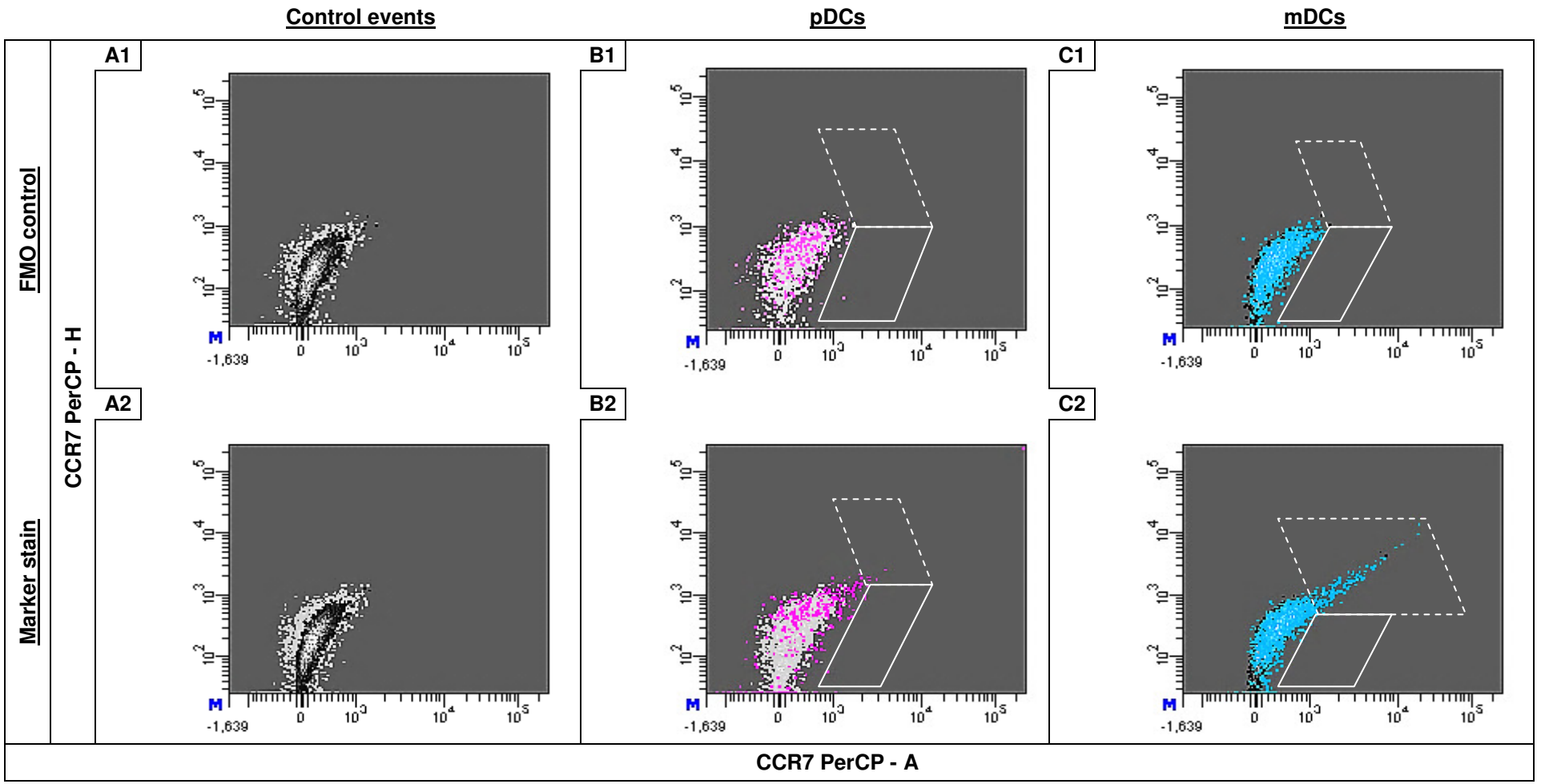

Figure 4.4: pDC and mDC staining profile of CCR7 and relevant FMO control

Graph A1-C1 and A2-C2 represents the control, pDC (pink-coloured) and mDC (blue-coloured) events upon CCR7 FMO control and marker staining, respectively. B1-2 and C1-2contains DCs (to the front) and control events (grey-coloured for pDCs and black-coloured for mDCs, displayed to the back of the DC population) to show the relationship of pDCs and mDCs to control events. The white dash border gate was used to capture positive events for statistical analysis. Events within the solid gate were not regarded as positive.

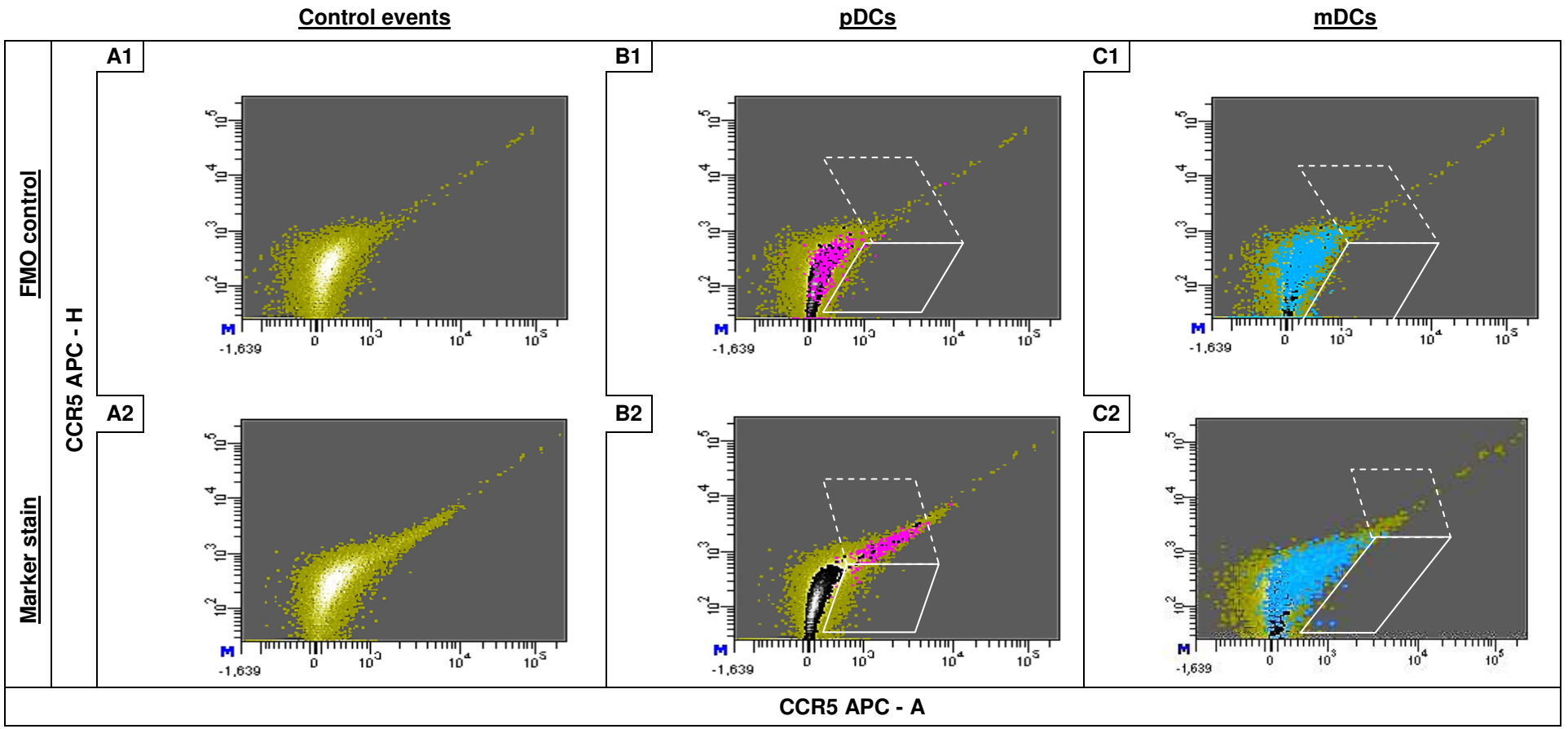

Figure 4.5: pDC and mDC staining profile of CCR5 and relevant FMO control

Graph A1-C1 and A2-C2 represents the control, pDC (pink-coloured) and mDC (blue-coloured) events upon CCR5 FMO control and marker staining, respectively. B1-2 and C1-2 contains DC (to the front) and control events (black and brown-coloured and displayed to the back of the DC population) to show the relationship of pDCs and mDCs to control events. The white dash border gate was used to capture positive events for statistical analysis. Events within the solid gate were not regarded as positive. ***Note the different placement of the gate in the FMO control vs. the marker stain for the pDCs and mDCs. In the latter stain the gate was placed in reference to the tail of positive events displayed by the brown coloured control events as the gate placed according to FMO control was not sufficient in capturing pDC and mDC positive CCR5 events, attributed to data spread difference in the channel upon negative and positive expression of the marker.***

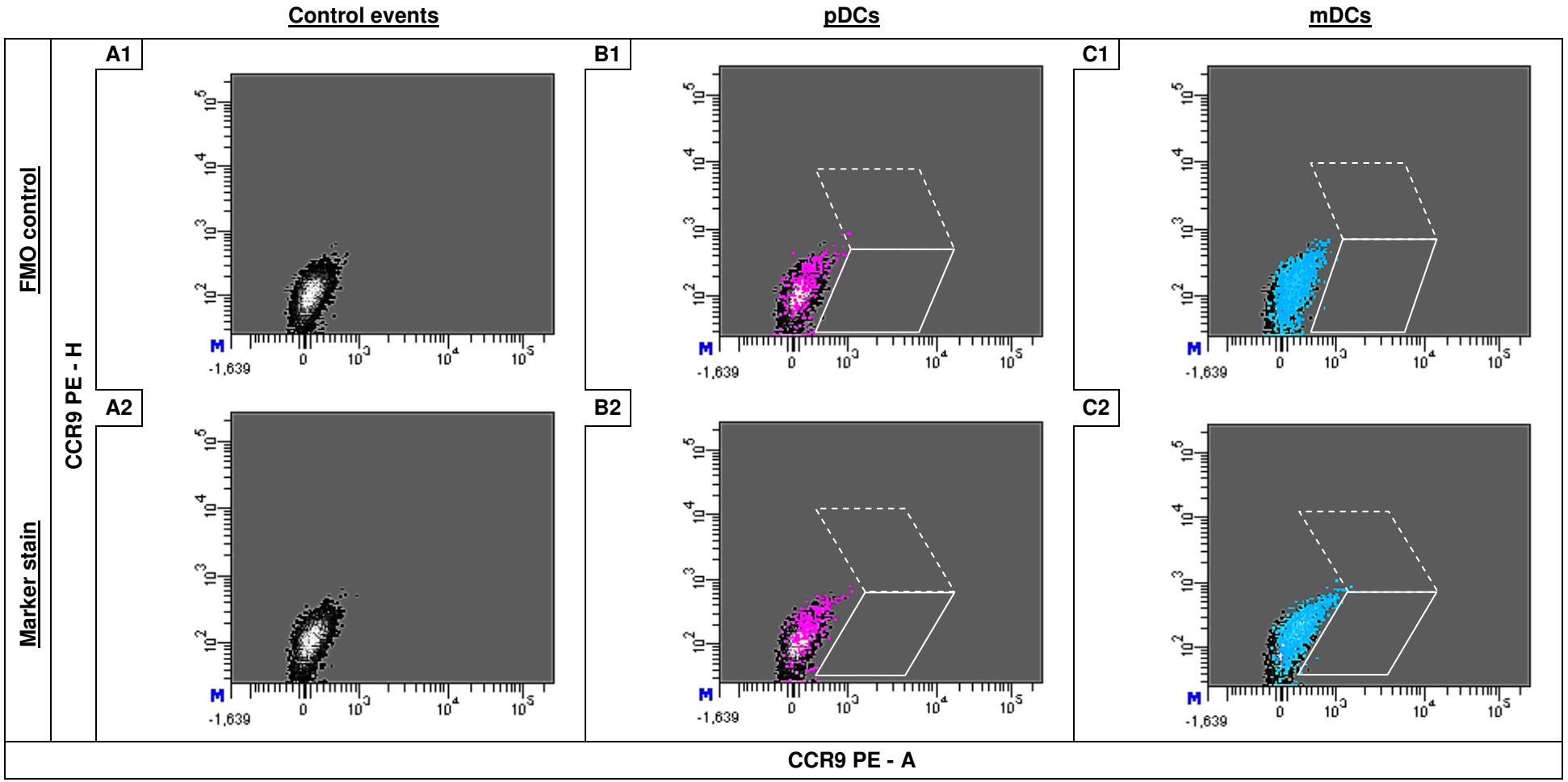

Figure 4.6: pDC and mDC staining profile of CCR9 and relevant FMO control

Graph A1-C1 and A2-C2 represents the control, pDC (pink-coloured) and mDC (blue-coloured) events upon CCR9 FMO control and marker staining, respectively. B1-2 and C1-2contains DC (to the front) and control events (black-coloured and displayed to the back of the DC population) to show the relationship of pDCs and mDCs to control events. The white dash border gate was used to capture positive events for statistical analysis. Events within the solid gate were not regarded as positive.

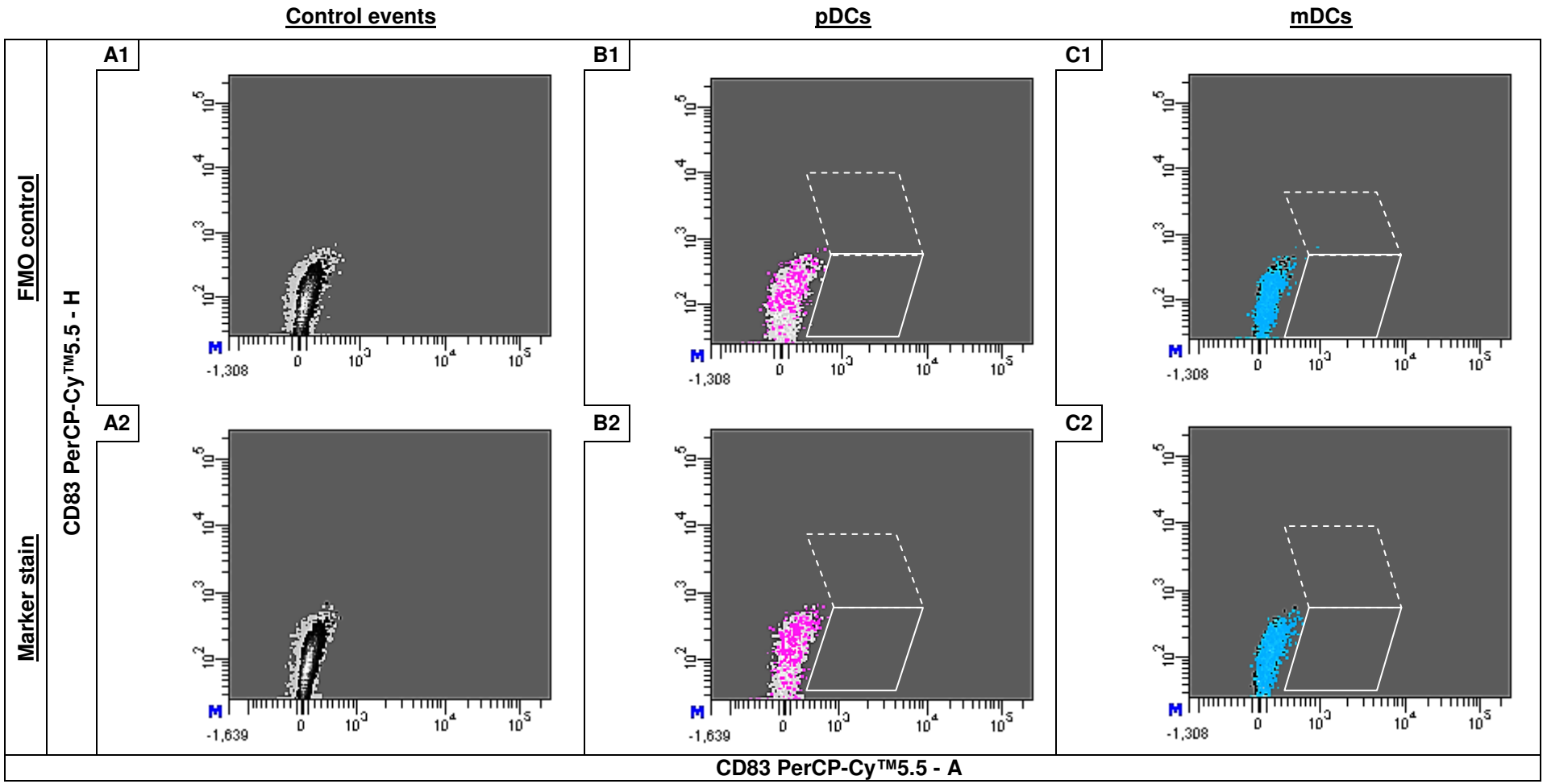

Figure 4.7: pDC and mDC staining profile of CD83 and relevant FMO control

Graph A1-C1 and A2-C2 represents the control, pDC (pink-coloured) and mDC (blue-coloured) events upon CD83 FMO control and marker staining, respectively. B1-2 and C1-2 contains DC (to the front) and control events (grey-coloured for pDCs and black-coloured for mDCs, displayed to the back of the DC population) to show the relationship of pDCs and mDCs to control events. The white dash border gate was used to capture positive events for statistical analysis. Events within the solid gate were not regarded as positive.

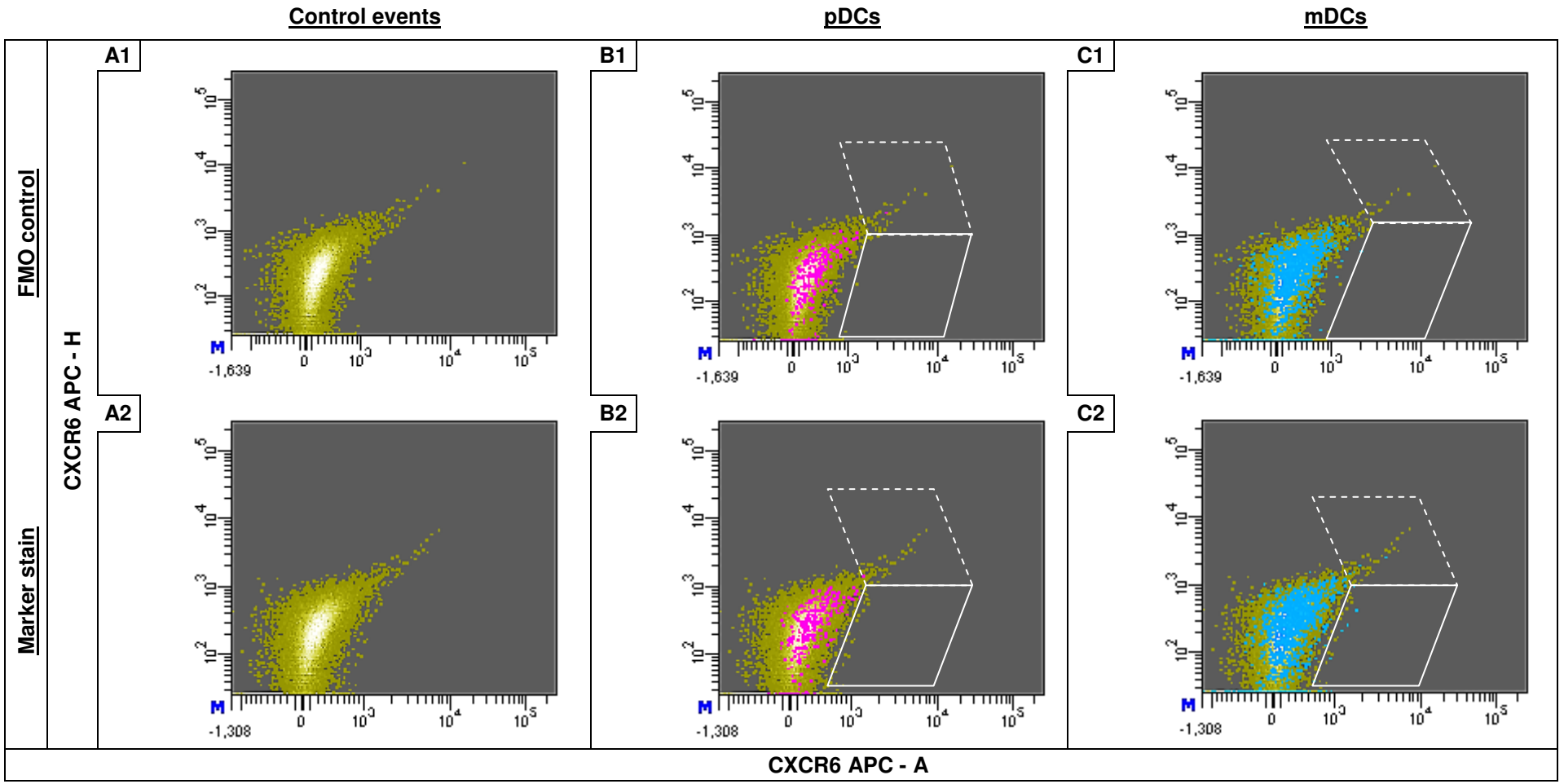

Figure 4.8: pDC and mDC staining profile of CXCR6 and relevant FMO control

Graph A1-C1 and A2-C2 represents the control, pDC (pink-coloured) and mDC (blue-coloured) events upon CXCR6 FMO control and marker staining, respectively. B1-2 and C1-2contains DC (to the front) and control events (brown-coloured and displayed to the back of the DC population) to show the relationship of pDCs and mDCs to control events. The white dash border gate was used to capture positive events for statistical analysis. Events within the solid gate were not regarded as positive.

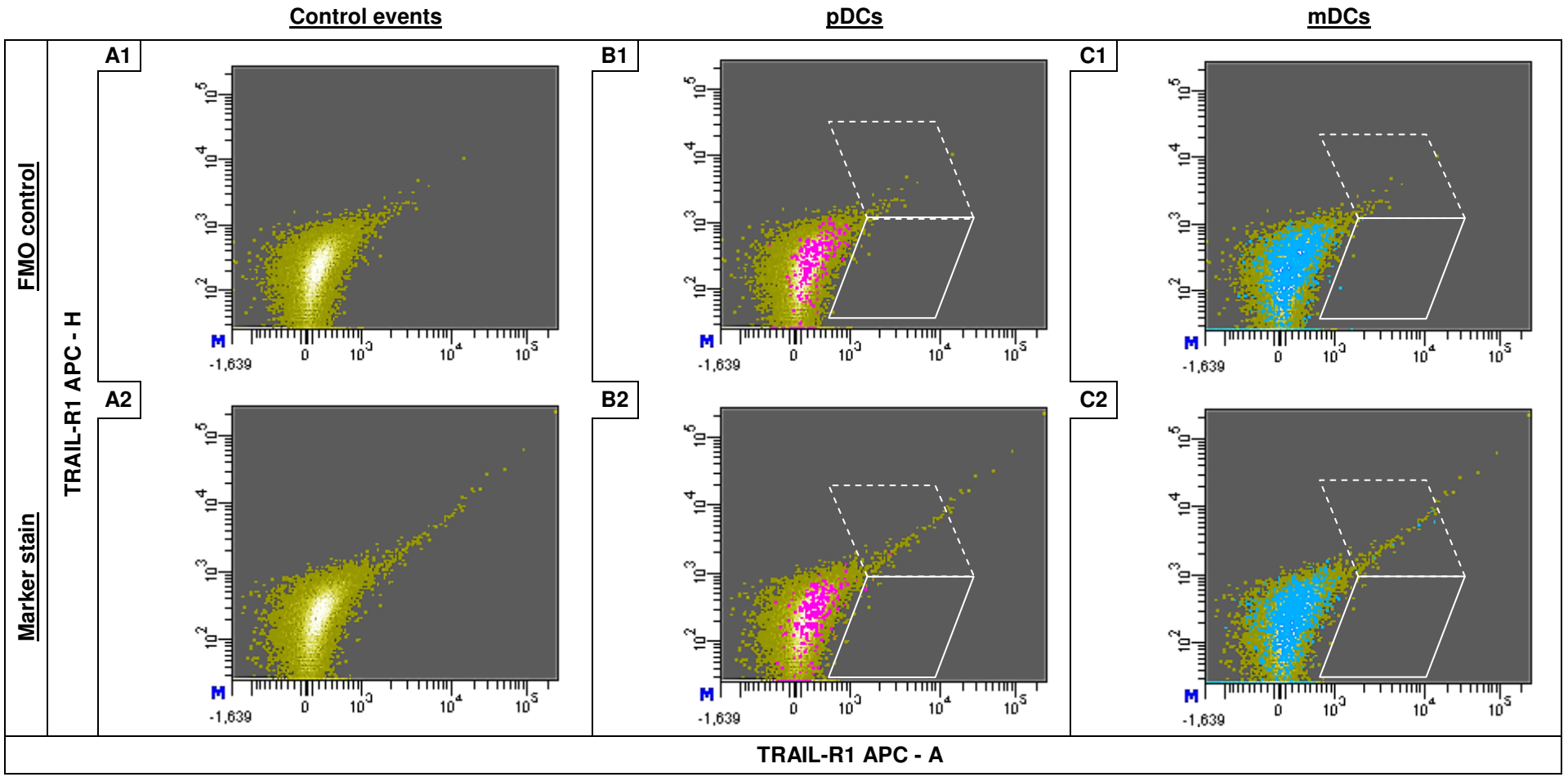

Figure 4.9: pDC and mDC staining profile of TRAIL-R1 and relevant FMO control

Graph A1-C1 and A2-C2 represents the control, pDC (pink-coloured) and mDC (blue-coloured) events upon TRAIL-R1 FMO control and marker staining, respectively. B1-2 and C1-2 contains DC (to the front) and control events (brown-coloured and displayed to the back of the DC population) to show the relationship of pDCs and mDCs to control events. The white dash border gate was used to capture positive events for statistical analysis. Events within the solid gate were not regarded as positive.

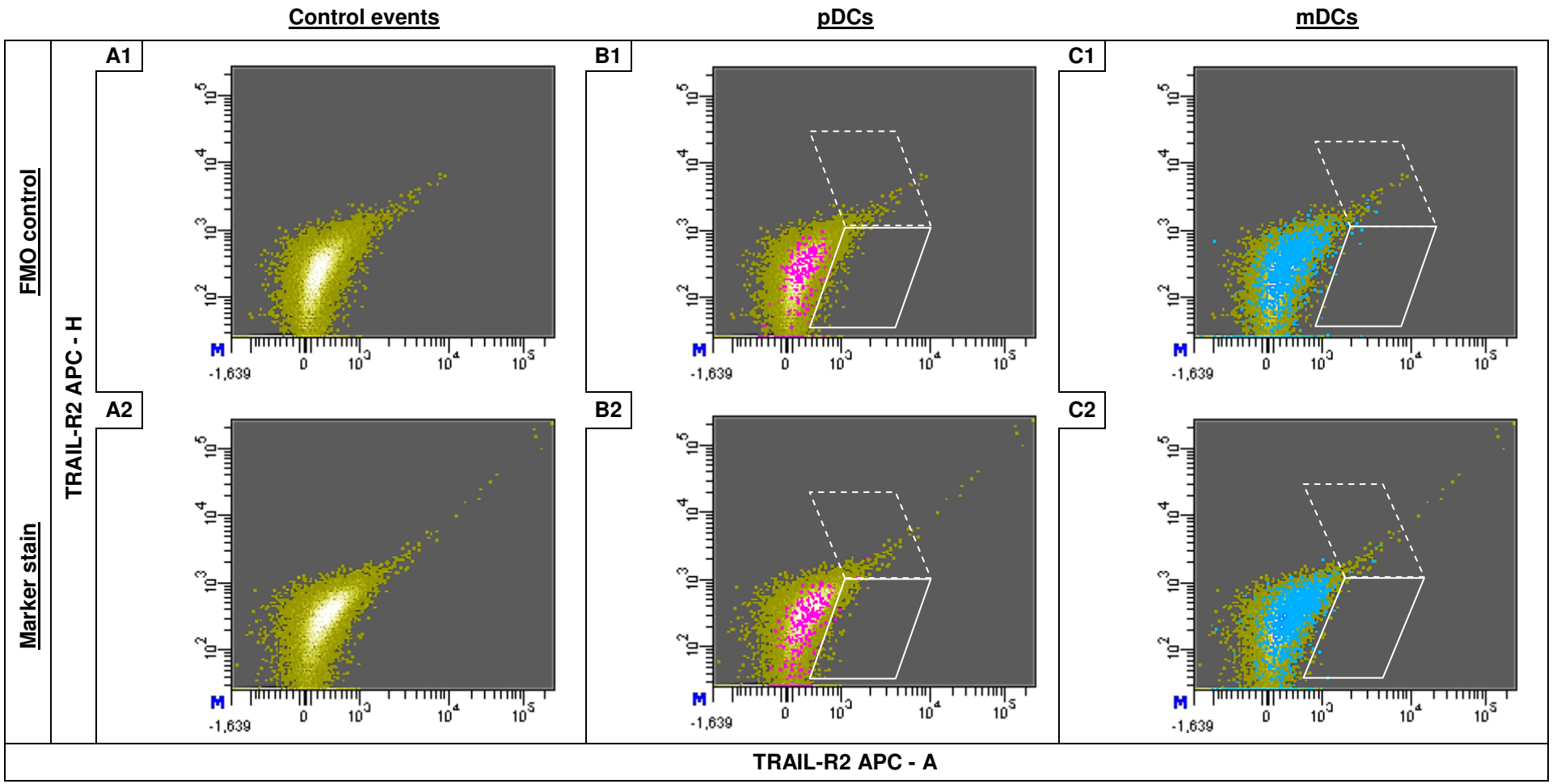

Figure 4.10: pDC and mDC staining profile of TRAIL-R2 and relevant FMO control

Graph A1-C1 and A2-C2 represents the control, pDC (pink-coloured) and mDC (blue-coloured) events upon TRAIL-R2 FMO control and marker staining, respectively. B1-2 and C1-2 contains DC (to the front) and control events (brown-coloured and displayed to the back of the DC population) to show the relationship of pDCs and mDCs to control events. The white dash border gate was used to capture positive events for statistical analysis. Events within the solid gate were not regarded as positive.

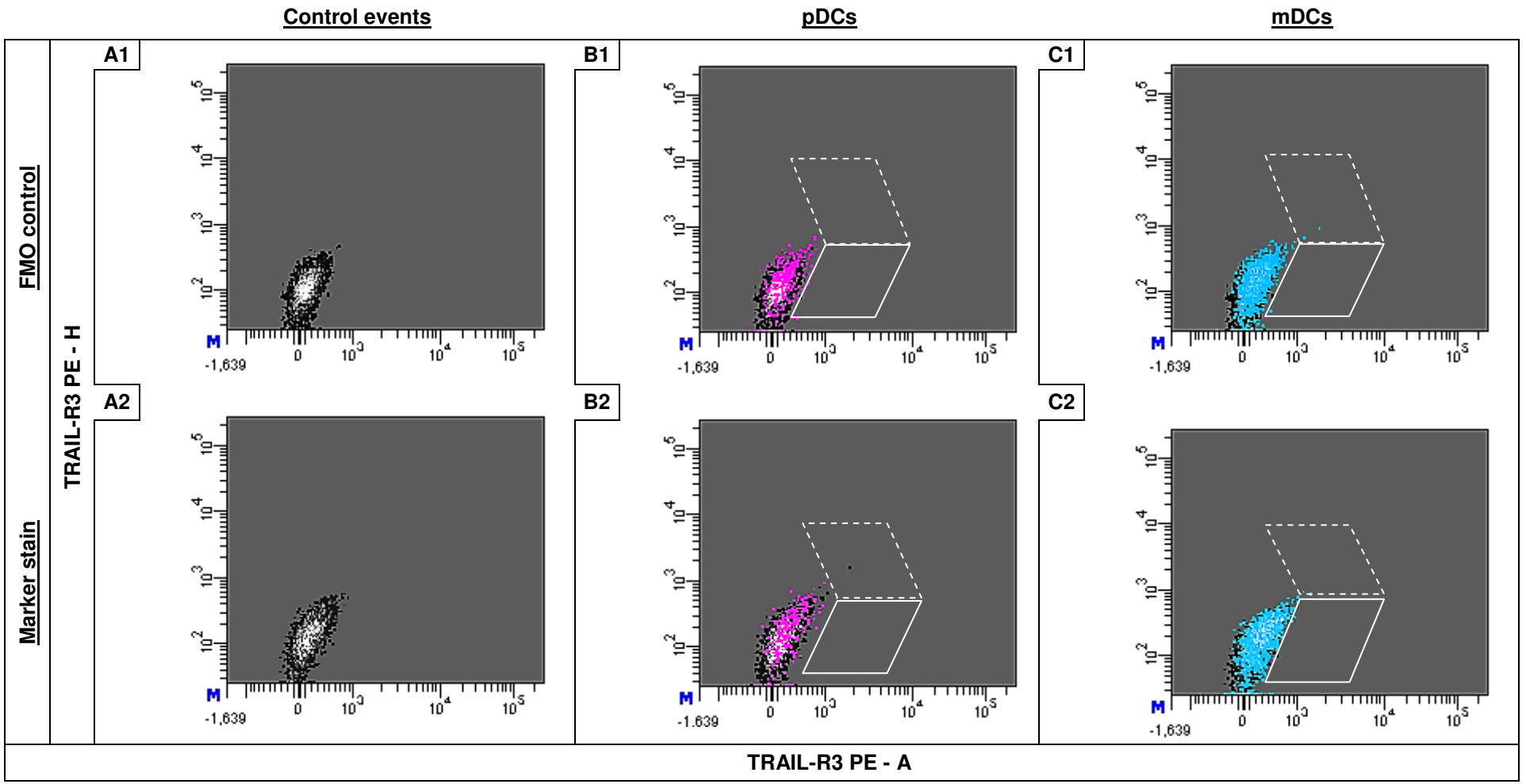

Figure 4.11: pDC and mDC staining profile of TRAIL-R3 and relevant FMO control

Graph A1-C1 and A2-C2 represents the control, pDC (pink-coloured) and mDC (blue-coloured) events upon TRAIL-R3 FMO control and marker staining, respectively. B1-2 and C1-2contains DC (to the front) and control events (black-coloured and displayed to the back of the DC population) to show the relationship of pDCs and mDCs to control events. The white dash border gate was used to capture positive events for statistical analysis. Events within the solid gate were not regarded as positive.

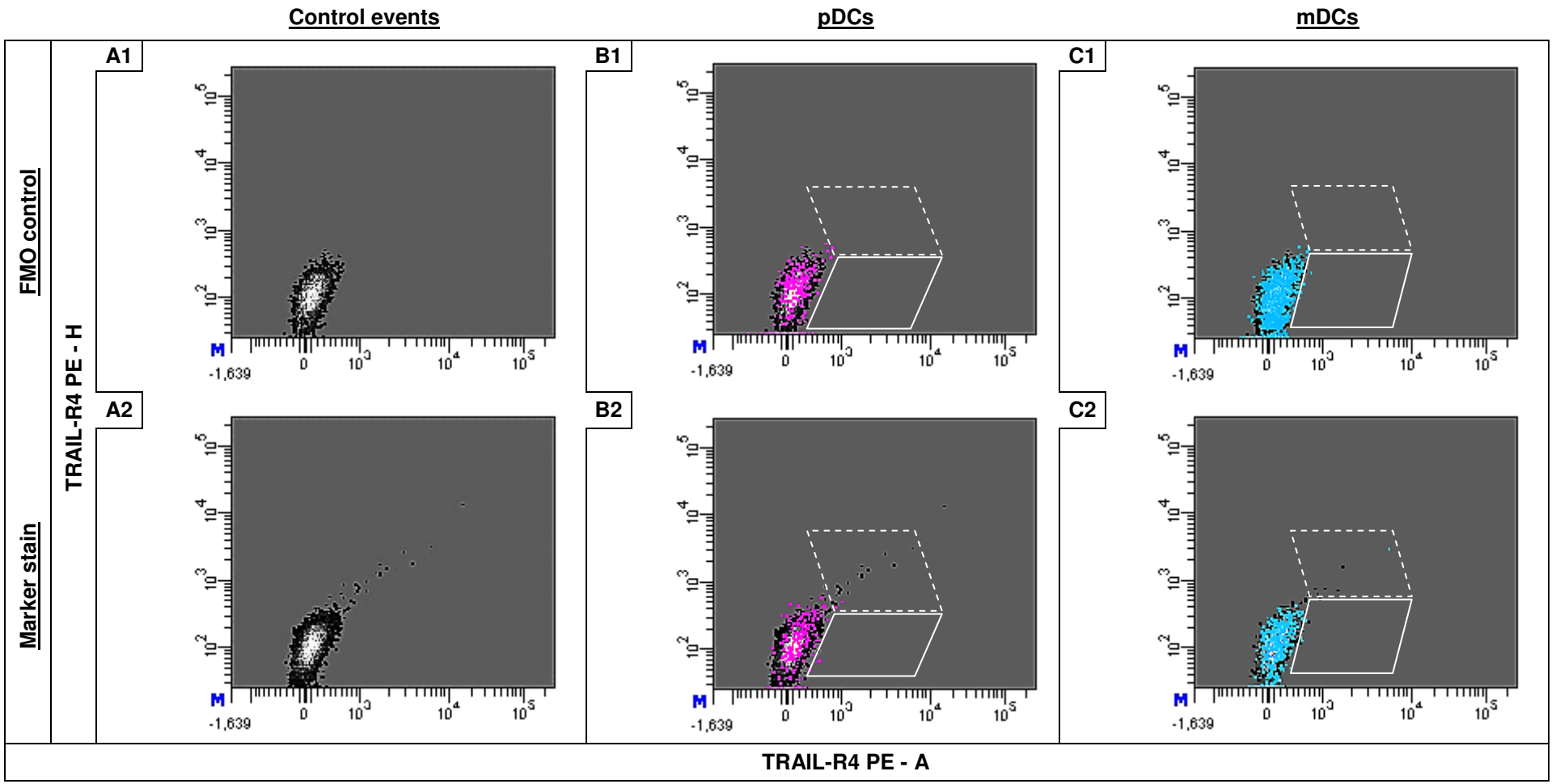

Figure 4.12: pDC and mDC staining profile of TRAIL-R4 and relevant FMO control

Graph A1-C1 and A2-C2 represents the control, pDC (pink-coloured) and mDC (blue-coloured) events upon TRAIL-R4 FMO control and marker staining, respectively. B1-2 and C1-2 contains DC (to the front) and control events (black-coloured and displayed to the back of the DC population) to show the relationship of pDCs and mDCs to control events. The white dash border gate was used to capture positive events for statistical analysis. Events within the solid gate were not regarded as positive.

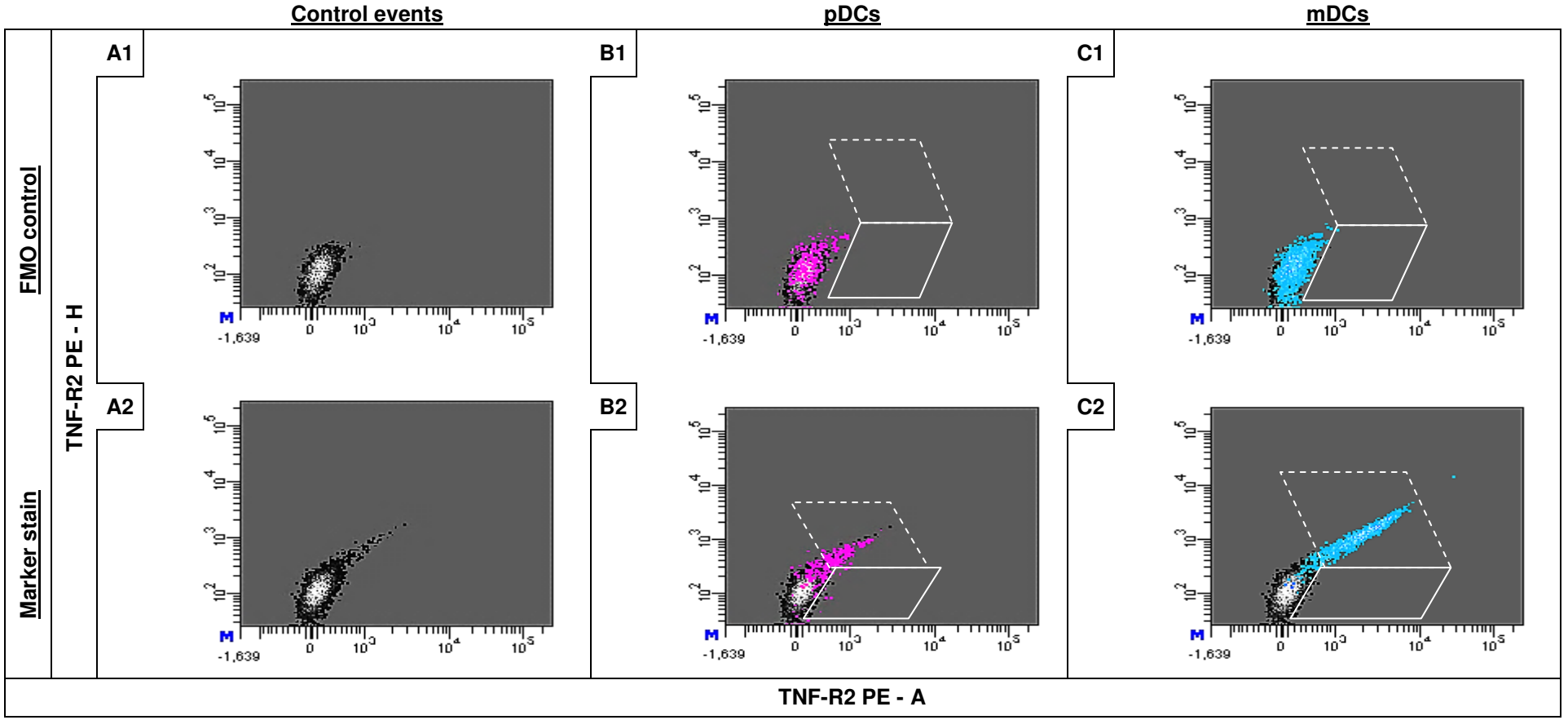

Figure 4.13: pDC and mDC staining profile of TNF-R2 and relevant FMO control

Graph A1-C1 and A2-C2 represents the control, pDC (pink-coloured) and mDC (blue-coloured) events upon TNF-R2 FMO control and marker staining, respectively. B1-2 and C1-2 contains DC (to the front) and control events (black-coloured and displayed to the back of the DC population) to show the relationship of pDCs and mDCs to control events. The white dash border gate was used to capture positive events for statistical analysis. Events within the solid gate were not regarded as positive. ***Note the different placement of the gate in the FMO control vs. the marker stain for the mDCs. In the latter stain the gate was placed in reference to black coloured negative events as the gate placed according to FMO control was not sufficient in capturing positive TNF-R2 events, attributed to data spread difference in the channel upon negative and positive expression of the marker.***

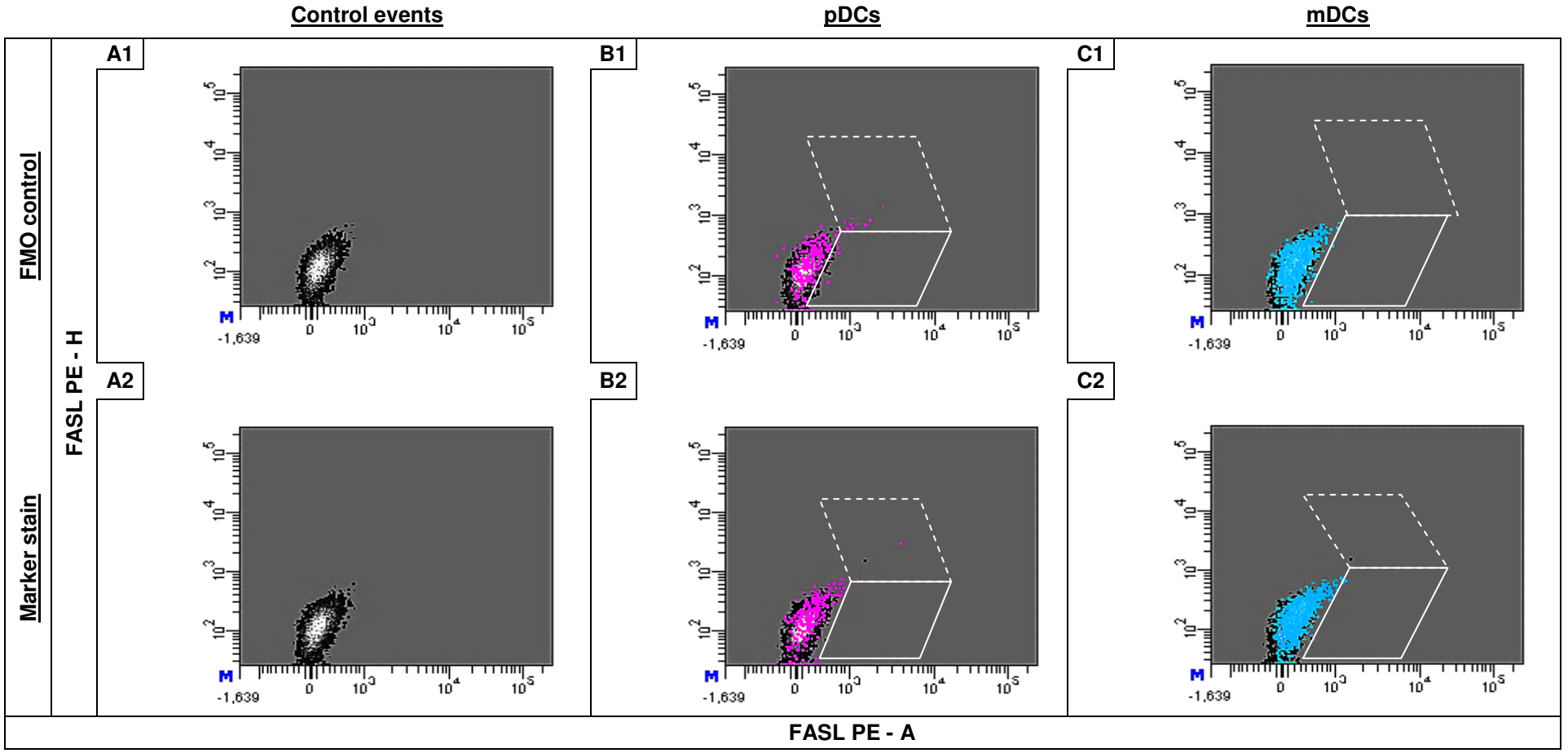

Figure 4.14: pDC and mDC staining profile of FASL and relevant FMO control

Graph A1-C1 and A2-C2 represents the control, pDC (pink-coloured) and mDC (blue-coloured) events upon FASL FMO control and marker staining, respectively. B1-2 and C1-2 contains DC (to the front) and control events (black-coloured and displayed to the back of the DC population) to show the relationship of pDCs and mDCs to control events. The white dash border gate was used to capture positive events for statistical analysis. Events within the solid gate were not regarded as positive. ***Note the high level of non-specific binding in the FMO control of pDCs.***

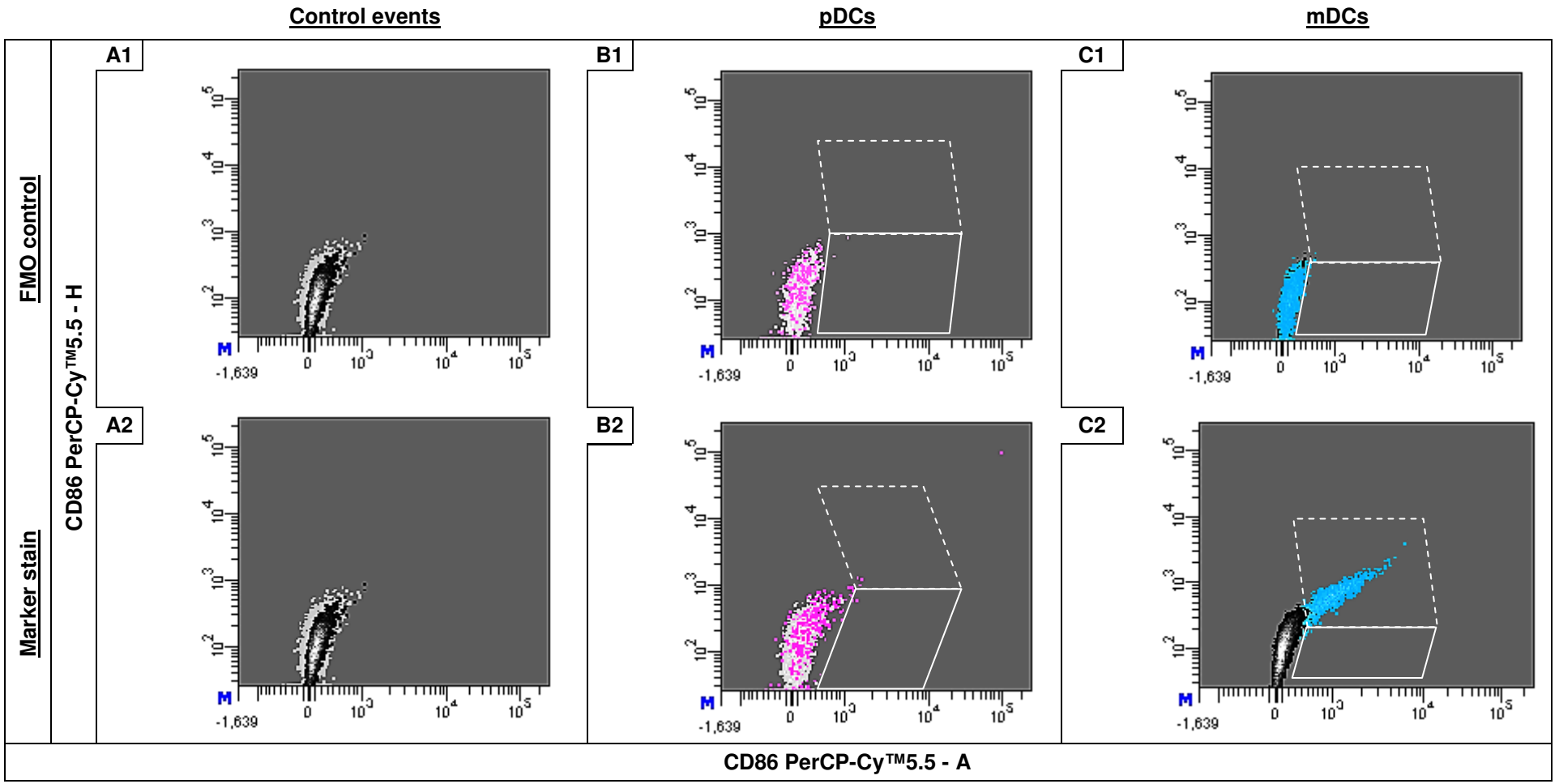

Figure 4.15: pDC and mDC staining profile of CD86 and relevant FMO control

Graph A1-C1 and A2-C2 represents the control, pDC (pink-coloured) and mDC (blue-coloured) events upon CD86 FMO control and marker staining, respectively. B1-2 and C1-2 contains DC (to the front) and control events (grey-coloured for pDCs and black-coloured for mDCs, displayed to the back of the DC population) to show the relationship of pDCs and mDCs to control events. The white dash border gate was used to capture positive events for statistical analysis. Events within the solid gate were not regarded as positive.

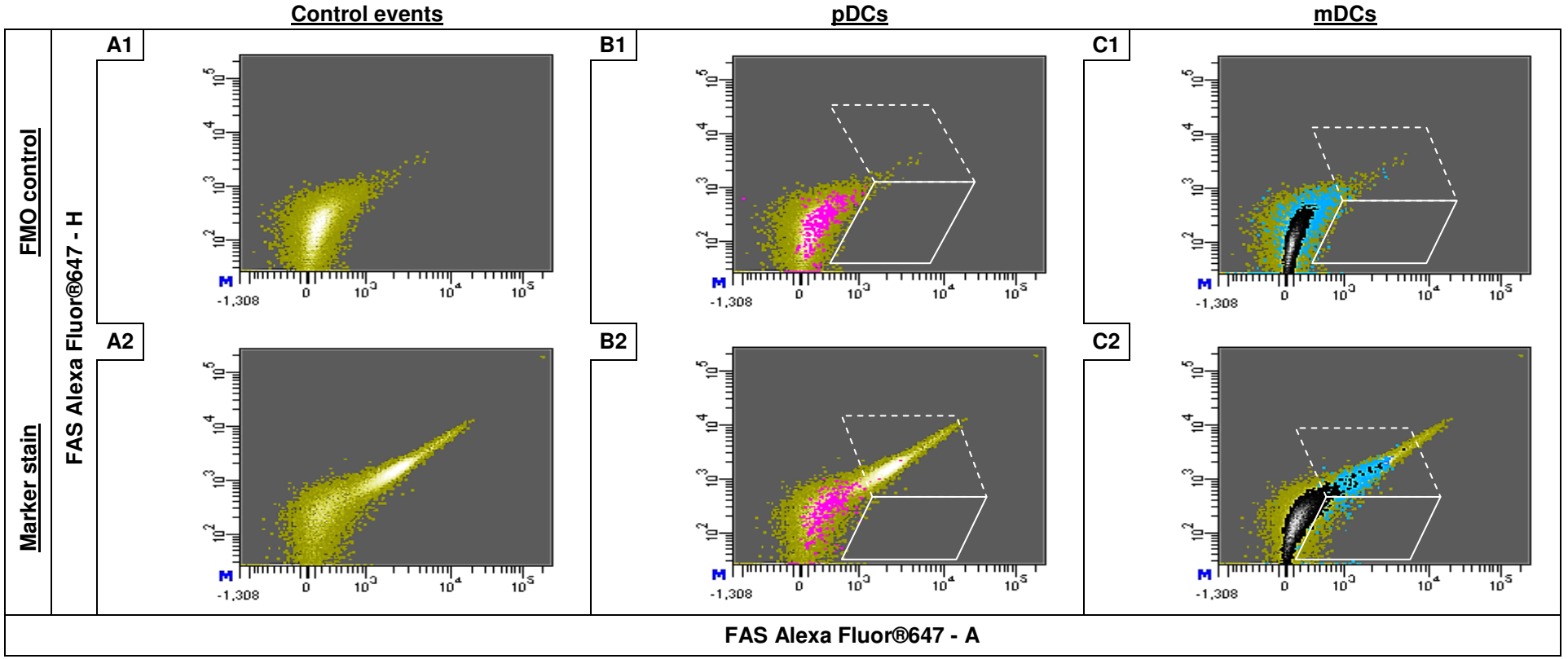

Figure 4.16: pDC and mDC staining profile of FAS and relevant FMO control

Graph A1-C1 and A2-C2 represents the control, pDC (pink-coloured) and mDC (blue-coloured) events upon FAS FMO control and marker staining, respectively. B1-2 contains pDC (to the front) and control events (brown-coloured events, displayed to the back of the DC population) and C1-2 contain mDC events (to the front) and control events (black and brown-coloured events, displayed to the back of the DC population) to show the relationship of pDCs and mDCs to control events. The white dash border gate was used to capture positive events for statistical analysis. Events within the solid gate were not regarded as positive. ***Note the different placement of the gate in the FMO control vs. the marker stain for the mDCs. In the latter stain the gate was placed in reference to black coloured negative events as the gate placed according to FMO control was not sufficient in capturing mDC positive FAS events, attributed to data spread difference in the channel upon negative and positive expression of the marker.***

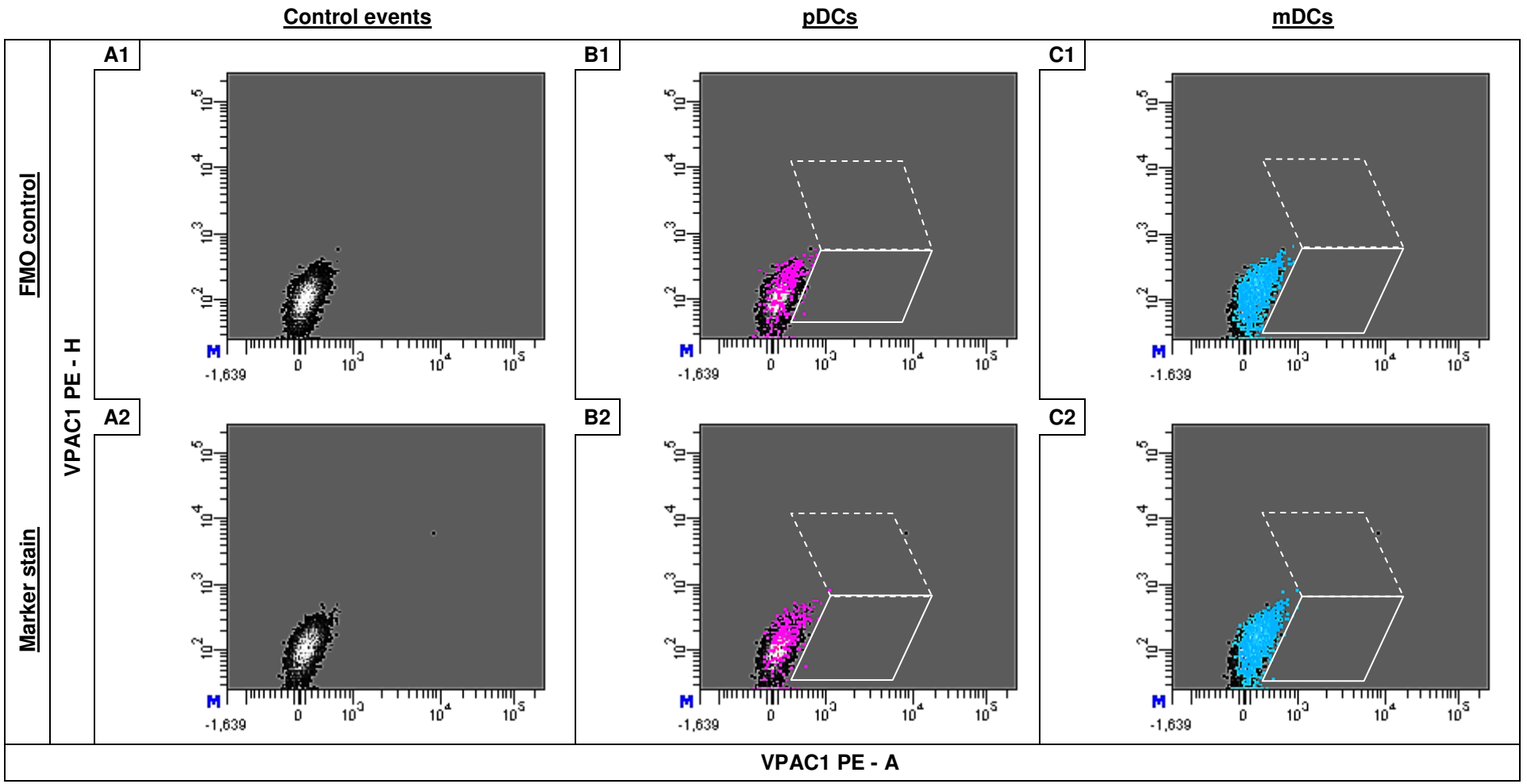

Figure 4.17: pDC and mDC staining profile of VPAC1 and relevant FMO control

Graph A1-C1 and A2-C2 represents the control, pDC (pink-coloured) and mDC (blue-coloured) events upon VPAC1 FMO control and marker staining, respectively. B1-2 and C1-2 contains DC (to the front) and control events (black-coloured and displayed to the back of the DC population) to show the relationship of pDCs and mDCs to control events. The white dash border gate was used to capture positive events for statistical analysis. Events within the solid gate were not regarded as positive.

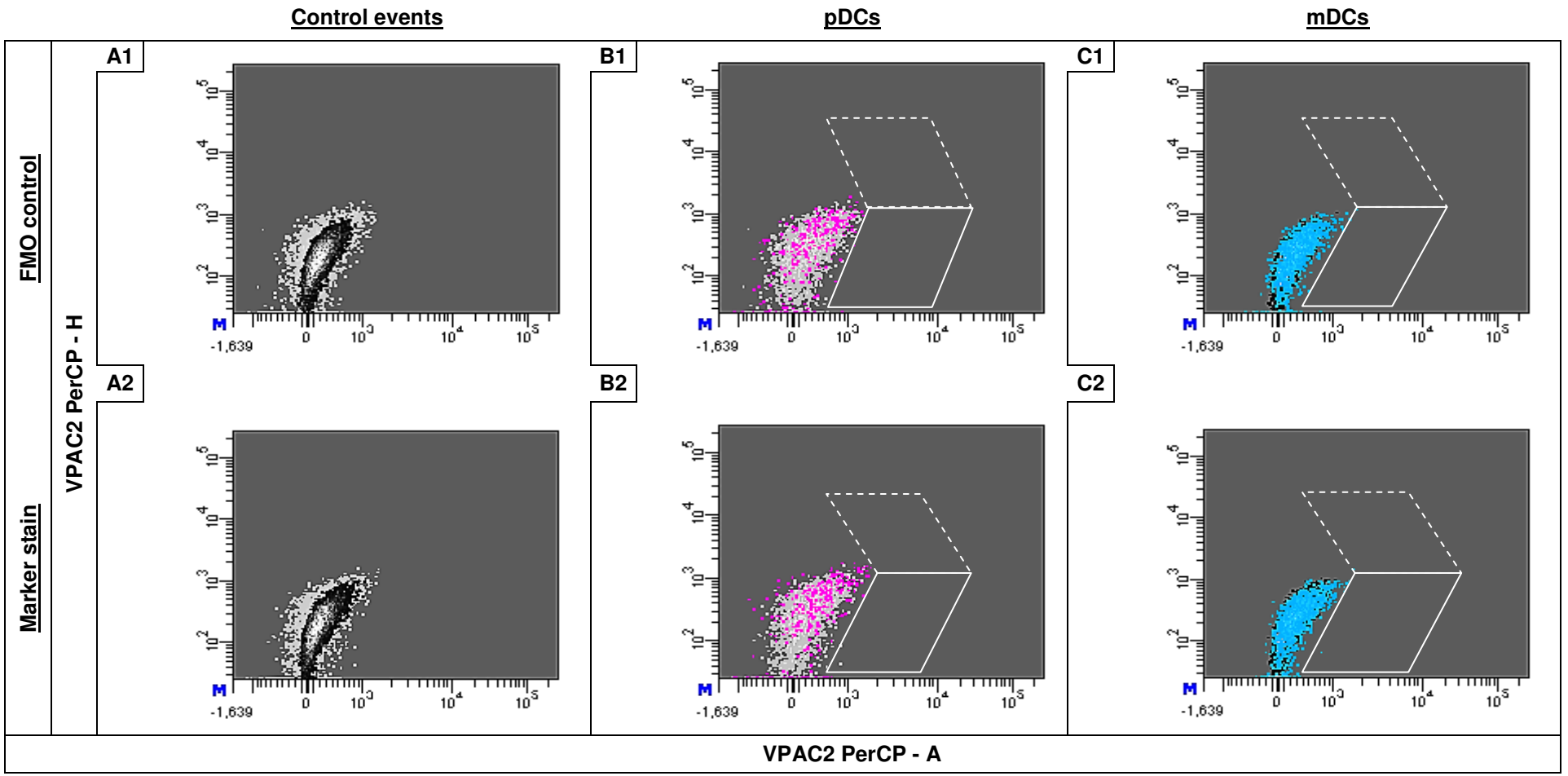

Figure 4.18: pDC and mDC staining profile of VPAC2 and relevant FMO control

Graph A1-C1 and A2-C2 represents the control, pDC (pink-coloured) and mDC (blue-coloured) events upon VPAC2 FMO control and marker staining, respectively. B1-2 and C1-2 contain DC (to the front) and control events (grey coloured for pDCs, black-coloured for mDCs and displayed to the back of the DC population) show the relationship of pDCs and mDCs to control events. The white dash border gate was used to capture positive events for statistical analysis. Events within the solid gate were not regarded as positive.

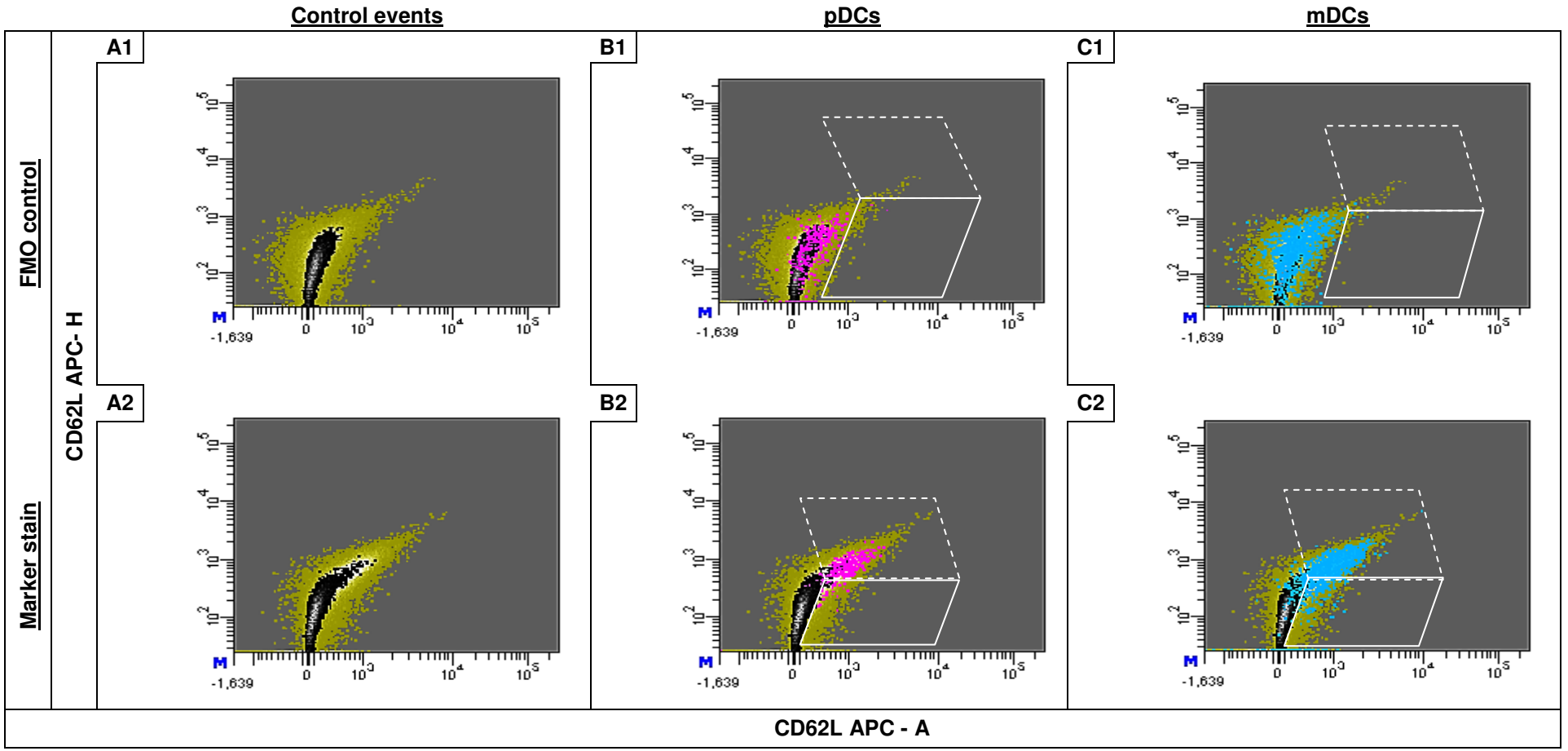

Figure 4.19: pDC and mDC staining profile of CD62L and relevant FMO control

Graph A1-C1 and A2-C2 represents the control, pDC (pink-coloured) and mDC (blue-coloured) events upon CD62L FMO control and marker staining, respectively. B1-2 and C1-2 contain DC (to the front) and control events (black and brown-coloured events, displayed to the back of the DC population) to show the relationship of pDCs and mDCs to control events. The white dash border gate was used to capture positive events for statistical analysis. Events within the solid gate were not regarded as positive. ***Note the different placement of the gate in the FMO control vs. the marker stain for both DC populations. In the latter stain the gate was placed in referenced to black coloured negative events as the gate placed according to FMO control was not sufficient in capturing CD62L events, attributed to data spread difference in the channel upon negative and positive expression of the marker.***

4.3.9 Flow cytometric analyses: Gating strategy used to identify the DC subsets for phenotypic profiling

An overall two step gating strategy was employed to, firstly, define the pDC and mDC subsets from the heterogeneous cell population in whole blood and, secondly to determine the expression profile of the 17 markers listed in Table 4.2 for both DC subsets. The gating strategy entailed the use of two-parameter density plots (these plots allow for the graphical presentations of the properties of events or cells according to two defined parameters, simultaneously. One dot represents one event. The X-axis and Y-axis were scaled in four log decades from which the signal intensity (MFI) of the marker of interest can be determined.) Moreover, hierarchical gating was used to detect the pDC and mDC population, characterised as HLA-DR^{+}CD11c^{-}CD123^{+}LIN1^{DIM} and HLA-DR^{+} CD11c^{+}CD123^{DIM}LIN1^{DIM}, respectively. Recall that $^{+}$refers to a bright positive expression of the relevant marker, ^{DIM} refers to an expression of intermediate intensity and $^{-}$ refers to the marker not being expressed. Data analyses were performed using the BD FACSDiva™ software v6.1.3 (BD Biosciences, San Jose, CA).

Prior to defining the DC subsets, or any other cell population of interest, total acquired events should be separated into singlet and doublet populations and only the former selected for further analysis. Singlets are recorded by a flow cytometer as one event, consequently also doublets, which in fact are two or more bound particles which should be excluded from the data analyzed. Identification of singlets was performed by displaying total acquired events in a FSC – H vs. FSC - A and collected using a polygon gate, labeled as P1 (Figure 4.20 A). Following this, P1 events were then displayed in a SSC – A vs. FSC - A density plot and a broad P2 polygon gate drawn to select the monocyte and lymphocyte population. The morphological properties (granularity and size) of pDCs and mDCs, position both the DC subsets between the monocyte and lymphocyte populations in such a density plot (Figure 4.20B). Events of the P2 polygon gate was then displayed in a HLA-DR - A vs. CD11c - A density plot and a broad gate, P3 and P4 respectively, drawn to collect HLA-DR^{+}CD11c^{-} and HLA-DR^{+}CD11c^{+} events, respectively (Figure 4.20 C and D). These events were then displayed, separately, in a CD123 - A vs. LIN1 - A density plot. The CD123^{+}LIN1^{DIM} events identified within the HLA-DR^{+}CD11c^{-} populations and the CD123^{DIM}LIN1^{DIM} events of the HLA-DR^{+}CD11c^{+} population, defined the pDC and mDC populations respectively (Figure 4.20 E and F, respectively).

This gating strategy is an adaption to the method described in a majority of DC related publications in which singlet events are collected in a HLA-DR^{+}LIN1^{DIM} density plot followed by identifying pDCs (CD123^{+}CD11c^{-}) and mDCs (CD123^{DIM}CD11c^{+}) from a CD123 vs. CD11c density plot. This gating strategy was found optimal for the identification of DCs from acquired events in the control study group but it was not sufficient for most of the HIV-1 and HIV-1-related study groups, presumably due to HIV-1- associated changes on cellular level. This prompted the design of the abovementioned gating strategy which enabled optimal identification of DCs from the control, HIV-1 and HIV-1-related study groups.

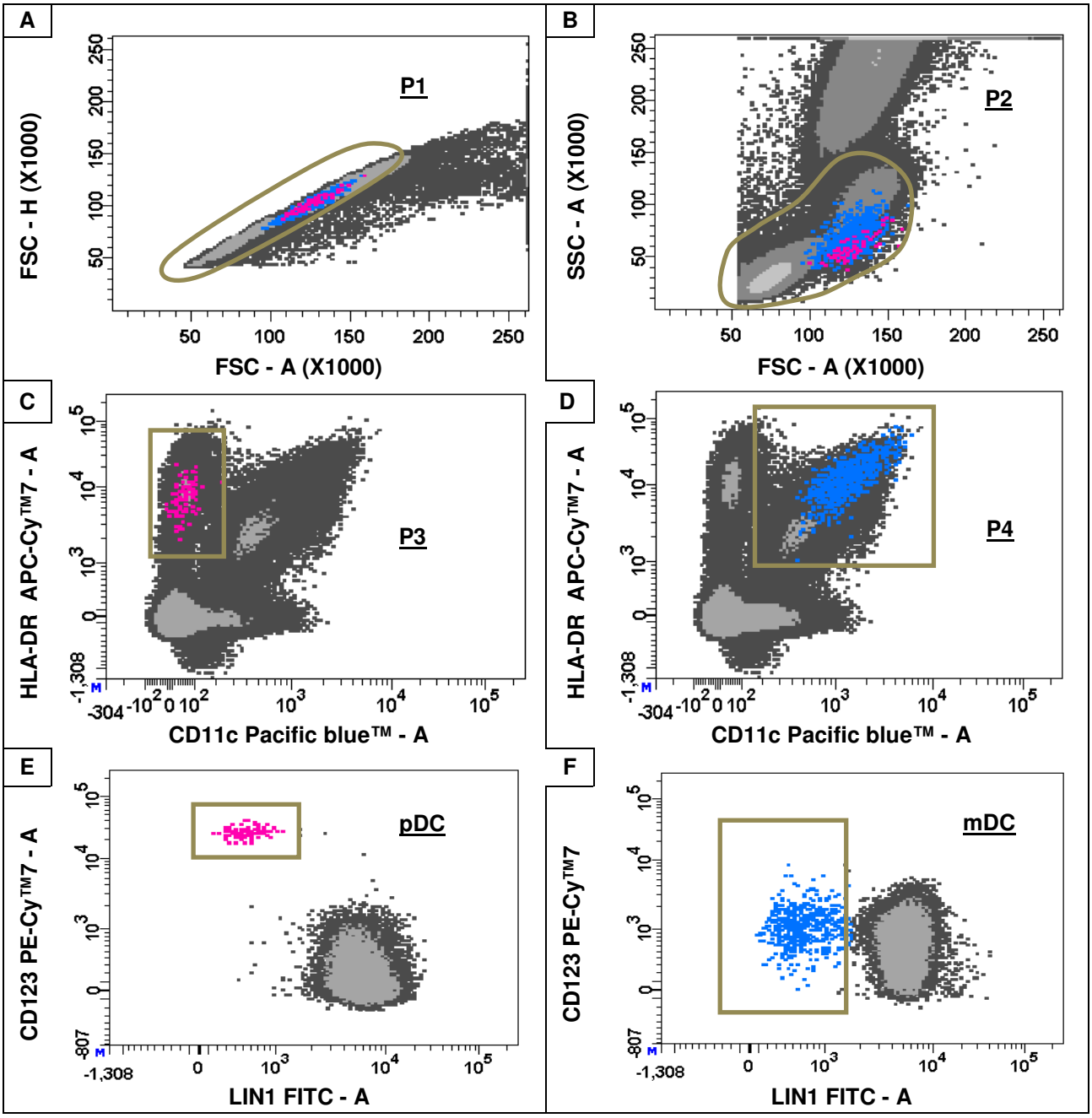

Figure 4.20: Gating strategy to identify the DC subsets for phenotypic analyses

Singlets were collected in a P1 gate using a FSC - H vs. FSC - A density plot, and then displayed in SSC - A vs. FSC - A density plot. A broad gate (P2) used to identify events between the monocyte and lymphocyte population. These events were further sequentially analysed in an HLA-DR - A vs. CD11c - A and CD123 - A vs. LIN1 - A density plots to collect HLA-DR^{+}CD11c^{-}CD123^{+}LIN1^{DIM} and HLA-DR^{+}CD11c^{+}CD123^{DIM}LIN1^{DIM} events defined as pDCs (pink-coloured) and mDCs (blue coloured), respectively.

4.3.10 Distinguishing between mDC and non-mDC contaminating events within the LIN1^{DIM} population

The described DC subset identification gating strategy (Figure 4.20) was optimal in differentiating pDCs and mDCs from total acquired flow cytometric events for subsequent analyses of expression of markers of interest, however, in some cases the study observed LIN1^{DIM} mDC events with questionable high density (Figure 4.21 A vs. B, displaying HLA-DR^{+}CD11c^{+} events in a CD123 vs. LIN1 density plot) which is in contrast to the well-described extreme low number distribution of these cells in peripheral blood. It became apparent via the analyses of TNF-R2 expression by mDCs that these events included two clearly different populations, a low density TNF-R2^{DIM} (mDC events) and high density TNF-R2^{BRIGHT} (non-DC events) (Figure 4.21 D, blue and purple coloured events, respectively). In contrast TNF-R2 analyses of mDC events of the data set depicted in Figure 4.21 A only showed low density TNF-R2^{DIM} mDC events (Figure 4.21 C). Hence, these non-DC events needed to be excluded from mDC gating events so to ensure analysis of exclusively mDC specific marker expression. Also the differential expression of TNF-R2 made it possible to collect mDC specific events for further analyses of markers included in the related marker panel (Panel E, refer to Table 4.2). However, for the remaining panels where TNF-R2 was not present an alternative gating strategy had to be devised, preferably using markers present in all the panels, hence, relying on the differential expressing of DCID markers as tool to extract mDC specific events from contaminating non-DC events (refer to Figure 4.21). The study evaluated the TNF-R2^{DIM} mDC and TNF-R2^{BRIGHT} non-DC population observed in the TNF-R2 vs. LIN1 density plot (Figure 4.21 C, D), in a HLA-DR vs. LIN1 density plot and were able to locate “true” mDC events separate from non-DC events as these displayed a higher HLA-DR MFI than non-DC events (Figure 4.21 F; E depicts dataset without non-DC events). In addition, the current study also observed that analyses of events in a CD86 vs. HLA-DR density plot, allowed for distinguishing “true” mDCs from non-DC events (Figure 4.21 H; F depicts dataset without non-DC events).

These findings suggested that in flow cytometric analysis of blood mDCs in HIV-1 studies the addition of TNF-R2 or CD86 to a marker panel could guide a more sensitive “isolation” of the mDC subset from acquired events. Its proposed that these contaminating events observed in the mDC defining gate are due to changes induced by HIV-1 infection on cells encompassing the LIN1^{+} population (T lymphocytes, macrophages, monocytes, neutrophils, B Lymphocytes, eosinophils and NKL’s) or natural differences between donors.

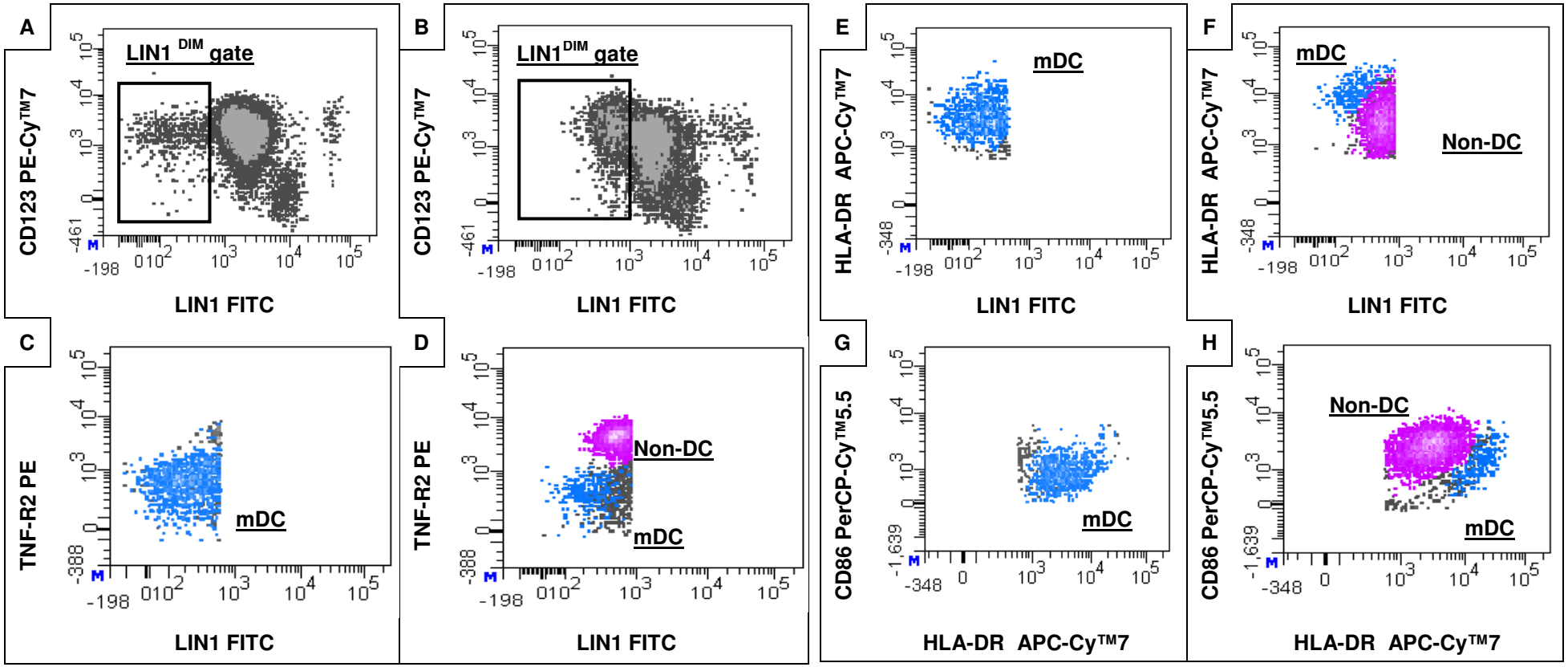

Figure 4.21: Distinguishing between mDC and non-mDC contaminating events within the LIN1^{DIM} population

Graph A and B, respectively, show examples of data sets with low and high density LIN1^{DIM} events when *HLA-DR^{+}CD11c^{+} events (refer to Figure 4.20) were analysed in a CD123 vs. LIN1 density plot. Analyses of LIN1^{DIM} events of A (displayed in C) revealed TNF-R2^{DIM} expressing events (blue-coloured) in comparison to the analyses of B (displayed in D) which shows, in addition to the TNF-R2^{DIM}, alsoTNF-R2^{BRIGHT} (purple-coloured) events. The latter were regarded as non-DC events. Differentiation of TNF-R2^{DIM}mDC from TNF-R2^{BRIGHT} non-DC events was also performed in a HLA-DR vs. LIN1 density plot so to define a method using DCID markers in the analyses of mDC-specific events in panels where TNF-R2 was not present. mDC events were identified as the events with higher HLA-DR MFI (dataset of C (mDC events) displayed in E vs. dataset of D (DC and non-DC events) displayed in F). A CD86 vs. HLA-DR density plot could also be used to distinguish mDC from non-mDC events in cases of high density LIN1^{DIM} events (G displaying mDC events vs. H displaying dataset with DC and non-DC events).*

4.3.11 Statistical analyses

Comparative analyses of the expression of markers of interest by pDCs and mDCs were performed as defined in section 3.3.8. These tests were performed using the Graphpad Prism version 5.00 software (San Diego, California, USA). Refer to Table 3. 4 for the summary of the method used to report significant and non-significant data as well as the corresponding p value range.

.

4.4 Results and discussion

4.4.1 Defining marker expression related to apoptosis, migration, activation/maturation on both DC subsets during HIV-1 infection.

4.4.1.1 Expression profile of the activation markers: CD80, CD86, CD62L and maturation marker CD83 on blood DCs of the control, HIV-1 and HIV-1-related study groups.

CD62L was found constitutively and positively expressed by pDCs and mDCs respectively. mDCs also positively expressed CD86 while no expression of this marker was found on pDCs. In both DC subsets CD80 and CD83 expression was absent.

Assessing activation/maturation marker expression in healthy controls found a significant shift in MFI between CD86 and CD62L staining of mDCs as well as CD62L staining of pDCs when compared to the relevant FMO stain/internal control. Accordingly, the staining profile showed positive expression of CD62L by mDCs (Figure 4.19 C1-C2) and constitutive expression of CD62L and CD86 by pDCs (Figure 4.19 B1-B2) and mDCs (Figure 4.15 C1-C2), respectively. These DC subsets were designated as $CD86^+$mDCs, $CD62L^+$mDCs and $CD62L^+$pDCs. The CD86 staining profile of pDCs (Figure 4.15 B1-B2) as well as that of CD80 (Figure 4.3 B1-B2, C1-C2), CD83 (Figure 4.7 B1-B2, C1-C2)) on both DC subsets was similar to that of the relevant FMO stain/internal controls. Accordingly, this confirmed negative expression of these markers on blood DCs.

HIV-1 infection induced a significantly higher distribution of $CD86^+$mDCs which normalises during ARV therapy

The median percentage $CD86^+$mDCs was significantly higher in the ARV^-HIV-1 study group ($p \leq 0.05$) compared to the control study group. These may resemble mDCs that have responded to the HHF milieu and initiate export from blood to secondary lymphoid tissue. In a similar comparison, a higher median percentage of $CD86^+$mDCs was observed in the ARV^-HIV-1/TB study group, although the change was not significant. Notably, normalization of the $CD86^+$mDCs subset distribution was observed during ARV therapy. The median percentage $CD86^+$mDCs was significantly declined in the ARV^+HIV-1 study group ($p = 0.01$) compared to the ARV^-HIV-1 study group. However, a similar decline was not observed in the ARV^+HIV-1/TB study group. The normalization effect observed with the ARV^+HIV-1 study group and lack thereof observed in the ARV^+HIV-1/TB study group could be due to the significant difference in time on therapy between these study groups which was 18 months in the former and 5.5 months in the latter study group (Table 4.3, Figure 4.22 C)

No significant change in the distribution of $CD62L^+$pDCs and $CD62L^+$mDCs or expression profile of the negatively expressed CD80 and CD83 markers during HIV-1 infection

No significant change in the median percentage $CD62L^+$pDCs was observed in the HIV-1 and HIV-1 related study groups when compared to that of the healthy controls (Table 4.3, Figure 4.22 A). Although a higher median percentage of $CD62L^+$mDCs was observed in the ARV^-HIV-1 and ARV^+HIV-1 study groups the change was not significant. Nonetheless, an interesting trend was observed with the $CD62L^+$mDC subsets.

Compared to the higher distribution of $CD62L^{+}$mDCs in both the ARV^{-}HIV-1 and ARV^{+}HIV-1 study groups a decline in the median percentage $CD62L^{+}$mDCs was observed in the corresponding ARV^{-}HIV-1/TB and ARV^{+}HIV-1/TB study groups. It was proposed this finding may be related to the anti-TB treatment. Furthermore, no significant change in the staining pattern was observed when the expression profile of the negatively expressed activation (CD80) and maturation markers (CD83) on both DCs of the healthy control study group was compared to that of the HIV-1 and HIV-1 related study groups (data not shown).

Our findings was in agreement with the reports of Sehgal M, *et al.* (2014) and Benlahrech A, *et al.* (2012) in which similar 1) distribution frequency of $CD62L^{+}$pDCs and $CD62L^{+}$mDCs and 2) expression profile of CD80 and CD83 on blood DCs between healthy controls and HIV-1 infected individuals was observed, Notably, other studies have reported differently on the level of CD83 and CD86 expression on DCs during HIV-1 infection. Dillon SM, *et al.* (2008), in contrast to Yonkers NL, *et al. (*2011), did not observe statistical significant difference in levels of CD83 and CD86 expression by DCs between the healthy controls and HIV-1 infected patients. However, Yonkers NL, *et al. (*2011) reported on significantly higher expression of these markers in HIV infected patients with regard to mDCs, while observing tendency of higher expression by pDCs. It was proposed these contrasting findings might be related to viral load variability; however, the viral load of the HIV infected participants of Dillon's study was much higher than that of Yonkers's. These conflicting reports might be due to the diversity of the subjects investigated (stages of disease, donor specificity) and factors regarding experimental design.

Table 4.3: Summary of the CD4 and CD8 T lymphocyte percentage; CD4:CD8 ratio, viral load (as applicable) as well as the percentage distribution of DC subsets positively expressing markers of apoptosis, migration and activation of the control, HIV-1 and HIV-1-related study groups.

		Study groups				
		Control	**ARV$^-$HIV-1**	**ARV$^-$HIV-1/TB**	**ARV$^+$HIV-1**	**ARV$^+$ HIV-1/TB**
CD4 T cells	**Me^a**	881	354	207	339	319
	R^a	412 - 1694	14 - 1175	51 - 598	137 - 1072	52 - 1274
	Me^b	44	23	14.5	19.5	20
	R^b	22 - 62	4 - 39	7 - 30	7 - 31	4 - 47
CD8 T cells	**Me^a**	601	863	1067	1147	805
	R^a	161 - 2545	187 - 2940	229 - 3106	346 - 2962	306 - 2988
	Me^b	30	51	60.5	56.5	60
	R^b	14 - 52	23 - 77	45 - 85	33 - 82	34 - 85
CD4:CD8 Ratio	**Me^c**	1.47	0.45	0.24	0.37	0.34
	R^c	0.43-3.54	0.07-1.45	0.08-0.6	0.1-0.95	0.08-1.39
CD86$^+$mDC	**Me^d**	86.45	92.5	92.95	87.6	91.2
	R^d	60.70 – 98.2	61.5 - 100	66.7 - 100	58.5 - 100	62.6 - 100
FAS$^+$mDC	**Me^d**	92	92.7	95.2	89.70	91.40
	R^d	71.4 – 99.8	69 - 100	63.7 - 100	73.3 – 100	71.4 - 100
TNF-R2$^+$ mDC	**Me^d**	90.65	89.95	93.6	91.7	91
	R^d	29.4 - 99.10	37.9 – 99.6	59.5 - 100	48.9 – 99.5	62.1 – 98.5
TNFR2$^+$ pDC	**Me^d**	49.5	84.4	81.5	80.3	46.9
	R^d	3.7 – 96.7	6.1 - 99.10	20.4 - 100	4 - 100	10.8 -88.7
CCR5$^+$pDC	**Me^d**	83.89	81.98	N/A	68.39	58.62
	R^d	22.63-100	15.07-99.4		13.53-91.65	32.47-91.33
CD62L$^+$pDC	**Me^d**	91.86	91.99	93.8	93.79	90.76
	R^d	26.67 -100	52.60 - 100	60 - 100	66.12 - 100	63.84 - 98.40
CD62L$^+$mDC	**Me^d**	60.97	70.89	59.7	75.63	66.05
	R^d	37.88 – 92.18	17.8 - 94.84	37.04 - 81	30.10 – 91.6	36.3 – 92.6
Viral load	**Me^e**	N/A	8.9 x10^3	7.3 x10^4	LOD	LOD
	R^e		LOD - 3.5 x10^6	340 - 3.3 x10^6	LOD - 1.8x10^5	LOD - 7,1x10^5

Data indicated as
Me^a *= Median cells/µl,*
R^a *= Range cells/µl,*
Me^b *= Median % of CD45$^+$CD3$^+$ events,*
R^b *=Range % of CD45$^+$CD3$^+$ events,*
Me^c *= Median ratio of CD4 Lymphocyte absolute number to CD8 T lymphocyte absolute number*
R^c *=Range of the CD4:CD8 ratio values*
Me^d *= Median % of positive marker expressing DCs,*
R^d *= Range % of positive marker expressing DCs,*
Me^e *= Median RNA copies/ml,*
R^e *= Range RNA copies/ml*

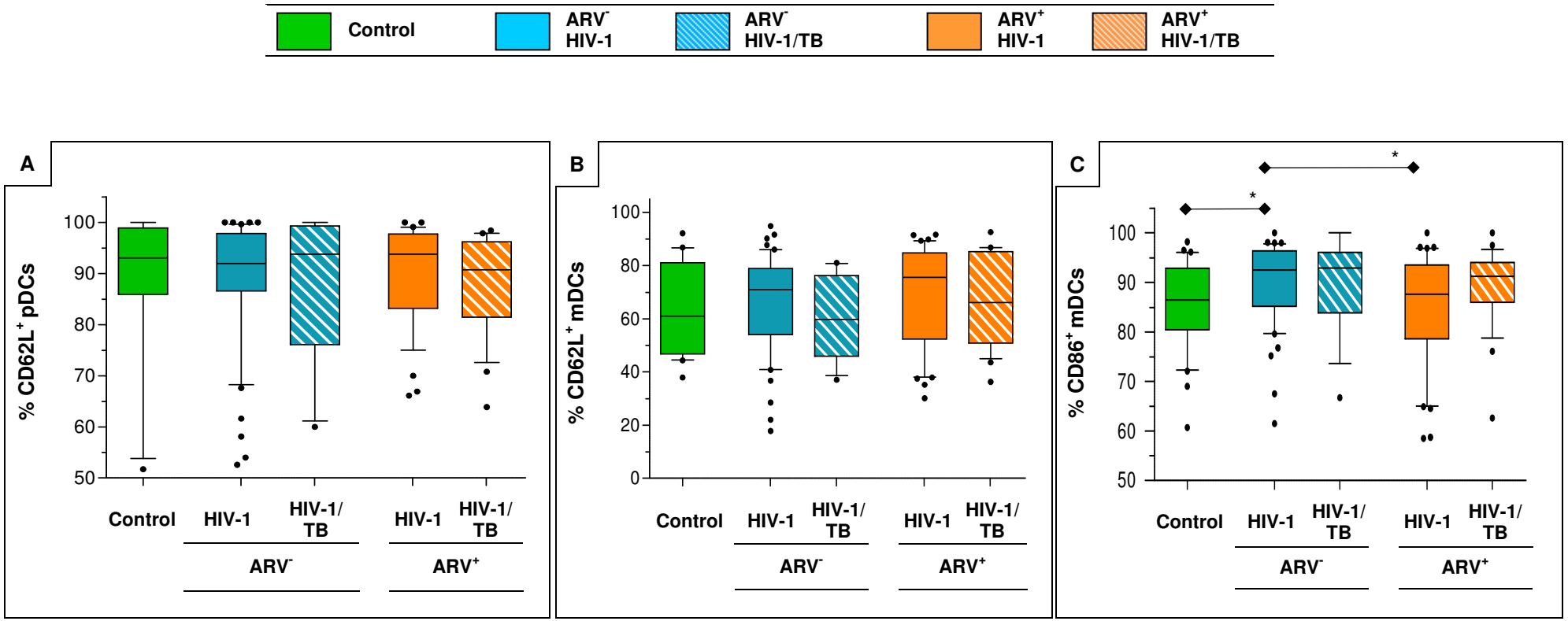

Figure 4.22: CD62L$^+$pDCs, CD62L$^+$mDCs and CD86$^+$mDCs subset distribution of the control, HIV-1 and HIV-1 related study groups

Peripheral whole blood was stained with mAbs to detect the percentage pDCs and mDCs expressing CD62L or CD86 using multi-parameter flow cytometry. The box and whiskers plot graphically represents the frequency distribution of the percentage CD62L$^+$pDCs (A), CD62L$^+$mDCs (B) and CD86+mDCs (C) of the control, HIV-1 and HIV-1-related study groups. Each boxplot shows the 10-90 percentile range of data (whiskers) and horizontal line the median value. Outliers are represented by black enclosed circles. Horizontal lines with diamond arrows indicate the specific study group comparison of interest and an asterisk(s) the significance. Refer to Table 3.4 for a description of the method used to indicate the level of statistical significance.

4.4.1.2 Expression profile of the apoptotic markers: TNF-R2, FAS, TRAIL receptors (R1-R4) and FASL on blood DCs of the control, HIV-1 and HIV-1-related study groups.

TNF-R2 was found positively and constitutively expressed by pDCs and mDCs, respectively. FAS expression was absent on pDCs and constitutively expressed by mDCs. The four TRAIL receptors as well as FASL were found negatively expressed by both DC subsets.

Assessing the expression of markers related to apoptosis on blood DCs in healthy individuals showed a distinct shift in MFI between TNF-R2 and related FMO/internal control stain for both DC subsets (Figure 4.13) as well as FAS staining on mDCs. The staining pattern revealed constitutive expression of FAS and TNF-R2 by mDCs and positive expression of the latter marker on pDCs. These blood DC subsets were designated as FAS^+mDCs, $TNF\text{-}R2^+$mDCs, $TNF\text{-}R2^+$pDCs, respectively. In contrast, a similar staining profile between marker and related FMO/internal control stain with no change in MFI was observed with TRAIL-R1 (Figure 4.9), TRAIL-R2 (Figure 4.10), TRAIL-R3 (Figure 4.11), TRAIL-R4 (Figure 4.12) and FASL (Figure 4.14) on both DC subsets as well as FAS (Figure 4.16) on pDCs. This staining pattern for these markers confirmed negative expression of these markers on DCs from fresh whole blood.

HIV-1 and HIV-1/TB co-infection associated changes on TNF-R2 expression

The median percentage $TNF\text{-}R2^+$pDCs was higher in the ARV^-HIV-1 and ARV^-HIV-1/TB study groups compared to the control study group, however, the change was not significant. Notably, a significantly reduced median percentage of $TNF\text{-}R2^+$pDCs was observed in the ARV^+HIV-1/TB study group compared to the ARV^-HIV-1/TB study group. The reason for this change is not clear as the median time on ARV therapy for the ARV^+HIV-1/TB study group was 5.5 months which was much shorter than the 18 months of the ARV^+HIV-1 study group showing only slightly reduced median percentage levels of $TNF\text{-}R2^+$pDCs. The significant change in median percentage $TNF\text{-}R2^+$pDCs can possibly be attributed to anti-TB therapy as the median time on anti-TB therapy for the ARV^+HIV-1/TB study group was 3 months compared to that of the ARV^-HIV-1/TB study group which was < 1 month (Figure 4.23A)

No significant change was observed in the median percentage $TNF\text{-}R2^+$mDCs between the ARV^-HIV-1 study group and control study group, however, a significantly higher median frequency of $TNF\text{-}R2^+$mDCs was observed in the ARV^-HIV-1/TB study group ($p \leq 0.05$). Also, the median percentage $TNF\text{-}R2^+$mDCs was significantly higher in the ARV^-HIV-1/TB study group compared to the ARV^-HIV-1 study group ($p \leq 0.05$) which may indicate the effect of the TB co-infection. A decline in the median percentage $TNF\text{-}R2^+$mDCs was observed in the ARV^+HIV-1/TB study group which trended towards significance ($p = 0.13$) (Figure 4.23B). The percentage FAS^+mDCs of the HIV-1 and HIV-1 related study groups was comparable to the control study group. Hence, neither an HIV-1 nor HIV-1/TB co-infection induced a change in the distribution frequency of the FAS^+mDCs subsets. However, a slightly lower median percentage of FAS^+mDCs was observed in the ARV^+HIV-1 study group compared to the ARV^-HIV-1 study group which trended towards significance ($p = 0.08$) (Figure 4.23C).

The negative staining profile of TRAIL R1-R4 and FASL on both DC subsets as well as FAS on pDCs as observed in healthy controls was also observed in the HIV-1 and HIV-1 related study groups (data not

shown). Collectively, the data indicated that HIV-1 infection and HIV-1/TB co-infection had no impact on the expression of these markers on blood DCs. It is suggested that future studies also focus on MFI data to evaluate marker density changes.

The expression profile of TRAILs cognate receptors has not been widely documented, however putative negative expression by blood DCs in healthy individuals was considered due to the absence of significant TRAIL-R1 and TRAIL-R2 expression on DCs from cord blood (Peng P, *et al.* 2011). However, assays investigating the expression of the four TRAIL receptors using mo-DCs (significant of tissue resident DCs, namely, immature DC and mature DCs) showed positive expression of TRAIL-R2 and TRAIL-R3 (notably, lacking expression of TRAIL-R1 and TRAIL-R4) (Leverkus M, *et al.* 2000). These findings may be indicative of TRAIL receptor up-regulation at different stages of DC development. The FAS and FASL molecules have also been reported by Dillon SM and colleagues (2011) as markers negatively expressed by blood pDCs and mDCs in healthy individuals. In line with the current study's findings, Dillon SM *et al.* (2011) also did not observe a significant change in FAS and FASL expression on blood mDCs and pDCs between healthy individuals and HIV-1 infected patients.

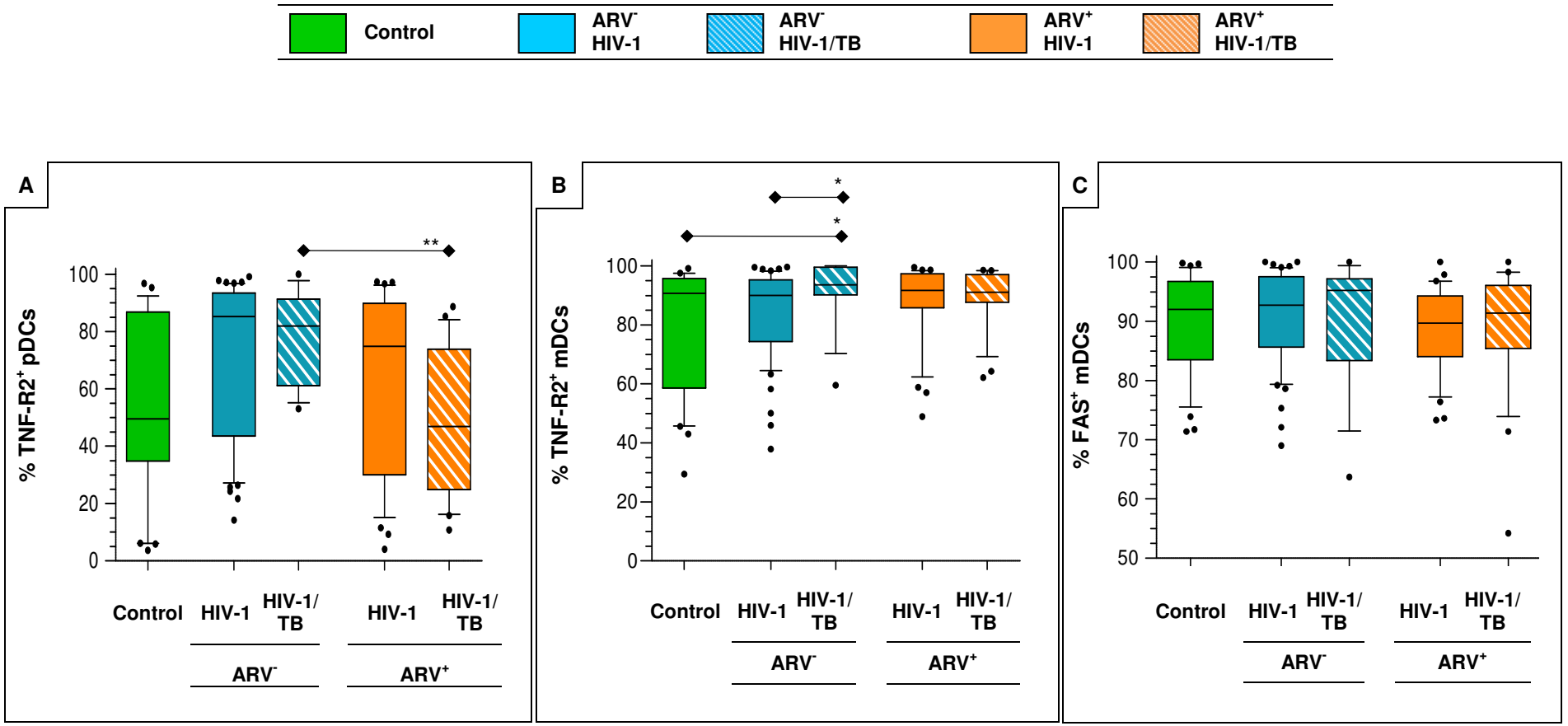

Figure 4. 23: TNF-R2$^+$pDC, TNF-R2$^+$mDC and FAS$^+$mDC subsets distribution of the control, HIV-1 and HIV-1 related study groups

Peripheral whole blood was stained with mAbs to detect the percentage pDCs and mDCs expressing TNF-R2 or FAS using multi-parameter flow cytometry. The box and whiskers plot graphically represents the frequency distribution of the percentage TNF-R2$^+$pDCs (A), TNF-R2$^+$ mDCs (B) and FAS$^+$mDCs (C) of the control, HIV-1 and HIV-1-related study groups. Each boxplot shows the 10-90 percentile range of data (whiskers) and horizontal line the median value. Outliers are represented by an enclosed circle. Horizontal lines with diamond arrows indicate the specific study group comparison of interest and an asterisk(s) the significance. Refer to Table 3.4 for a description of the method used to indicate the level of statistical significance.

4.4.1.3 Expression profile of the chemokine markers: CCR5, CCR7, CCR9 and CXCR6 on blood DCs of the control, HIV-1 and HIV-1-related study groups.

CCR5 was found positively expressed by pDCs and negatively by mDCs. The expression of CCR7, CCR9 and CXCR6 was found negative on both DC subsets.

Assessing chemokine marker expression in healthy controls found a significant change in the staining profile and MFI in the marker stain compared to the FMO control stain of CCR5 on pDCs confirming positive expression of CCR5 by pDCs (Figure 4.5 B1-B2). The expression profile of CCR5 on mDCs (Figure 4.5 C1-2) as well as CCR7 (Figure 4.4), CCR9 (Figure 4.6) and CXCR6 (Figure 4.8) on both DC subsets matched the profile of corresponding FMO stain/internal control and indicated negative expression of these markers.

ARV therapy reduced the frequency of CCR5$^+$pDC subsets

HIV-1 infection did not induce a change in the distribution of CCR5$^+$pDCs as the median percentage CCR5$^+$pDCs was similar between the control and ARV$^-$HIV-1 study group. Notably, comparing the median percentage CCR5$^+$pDCs of both these study groups to the ARV$^+$HIV-1 study group a significantly lower median percentage of CCR5$^+$pDCs was observed (Figure 4.24). The decline in CCR5$^+$pDC distribution to levels below that of the control study group may indicate an inhibitory role induced by ARV therapy. This may lead to suboptimal responses to the CCR5 ligands and reduced migration to secondary lymphoid tissue and subsequent activation of the adaptive immune responses. Notably, the number of flow cytometry acquired events was extremely low in the HIV-1/TB study group and adequately analyses could not be performed, hence, this data point was removed from CCR5 statistical analyses.

HIV-1 infection incurred no change in the expression profile of the negatively expressed chemokine markers

HIV-1 and HIV-1/TB infection did not influence CCR9 and CXCR6 marker expression on blood DCs as the expression profile between the control, HIV-1 and HIV-1-related study groups was similar (data not shown). In regard to these findings, the study could not provide conclusive evidence that declining DC numbers are the result of enhanced export from blood in response to inflammatory signaling generated at infected/inflamed sites in the GIT and/or lungs. Possibly, the choice of markers was not sufficient for the purpose intended, hence, the study proposed to investigate a broader range of chemokine markers involved in directing migration to these sites during the relevant infection. However, in view of observing no changes in expression of these migratory marker expression on blood DCs when examined in conditions known for intestinal and pulmonary infection, it was proposed that phenotypic changes during localised infection is maybe restricted to tissue-specific DCs. Furthermore, it was theorised that the blood DCs that have left circulation to perform a homeostatic function in tissue are more prone to anticipated phenotypic changes upon exposure to the milieu of the specific tissue compartment. This theory was based on findings from a study conducted by Mann ER, *et al.* (2012) who showed the differentiation of blood DCs into a gut-specific phenotype with homeostatic function upon *in vitro* exposure to supernatant collected from colonic biopsies.

Analysis of CCR7 (lymphoid homing marker) expression on DCs was complex due to inconsistent marker expression. The staining profile observed during analyses was in certain cases different to but in majority of cases similar to that of the FMO stain/internal control (Data not shown). Possibly, this may be related to

donor specificity, however, the majority of cases showed no expression of CCR7. Notably, a study by Patterson S, *et al*. (2005) showed no expression of CCR7 in freshly isolated blood DCs while observing upregulated expression only in pDCs after a 2 day culture with GM-CSF and IL-4.

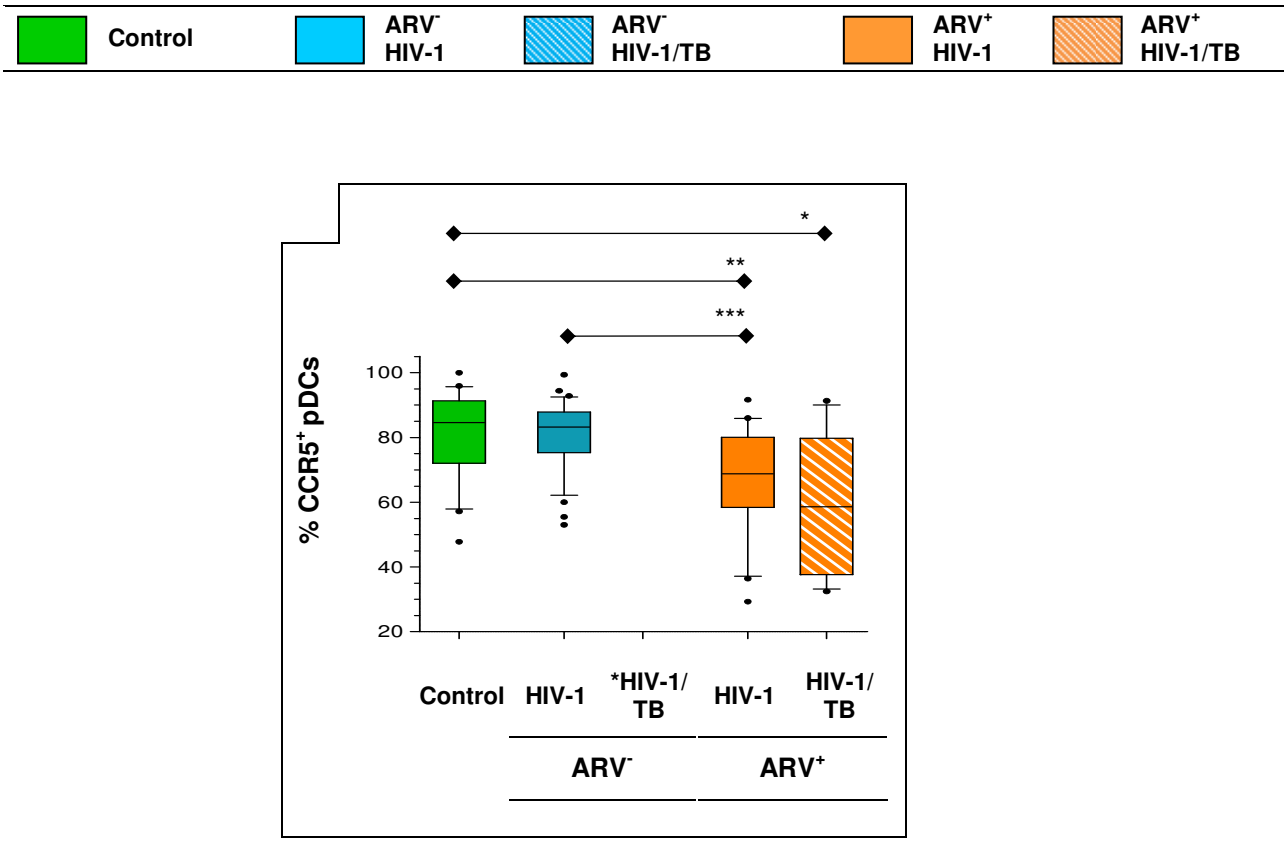

Figure 4. 24: CCR5$^+$pDC subset distribution of the control, HIV-1 and HIV-1 related study groups

Peripheral whole blood was stained with mAbs to detect the percentage pDCs and mDCs expressing CCR5 using multi-parameter flow cytometry. The box and whiskers plot graphically represents the frequency distribution of the percentage CCR5$^+$pDCs of the control, HIV-1 and HIV-1-related study groups. Each boxplot shows the 10-90 percentile range of data (whiskers) and horizontal line the median value. Outliers are represented by an enclosed circle. Horizontal lines with diamond arrows indicate the specific study group comparison of interest and an asterisk(s) the significance. Refer to Table 3.4 for a description of the method used to indicate the level of statistical significance. ***Note:** an insufficient number of events were obtained from samples of the HIV-1/TB study group, hence, adequate statistical analysis could not be performed and a graph excluding the boxplot for this study group was generated.*

4.5 Conclusion

In this study, it was proposed that declining numbers of pDCs and mDCs might be the net result of persistent exposure and/or response to the milieu of harmful viral elements, excessive host inflammatory agents and/or gut "leaking" elements in circulation during HIV-1 infection. In view of this, escalating frequencies in cellular mechanisms such as apoptosis, activation and cell mobilisation (either due to increased antigen capture for presentation in the lymph nodes and/or chemotactic movement in response to inflammatory signals generated at sites of infection) were proposed as three possible scenarios that could explain the decline of pDCs and mDCs from peripheral blood during HIV-1 infection. Accordingly, the present study examined the residual pool of blood pDCs and mDCs of chronically HIV-1 and HIV-1/TB co-infected as well as ARV treated patients for *ex vivo* surface expressed markers related to apoptosis, migration and activation. It was proposed that the effect of chronic exposure to the HIV-1 induced milieu in circulation would be mirrored by a change in the expression of these markers and possibly indicates their role in DC number loss. In summary the following was found

1) Negative marker expression in the control study group with no significant change when compared to HIV-1 and HIV-1-related study groups, these included
    a) the migratory markers CCR5 on mDCs, CCR9 and CXCR6 on both DC subsets,
    b) the apoptotic markers TRAIL R1 – R4 and FASL on both DC subsets and FAS on pDCs
    c) the activation markers CD80 and CD83 on both DC subsets, and CD86 on pDCs

2) Positive expression of markers in the control study group with no significant change when compared to the HIV-1 and HIV-1 related study groups, these included
    a) the activation marker CD62L on both DC subsets
    b) the apoptotic marker FAS on mDCs

    It was suggested that future studies also investigate MFI data of positively expressed marker to evaluate marker density changes during HIV-1 infection.

3) Positive expression of markers in the control study group showing a significant change when compared to the HIV-1 and HIV-1 related study groups.
    a) the activation marker CD86 on mDCs
    b) the migratory marker CCR5 on pDCs
    c) the apoptotic marker, TNF-R2 on pDCs and mDCs.

In view of the substantiated reports on viral elements and upregulated host factors in circulation during HIV-1 infection, the stable CD62L and FAS expression was interesting. Possibly, this signifies that DCs are conditioned not to respond to antigen while in peripheral circulation (possibly an inherent preventative process of precursor DCs in blood). It was proposed that DC phenotype change or differentiation may be 1) significant of antigen encountered DCs in lymphatic circulation or 2) restricted to tissue-resident DCs. Furthermore, the study contemplated the significance of positive FAS and CD62L marker expression. It was proposed this to 1) imply the marker as phenotypically positive but on a functional level, temporarily "dormant" and 2) defined as a preset "time saving" mode that, in the event of cellular activation, not much time is wasted on pre-events such as gene regulation when prompt response to antigen is required.

It was further proposed that persistent exposure to the HIV-1 induced milieu in circulation, in addition to playing a part in the decline of DCs from peripheral blood, may induce exhaustion of DCs and in turn affect their function. Hence, the third part of the study aimed at investigating the functional abilities of the current blood DC pool in circulation of HIV-1 infected patients upon pathogenic *in vitro* stimulation.

4.6 References

Books

Abbas AK, Lichtman AH, Pillai S. Cellular and Molecular Immunoloy. 7th ed. USA: Elsevier Saunders. 2012. p158.

Journals

Agostini, C., Cabrelle, A., Calabrese, F., Bortoli, M., Scquizzato, E., Carraro, S., Miorin, M., Beghè, B., Trentin, L., Zambello, R., *et al*. (2005). Role for CXCR6 and its ligand CXCL16 in the pathogenesis of T-cell alveolitis in sarcoidosis. Am. J. Respir. Crit. Care Med. *172*, 1290–1298.

Ajuebor, M.N., Hogaboam, C.M., Kunkel, S.L., Proudfoot, A. E. and Wallace, J.L. (2001). The chemokine RANTES is a crucial mediator of the progression from acute to chronic colitis in the Rat. J. Immunol. *166*, 552–558.

Arican, O., Aral, M., Sasmaz, S., and Ciragil, P. (2005). Serum levels of TNF-alpha, IFN-gamma, IL-6, IL-8, IL-12, IL-17, and IL-18 in patients with active psoriasis and correlation with disease severity. Mediators Inflamm. *5*, 273–279.

Arrieta, M.C., Madsen, K., Doyle, J., and Meddings, J. (2009). Reducing small intestinal permeability attenuates colitis in the IL10 gene-deficient mouse. Gut *58*, 41–48.

Baumgarth, N., and Roederer, M. (2000). A practical approach to multicolor flow cytometry for immunophenotyping. J. Immunol. Methods *243*, 77–97.

Benlahrech, A., Yasmin, A., Westrop, S.J., Coleman, A., Herasimtschuk, A., Page, E., Kelleher, P., Gotch, F., Imami, N., and Patterson, S. (2012). Dysregulated immunophenotypic attributes of plasmacytoid but not myeloid dendritic cells in HIV-1 infected individuals in the absence of highly active anti-retroviral therapy. Clin. Exp. Imunol. *170*, 212–221.

Boni, C., Fisicaro, P., Valdatta, C., Amadei, B., Di Vincenzo, P., Giuberti, T., Laccabue, D., Zerbini, A., Cavalli, A., Missale, G., *et al*. (2007). Characterization of Hepatitis B virus (HBV)-specific T-cell dysfunction in chronic HBV infection. J. Virol. *81*, 4215–4225.

Breen, E.C. (2002). Pro- and anti-inflammatory cytokines in human immunodeficiency virus infection and acquired immunodeficiency syndrome. Pharmacol. Ther. *95*, 295–304.

Brenchley, J.M., Price, D.A., and Douek, D.C. (2006a). HIV disease: fallout from a mucosal catastrophe? Nat. Immunol. *7*, 235–239.

Brenchley, J.M., Price, D.A., Schacker, T.W., Asher, T.E., Silvestri, G., Rao, S., Kazzaz, Z., Bornstein, E., Lambotte, O., Altmann, D., *et al*. (2006b). Microbial translocation is a cause of systemic immune activation in chronic HIV infection. Nat. Med. *12*, 1365–1371.

Brockman, M. a, Kwon, D.S., Tighe, D.P., Pavlik, D.F., Rosato, P.C., Sela, J., Porichis, F., Le Gall, S., Waring, M.T., Moss, K., *et al*. (2009). IL-10 is up-regulated in multiple cell types during viremic HIV infection and reversibly inhibits virus-specific T cells. Blood *114*, 346–356.

Brown, K.N., Trichel, A., and Barratt-Boyes, S.M. (2007). Parallel loss of myeloid and plasmacytoid dendritic cells from blood and lymphoid tissue in simian AIDS. J. Immunol. 6958–6967.

Cantin, R., Méthot, S., and Tremblay, M.J. (2005). Plunder and Stowaways: Incorporation of cellular proteins by enveloped viruses. J. Virol. *79*, 6577–6587.

Chang, W.L.W., Baumgarth, N., Meghan, K., Lee, C.Y.D., Baron, C.A., Gregg, J.P., and Barry, P.A. (2007). Exposure of myeloid dendritic cells to exogenous or endogenous IL-10 during maturation determines their longevity. J. Immunol. *178*, 7794–7804.

Chen, Y., Hwang, S., Chan, V., Chung, N., Wang, S., Li, Z., Ma, J., CW, L., Hsieh, Y., Chang, K., *et al*. (2013). Binding of HIV-1 gp120 to DC-SIGN promotes ASK-1-dependent activation-induced apoptosis of human dendritic cells. PLoS Pathog. *9*, 1–17.

Damås, J.K., Landrø, L., Fevang, B., Heggelund, L., Frølanda, S., and Aukrusta, P. (2009). Enhanced levels of the CCR7 ligands CCL19 and CCL21 in HIV infection: correlation with viral load, disease progression and response to highly active antiretroviral therapy. AIDS *23*, 135–138.

Das, S.N., Khare, P., Singh, M.K., and Sharma, S.C. (2011). Fas receptor (CD95) & Fas ligand (CD 178) expression in patients with tobacco-related intraoral squamous cell carcinoma. Indian J. Med. Res. *134*, 54–60.

Davalos-Misslitz, A.C.M., Rieckenberg, J., Willenzon, S., Worbs, T., Kremmer, E., Bernhardt, G., and Förster, R. (2007). Generalized multi-organ autoimmunity in CCR7-deficient mice. Eur. J. Immunol. *37*, 613–622.

De, S.K., Devadas, K., and Notkins, A.L. (2002). Elevated levels of Tumor Necrosis Factor Alpha (TNF-alpha) in Human Immunodeficiency Virus type 1-transgenic mice: prevention of death by antibody to TNF-alpha. J. Virol. *76*, 11710–11714.

Degli-Esposti, M.A., Smolak, P.J., Walczak, H., Waugh, J., Huang, C.-P., Dubose, R.F., Goodwin, R.G., and Smith, C.A. (1997a). Cloning and characterization of TRAIL-R3, a Novel Member of the emerging TRAIL Receptor family. J. Exp. Med. *186*, 1165–1170.

Degli-Esposti, M.A., Dougall, W.C., Smolak, P.J., Waugh, J.Y., Smith, C.A., and Goodwin, R.G. (1997b). The novel receptor TRAIL-R4 induces NF-kappa B and protects against TRAIL-mediated apoptosis, yet retains an incomplete death domain. Immunity *7*, 813–820.

de Milito, A., Hejdeman, B.O., Albert, J., Aleman, S.O.O., Sönnerborg, A., Zazzi, M., and Chiodi, F. (2000). High plasma levels of soluble Fas in HIV type 1-infected subjects are not normalised during highly active antiretroviral therapy. AIDS Res. Hum. Retroviruses *16*, 1379–1384.

de Vries, E.G.E., Gietema, J.A., and de Jong, S. (2006). Tumor necrosis factor-related apoptosis-inducing ligand pathway and its therapeutic implications. Clin. Cancer Res. *12*, 2390–2393.

Dickie, P., Felser, J., Eckhaus, M., Bryant, J., Silver, J., Marinos, N., and Notkins, A.L. (1991). HIV-associated nephropathy intransgenic mice expressing HIV-1 genes. Virology *185*, 109–119.

Dillon, S.M., Robertson, K.B., Pan, S.C., Mawhinney, S., Meditz, A.L., Folkvord, J.M., Connick, E., McCarter, M.D., and Wilson, C.C. (2008). Plasmacytoid and myeloid dendritic cells with a partial activation phenotype accumulate in lymphoid tissue during asymptomatic chronic HIV-1 infection. J. Acquir. Immune Defic. Syndr. *48*, 1–12.

Dillon, S.M., Friedlander, L.J., Rogers, L.M., Meditz, A.L., Folkvord, J.M., Connick, E., McCarter, M.D., and Wilson, C.C. (2011). Blood myeloid dendritic cells from HIV-1-infected individuals display a proapoptotic profile characterized by decreased Bcl-2 levels and by caspase-3+ frequencies that are associated with levels of plasma viremia and T cell activation in an exploratory st. J. Virol. *85*, 397–409.

Dunn, C., Brunetto, M., Reynolds, G., Christophides, T., Kennedy, P.T., Lampertico, P., Das, A., Lopes, A.R., Borrow, P., Williams, K., *et al*. (2007). Cytokines induced during chronic hepatitis B virus infection promote a pathway for NK cell-mediated liver damage. J. Exp. Med. *204*, 667–680.

Eppert, B.L., Motz, G.T., Wortham, B.W., Flury, J.L., and Borchers, M.T. (2010). CCR7 deficiency leads to leukocyte activation and increased clearance in response to pulmonary Pseudomonas aeruginosa infection. Infect. Immun. *78*, 2099–2107.

Falschlehner, C., Emmerich, C.H., Gerlach, B., and Walczak, H. (2007). TRAIL signalling: Decisions between life and death. Int. J. Biochem. Cell Biol. *39*, 1462–1475.

Fang, L., Sun, L., Hu, F., and Chen, Q. (2013). Effects of FasL Expression in oral squamous cell cancer. Asian Pacific J. Cancer Prev. *14*, 281–285.

Faustman, D.L., and Davis, M. (2013). TNF Receptor 2 and disease: autoimmunity and regenerative medicine. Front. Immunol. *4*, 1–8.

Ferguson, T.A., and Griffith, T.S. (2006). A vision of cell death : Fas ligand and immune privilege 10 years later. Immunol. Rev. *213*, 228–238.

Forman, M.A., and Gupta, R.K. (2007). Tandem dyes for flow cytometry: can we overcome quality concerns? MLO. Med. Lab. Obs. 24, 26.

Gasper-Smith, N., Crossman, D.M., Whitesides, J.F., Mensali, N., Ottinger, J.S., Plonk, S.G., Moody, M.A., Ferrari, G., Weinhold, K.J., Miller, S.E., *et al.* (2008). Induction of plasma (TRAIL), TNFR-2, Fas ligand, and plasma microparticles after human immunodeficiency virus type 1 (HIV-1) transmission: implications for HIV-1 vaccine design. J. Virol. *82*, 7700–7710.

Gelderblom HR, Reupke, H., and Pauli, G. (1985). Loss of envelope antigens if HTLV-III/LAV, a factor in AIDS pathogenesis. The Lancet. 1016–1017.

Gimsa, U., Mitchison, N.A., and Brunner-weinzierl, M.C. (2013). Immune privilege as an intrinsic CNS property: astrocytes protect the CNS against T-cell-mediated neuroinflammation. Mediators Inflamm. *2013*, 1–11.

Gomes-Santos, A.C., Moreira, T.G., Castro-Junior, A.B., Horta, B.C., Lemos, L., Cruz, D.N., Guimarães, M.A.F., Cara, D.C., McCafferty, D.-M., and Faria, A.M.C. (2011). New insights into the immunological changes in IL-10-deficient mice during the course of spontaneous inflammation in the gut mucosa. Clin. Dev. Immunol. *2012*, 1–13.

Green, D.S., Center, D., and Cruikshank, W.W. (2009). Human immunodeficiency virus type 1 gp120 reprogramming of CD4+ T-cell migration provides a mechanism for lymphadenopathy. J. Virol. *83*, 5765–5772.

Gregory, M.S., Repp, A.C., Holhbaum, A.M., Saff, R.R., Marshak-Rothstein, A., and Ksander, B.R. (2002). Membrane Fas ligand activates innate immunity and terminates ocular immune privilege. J. Immunol. *169*, 2727–2735.

Gregory, M.S., Hackett, C.G., Abernathy, E.F., Lee, K.S., Saff, R.R., Hohlbaum, A.M., Moody, K.-S.L., Hobson, M.W., Jones, A., Kolovou, P., *et al.* (2011). Opposing roles for membrane bound and soluble Fas ligand in glaucoma-associated retinal ganglion cell death. PLoS One *6*, 1–13.

Guadalupe, M., Reay, E., Sankaran, S., Prindiville, T., Flamm, J., Mcneil, A., and Dandekar, S. (2003). Severe CD4 + T-cell depletion in gut lymphoid tissue during primary Human Immunodeficiency Virus type 1 infection and substantial delay in restoration following Highly Active Antiretroviral Therapy. J. Virol. *77*, 11708–11717.

Hartigan, A.J., Westwick, J., Jarai, G., and Hogaboam, C.M. (2009). CCR7 deficiency on dendritic cells enhances fungal clearance in a murine model of pulmonary invasive aspergillosis. J. Immunol. *183*, 5171–5179.

Herbeuval, J.-P., Boasso, A., Grivel, J.-C., Hardy, A.W., Anderson, S.A., Dolan, M.J., Chougnet, C., Lifson, J.D., and Shearer, G.M. (2005). TNF-related apoptosis-inducing ligand (TRAIL) in HIV-1-infected patients and its in vitro production by antigen-presenting cells. Blood *105*, 2458–2464.

Herzenberg, L.A., Tung, J., Moore, W.A., Herzenberg, L.A., and Parks, D.R. (2006). Interpreting flow cytometry data: a guide for the perplexed. Nat. Immunol. *7*, 681–685.

Holland, P.M. (2014). Death receptor agonist therapies for cancer, which is the right TRAIL? Cytokine Growth Factor Rev. *25*, 185–193.

Hosaka, N., Oyaizu, N., Kaplan, M.H., Yagita, H., and Pahwa, S. (1998). Membrane and soluble forms of Fas (CD95) and Fas ligand in peripheral blood mononuclear cells and in plasma from Human Immunodeficiency Virus – infected persons. J. Infect. Dis. *178*, 1030–1039.

Huang, K.-J., Su, I.-J., Theron, M., Wu, Y.-C., Lai, S.-K., Liu, C.-C., and Lei, H.-Y. (2005). An interferon-gamma-related cytokine storm in SARS patients. J. Med. Virol. *75*, 185–194.

Hulspas, R., O'Gorman, M.R.G., Wood, B.L., Gratama, J.W., and Sutherland, D.R. (2009). Considerations for the control of background fluorescence in clinical flow cytometry. Cytom. Part B Clin. Cytom. *76B*, 355–364.

Hütter, G., Nowak, D., Mossner, M., Ganepola, S., Müßig, A., Allers, K., Schneider, T., Hofmann, J., Kücherer, C., Blau, O., *et al.* (2009). Long-term control of HIV by CCR5 Delta32/Delta32 stem-cell transplantaion. N. Engl. J. Med. *360*, 692–698.

Ikomey, G.M., Okomo-Assoumou, M.-C., Atashili, J., Mesembe, M.T., Mukwele, B., Lyonga, E., Eyoh, A., and Ndumbe, P.M. (2012). Plasma concentrations of soluble Fas receptors (Fas) and Fas ligands (FasL) in relation to CD4+ cell counts in HIV-1 positive and negative patients in Yaounde, Cameroon. BMC Res. Notes *5*, 322.

Ivetic, A., and Ridley, A.J. (2004). The telling tail of L-selectin. Biochem. Soc. Trans. *32*, 1118–1121.

Jackson, L.A., Drevets, D.A., Dong, Z., Greenfield, R.A., and Murphy, J.W. (2005). Levels of L-selectin (CD62L) on human leukocytes in disseminated Cryptococcosis with and without associated HIV-1 infection. J. Infect. Dis. *191*, 1361–1367.

Junt, T., Scandella, E., Förster, R., Krautwald, S., Lipp, M., Hengartner, H., Ludewig, B., Fo, R., and Krebs, P. (2004). Impact of CCR7 on priming and distribution of antiviral effector and memory CTL. J. Immunol. *173*, 6684–6693.

Kahnert, A., Höpken, U.E., Stein, M., Bandermann, S., Lipp, M., and Kaufmann, S.H.E. (2007). Mycobacterium tuberculosis triggers formation of lymphoid structure in murine lungs. J. Infect. Dis. *195*, 46–54.

Kaur, S., White, S., and Bartold, P.M. (2013). Periodontal disease and rheumatoid arthritis: a systematic review. J. Dent. Res. *92*, 399–408.

Keating, S.M., Golub, E.T., Nowicki, M., Young, M., Anastos, K., Crystal, H., Cohen, M.H., Zhang, J., Greenblatt, R.M., Desai, S., *et al.* (2011). The effect of HIV infection and HAART on inflammatory biomarkers in a population-based cohort of women. AIDS *25*, 1823–1832.

Kennedy, R.J., Hoper, M., Deodhar, K., Erwin, P.J., Kirk, S.J., and Gardiner, K.R. (2000). Interleukin 10-deficient colitis: new similarities to human inflammatory bowel disease. Br. J. Surg. *87*, 1346–1351.

Klinger, A., Gebert, A., Bieber, K., Kalies, K., Ager, A., Bell, E.B., and Westermann, J. (2009). Cyclical expression of L-selectin (CD62L) by recirculating T cells. Int. Immunol. *21*, 443–455.

Kocks, J.R., Adler, H., Danzer, H., K, H., Jonigk, D., Lehmann, U., and Förster, F. (2009). Chemokine receptor CCR7 contributes to a rapid and efficient clearance of lytic murine γ-herpes virus 68 from the lung, whereas bronchus-associated lymphoid tissue harbors virus during latency. J. Immunol. *182*, 6861–6869.

Kopp, J.B., Rooney, J.F., Wohlenberg, C., Dorfman, N., Marinos, N.J., Bryant, J.L., Katz, S.I., Notkins, A.L., and Klotman, P.E. (1993). Cutaneous disorders and viral gene expression in HIV-1 transgenic mice. AIDS Res. Hum. Retroviruses *9*, 267–275.

Kourtis, A.P., Nesheim, S.R., Thea, D., Ibegbu, C., Nahmias, A.J., and Lee, F.K. (2000). Correlation of virus load and soluble L-selectin , a marker of immune activation , in pediatric HIV-1 infection. AIDS *14*, 2429–2436.

Kühn, R., Löhler, J., Rennick, D., Rajewsky, K., and Müller, W. (1993). Interleukin-10-deficient mice develop chronic enterocolitis. Cell *75*, 263–274.

Leverkus, M., Walczak, H., Mclellan, A., Fries, H.-W., Terbeck, G., Bröcker, E.-B., and Kämpgen, E. (2000). Maturation of dendritic cells leads to up-regulation of cellular FLICE-inhibitory protein and concomitant down-regulation of death ligand – mediated apoptosis. Am. Soc. Hematol. *96*, 2628–2632.

Liu, J.H., Wei, S., Lamy, T., Li, Y., PK, E.-B., Djeu, J.Y., Thomas, P., and Loughran, J. (2002). Blockade of Fas-dependent apoptosis by soluble Fas in LGL leukemia. Blood *100*, 1449–1453.

Liu, P., Overman, R.G., Yates, N.L., Alam, S.M., Vandergrift, N., Chen, Y., Graw, F., Freel, S.A., Kappes, J.C., Ochsenbauer, C., *et al.* (2011). Dynamic antibody specificities and virion concentrations in circulating immune complexes in acute to chronic HIV-1 infection. J. Virol. *85*, 11196–11207.

Liu, Z., Zhang, P., Ma, Y., Chen, H., Zhou, Y., Zhang, M., Chu, Z., and Qin, H. (2011). Lactobacillus plantarum prevents prevents the development of colitis in IL-10-deficient mouse by reducing the intestinal permeability. Mol. Biol. Rep. *38*, 1353–1361.

Ludewig, B., Graf, D., Gelderblom, H.R., Becker, Y., Kroczek, R.A., and Pauli, G. (1995). Spontaneous apoptosis of dendritic cells is efficiently inhibited by TRAP (CD40-ligand) and TNF-α, but strongly enhanced by interleukin-10.pdf. Eur. J. Immunol. *25*, 1943–1950.

Madsen, K.L., Malfair, D., Gray, D., Doyle, J.S., Jewell, L.D., and Fedorak, R.N. (1999). Interleukin - 10 gene-deficient mice develop a primary intestinal permeability defect in response to enteric microflora. Inflamm. Bowel Dis. *5*, 262–270.

Maecker, H.T., Frey, T., Nomura, L.E., and Trotter, J. (2004). Selecting fluorochrome conjugates for maximum sensitivity. Cytom. Part A *62A*, 169–173.

Malaponte, G., Bevelacqua, V., Li Volti, G., Petrina, M., Nicotra, G., Sapuppo, V., Li Volti, S., Travali, S., and Mazzarino, M.C. (2004). Soluble adhesion molecules and cytokines in children affected by recurrent infections of the upper respiratory tract. Pediatr. Res. *55*, 666–673.

Mandl, J.N., Barry, A.P., Vanderford, T.H., Kozyr, N., Chavan, R., Klucking, S., Barrat, F.J., Coffman, R.L., Staprans, S.I., and Feinberg, M.B. (2008). Divergent TLR7 and TLR9 signaling and type I interferon production distinguish pathogenic and nonpathogenic AIDS virus infections. Nat. Med. *14*, 1077–1087.

Mann, E.R., Bernardo, D., Al-Hassi, H.O., English, N.R., Clark, S.K., McCarthy, N.E., Milestone, A.N., Cochrane, S.A., Hart, A.L., Stagg, A.J., *et al.* (2012). Human gut-specific homeostatic dendritic cells are generated from blood precursors by the gut microenvironment. Inflamm. Bowel Dis. *18*, 1275–1286.

Matloubian, M., Lo, C.G., Cinamon, G., Lesneski, M., Xu, Y., Brinkmann, V., Allende, M., Proia, R., and JG, C. (2004). Lymphocyte egress from thymus and peripheral lymphoid organs is dependent on S1P receptor 1. Nature *427*, 355–360.

Mavigner, M., Cazabat, M., Dubois, M., L'Faqihi, F., Requena, M., Pasquier, C., Klopp, P., Amar, J., Alric, L., Barange, K., *et al.* (2012). Altered CD4 + T cell homing to the gut impairs mucosal immune reconstitution in treated HIV-infected individuals. J. Clin. Invest. *122*, 62–69.

Monsalvo, A.C., Batalle, J.P., Lopez, M.F., Krause, J.C., Klemenc, J., Hernandez, J.Z., Maskin, B., Bugna, J., Rubinstein, C., Aguilar, L., *et al*. (2011). Severe pandemic 2009 H1N1 influenza disease due to pathogenic immune complexes. Nat. Med. *17*, 195–199.

Montes de Oca Arjona, M., Pérez Cano, R., Orozco, M.J., Martín Aspas, A., Guerrero, F., Fernández Gutiérrez Del Álamo, C., and Girón-González, J.A. (2005). Absence of favourable changes in circulating levels of interleukin-16 or beta-chemokine concentration following structured intermittent interruption treatment of chronic human immunodeficiency virus infection. Clin Microbiol Infect *11*, 57–62.

Morgan, A.J., Guillen, C., Symon, F.A., Huynh, T.T., Berry, M.A., Entwisle, J.J., Briskinz, M., Pavord, I.D., and Wardlaw, A.J. (2005). Expression of CXCR6 and its ligand CXCL16 in the lung in health and disease. Clin. Exp. Allergy *35*, 1572–1580.

Muller, W.A. (2013). Getting Leucocytes to the sites of inflammation. Vet. Pathol. *50*, 7–22.

Nishimura, M., Kuboi, Y., Muramoto, K., Kawano, T., and Imai, T. (2009). Chemokines as novel therapeutic targets for inflammatory bowel disease. Ann. N. Y. Acad. Sci. *1173*, 350–356.

O' Reilly LA, Tai L, Lee L, Kruse EA, Grabow S, Fairlie WD, Haynes NM, Tarlinton DM, Zhang JG, Belz GT, Smyth MJ, Bouillet P, Robb L, S.A. (2009). Membrane-bound Fas ligand only is essential for Fas-induced apoptosis. J. Exp. Med. *461*, 659–665.

Orsilles, M.A., Pieri, E., Cooke, P., and Caula, C. (2006). IL-2 and IL-10 serum levels in HIV-1-infected patients with or without active antiretroviral therapy. Acta Pathol. Microbiol. Immunol. Scand. *114*, 55–60.

Ozbalkan, Z., Efe, C., Cesur, M., Ertek, S., Nasiroglu, N., Berneis, K., and Rizzo, M. (2010). An update on the relationships between rheumatoid arthritis and atherosclerosis. Atherosclerosis *212*, 377–382.

Pan, G., O' Rourke, K., Chinnaiyan, A.M., Gentz, R., Ebner, R., Ni, J., and Dixit, V.M. (1997). The receptor for the cytotoxic ligand TRAIL. Science *276*, 111–113.

Papadakis, K.A., Prehn, J., Nelson, V., Cheng, L., Binder, S.W., Ponath, P.D., Andrew, D.P., and Targan, S.R. (2000). The role of Thymus-expressed chemokine and its receptor CCR9 on lymphocytes in the regional specialization of the mucosal immune system. J. Immunol. *165*, 5069–5076.

Patterson, S., Donaghy, H., Amjadi, P., Gazzard, B., Gotch, F., and Kelleher, P. (2005). Human BDCA-1-positive blood Dendritic Cells differentiate into phenotypically distinct immature and mature populations in the absence of exogenous maturational stimuli: differentiation failure in HIV infection. J. Immunol. *174*, 8200–8209.

Pelsers, M.M.A.L., Hermens, W.T., and Glatz, J.F.C. (2005). Fatty acid-binding proteins as plasma markers of tissue injury. Clin. Chim. Acta *352*, 15–35.

Peng, P., Yan, Y., and Keng, S. (2011). Exosomes in the ascites of ovarian cancer patients: origin and effects on anti-tumor immunity. Oncol. Rep. *25*, 749–762.

Peppa, D., Gill, U.S., Reynolds, G., Easom, N.J.W., Pallett, L.J., Schurich, A., Micco, L., Nebbia, G., Singh, H.D., Adams, D.H., *et al*. (2013). Up-regulation of a death receptor renders antiviral T cells susceptible to NK cell-mediated deletion. J. Exp. Med. Med. *210*, 99–114.

Perfetto, S.P., Chattopadhyay, P.K., and Roederer, M. (2004). Seventeen-colour flow cytometry: unravelling the immune system. Nat. Rev. Immunol. *4*, 648–655.

Pfeffer, K. (2003). Biological functions of tumor necrosis factor cytokines and their receptors. Cytokine Growth Factor Rev. *14*, 185–191.

Pham, T.H.M., Okada, T., Matloubian, M., Lo, C.G., and Jason G, C. (2008). S1P1 receptor signaling overrides retention mediated by Gαi - coupled receptors to promote T cell egress. Immunity *28*, 122–133.

Piddubna, A.I., and Chemych, M.D. (2013). IL-4, IL-10, TNF-α profile and immunological changes in North-Eastern Ukrainian HIV-infected individuals. HIV AIDS Rev. *12*, 68–72.

Raffler, N.A., Rivera-Nieves, J., and Ley, K. (2005). L-selectin in inflammation, infection and immunity. Drug Discov. Today Ther. Strateg. *2*, 213–220.

Raport, C.J., Gosling, J., Schweickart, V.L., Gray, P.W., and Charo, I.F. (1996). Molecular cloning and functional characterization of a novel human CC chemokine receptor (CCR5) for RANTES , MIP-1 β , and MIP-1α. J. Biol. Chem. *271*, 17161–17166.

Rehermann, B. (2009). Hepatitis C virus versus innate and adaptive immune responses : a tale of coevolution and coexistence. J. Clin. Invest. *119*, 1745–1754.

Reimold, A.M. (2003). New indications for treatment of chronic inflammation by TNF-alpha blockade. Am. J. Med. Sci. *325*, 75–92.

Rosen, S.D. (2004). Ligands for L-selectin: homing, inflammation, and beyond. Annu. Rev. Immunol. *22*, 129–156.

Rychert, J., Strick, D., Bazner, S., Robinson, J., and Rosenberg, E. (2010). Detection of HIV gp120 in plasma during early HIV infection is associated with increased proinflammatory and immunoregulatory cytokines. AIDS Res. Hum. Retroviruses *26*, 1139–1145.

Sehgal, M., Zeremski, M., Talal, A.H., Khan, Z.K., Capocasale, R., Philip, R., and Jain, P. (2014). Host genetic factors and dendritic cell responses associated with the outcome of interferon/ribavirin treatment in HIV-1/HCV co-infected individuals. Clin. Cell. Immunol. *5*, 1–12.

Sprick, M.R., Weigand, M.A., Rieser, E., Rauch, C.T., Juo, P., Blenis, J., Krammer, P.H., and Walczak, H. (2000). FADD/MORT1 and caspase-8 are recruited to TRAIL receptors 1 and 2 and are essential for apoptosis mediated by TRAIL receptor 2. Immunity *12*, 599–609.

Stenqvist, A.C., Nagaeva, O., Baranov, V., and Mincheva-Nilsson, L. (2013). Exosomes secreted by human placenta carry functional Fas ligand and TRAIL molecules and convey apoptosis in activated immune cells, suggesting exosome-mediated immune privilege of the fetus. J. Immunol. *191*, 5515–5523.

Stenstad, H., Ericsson, A., Johansson-Lindbom, B., Svensson, M., Marsal, J., Mack, M., Picarella, D., Soler, D., Marquez, G., Briskin, M., *et al.* (2006). Gut-associated lymphoid tissue – primed CD4 + T cells display CCR9-dependent and -independent homing to the small intestine. Blood *107*, 3447–3454.

Strober, W., Zhang, F., Kitani, A., Fuss, I., and Fichtner-Feigl, S. (2010). Pro-inflammatory cytokines underlying the inflammation of Crohn's Disease. Curr. Opin. Gastroenterol. *26*, 310–317.

Su, D.-L., Lu, Z.-M., Shen, M.-N., Li, X., and Sun, L.-Y. (2012). Roles of pro- and anti-inflammatory cytokines in the pathogenesis of SLE. J. Biomed. Biotechnol. *2012*, 1–15.

Suda, T., Hashimoto, H., Tanaka, M., Takahiro, O., and Shigekazu, N. (1997). Membrane Fas Ligand kills human peripheral blood T lymphocytes, and soluble Fas Ligand blocks the killing. J. E *186*, 2045–2050.

Sun, Y., Jin, C., Zhan, F., Wang, X., Liang, M., Zhang, Q., Ding, S., Guan, X., Huo, X., Li, C., *et al.* (2012). Host cytokine storm is associated with disease severity of severe fever with thrombocytopenia syndrome. J. Infect. Dis. *206*, 1085–1094.

Thibault, S., Tardif, M.R., Gilbert, C., and Tremblay, M.J. (2007). Virus-associated host CD62L increases attachment of human immunodeficiency virus type 1 to endothelial cells and enhances trans infection of CD4+ T lymphocytes. J. Gen. Vrology *88*, 2568–2573.

Walczak, H., Degli-Esposti, M.A., Johnson, R.S., Smolak, P.J., Waugh, J.Y., Boiani, N., Timour, M.S., Gerhart, M.J., Schooley, K.A., Smith, C.A., *et al*. (1997). TRAIL-R2: a novel apoptosis-mediating receptor for TRAIL. EMBO J. *16*, 5386–5397.

Walker, N.F., Meintjes, G., and Wilkinson, R.J. (2013). HIV-1 and the immune response to TB. *8*, 57–80.

Wauquier, N., Becquart, P., Padilla, C., Baize, S., and Leroy, E.M. (2010). Human fatal Zaire Ebola virus infection is associated with an aberrant innate immunity and with massive lymphocyte apoptosis. PLoS Negl. Trop. Dis. *4*, 1–10.

Wendland, M., Czeloth, N., Mach, N., Malissen, B., Kremmer, E., Pabst, O., and Forster, R. (2007). CCR9 is a homing receptor for plasmacytoid dendritic cells to the small intestine. Proc. Natl. Acad. Sci. U. S. A. *104*, 6347–6352.

Wiley, S.R., Schooley, K., Smolak, P.J., Din, W.S., Huang, C.P., Nicholl, J.K., Sutherland, G.R., Smith, T.D., Rauch, C., Smith, C.A., *et al*. (1995). Identification and characterization of a new member of the TNF family that induces apoptosis. Immunity *3*, 673–682.

Winter, S., Rehm, A., Wichner, K., Scheel, T., Batra, A., Siegmund, B., Berek, C., Lipp, M., and Höpken, U.E. (2011). Manifestation of spontaneous and early autoimmune gastritis in CCR7-deficient mice. Am. J. Pathol. *179*, 754–765.

Yang, S., Liu, F., Wang, Q.J., Rosenberg, S.A., and Morgan, R.A. (2011). The shedding of CD62L (L-selectin) regulates the acquisition of lytic activity in human tumor reactive T lymphocytes. PLoS One *6*, 1–10.

Ye, P., Kazanjian, P., Kunkel, S.L., and Kirschner, D.E. (2004). Lack of good correlation of serum CC-chemokine levels with human immunodeficiency virus-1 disease stage and response to treatment. J. Lab. Clin. Med. *143*, 310–319.

Yonkers, N.L., Rodriguez, B., Asaad, R., Lederman, M.M., and Anthony, D.D. (2011). Systemic immune activation in HIV infection is associated with decreased MDC responsiveness to TLR ligand and inability to activate naive CD4 T-cells. PLoS One *6*, 1–10.

Zhang, X.D., Nguyen, T., Thomas, W.D., Sanders, J.E., and Hersey, P. (2000). Mechanisms of resistance of normal cells to TRAIL induced apoptosis vary between different cell types. Fed. Eur. Biochem. Soc. Lett. *482*, 193–199.

Chapter 5

Response of peripheral blood pDCs and mDCs of HIV-1 infected individuals to Toll-like receptors (TLR) stimulation and immunemodulation.

5.1 Introduction

HIV infection is associated with an increased risk for the development of opportunistic infections which may be indicative of reduced level of protection upon exposure to other viral or bacterial pathogens. Several study groups have reported on the altered function of DCs from HIV-1 infected individuals (as reviewed by Miller E and Bhardwaj N, 2013). In particular, Donaghy H and colleagues (2003) observed reduced proliferation of T lymphocytes from uninfected individuals when stimulated with allogeneic DCs from HIV-1 infected compared to DCs from uninfected individuals in a MLR assay. Also, altered cytokine production has been described, in particular, modification of IFN-α production has been extensively recorded. Notably, the changes associated with this cytokine during HIV-1 infection are perplexing. In parallel to the observed elevation in serum IFN-α during HIV-1 infection are reports on the significant reduction (from the blood) in the numbers of the cells that primarily produces this cytokine, namely pDCs. In better understanding this paradox, Lehman *et al.* (2008) investigated the relationship between pDC numbers and IFN-α mRNA levels in lymphoid tissue. The study proposed that a high serum IFN-α level may be the result of elevated IFN-α mRNA expression in lymphoid tissues, which in turn may be related to an influx of pDCs in the lymph nodes as a response to HIV-1 infection. However, the authors found the lymphoid compartment to house unchanged pDC numbers during HIV-1 infection in various stages of HIV-1 disease progression. Also, unaltered expression of IFN-α mRNA levels in various lymphoid tissues (cervical, axillary and inguinal lymph nodes and tonsils) was observed. Notably, the authors showed that pDCs in peripheral blood of HIV-1 infected individuals exhibited a 100 fold higher expression of IFN-α mRNA as well as increased intracellular expression of IFN-α compared to controls. They referred to this finding as an overproduction of IFN-α. Accordingly, the current study proposed this phenomenon to ultimately result in cellular exhaustion and reduced response when challenged with other invading viral/bacterial stimuli. Accordingly, Martinson JA, *et al.* (2007) observed significantly reduced levels of IFN-α upon *in vitro* TLR7 priming of pDCs and peripheral blood mononuclear cells (PBMCs) from HIV-1 infected patients. Donhauser N, *et al.* (2012) also reported on reduced IFN-α production upon *in vitro* TLR 9 stimulation of pDCs which seem to directly correlate with CD4 T lymphocyte counts.

Vital to the initiation of normal inflammation in response to invading pathogens is down-regulation of immune responses post-infection. However, in HIV-1 infection the immune system is not able to clear the virus (in absence of ARV) and with a persistent pool of viral and gut leakage antigens, inflammatory conditions persist (one of the driving forces of the disease), which is detrimental to the host. To date research has not been able to find a way to fully clear the HIV and available treatment is limited to the chronic use of ARVs to control viral replication. Conversely, this form of treatment is associated with various harmful long-term side effects and increasing reports of drug resistance. Nonetheless, it remains the only available intervention to control HIV-1 replication and provides general alleviation of damage/pressure of HIV-1-associated immune activation. Hence, while various strategies to cure HIV-1/AIDS disease are being investigated, in the interim, improved ARV treatments and/or development of new interventions are also priority. Accordingly, a sub-

project to this study focused on investigating the impact of a natural agent (neuropeptide) with reported anti-inflammatory properties, namely, VIP, on activated mDCs(Delgado M, *et al.* 2004[a]). This is also a sub-project to a bigger study aiming at investigating alternative or cognate anti-HIV-1 treatment strategies, in particular, targeting HIV-1 associated chronic immune activation and inflammatory responses using VIP.

Briefly, VIP is a neuropeptide consisting of 28 amino acids and as reviewed by Harmar AJ, *et al.* (2012), it has been identified to play a role in various diverse compartments of the body e.g. central nervous system, immune system and the GIT. Upon engagement with its cognate G-protein coupled receptors, VPAC1 and VPAC2, adenylate cyclase is stimulated resulting in the subsequent production of cyclic adenosine monophosphate (cAMP) (as reviewed by Dickson L and Finlayson K (2009)). Notably, raised intracellular cAMP levels have been linked to suppression of innate immune functions, in particular modulation of 1) phagocytic and microbiocidal activity and 2) various inflammatory cytokine expressions (down-regulating TNF-α and IL-12, while up-regulating IL-10)(Delgado M, *et al.* 2004[b]). Also, the inhibitory effect of VIP on immune related molecules such as prostaglandin E_2 (PGE_2), an autocoid hormone (autocrine or paracrine but not endocrine acting) that plays a role in inflammation, has been described. Under normal inflammatory conditions PGE_2 and cyclooxygenase-2 (COX-2) (an isoenzyme which is in involved in the conversion of arachidonic acid into precursor PGE_2, namely prostaglandin H) are up-regulated. However, Gonzalez-Rey E and Delgado M (2008) showed decreased production of both PGE_2 in culture supernatants and COX-2 in cell lysates of LPS or LPS/IFN-γ stimulated microglia, bone-marrow derived DCs and peritoneal macrophages (cells isolated from experimental mice) when incubated with VIP. The authors also determined that the inhibitory effect is exerted via the interaction of VIP with the cognate VPAC1 receptor. On a molecular level the authors were able to link VIP inhibition to the down-regulation of NF-κB induced trans-activation of the COX-2 promoter via decreased binding of p65, a major component of the NF-κB transcription factor, to the promoter.

Another study demonstrated that VIP regulation of the NF-κB transcription factor inhibited the function of Langerhans cells (DCs of the epidermis) (Ding W, *et al.*2007). The study explained that inactive NF-κB consists of mainly a p50/p65 heterodimer and are bound to the IκB inhibitory protein in the cytoplasm of unstimulated cells. Upon activation, i.e. cellular response to various stimuli (LPS, pro-inflammatory cytokines, etc.), the inhibitory protein is phosphorylated and degraded by IκB kinases (IKK). This results in the release of the p50/p65 NF-κB heterodimers and subsequent translocation to the nucleus where it acts upon binding sites on DNA, activating the transcription of various genes. Accordingly, the cytosol of unstimulated cells contains a higher ratio of IκB to IKK protein with an inverted ratio upon stimulation. However, the authors showed that dual incubation of LPS and VIP induced cytosolic IκB to IKK ratios similar to that of unstimulated Langerhans cells. Also, it was found that VIP plays a role in preventing degradation of the IκB protein. Moreover, Ding W, *et al.* (2007), interested in determining the outcome of VIP induced inhibition of NF-κB function on cytokine production, showed a significant decline in supernatant TNF-α of LPS stimulated Langerhans cell cultures treated with VIP.

Only a few studies have investigated VIP during HIV-1 infection, even less have reported on VIP and blood DCs. Fabricius D,*et al*. (2006) used confocal microscopy to show cell surface expression of both VPAC1 and VPAC2 receptors and associated mRNA transcripts in blood pDCs. A crucial observation of this study was the significant decline in production of IFN-α upon *in vitro* stimulation of pDCs with cytosine-phosphodiester-guanine oligodeoxynucleotides (CpG ODN) and treatment with VIP. It was also reported that the level of IFN-α in the culture supernatant indirectly correlated with increasing dosages of VIP. Furthermore, an increase in the expression of CD86 and MHC class II, whilst a down-regulation of the MHC class I was observed in VIP treated vs. untreated CpG ODN stimulated pDCs. On a functional level, the authors observed suppressed CD4 T lymphocyte proliferation in MLR experiments when incubated with VIP pre-treated pDCs.

In the current study evaluation of DC function and immunemodulation was performed after *in vitro* TLR stimulation of these cells. The responses were evaluated via similar markers related to apoptosis and migration that were used in Chapter 4 to profile the phenotype of DC that constitute the residual DC pool during HIV-1 infection. Similar to the contemplated readout of the previous chapter the current study proposed that aberrant function may reflect as modified marker expression with regard to 1) *ex vivo* markers related to apoptosis and chemotaxis and 2) *in vivo* cytokine expression when compared to the marker profile obtained from an uninfected system. A sub-project of the study aimed to ascertain whether these modifications could be dampened or reversed via treatment with the immunemodulatory VIP agent. A brief description on the *ex vivo* and *in vivo* markers used in the current study to evaluate activated DCs are discussed in sections 5.1.1 - 5.1.2.

5.1.1 Investigating *ex vivo* apoptotic and migration marker expression on whole blood TLR stimulated mDCs and pDCs

This part of the study focused on the *ex vivo* profiling of TLR activated blood DCs, targeting markers associated with apoptosis (TNF-R2, TRAIL-R1 and TRAIL-R2) and migration (CCR5, CCR7, CCR9). These markers were also used to profile the DC phenotype in fresh whole blood as described in Chapter 4. Refer to the latter chapter for a description on these cell surface markers.

5.1.2 Investigating *in vivo* cytokine expression in whole blood TLR stimulated mDCs and pDCs

This part of the study focused on the *in vivo* profiling of TLR stimulated blood DCs to assess the production of IFN-α (pDC specific), IL12p40 (mDC specific) and TNF-α (produced by both pDCs and mDCs). These cytokines are members of the proinflammatory cytokine family. **IFN-α (type 1 Interferon)** is an important effector molecule of the immune system and as described by the cofounders, Isaacs A and Lindenmann J (1957), is an “abortive product of virus multiplication”. Also, these cells are referred to as professional IFN-α producing cells due to their superior ability to produce high amounts of IFN-α in response to viral infections (as reviewed byFitzgerald-Bocarsly P, *et al.* 2008). In particular, the per cell production of IFN-α in pDCs are 10 times higher compared to monocytes (as reviewed by McKenna K *et al.* 2005; Fitzgerald-Bocarsly P, 2002;Cella M, *et al.* 1999).Molecular analyses have shown that upon TLR7 stimulation of highly purified pDCs, IFN-α-associated genes constitute the majority of genes transcribed and include several subsets of this cytokine (IFN-α2, -α5, -α6, -α8, -α1/13, -α10, -α14, -α16, -α17 and -α21) as well as IFN-β (Birmachu W, *et al.* 2007). **TNF-α** has potent endocrine function and works synergistically with interferons. It is also a

multifunctional molecule that plays a role in the induction of cell death and activation and/or co-stimulation. As reviewed by Sedger LM and McDermott MF (2014), TNF is a multifunctional molecule that 1) acts together with IL-1β in induction of inflammation 2) is a potent inducer of IL-6 and 3) promotes the differentiation of monocytes/macrophages. **ILp40** and ILp35 constitute the IL-12 70-kDA heterodimeric protein. Specifically, the ILp40 subunit is expressed by DCs, macrophages and microglia. It functions as a chemoattractant to macrophages and plays a role in the migration of DCs stimulated by bacterial antigen (Cooper AM and Khadar SA, *et al*. 2006)

Main research focus

The waning of DCs from peripheral blood during HIV-1 infection most probably adds pressure to the remaining DC pool in circulation to provide adequate immune support in the face of other antigen encounters. Also, as HIV-1 infection is associated with the development of opportunistic infection, invading pathogens may add further tension on the DC compartment. It was proposed that these cells have suboptimal functionality which may reflect via changes in signature cytokine production and modification of cell surface markers upon activation. If so, and in view of the lack of DC number recovery during therapy, it was of further interest to determine the possible role of ARV in function recovery.

Main study aim:

The aim of the current study was to assess the functional capacity of the current pool of blood pDCs and mDCs of chronically HIV-1 mono, HIV-1/TB dual infected as well as ARV treated individuals

Study objectives

- ***to stimulate DCs in vitro using specific agonists to TLR 4 (expressed on mDCs), TLR 7/8 (expressed on both pDCs and mDCs) and TLR 9 (expressed on pDCs)***
- ***to phenotypically characterise TLR activated DCs via the expression of cell surface markers (similar to those used in chapter 4) related to apoptosis (TNF-R2, TRAIL R1 and R2) and homing (CCR5, CCR7 and CCR9)***
- ***to evaluate intracellular production of TNF-α, IL12p40 (mDC-specific) and IFN-α(2b) (pDC-specific)***

Sub-project aim:

The sub-aim of the study was to examine the impact of the immunemodulatory peptide VIP on in vitro activated DCs

Sub project objectives

- ***to evaluate the expression of the immunemodulatory receptors VPAC1 and VPAC2 in fresh whole blood (cell surface, assayed in Chapter 4) and TLR stimulated whole blood (cell surface and intra-vesicular)***
- ***to evaluate the expression of cell surface and intracellular markers in VIP treated vs. untreated TLR stimulated DCs.***

5.2 Outline of the study

Refer to sections 5.3.1 - 5.3.11 for a detailed description on sample collection and processing

SAMPLE COLLECTION					
Patient recruitment, blood collection by venesection at various clinics in the Western Cape, South Africa					
3 Study groups: Control, ARV$^-$HIV-1 and ARV$^+$HIV-1					
↓					
WHOLE BLOOD					**PLASMA**
50µl	48 x ±200µl				1ml
↓	↓				↓
	TLR STIMULATION				
	6 x neat, 6 x neat + VIP	6 x LPS (TLR4 ligand), 6 x LPS + VIP	6 x R848 (TLR7/8 ligand), 6 x R848 + VIP	6 x CpG ODN (TLR9 ligand), 6 x CpG ODN + VIP	
↓	↓				↓
4-COLOUR FLOW CYTOMETRIC QUANTIFICATION	**8-COLOUR FLOW CYTOMETRIC PROFILING**				**REAL TIME PCR QUANTIFICATION**
CD4 and CD8 T cells **ASSAY:** Staining with BD MultiTEST™ mAbs: CD3 FITC, CD8 PE, CD45 PerCP, CD4 APC in BD TruCOUNT^{TM} tube	**TLR stimulated pDCs and mDCs** **ASSAY:** Staining with DCID and marker specific m Abs as set out in the panels below:				**Viral load** **ASSAY:** ABBOTT Real Time HIV-1 PCR assay (ABBOTT m2000rt)/ bioMérieuxNucliSensEasy Q® HIV-1, v1.2 test
	Cell surface markers			Intracellular markers	
	Panel 1	Panel 2	Panel 3	Panel 4	Panel 5
	TRAIL-R2, TNF-R2	TRAIL-R1, VPAC 1, VPAC 2	CCR 5, CCR 7, CCR 9,	TNF-α, VPAC 1, VPAC 2	IL12p40, IFN-α(2b)
↓	↓				↓
	DATA COLLECTED				
CD4 and 8 T cells - count (cells/µl)	**TLR stimulated pDCs and mDCs** - % pDC/mDCs positively expressing cell surface and intracellular markers				**Viral load** - RNA copies/ml

5.3 Material and Methods

5.3.1 Study groups and clinical data

A subset of recruits of the Control (n=17), ARV$^-$HIV-1 (n=22) and ARV$^+$HIV-1 (n=24) study groups of chapter 4 were simultaneously also employed in this third part of the study. Enlistees to these study groups were enrolled (Aug 2011- Mar 2012) according to the criteria defined in Table 3.1. The ARV regimen TDF, Lamivudine, EFV was used by 60%; the Stavudine, Lamivudine, EFV regimen used by 20%; the Stavudine, Lamivudine, NVP regimen used by 15% and the TDF, Lamivudine, NVP regimen used by 5% of total recruits of the ARV$^+$HIV-1 study group. Participants were recruited from state clinics in a peri-urban area of Cape Town, South Africa, which included Idasvalley (14% of total recruits), Durbanville (41%), Kuilsriver (5%), Tygerberg (5%) and the Desmond Tutu Emavundleni Clinic Site in Khayelitsha (35%). The participants from Khayelitsha were enlistees of primarily the control and ARV$^-$ HIV-1 study group. Demographic and clinical data of the participants in each study group are shown in Table 5.1.

Informed consent was obtained from all the study participants. The study was reviewed and approved by the HREC of the Faculty of Medicine and Health Sciences of Stellenbosch University (Ethics reference number N08/02/057). Ethical approval for the collection and analysis of blood samples from participants recruited at the Desmond Tutu Emavundleni Clinic Site in Khayelitsha was initially obtained from the REC of the Health Sciences Faculty of UCT (Ethics reference number 417/2006) with subsequent amendments to the project approved by the HREC of US.

Table 5.1: Demographic and clinical data of the participants in the study groups analysed to investigate TLR responses of blood pDCs and mDCs

	Study groups		
	Control	**ARV$^-$HIV-1**	**ARV$^+$HIV-1**
Total (n)	17	22	24
Male: Female			
nr	9:8	3:19	11:13
%	53:47	14:86	46:54
Age[a]			
Median	28	32	42
Range	19 - 58	22 - 50	19 - 55
Time on ARV therapy[b]			
Median	N/A	N/A	13.5
Range			<1 - 75

[a] *Age median and range expressed in years*
[b] *Time on treatment median and range expressed in months*

5.3.2 Whole blood TLR stimulation

5.3.2.1 Determining optimal TLR ligand concentration

Whole blood TLR stimulated *in vitro* cultures were prepared using TLR ligands (TLR-L) purchased from InvivoGen (San Diego, CA). Table 5.2 lists the initial TLRs targeted to activate DCs, provides the name and a brief description on their corresponding ligand as well as their expression properties on pDCs and/or mDCs. TLR-Ls were provided as a lyophilised pellet and were reconstituted in supplied endotoxin free physiological water (NaCl 0.9%) according to the specifications of the manufacturer (InvivoGen, San Diego, CA). Aliquots, sufficient for the execution of 3 consecutive cultures, were prepared and stored at -20°C. This was performed to prevent multiple freeze/thaw cycles that could affect the stability of the ligand. InvivoGen also provided the recommended TLR-L concentration range for *in vitro* culturing of cells and the current study used these as peripheral boundary titers for the dilution series intended to determine the optimum ligand concentration. Accordingly, dilutions performed for the 1) FSL, Poly I: C, R848 and LPS ligands entailed a ten–fold titration series and 2) Pam3CSK4, FLA-ST and CpG 2395 ligands entailed preparing one midpoint titer between the set boundary titers. Ligands were serially diluted in 1x PBS pH 7.4 (Gibco® Carlsbad, CA, USA). Table 5.3 summarises the reconstituted stock concentrations, manufacturer's recommended concentration range and the titers of the dilution series prepared for each of the seven ligands investigated.

The prepared titers were incubated with whole blood from an HIV-1uninfected donor for 18h. Subsequently, DC activation was evaluated via the expression of the activation markers CD86 and CD80 (refer to Table 4.2 for details on the conjugated fluorochrome, clone, isotype and manufacturer regarding the latter two mAbs) and maturation marker CD83 (conjugated to APC, clone: HB15e, isotype: Mouse $IgG_{1,\kappa}$ obtained from BD Biosciences, San Jose, CA). Whole blood stimulation and post-stimulation cell surface marker staining were performed following the procedure outlined in section 5.3.4. The percentage DCs positively expressing the activation and maturation markers as well as the MFI of these were recorded for each of the different titration points of the seven ligands and plotted on a line graph. Accordingly, the single titration point showing the highest level of functional responses were identified and used as the optimal ligand concentration for subsequent TLR stimulation experiments. Optimal concentrations for the ligands Pam 3CSK4, FSL-1, Poly I:C, LPS, FLA-ST, R848 and CpG ODN 2395 type C were 0.55 µg/ml, 0.1 µg/ml, 10 µg/ml, 0.1 µg/ml, 0.1 µg/ml, 0.5 µg/ml and 5 µM, respectively. This procedure was repeated using whole blood from an unrelated HIV-1 uninfected donor to examine the reproducibility of results and to eliminate any possible donor bias.

Table 5.2: Description of the TLR ligands

TLR	Name of synthetic or natural TLR-ligand	Description of the component recognised by TLR[a]	Expression by blood DC subset[b]
1 and 2	Pam3CSK4	Acylated amino terminus of bacterial lipoproteins found in the cell wall of both Gram Positive and Gram Negative bacteria. Pam3CSK4 is a synthetic analog.	mDCs:TLR 1 & 2 pDCs: TLR 1
2 and 6	FSL-1	Lipoylated N-terminal diacylated cysteine residue of the LP44 of *Mycoplasma salivarium*. FSL-1 is the synthetic analog.	mDCs: TLR 2 & 6 pDCs: TLR 6
3	Polyinosinic-polycytidylic acid (Poly I:C)	Poly I:C, a synthetic analog, represents a molecular pattern associated with dsRNA of viruses. The high molecular weight type was used.	mDCs
4	Lipopolysaccharide (LPS)	LPS is the structural component of the outer wall of Gram Negative bacteria, with the shape of Lipid A driving the stimulatory response. An ultrapure preparation from the *Escherichia coli* strain 0111:B4 was used.	mDCs
5	FLA-ST	FLA-ST is an ultrapure preparation of bacterial flagellin, the component associated with motility. The preparation was purified from *Salmonella Typhimurium*.	mDCs
7 and 8	R848	Resiquimod 848 (R848) is an imidazoquinoline compound, used clinically as an asynthethic immunemodulatory drugs against viral infections. It mimics the TLR7/8's natural ligand, ssRNA from viruses.	mDCs: TLR 8 pDCs: TLR 7
9	CpG Oligo-deoxynucleotides (ODN) 2395, Type C	CpG ODNs are synthetic short single stranded unmethylated DNA containing a series of only Cytosine (C) and Guanine (G) nucleotides on a phosphodiester backbone. CpG ODN's are predominantly present in bacterial DNA	pDCs

[a] *Information supplied by the manufacturer InvivoGen (San Diego, CA)*
[b] *Liu K-J, 2006;Iwasaki A and Medzhitov R, 2004;*

Table 5.3: Summary of ligand reconstituted stock concentration, manufacturer's recommended concentration range and the titers of the dilution series prepared for each of the seven ligands investigated.

Ligand	Reconstituted stock concentration	Recommended concentration range	Dilution series (optimal concentration are underlined)
Pam3CSK4	1 mg/ml	1 - 0.1 µg/ml	1, 0.55 and 0.1 µg/ml
FSL	100 µg/ml	1 – 0.001 µg/ml	1, 0.1, 0.01 and 0.001 µg/ml
Poly I:C	1 mg/ml	10 – 0.03 µg/ml	10, 1, 0.1 and 0.01 µg/ml
LPS	5 mg/ml	10 – 0.01 µg/ml	10, 1, 0.1 and 0.01 µg/ml
FLA-ST	100 µg/ml	0.1 – 0.01 µg/ml	0.1, 0.055 and 0.01 µg/ml
R848	1 mg/ml	5 - 0.05 µg/ml	5, 0.5 and 0.05 µg/ml
CpG ODN 2395, Type C	500 µM	5 - 1 µM	5, 3 and 1 µM

The underlined titre was found optimal and used in subsequent TLR stimulation experiments

5.3.2.2 Selection of markers to phenotypically characterise activated DCs from TLR stimulated cultures

Upon determining the optimal TLR-L concentrations for DC activation in whole blood *in vitro* cultures, the study next evaluated the expression of the cell surface markers employed in Chapter 4 (Table 4.2) on activated DCs. For this purpose, whole blood of an HIV-1 uninfected donor was incubated with optimal concentrations of the 7 ligands (Table 5.3) investigated. Whole blood stimulation and post-stimulation cell surface marker staining were performed according to the assay described in section 5.3.4 using the same mAbs volumes as specified in section 4.3.5. This experiment was repeated using whole blood from an unrelated HIV-1 uninfected donor to confirm reproducibility of results. The expression profile of these cell surface markers on TLR activated pDCs and mDCs were compared to that of the DC subsets in fresh whole blood (refer to Chapter 4). Markers that showed a clear change in expression (either an up-regulation or down modulation that signifies activation) were identified and selected for the analyses of DC responses in subsequent TLR experiments. In addition, some markers that showed minimal to no change in expression were also selected as their expression on pDCs and mDCs upon TLR stimulation in an HIV-1 setting was of interest. Accordingly, the final set of phenotypic markers included TRAIL-R1 and -R2, TNF-R2, CCR5, CCR7, CCR9, VPAC1 and VPAC2. These were regrouped into four new panels, labeled as Panel 1-3 (refer to Table 5.4). The markers previously used in phenotypic profiling of fresh whole blood but excluded from the mAb staining panels for phenotypic profiling of TLR stimulated DCs were CXCR6, TRAIL-R3, TRAIL-R4, FAS, FASL and CD62L. Also, TLR-Ls that accordingly showed a significant level of marker modulation, in either one or both the DC subsets, were identified and selected

to use in subsequent TLR experiments. These included LPS (ligand for TLR 4 and expressed on mDCs), CpG ODN (ligand for TLR9 and expressed on pDCs) and R848 (ligand for TLR7/8 and expressed on both DC subsets).

5.3.2.3 Intracellular profiling of TLR stimulated pDCs and mDCs

In addition to the four mAb panels employed for phenotypic profiling of activated pDCs and mDCs, two additional panels were introduced to investigate intracellular cytokine production by DCs and were labeled as Panel 4 and 5, respectively. Panel 4 included the mAb TNF-α Alexa Fluor®647 (used at an optimal volume of 0.5µl per reaction as determined by a titration assay, refer to 4.3.4) and Panel 5 the mAbs IL12p40 Alexa Fluor®647 (0.5µl) and IFN-α (2b) PE (refer to as IFN-α from this point on) (2 µl). These mouse anti-human mAbs were obtained from either Biolegend[1] (San Diego, CA) or BD Biosciences[2] (San Jose, CA). Panel 5 also included mAbs to investigate VPAC 1 (2 µl) and 2 (2 µl) expression on intracellular vesicles in activated pDCs and mDCs. Refer to Table 5.4 for clone and isotype information on the cell surface (Panel 1-3) and intracellular markers (Panel 4 and 5) investigated in the current study.

Table 5.4: mAb panels for cell surface and intracellular staining of TLR stimulated pDCs and mDCs

	Panels	Markers of interest	Clones	Isotype
mAbs for DCID		HLA-DR APC-Cy™7 CD123 PE-Cy7 CD 11c Pacific blue™ LIN1 FITC	Refer to Table 4.2	
mAbs for cell surface staining	Panel 1 +DCID	TRAIL-R2 APC TNF-R2 PE	Refer to Table 4.2	
	Panel 2 +DCID	TRAIL-R1 APC VPAC 2 PerCP VPAC 1 PE	Refer to Table 4.2	
	Panel 3 +DCID	CCR5 APC CCR7 PerCP CCR9 PE	Refer to Table 4.2	
mAbs for Intracellular staining	Panel 4 +DCID	TNF-α Alexa Fluor®647 [1] VPAC 1 PE VPAC 2 PerCP	MAb11 - 476031	Mouse IgG_1, κ mouse IgG_{2a} mouse IgG_1
	Panel 5 +DCID	IL12p40 Alexa Fluor®647 [1] IFN-α(2b) PE [2]	C11.5 7N4-1	Mouse IgG_1, κ Mouse IgG_1, κ

5.3.2.4 FMO staining controls and the autofluorescence factor

FMO staining controls were also used in this part of the study to, as described in section 4.3.7.2, discriminate between positive and negative events and identify false positive events brought on by background fluorescence (fluorochrome induced) as well as autofluorescence (cell induced). Autofluorescence refers to the intrinsic properties of cells that can cause spontaneous fluorescence. This includes reduced pyridine nucleotides and flavins that can be excited, specifically by the blue laser of a flow cytometer, resulting in the generation of false positive events. Furthermore, changes in physiological conditions (such as cell culturing) may cause an increase in the level of autofluorescence. Autofluorescence is generally assessed visually using a FL1 (FITC) vs. FL2 (PE) density plot due to the excitation and emission characteristics of autofluorescence being similar to that of the FITC and PE fluorochromes. In the current study assessment of autofluorescence was performed as indicated, however, good resolution was also observed when using a PerCP (FL3) vs. PE density plot. As indicated in Figure 5.1 B vs. A, in comparing the mDC event profile of a PE FMO stained control of TLR stimulated to that of fresh whole blood autofluorescence could be identified as a characteristic “tail of positive” events in activated mDCs. Accordingly, marker stained samples in which the PE conjugated marker displayed a similar event profile as the PE FMO control stain were regarded as negatively expressing the marker of interest and gates were appropriately placed to exclude these events from analyses. However, these gates needs to be adjusted/tightened when marker expression is true positive - distinguished by an absence of “tailed” events (Figure 5.1D) and displaying a mDC event profile similar to that of stained fresh whole blood (Figure 5.1 C) – to accurately capture these events for analyses (compare the position of the dashed line between Figure 5.1B and D). Notably, autofluorescence was a predominant feature of activated mDC population.

In this part of the study FMO control staining were performed concurrent with the evaluation of the expression of the17 phenotypic markers of Panel A-G (Table 4.3) in TLR stimulated whole blood (Refer to section 5.3.2.2). Stimulated whole blood from a healthy donor was prepared according to the procedure described in section 4.3.7.2. TLR stimulation and post-stimulation staining was performed as outlined in section 5.3.4. Literature recommends performing FMO staining controls with daily experiments, but as per reasons defined in section 4.3.7.2, the current study performed FMO staining controls once and used the resulting staining profile as a guide to analyze subsequently stained samples.

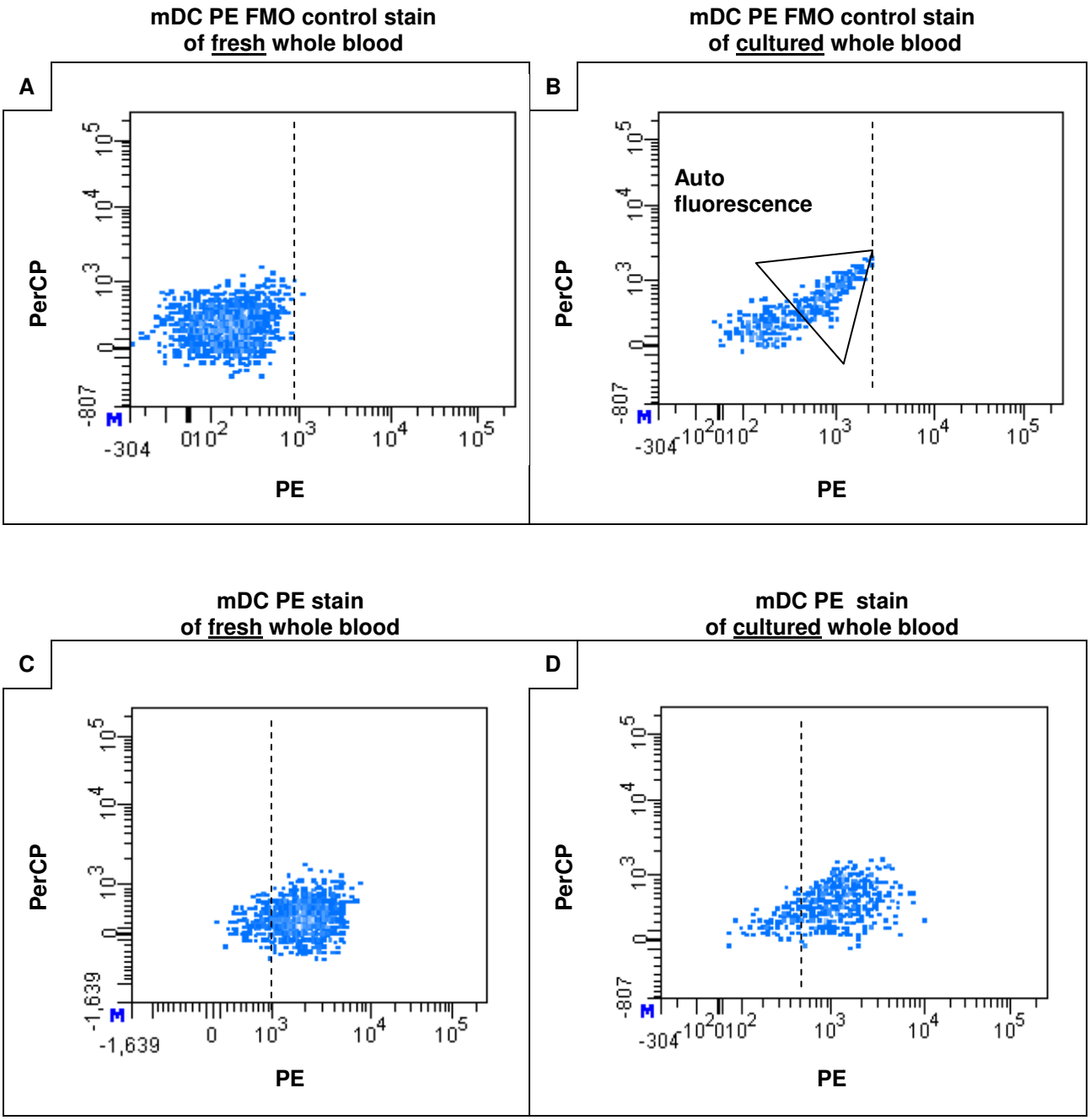

Figure 5.1 Description of the method used to detect autofluorescence

Detection of autofluorescence was performed by displaying events in a FL2 (PE) vs. FL3 (PerCP) density plot. Graph A displays a PE FMO control stain of mDCs in fresh whole blood where no autofluorescence was detected and graph B shows autofluorescence as a "tail of positive events" with PE FMO control stain of cultured whole blood. A change (visually inspected) in the expression profile of events from the PE FMO control to the marker stained sample of whole blood cultured mDCs (B vs. D) was indicative of true positive events for the marker of interest conjugated to PE. The dashed line shows the staining boundary which is fixed to compare FMO control to marker stain in fresh whole blood, however, it needs to be adjusted between the FMO control and marker stain of cultured whole blood.

5.3.3 General specimen processing

Each of the participants enrolled in the study was allocated a patient number and all laboratory procedures were performed in reference to this number. Whole blood (2 x 10 ml) was aseptically obtained by venisection puncture in Sodium Heparin vacutainer tubes (BD Biosciences, San Jose, CA) (optimal for cell culturing as reported by Petrovsky N and Harrison LC, 1995) and used in the whole blood *in vitro* TLR stimulation assay. Whole blood was also collected in EDTA vacutainer tubes (10ml) (BD Biosciences, San Jose, CA) and used for determining CD4 and CD8 T lymphocytes counts (refer to section 3.3.6), phenotypic profiling of pDCs and mDCs (Chapter 4) as well as viral load quantification (refer to section 3.3.7). Processing of samples was at all times performed under sterile conditions in a biosafety cabinet (NUAIRE biological class II safety cabinet). Barrier pipette tips were used for the sterile preparation of *in vitro* whole blood cultures. Centrifugation was performed using a Hettich Rotanta 460R benchtop centrifuge (Massachussets, USA).

5.3.4 Whole blood TLR stimulation and mAb staining assay

Whole blood TLR stimulated cultures were prepared in appropriately labeled (stimulant, patient nr) 12 x 75 mm, 5 ml round bottom sterile, pyrogen-free polystyrene capped BD Falcon™ tubes (BD Biosciences, San Jose, CA). Section 5.2 shows the layout of sample preparation per patient for the TLR stimulation assay. For the profiling of cell surface marker expression on activated DCs, separate test tubes were prepared to which 10 µl of R848, LPS, CpG ODN and 1x PBS pH 7.4 (Gibco® Carlsbad, CA, USA) was added, respectively. In addition, a duplicate set of reactions were simultaneously prepared to which VIP (5ul, [final] = $1x10^{-8}$M, (Delgado M, *et al.* 2004[a]) was added. Similar reactions were prepared to examine intracellular cytokine production of activated DCs. Additionally, and concurrent with the addition of stimulus/PBS, the protein transport inhibitor Brefeldin A (5µl, [final] = 1:1000) was added to each of these reactions. This was performed to prevent cellular release of cytokines from both DC subsets as well as other responding cells so to a) allow for measuring the level of expression of the cytokines of interest produced by DCs specifically and b) prevent the release of other cytokines that may influence IFN-α production of DCs upon *in vitro* challenge. The total test volume, with the addition of whole blood, was 200 µl. These samples were gently vortexed and incubated at a 5º slant in a humidified 37^0C, 5% CO_2 incubator (NuAire Autoflow NU-5510). The incubation period for optimum cell surface and intracellular cytokine analysis was performed at 18 and 4.5 hours, respectively.

Immediately after the incubation period, samples destined for the profiling of cell surface marker expression on activated DCs were stained with applicable mAbs. The relevant mAb cocktail (Panel 1-3, Table 5.4) was freshly prepared in staining buffer (0.4% heat-inactivated foetal calf serum in 1 x PBS pH 7.4 (Gibco® Carlsbad, CA, USA)) and a volume of 50µl added to the TLR stimulated samples, the samples were gently vortexed and incubated for 30 min at room temperature. Red blood cell lysing was performed with 1.8 ml 1 x BD FACS lysing solution (BD Biosciences, San Jose, CA), the samples were gently vortexed and incubated for 10 min in the dark at room temperature. The cells were centrifuged for 5 min at 400 x g and after discarding the supernatant staining buffer (2 ml) was added. Washing with staining buffer was performed twice. Discarding of the supernatant entailed inverting the tube to dispose the fluid in biological hazard container and blotting the inverted tube dry on absorbent paper to remove excess fluid. The samples prepared for examining cell surface expression were resuspended in 350 µl

staining buffer and immediately acquired on a BD FACSCanto II™ flow cytometer (BD Biosciences, San Jose, CA). A threshold was set on 30 000 for the FSC and 200 for the FITC (LIN1) detector. A maximum of 750 000 total events were acquired. Data on the height (H), area (A) and width (W) of the fluorescence pulse generated in the different channels was collected.

The TLR stimulated samples prepared for the examination of intracellular cytokine production were firstly stained with the DCID cell surface markers, lysed and washed following the procedure as described above. The cell pellet was then either stored in 1ml staining buffer at 4ºC for processing the next day or immediately subjected to fixation and permeabilisation. This entailed adding 100µl of the BD Cytofix/Cytoperm™ reagent (BD Biosciences, San Jose, CA) to the cell pellet and incubating the sample for 20 min at 4°C in the dark. Following this, 500 µl Permwash buffer (BD Biosciences, San Jose, CA) was added to the sample and centrifuged at 400 x g at 4°C for 5 min. The supernatant was discarded and a cocktail of the mAbs of Panel 4 and 5 (refer to Table 5.4) were freshly prepared in permwash buffer. A volume of 50µl was then added to the samples and incubated for 30 min at 4°C in the dark. Two wash steps followed, the first was performed with Permwash buffer (500 µl) and the second in staining buffer (2 ml) at 400 x g and 4°C for 5 min. The sample was resuspended in 250 µl staining buffer and immediately acquired on a BD FACSCanto II™ flow cytometer (BD Biosciences, San Jose, CA). A threshold was set at 30 000 for the FSC detector and maximum of 450 000 total events were acquired. Data on the height (H), area (A) and width (W) of the fluorescence pulse generated in the different channels was collected.

5.3.5 Flow cytometric detection of nonviable DCs in TLR stimulated whole blood cultures

The 7-AAD nucleic acid dye was used to detect nonviable DCs. Two additional control samples per patient were prepared to detect nonviable pDCs and mDCs from the 4.5h and 18 h stimulations (incubation periods for the *in vitro* detection of intracellular cytokine production and cell surface receptor expression, respectively). These samples were prepared by stimulating (4.5h and 18h incubation periods) whole blood (190 µl) from each of the patients,followed by staining with DCID markers and 7–AAD dye (according to the specification of the manufacturer, BD Biosciences, San Jose, CA), to detect non-viable pDCs and mDCs. Note that 7-AAD fluorescence is detected in the PerCP detector. The pDC and mDC population was defined from the total acquired events following the gating strategy as previously described (Figure 4.20). The boundary of negatively stained 7-AAD events was determined by staining unstimulated whole blood cultures with only the DCID surface markers. Hence, events from TLR stimulated samples were classified as positive for 7-AAD when detected outside of the negative staining boundary. Literature recommends the inclusion of the 7-AAD dye within each of the panels designed in a multi-colour experiment so to identify and exclude nonviable cells during analyses of acquired events. However, as the current study was limited with regard to availability of detectors (only able to employ 7 of the 8 accessible channels of the BD FACSCanto™ II 8-colour flow cytometer (BD Biosciences, San Jose, CA) due to the fact that most markers used in the study, at the time of panel design, was not available conjugated to either the fluorochromes AmCyan or V500 that emit light within the 8th channel (510/50 BP filter of the Violet laser) the PerCP detector could not be used as a dedicated channel for the detection of non-viable 7-AAD fluorescing cells. Nonetheless, 7-AAD staining was performed separately and used to monitor non-viable pDCs and mDCs during the TLR experiments.

5.3.6 Statistical analyses

Comparative analyses of DC function were performed using data collected on DCs positively expressing cell surface markers and intracellular cytokines of interest in TLR–L stimulated and unstimulated cultures (alternatively also refer to as TLR-L^- cultures). Assessment of the data collected was performed as follows:

- **to assess the general TLR activation profile** each of the TLR-L^+ cultures were compared to TLR-L^- culture of the control study group. The non-parametric two tailed Mann-Whitney t test was applied;
- **to assess the activation abilities of DCs during HIV-1 infection** TLR-L^+/TLR-L^- cultures of the ARV^- HIV-1 and ARV^+HIV-1 study groups were separately compared to the control study group. Spontaneous levels of marker change in the TLR-L^+ cultures were similarly investigated. The non-parametric two tailed Mann-Whitney t test was applied;
- **to assess the effect of VIP:** VIP treated TLR-L^- and TLR-L^+ cultures were compared to corresponding VIP untreated TLR-L^- and TLR-L^+ cultures of the control, ARV^-HIV-1 and ARV^+HIV-1 study groups. The non-parametric two tailed Mann-Whitney t test was applied.

Statistical analysis was performed using the Graphpad Prism version 5.00 software (San Diego, California, USA). Refer to Table 3.4 for the summary of the method used to report significant and non-significant data as well as the corresponding P value range.

5.4 Results and Discussion

5.4.1 Defining marker expression related to apoptosis, migration/homing and immunemodulation on both DC subsets upon *in vitro* TLR activation during HIV-1 infection.

5.4.1.1 Profiling apoptotic markers TNF-R2, TRAIL–R1 and TRAIL-R2 expression on TLR activated DCs

Whole blood TLR-L$^+$ cultures (LPS and R848) of HIV-1 infected individuals show significantly higher frequencies of TNF-R2$^+$pDCs, while reduced levels were observed in TLR-L$^+$ cultures of ARV treated individuals

Compared to the TNF-R2 pDC profile obtained from fresh whole blood (Figure 4.23), a reduced frequency of TNF-R2$^+$pDCs were observed in the TLR-L$^-$ culture of the control, ARV$^-$HIV-1 and ARV$^+$HIV-1 study groups. This may be due to signal deprivation considering that these cells were removed from the host and/or cultured in suboptimal *ex vivo* conditions in the synthetic environment. The TLR-L$^-$ culture of the ARV$^-$HIV-1 study group showed a significantly higher median percentage of TNF-R2$^+$pDCs when compared to that of the control study group ($p \leq 0.0001$). This may be an indication of the activation status of these cells in response to the HIV/host induced milieu of pathogenic/inflammatory molecules. The median percentage TNF-R2$^+$pDC of the ARV$^+$HIV-1 study group was significantly reduced when compared to theARV$^-$HIV-1 study group ($p = 0.005$) and similar to the control study group. ARV seems to have a recovery effect on the TNF-R2$^+$pDCs subsets. Assessment of the TNF-R2$^+$pDC profile in TLR-L$^+$ cultures via the control study group, the study found a significantly higher frequency of TNF-R2$^+$pDCs in the LPS ($p < 0.0001$), CpG ODN ($p < 0.0001$) and R848 ($p < 0.0001$) cultures when compared to the unstimulated culture. Clearly, pDCs responded to the TLR-L signal by upregulating TNF-R2 expression. In the LPS ($p = 0.002$) and R848 ($p = 0.01$) culture the median percentage of TNF-R2$^+$pDCs was significantly higher in the ARV$^-$HIV-1 study group compared to the control study group. In the CpG ODN culture the median percentage of TNF-R2$^+$pDCs was similar between these study groups. ARV therapy seemed to reduce the frequency of the TNF-R2$^+$pDC subset as significantly lower median percentage of TNF-R2$^+$pDCs was observed in the ARV$^+$HIV-1 study group compared to ARV$^-$HIV-1 study group of the LPS culture ($p = 0.05$). This adjusted frequency distribution of TNF-R2$^+$pDCs in the ARV$^+$HIV-1 study group was comparable to that of the control study group. Notably, reduced median percentage of TNF-R2$^+$pDCs was also observed in the ARV$^+$HIV-1 study group of the CpG ODN culture ($p < 0.0001$) and R848 culture ($p < 0.0001$) when compared to the ARV$^-$HIV-1 study group. These immune recovery levels were even significantly lower than the median percentageTNF-R2$^+$pDCs of the control study group (CpG ODN culture: $p < 0.0001$), trending towards significance in the R848 culture ($p = 0.1$). These findings suggested that ARV therapy has an inhibitory effect on the expression of TNF-R2 when DCs are activated by related signals (Figure 5.2, Table 5.6).The degree of decline below that of the healthy controls is unexpected and concerning as it may indicate ARV therapy negatively affecting immune responses.

The frequency distribution of TNF-R2$^+$mDCs of the control, ARV$^-$HIV-1 and ARV$^+$HIV-1 study group of the TLR-L$^-$ cultures were mostly similar to that of fresh whole blood. Also, the study found no significant difference in TNF-R2$^+$mDCs frequency distribution between the control, ARV$^-$HIV-1 and ARV$^+$HIV-1 study groups of the TLR-L$^-$ culture. Assessing the activation profile via responses by the control study group, no significant difference between unstimulated and the LPS and R848 cultures was found. However, comparison with the CpG ODN culture showed a tendency ($p = 0.05$) towards a lower TNF-R2$^+$mDCs frequency distribution. Compared to the control, the ARV$^-$HIV-1 study group of the CpG ODN culture showed a significant higher median percentage of TNF-R2$^+$mDCs ($p = 0.046$) while in the LPS and R848 culture we observed a tendency toward higher TNF-R2$^+$mDCs frequency ($p = 0.14$, $p = 0.14$, respectively) in the ARV$^-$HIV-1 study group. Notably, the TLR-L$^+$ cultures of the ARV$^+$HIV-1 study group compared to that of the ARV$^-$HIV-1 study group showed a significantly lower median percentage of TNF-R2$^+$mDCs (LPS: $p = 0.009$, CpG ODN: $p < 0.0001$; R848: $p = 0.0007$). This decline of TNF-R2$^+$mDCs as observed with the ARV$^+$HIV-1 study group when compared to the control study grouped was significant for the CpG ODN culture ($p = 0.0034$) and tended towards significance for the R848 culture ($p = 0.11$). Similar to TNF-R2$^+$pDCs, ARV therapy also has an immune-inhibitory effect on TNF-R2$^+$mDCsto a degree lower than the healthy control study group. No significant change in the frequency distribution of TNF-R2$^+$pDCs or TNF-R2$^+$mDCs was observed between VIP treated and untreated TLR-L$^+$ cultures of all three the study groups investigated (Figure 5.3, Table 5.7).

The markers TRAIL-R1 and TRAIL-R2, like in fresh whole blood, were found to be unexpressed by both DC subsets of all the study groups in the TLR-L$^-$ cultures. Also, no change in expression was observed upon *ex vivo* stimulation with the R848, LPS or CpG ODN ligands (data not shown).

In contrast to the decline in the frequency of TNF-R2$^+$pDCs and TNF-R2$^+$mDCs of the ARV$^+$HIV-1 study group when compared to the ARV$^-$HIV-1 study group for all the TLR-L$^+$ cultures (Figure 5.2 and Figure 5.3), the immune status parameters (CD4 and CD8 T lymphocyte absolute count and CD4:CD8 ratio, Table 5.5) were similar between these study groups. Although ARV therapy did not incur a change in parameters related to immune status after an approximate 1 year of ARV therapy, it seemed that it did affect the function of DCs.

Table 5.5 Summary of the CD4 T and CD8 T lymphocytes absolute numbers; CD4:CD8 ratio and viral load (as applicable) of the control, HIV-1 and HIV-1-related study groups.

		Study groups		
		Control	**ARV$^-$HIV-1**	**ARV$^+$HIV-1**
CD4 T cells	**Me^a, R^a**	799, 412 - 1694	331, 14 - 909	323, 143 - 1072
	Me^b, R^b	42, 26-54	21.5, 4-39	19.5, 8-31
CD8 T cells	**Me^a, R^a**	602, 205 - 1048	828, 187 - 2940	1093, 346 - 2962
	Me^b, R^b	29, 15-40	50.5, 41-77	51.5, 34-82
CD4:CD8 Ratio	**Me^c, R^c**	1.34, 0.5-2.9	0.42, 0.07-0.89	0.41, 0.11-0.72
Viral load	**Me^e, R^e**	N/A	$1.5x10^4$, LOD - $3.5x10^6$	LOD, LOD - 310

Data indicated as
Me^a = Median cells/µl, **R^a** = Range cells/µl, **Me^b** = Median % of CD45$^+$CD3$^+$ events,
R^b = Range % of CD45$^+$CD3$^+$ events, **Me^c** = Median ratio of CD4 Lymphocyte absolute number to CD8 T lymphocyte absolute number, **R^c** = Range of the CD4:CD8 ratio values, **M^e** = Median RNA copies/ml,
R^e = Range RNA copies/ml

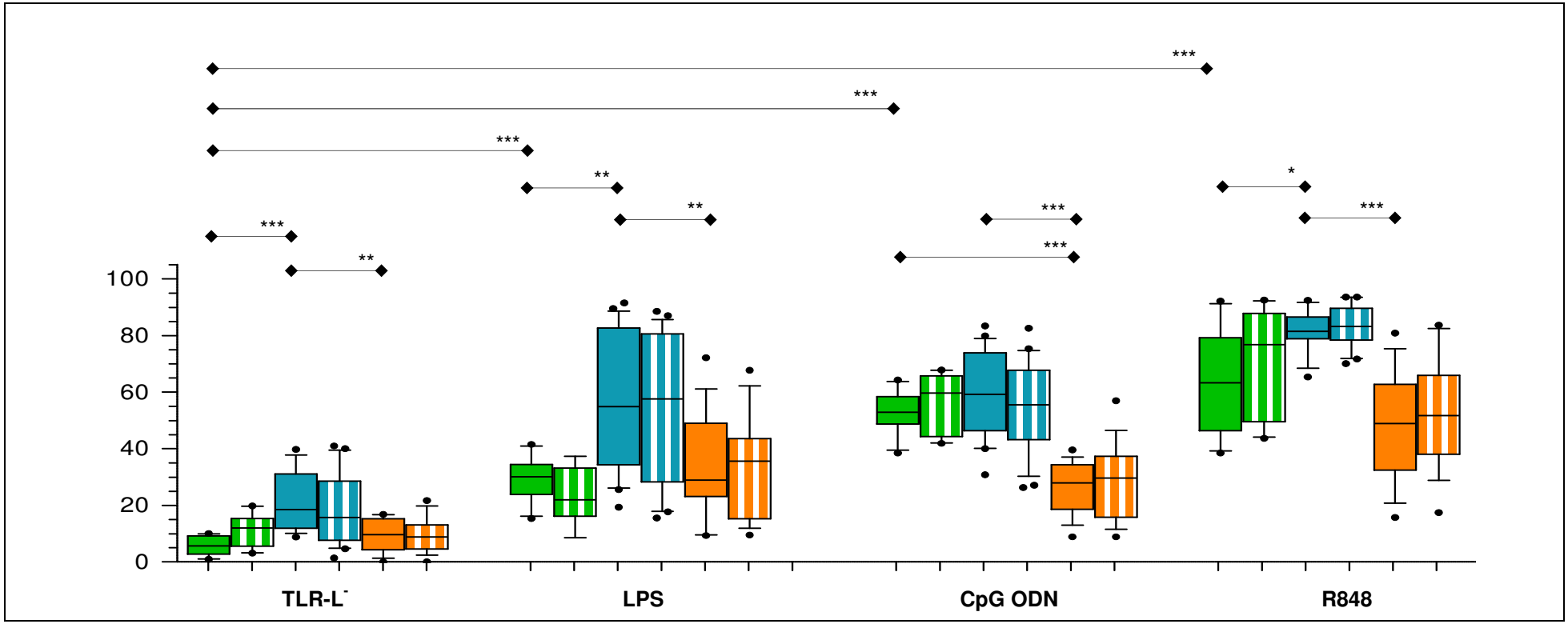

Figure 5.2: Frequency distribution of TNF-R2$^+$pDCs in R848, LPS and CpG ODN stimulated whole blood cultures of the control, ARV$^-$HIV-1 and ARV$^+$HIV-1study groups

TLR-L$^-$ and TLR-L$^+$ (R848, LPS, CpG ODN) whole blood cultures, set up to assess cell surface expression, were incubated for 18h and afterwards stained with mAbs to examine the expression of TNF-R2 on pDCs using multi-parameter flow cytometry. The box and whiskers plot represents the percentage TNF-R2$^+$pDC of the control, ARV$^-$HIV-1 and ARV$^+$HIV-1 study groups per whole blood culture. Each boxplot shows the 10-90 percentile range of data (whiskers) and horizontal line the median value. Outliers are represented by black enclosed circles. Horizontal lines with diamond arrows indicate the specific study group comparison of interest and an asterisk(s) the significance. Refer to Table 3.4 for a description of the method used to indicate the level of statistical significance.

Table 5.6 Summary of TNF-R2$^+$pDCs frequency in TLR-L$^-$ and TLR-L$^+$ whole blood cultures of the control, ARV$^-$HIV-1 and ARV$^+$HIV-1 study groups

Study groups						
TNF-R2$^+$pDCs	**Control**		**ARV$^-$HIV-1**		**ARV$^+$HIV-1**	
	TLR-L$^-$	**TLR-L$^-$ + VIP**	**TLR-L$^-$**	**TLR-L$^-$ + VIP**	**TLR-L$^-$**	**TLR-L$^-$ + VIP**
Minimum %	0.92	3.12	8.82	1.38	2.17	3.46
Median %	5.65	12.00	18.56	15.71	10.12	8.97
Maximum %	10.05	19.80	39.75	41.03	16.79	21.69
	R848	**R848 + VIP**	**R848**	**R848 + VIP**	**R848**	**R848 + VIP**
Minimum %	38.51	43.70	65.31	70.00	15.73	17.44
Median %	63.30	76.77	81.46	83.18	48.97	51.72
Maximum %	92.18	92.52	92.45	93.59	80.88	83.64
	LPS	**LPS + VIP**	**LPS**	**LPS + VIP**	**LPS**	**LPS + VIP**
Minimum %	15.36	8.530	19.39	15.54	9.300	9.520
Median %	30.11	21.95	54.86	57.56	28.90	35.56
Maximum %	41.58	37.30	91.47	88.55	72.16	67.74
	CpG ODN	**CpG ODN + VIP**	**CpG ODN**	**CpG ODN + VIP**	**CpG ODN**	**CpG ODN + VIP**
Minimum %	38.45	41.94	30.77	26.32	8.860	8.890
Median %	52.91	59.65	59.23	55.54	27.92	29.64
Maximum %	64.29	67.82	83.43	82.61	39.52	56.96

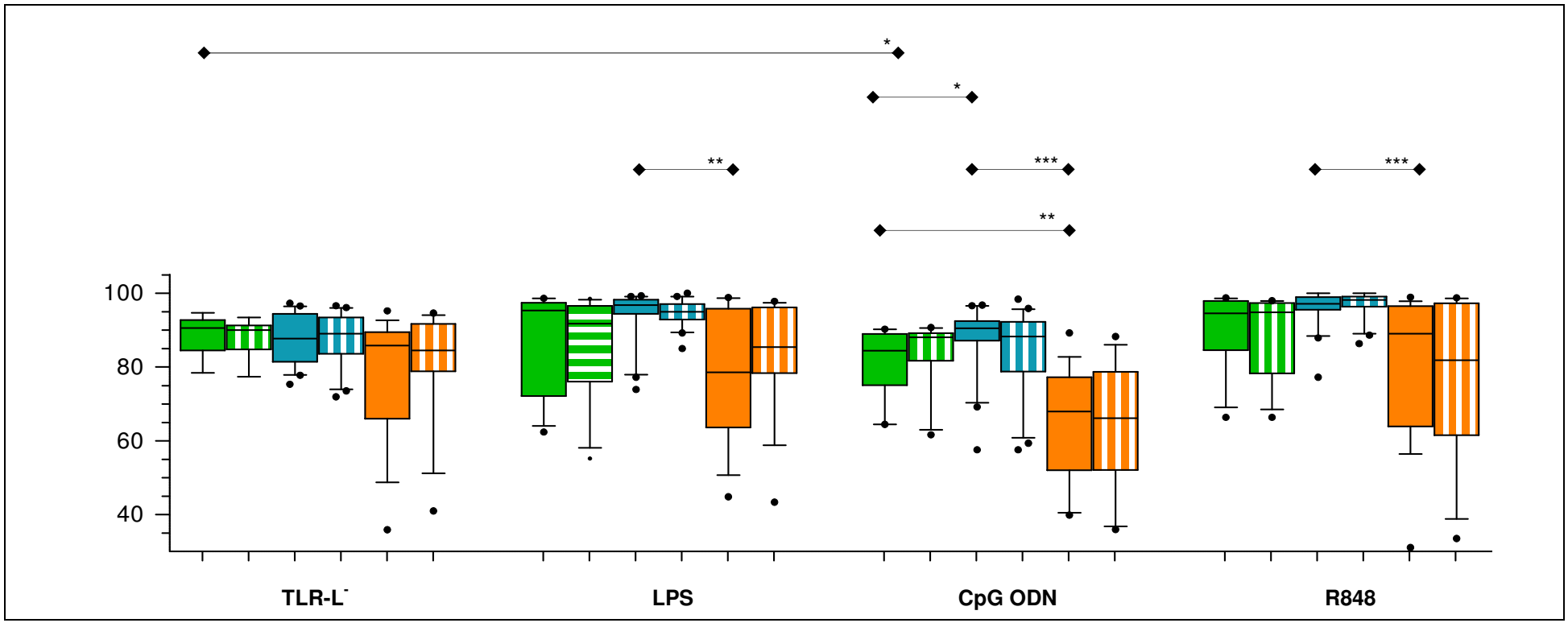

Figure 5.3 Frequency distribution of TNF-R2$^+$mDCs in R848, LPS and CpG ODN stimulated whole blood cultures of the control, ARV$^-$HIV-1 and ARV$^+$HIV-1study groups

TLR-L$^-$ and TLR-L$^+$ (R848, LPS, CpG ODN) whole blood cultures, set up to assess cell surface expression, were incubated for 18h and afterwards stained with mAbs to examine the expression of TNF-R2 on mDCs using multi-parameter flow cytometry. The box and whiskers plot represents the percentage TNF-R2$^+$mDC of the control, ARV$^-$HIV-1 and ARV$^+$HIV-1 study groups per whole blood culture. Each boxplot shows the 10-90 percentile range of data (whiskers) and horizontal line the median value. Outliers are represented by black enclosed circles. Horizontal lines with diamond arrows indicate the specific study group comparison of interest and an asterisk(s) the significance. Refer to Table 3.4 for a description of the method used to indicate the level of statistical significance.

Table 5.7: Summary of TNF-R2$^+$mDCs frequency in TLR-L$^-$ and TLR-L$^+$ whole blood cultures of the control, ARV$^-$HIV-1 and ARV$^+$HIV-1 study groups

	Study groups					
TNF-R2$^+$mDCs	**Control**		**ARV$^-$HIV-1**		**ARV$^+$HIV-1**	
	TLR-L$^-$	**TLR-L$^-$ + VIP**	**TLR-L$^-$**	**TLR-L$^-$ + VIP**	**TLR-L$^-$**	**TLR-L$^-$ + VIP**
Minimum %	78.41	77.40	75.32	71.88	35.88	41.00
Median %	90.51	90.00	87.68	89.01	85.80	84.48
Maximum %	94.68	93.45	97.24	96.61	95.18	94.62
	R848	**R848 + VIP**	**R848**	**R848 + VIP**	**R848**	**R848 + VIP**
Minimum %	66.39	66.38	77.24	86.29	31.10	33.50
Median %	94.51	94.80	97.13	98.13	88.97	81.80
Maximum %	98.78	97.96	100.0	100.0	98.92	98.77
	LPS	**LPS + VIP**	**LPS**	**LPS + VIP**	**LPS**	**LPS + VIP**
Minimum %	62.37	55.20	73.92	85.00	44.86	43.36
Median %	95.24	91.74	96.77	94.95	78.54	85.37
Maximum %	98.63	98.44	99.29	100.0	98.84	97.79
	CpG ODN	**CpG ODN + VIP**	**CpG ODN**	**CpG ODN + VIP**	**CpG ODN**	**CpG ODN + VIP**
Minimum %	64.42	61.61	57.57	57.58	39.84	35.92
Median %	84.38	87.99	90.45	88.22	67.89	66.13
Maximum %	90.21	90.66	96.73	98.36	89.19	88.24

5.4.1.2 Profiling chemotactic markers CCR5, CCR7 and CCR9 expression on TLR activated DCs

Compared to the positive CCR5 staining of pDCs in fresh whole blood, complete down-regulation of this marker in the TLR-L cultures was observed. Lack of expression of CCR5 by mDCs as observed in fresh whole blood was also observed in TLR-L cultures. Also the negative staining profile of CCR7 and CCR9 for both DC subsets in TLR-L cultures was similar to that of fresh whole blood (data not shown).

5.4.1.3 Profiling immunemodulatory markers VPAC1 and VPAC2 on fresh and TLR activated whole blood

The staining profile of the FMO control and marker stain samples of VPAC1 and VPAC2for both DC subsets was similar in fresh and TLR stimulated whole blood cultures. This was indicative of DC subsets negatively expressing the immunemodulatory markers evaluated for both cell surface and intra-vesicular expression.

5.4.1.4 Profiling intracellular expression of IFN-α, TNF-α and IL12p40 on TLR activated DCs

The whole bloodR848 culture of HIV-1 infected individuals showed significantly higher frequencies of IFN-α$^+$pDCs whilst normalisation of responses were observed in ARV treated individuals

IFN-α is a cytokine characteristically produced by pDCs. In assessing the TLR activation profile of IFN-α via the control study group, as expected, no spontaneous expression of IFN-α by pDCs in the unstimulated culture was observed. However, staining for this marker detected a high degree of IFN-α production by pDCs of the R848 stimulated whole blood culture. Both the CpG ODN and LPS cultures showed no to minimal IFN-α production by pDCs. Specifically, the R848 culture of the control study group showed a significantly higher median percentage of IFN-α$^+$pDCs when compared to TLR-L$^-$ culture of this study group ($p \leq 0.0001$). R848 stimulated whole blood cultures of the ARV$^-$HIV-1 study group showed a significantly higher frequency of IFN-α$^+$pDCs compared to the control study group ($p = 0.04$). A similar observation was reported in a study that investigated IFN-α supernatant levels of purified pDC stimulated with R848. The report also showed that cytokines IL-6, MIP-1α, MIP-1β and RANTES were also produced in higher levels in HIV infected individuals compared to controls (Sabado RL, *et al.* 2010). This is in contrast to the findings of Martinson JA, *et al.* (2007) who reported on the significantly lower percentage of IFN-α$^+$pDCs observed upon R848 stimulation of HIV-1 infected compared to uninfected individuals. Normalisation was observed with ARV therapy. The median percentage of IFN-α$^+$pDCs was significantly lower in the ARV$^+$HIV-1 study group compare to the ARV$^-$HIV-1 study group ($p = 0.004$). In addition, ARV therapyshowed to induce immune reconstitution with the levels of IFN-α$^+$pDCs observed in the ARV$^+$HIV-1 study groups being similar to the control study group.

In assessing the impact of VIP therapy, the study did not find the distribution of IFN-α$^+$pDCs to be significantly different between the VIP treated and untreated R848 whole blood cultures of the ARV$^-$HIV-1 and ARV$^+$HIV-1 study groups. Notably, in the ARV$^-$HIV-1 study group VIP treatment showed a tendency towards immunemodulation ($p = 0.15$) (Figure 5.4, Table 5.8).

Lower frequency of IL12p40$^+$mDC in R848 stimulated cultures of HIV-1 infected individuals whilst recovery was observed in ARV treated individuals

No IFN-α expression was observed by mDCs in neither of the TLR-L stimulated whole blood culture (data not shown). This was an expected outcome as IFN-α is not inherently produced by activated mDCs. In a similar way IL12p40 is a cytokine not characteristically produced by pDCs (IFN-α and IL12p40 also served as DC specific culture controls in the study). Accordingly, the study showed no production ofIL12p40 by pDCs in the LPS, CpG ODN and R848 whole blood cultures (data not shown). Notably, IL12p40 (a signature cytokine of mDCs) was detected at increased levels in mDCs upon R848 stimulation of the control study group ($p < 0.0001$) compared to the TLR-L$^-$ culture.IL12p40 production by mDCs was not detected in the LPS and CpG ODN cultures. Notably, the study observed a significantly reduced median percentage of IL12p40$^+$mDCs in the ARV$^-$HIV-1 study group compared to the control study group ($p = 0.02$). This may indicate that HIV-1 infection plays an inhibitory role in the production of IL12p40. In contrast Martinson JA, *et al.* (2007) found a higher percentage of IL12p40/p70$^+$mDCs in the HIV-infected compared to the uninfected cohort upon R848 stimulation. Also Sabado RL *et al.* (2010) showed higher supernatant levels of IL12p40 produced by purified mDCs. Note that in both these studies the R848 incubation period was between 16 and 24h which may produce different results to the current study in which stimulation was performed for 4.5h. Notably, a study that pre-exposed moDCs of healthy controls to the plasma of HIV infected individuals followed by Poly I: C (TLR 3 stimulation) showed reduced levels of IL12p70 (a heterodimer consisting of p35 and p40) in culture compared to the control sample. Exposure of moDCs to the plasma of HIV infected individuals on cART showed recovery in IL12p70 levels (Miller EA, *et al. 2012).*In the current study, ARV therapy seemed to normalise the frequency ofIL12p40$^+$mDCs as an increase in IL12p40$^+$mDCs was observed when the median percentage of IL12p40$^+$mDCs of the ARV$^+$HIV-1 study group was compared to that of the ARV$^-$HIV-1 study group. The change trended towards significance ($p = 0.12$).

The current study showed that all three study groups of the R848 culture arm had lower median frequencies of IL12p40$^+$mDCs in the VIP treated compared to the untreated sample. A significant immunemodulatory effect was observed in the ARV$^-$HIV-1 study group.VIP treatment showed a significantly lower IL12p40$^+$mDCs frequency compared to the untreated R848 sample ($p = 0.04$). Notably, VIP treatment in the ARV$^-$HIV-1 study group showed a median percentage of IL12p40$^+$mDCs significantly lower than the control study group ($p<0.0001$). It was suggested that VIP treatment may result in the reduction of IL12p40 production to levels significant of inefficient immune responses, which would be detrimental to the host (Figure 5.5, Table 5.9).

The TNF-α$^+$pDC frequency was unaltered between R848 cultures of healthy, HIV-1 infected and ARV treated individuals

As with IFN-α and IL12p40, spontaneous production of TNF-α was not detected by both DC subsets in the unstimulated cultures. The TNF-α activation profile showed TNF-α production by mDCs in the LPS and R848 cultures, while pDCs stained positive for TNF-α only in the R848 culture. CpG ODN stimulation showed minimal TNF-α production by the DC subsets in the different study groups. pDC TNF-α production in the R848 culture ($p < 0.0001$) and mDC TNF-α production in the LPS ($p < 0.0001$) and

R848 ($p < 0.0001$) were significantly higher when compared to the unstimulated culture of the control study group. HIV-1 infection seem not to influence TNF-α production as similar median percentages of TNF-α^+pDCs was observed in the control, ARV$^-$HIV-1 and ARV$^+$HIV-1 study groups of the R848 culture. This finding is in contrast with a study by Martinson *et al.* (2007) who observed suppression in the production of TNF-α when pDCs of HIV infected individuals were stimulated with R848. Possibly the type of cell suspension stimulated may affect these contrasting findings. The author used PBMCs which is a processed cell suspension and exposed to manipulation vs. whole blood in the current study which resembles a more natural cell suspension (but also includes many other cell types than PBMC fractions).

The median percentage of TNF-α^+mDCs was not different between the ARV$^-$HIV-1 study group and control study group of the R848 culture. ARV therapy induced a significantly lower median TNF-α^+mDCs distribution in the ARV$^+$HIV-1 study group compared to the ARV$^-$HIV-1 study group of the R848 culture ($p = 0.01$). The decline was comparable to that of the control study group indicating the role of ARV therapy in immune function recovery. A similar phenomenon was also observed with the LPS culture. Whereas a higher frequency of TNF-α^+mDCs was observed in the ARV$^-$HIV-1 study group ($p = 0.003$) compared to the control study group, ARV treatment seemed to induce a significant change in the frequency of TNF-α^+mDCs. The median percentage of this subset was significantly lower in the ARV$^+$HIV-1 study group ($p = 0.004$) compared to the ARV$^-$HIV-1 study group.

VIP immunemodulation was apparent with TNF-α production by pDCs. A significantly lower median percentage TNF-α^+pDCs was found upon comparing the R848+VIP culture of the control study group ($p = 0.006$), ARV$^-$HIV-1 study group ($p = 0.03$) and ARV$^+$HIV-1 study group ($p= 0.02$) to corresponding untreated study groups (TNF-α^+pDCs: Figure 5.6, Table 5.10). Immunemodulation was not as profound with the TNF-α^+mDCs subset. A tendency to reduce the TNF-α^+mDCs subset frequency was observed when the R848+VIP culture of the control study group ($p = 0.19$) and ARV$^-$HIV-1 study group ($p = 0.1$) was compared to untreated R848 cultures. Similarly, a tendency to reduce immune activation was observed when the LPS+VIP culture of the ARV$^+$HIV-1 study group ($p =0.06$) and ARV$^-$HIV-1 study group ($p = 0.19$) was compared to corresponding untreated LPS culture (TNF-α^+mDCs: Figure 5.7, Table 5.11). Further investigation is needed to determine the efficacy of VIP treatment.

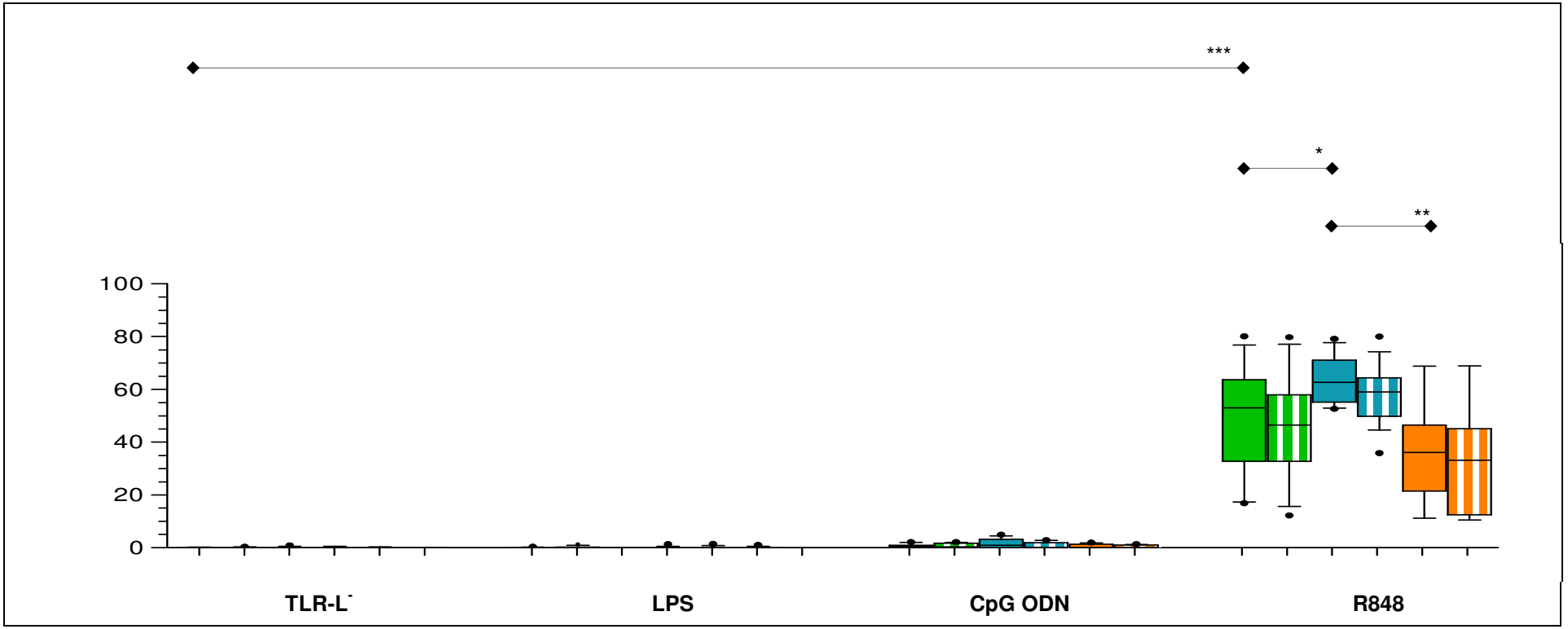

Figure 5.4: Frequency distribution of IFN-α^{+}pDCs in R848, LPS and CpG ODN stimulated whole blood cultures of the control, ARV^{-}HIV-1 and ARV^{+}HIV-1study groups

TLR-L^{-} and TLR-L^{+} (R848, LPS, CpG ODN) whole blood cultures, set up to assess intracellular cytokine production, were incubated for 4.5 hours and afterwards stained with mAbs to examine IFN-α expression by pDCs using multi-parameter flow cytometry. The box and whiskers plot represents the percentage $^{+}$pDCs of the Control, ARV^{-}HIV-1 and ARV^{+}HIV-1 study groups per whole blood culture. Each boxplot shows the 10-90 percentile range of data (whiskers) and IFN-α horizontal line the median value. Outliers are represented by black enclosed circles. Horizontal lines with diamond arrows indicate the specific study group comparison of interest and an asterisk(s) the significance. Refer to Table 3.4 for a description of the method used to indicate the level of statistical significance.

Table 5.8: Summary of IFN-α$^+$pDCs frequency in TLR-L$^-$ and TLR-L$^+$ whole blood cultures of the control, ARV$^-$HIV-1 and ARV$^+$HIV-1 study groups

	Study groups					
IFN-α$^+$pDCs	**Control**		**ARV$^-$HIV-1**		**ARV$^+$HIV-1**	
	TLR-L$^-$	**TLR-L$^-$ + VIP**	**TLR-L$^-$**	**TLR-L$^-$ + VIP**	**TLR-L$^-$**	**TLR-L$^-$ + VIP**
Minimum %	0	0	0	0	0	0
Median %	0	0	0	0	0	0
Maximum %	0.20	0.40	0.90	0.50	0.30	0
	LPS	**LPS + VIP**	**LPS**	**LPS + VIP**	**LPS**	**LPS + VIP**
Minimum %	0	0	0	0	0	0
Median %	0	0	0	0	0	0
Maximum %	0.40	1.40	0.0	1.30	1.40	1.10
	CpG ODN	**CpG ODN + VIP**	**CpG ODN**	**CpG ODN + VIP**	**CpG ODN**	**CpG ODN + VIP**
Minimum %	0	0	0	0	0	0
Median %	0.40	0.30	0.90	0.15	0	0
Maximum %	2.10	2.10	4.90	2.90	1.90	1.30
	R848	**R848 + VIP**	**R848**	**R848 + VIP**	**R848**	**R848 + VIP**
Minimum %	16.90	12.20	52.60	35.90	11.20	10.50
Median %	53.00	46.40	62.70	59.00	36.00	33.10
Maximum %	80.10	79.80	79.20	80.00	68.80	68.90

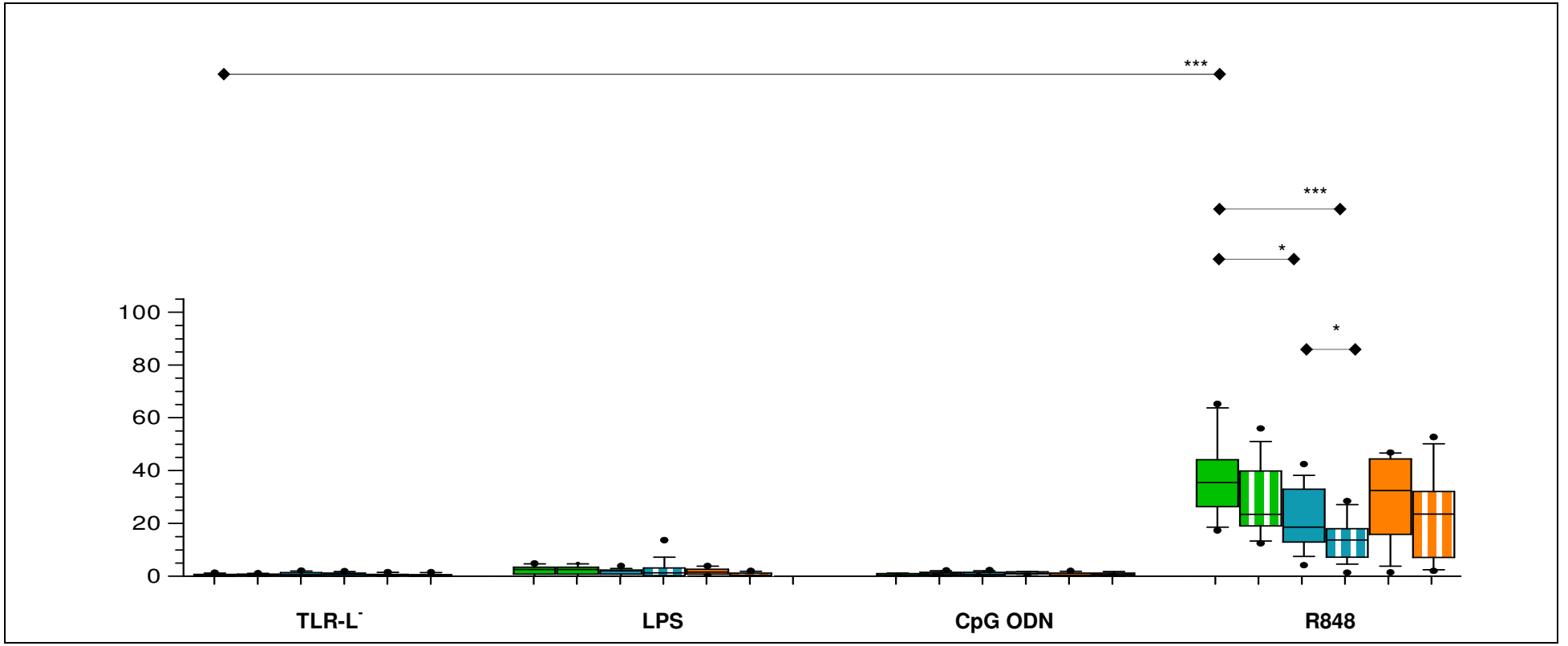

Figure 5.5 Frequency distribution of IL12p40^{+}mDCs in R848, LPS and CpG ODN stimulated whole blood cultures of the control, ARV^{-}HIV-1 and ARV^{+}HIV-1study groups

TLR-L^{-} and TLR-L^{+} (R848, LPS, CpG ODN) whole blood cultures, set up to assess intracellular cytokine production, were incubated for 4.5 hours and afterwards stained with mAbs to examine IL12p40 expression by mDCs using multi-parameter flow cytometry. The box and whiskers plot represents the percentage IL12p40 $^{+}$mDCs of the Control, ARV^{-}HIV-1 and ARV^{+}HIV-1 study groups per whole blood culture. Each boxplot shows the 10-90 percentile range of data (whiskers) and horizontal line the median value. Outliers are represented by black enclosed circles. Horizontal lines with diamond arrows indicate the specific study group comparison of interest and an asterisk(s) the significance. Refer to Table 3.4 for a description of the method used to indicate the level of statistical significance.

Table 5.9: Summary of IL12p40^{+}mDCs frequency in TLR-L^{-} and TLR-L^{+} whole blood cultures of the control, ARV^{-}HIV-1 and ARV^{+}HIV-1 study groups

	Study groups					
IL12p40^{+}mDCs	**Control**		**ARV^{-}HIV-1**		**ARV^{+}HIV-1**	
	TLR-L^{-}	**TLR-L^{-} + VIP**	**TLR-L^{-}**	**TLR-L^{-} + VIP**	**TLR-L^{-}**	**TLR-L^{-} + VIP**
Minimum %	0.0	0.0	0.0	0.0	0.0	0.0
Median %	0.30	0.60	0.60	0.70	0.45	0.30
Maximum %	1.40	1.10	2.10	1.90	1.60	1.60
	LPS	**LPS + VIP**	**LPS**	**LPS + VIP**	**LPS**	**LPS + VIP**
Minimum %	0.0	0.0	0.0	0.1000	0.0	0.0
Median %	2.550	2.550	2.050	1.300	1.600	0.4000
Maximum %	4.800	4.800	3.900	13.70	3.900	2.000
	CpG ODN	**CpG ODN + VIP**	**CpG ODN**	**CpG ODN + VIP**	**CpG ODN**	**CpG ODN + VIP**
Minimum %	0.0	0.0	0.0	0.1000	0.0	0.0
Median %	0.4000	0.8500	0.7000	1.000	0.4000	0.6000
Maximum %	1.200	2.200	2.300	1.800	2.000	1.800
	R848	**R848 + VIP**	**R848**	**R848 + VIP**	**R848**	**R848 + VIP**
Minimum %	7.20	12.50	4.20	1.40	1.50	2.00
Median %	32.90	23.40	18.50	13.75	32.45	23.50
Maximum %	65.30	56.00	42.40	28.50	46.90	52.70

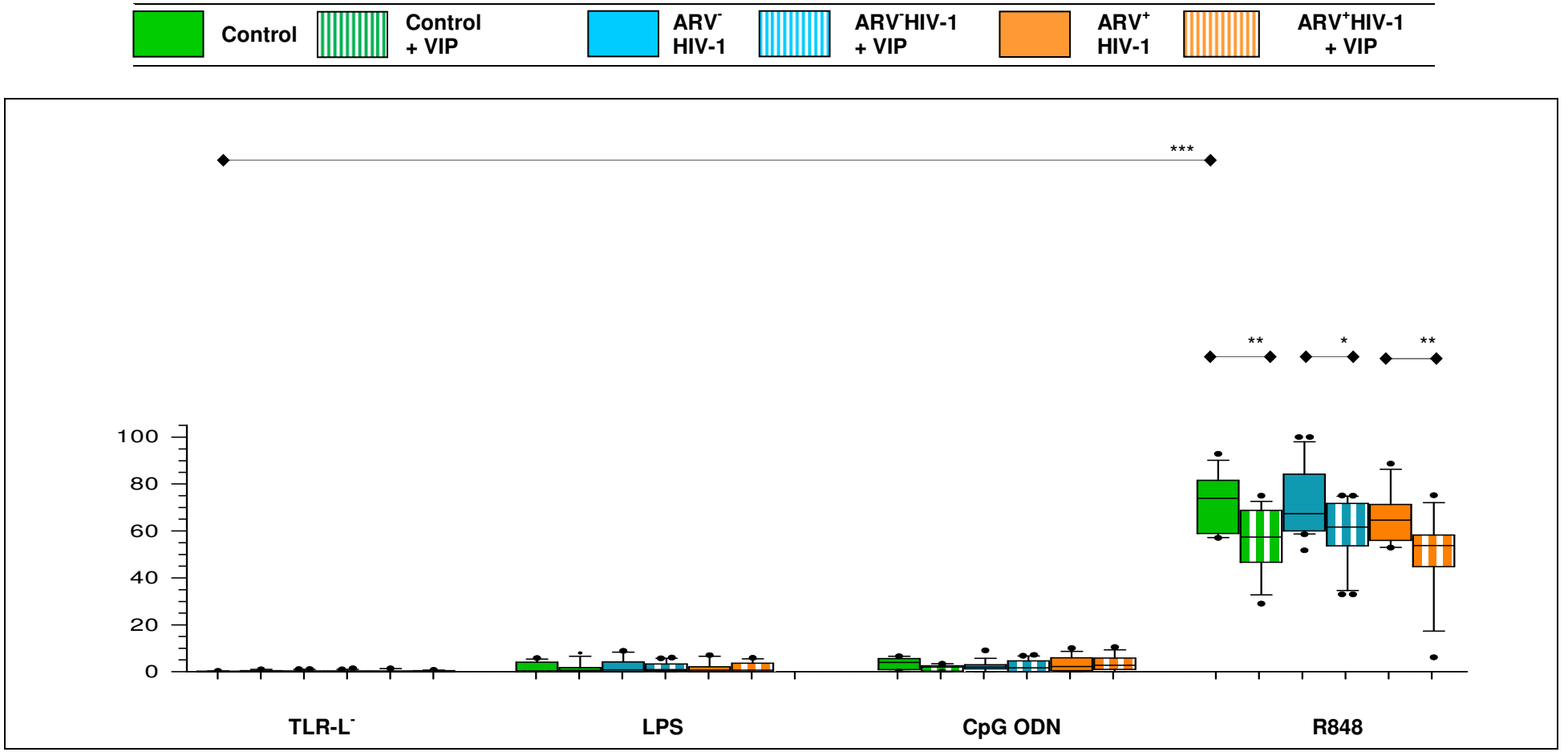

Figure 5.6: Frequency distribution of TNF-α$^+$pDCs in R848, LPS and CpG ODN stimulated whole blood cultures of the control, ARV$^-$HIV-1 and ARV$^+$HIV-1study groups

TLR-L$^-$ and TLR-L$^+$ (R848, LPS, CpG ODN) whole blood cultures, set up to assess intracellular cytokine production, were incubated for 4.5 hours and afterwards stained with mAbs to examine TNF-α expression by pDCs using multi-parameter flow cytometry. The box and whiskers plot represents the percentage TNF-α$^+$pDCs of the Control, ARV$^-$HIV-1 and ARV$^+$HIV-1 study groups per whole blood culture. Each boxplot shows the 10-90 percentile range of data (whiskers) and horizontal line the median value. Outliers are represented by black enclosed circles. Horizontal lines with diamond arrows indicate the specific study group comparison of interest and an asterisk(s) the significance. Refer to Table 3.4 for a description of the method used to indicate the level of statistical significance.

Table 5.10: Summary of TNFα^{+}pDCs frequency in TLR-L^{-} and TLR-L^{+} whole blood cultures of the control, ARV^{-}HIV-1 and ARV^{+}HIV-1 study groups

	Study groups					
	Control		ARV^{-}HIV-1		ARV^{+}HIV-1	
	TLR-L^{-}	TLR-L^{-} + VIP	TLR-L^{-}	TLR-L^{-} + VIP	TLR-L^{-}	TLR-L^{-} + VIP
Minimum %	0.0	0.0	0.0	0.0	0.0	0.0
Median %	0.0	0.0	0.0	0.0	0.0	0.0
Maximum %	0.4000	1.000	1.100	1.500	1.400	0.8000
	LPS	LPS + VIP	LPS	LPS + VIP	LPS	LPS + VIP
Minimum %	0.0	0.0	0.0	0.0	0.0	0.0
Median %	0.3500	0.6000	0.8000	0.9000	0.7000	0.7000
Maximum %	5.800	8.000	8.900	6.000	7.100	5.900
	CpG ODN	CpG ODN + VIP	CpG ODN	CpG ODN + VIP	CpG ODN	CpG ODN + VIP
Minimum %	0.1000	0.0	0.0	0.0	0.0	0.0
Median %	3.900	2.000	2.050	1.700	2.250	2.750
Maximum %	6.600	3.400	9.100	7.200	10.10	10.50
	R848	R848 + VIP	R848	R848 + VIP	R848	R848 + VIP
Minimum %	57.10	29.00	51.70	33.00	52.90	6.200
Median %	73.90	57.45	67.30	61.70	64.50	53.70
Maximum %	92.90	75.00	100.0	75.10	88.60	75.20

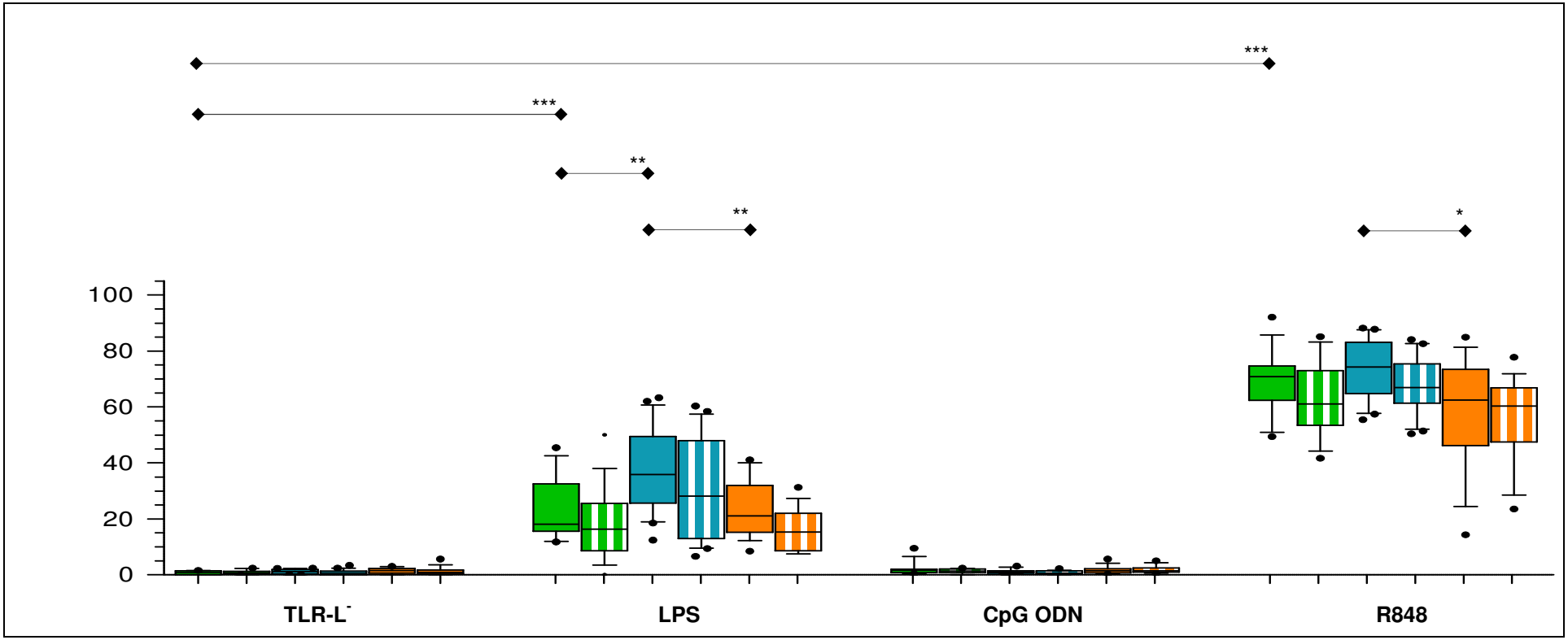

Figure 5.7: Frequency distribution of TNF-α$^+$mDCs in R848, LPS and CpG ODN stimulated whole blood cultures of the control, ARV$^-$HIV-1 and ARV$^+$HIV-1study groups

TLR-L$^-$ and TLR-L$^+$ (R848, LPS, CpG ODN) whole blood cultures, set up to assess intracellular cytokine production, were incubated for 4.5 hours and afterwards stained with mAbs to examine TNF-α expression by mDCs using multi-parameter flow cytometry. The box and whiskers plot represents the percentage TNF-α$^+$mDCs of the Control, ARV$^-$HIV-1 and ARV$^+$HIV-1 study groups per whole blood culture. Each boxplot shows the 10-90 percentile range of data (whiskers) and horizontal line the median value. Outliers are represented by black enclosed circles. Horizontal lines with diamond arrows indicate the specific study group comparison of interest and an asterisk(s) the significance. Refer to Table 3.4 for a description of the method used to indicate the level of statistical significance.

Table 5.11: Summary of TNFα^{+}mDC frequency in TLR-L^{-} and TLR-L^{+} whole blood cultures of the control, ARV^{-}HIV-1 and ARV^{+}HIV-1 study groups

	Study groups					
TNFα^{+}mDC	**Control**		**ARV^{-}HIV-1**		**ARV^{+}HIV-1**	
	TLR-L^{-}	**TLR-L^{-} + VIP**	**TLR-L^{-}**	**TLR-L^{-} + VIP**	**TLR-L^{-}**	**TLR-L^{-} + VIP**
Minimum %	0	0	0	0	0	00
Median %	0.75	0.70	1.15	0.60	1.55	0.90
Maximum %	1.60	2.40	2.40	3.40	3.00	5.60
	LPS	**LPS + VIP**	**LPS**	**LPS + VIP**	**LPS**	**LPS + VIP**
Minimum %	11.80	0	12.40	6.60	8.40	7.50
Median %	18.05	16.25	35.90	28.10	21.10	15.25
Maximum %	45.40	50.00	63.30	60.30	41.10	31.30
	CpG ODN	**CpG ODN + VIP**	**CpG ODN**	**CpG ODN + VIP**	**CpG ODN**	**CpG ODN + VIP**
Minimum %	0.40	0	0.20	0	0.20	0.50
Median %	1.70	1.35	1.00	0.60	1.50	1.50
Maximum %	9.50	2.40	3.10	2.20	5.60	5.00
	R848	**R848 + VIP**	**R848**	**R848 + VIP**	**R848**	**R848 + VIP**
Minimum %	49.40	41.60	55.40	50.40	14.30	23.50
Median %	70.80	61.00	74.30	66.90	62.50	60.30
Maximum %	92.10	85.10	88.20	84.00	84.90	77.70

5.5 Conclusion

In view of the reduced DC numbers during HIV-1 infection and complete lack of number correction during ARV therapy, it is believed that the remaining DC pool in circulation is under immense strain. In lower number capacity the cells are required to respond to persistent levels of 1) HIV antigen (in untreated infection) in circulation and 2) HIV-1 induced inflammatory signals whilst being bombarded by higher degree of invading pathogens due to the immunocompromised status of an HIV-infected system. The current study aimed to evaluate how effective DCs from an HIV-1 infected system respond to the third proposed stimulus and were activated *in vitro* by triggering TLR receptors that activate DCs to respond to signals of bacterial and viral origin. The responses were evaluated via markers associated with apoptosis and chemotaxis. In addition, cytokine responses were also assessed. In this part of the study whole blood TLR-L^- (unstimulated) and TLR-L^+ (LPS, R848, CpG ODN) cultures were prepared for each of the study groups to evaluate the level of spontaneous and activated cellular marker expression, respectively. The results were then grouped so to evaluated the responses from the control, ARV^-HIV-1 and ARV^+HIV-1 study group per culture. In the current study the following was found

1) DCs from HIV infected individuals effectively respond to TLR stimulation and the measured response was either greater (TNF-$R2^+$pDCs:LPS and R848,TNF-$R2^+$mDCs:CpG ODN, IFN-α+pDCs: R848, TNF-α+mDCs: LPS), lesser (IL12p40$^+$mDCs: R848)or similar (TNF-$R2^+$pDCs:CpG ODN, TNF-$R2^+$mDCs: LPS and R848, TNF-α+pDCs a R848) to the healthy control study group.
2) ARV therapy (approx. 1 year of treatment) had a restorative effect with reduction of responses comparable to the healthy control study group (TNF-$R2^+$pDCs: LPS and R848, IFN-α+pDCs: R848, IFN-α+pDCs: R848, TNF-α+mDCs: LPS,
3) immune-inhibitory effect of ARV therapy with reduction of responses significantly lower than the control study group (TNF-$R2^+$pDCs: CpG ODN, TNF-$R2^+$mDCs:CpG ODN)
4) spontaneous responses in unstimulated cultures: TNF-$R2^+$pDCs

DCs from a HIV-1 exposed environment showed heightened responses compared to unexposed DCs in most of the parameters investigated upon TLR stimulation. This may indicate the role that these cells play in driving inflammation during HIV infection. Nevertheless, the study showed that DCs are not functionally deprived during HIV-1 infection. Interestingly, as ARV therapy had seemingly no effect on the established parameters of immune status (no significant difference in CD4 and CD8 T lymphocyte counts as well as the CD4:CD8 ratio between the treated and untreated study groups) the results obtained from the TLR cultures were somewhat different. ARV therapy mostly corrected the changes induced by an HIV-1 infection to a degree that was comparable to the control study group. In some cases, ARV induced changes to levels lower than baseline (control study group). This may have adverse effects resulting in insufficient immune responses and would need to be investigated further. The reported discordancy has also been observed in Chapter 6 where ARV therapy fully recovered parameters of activation and exhaustion whilst having no effect on the signature parameters of immune status.VIP induced immune modulation of DC was limited and a more in-depth investigation is required into the use of VIP as an immunemodulatory agent for treating HIV-1 infection. In essence DC function is not impaired in chronic HIV-1 infection, rather these cells appear to respond more strongly to innate stimulation. ARV therapy appeared to normalize the hyper-responsive, but in certain instances may actually impair DC function.

5.6 References

Birmachu, W., Gleason, R.M., Bulbulian, B.J., Riter, C.L., Vasilakos, J.P., Lipson, K.E., and Nikolsky, Y. (2007). Transcriptional networks in plasmacytoid dendritic cells stimulated with synthetic TLR 7 agonists. BioMed Cent.Immunol.*8*, 1–19.

Cella, M., Jarrossay, D., Facchetti, F., Alebardi, O., Nakajima, H., Lanzavecchia, A., and Colonna, M. (1999).Plasmacytoid monocytes migrate to inflamed lymph nodes and produce large amounts of type I interferon. Nat. Med. *5*, 919–923.

Cooper, A.M., and Khader, S.A. (2006). IL-12p40: an inherently agonistic cytokine. Trends Immunol. 28, 33–38.

Delgado, M., Reduta, A., Sharma, V., and Ganea, D. (2004a). VIP/PACAP oppositely affects immature and mature dendritic cell expression of CD80/CD86 and the stimulatory activity for CD4+ T cells. J. Leukoc. Biol. *75*, 1122–1130.

Delgado, M., Pozo, D., and Ganea, D. (2004b).The significance of vasoactive intestinal peptide in immunomodulation.Pharmacol. Rev. *56*, 249–290.

Dickson, L., and Finlayson, K. (2009). VPAC and PAC receptors : From ligands to function. Pharmacol.Ther.*121*, 294–316.

Ding, W., Wagner, J.A., and Granstein, R.D. (2007).CGRP , PACAP , and VIP modulate Langerhans cell function by inhibiting NF-κB activation. J. Invest. Dermatol.*127*, 2357–2367.

Donaghy, H., Gazzard, B., Gotch, F., and Patterson, S. (2003). Dysfunction and infection of freshly isolated blood myeloid and plasmacytoid dendritic cells in patients infected with HIV-1. Blood *101*, 4505–4511.

Donhauser, N., Pritschet, K., Helm, M., Harrer, T., Schuster, P., Ries, M., Bischof, G., Vollmer, J., Smola, S., and Schmidt, B. (2012). Chronic immune activation in HIV-1 infection contributes to reduced interferon alpha production via enhanced CD40:CD40 ligand interaction. PLoS One *7*, 1–11.

Fabricius, D., O' Dorisio, M.S., Blackwell, S., and Jahrsdörfer, B. (2006). Human plasmacytoid dendritic cell function: inhibition of IFN-α secretion and modulation of immune phenotype by vasoactive intestinal peptide. J. Immunol. 5920–5927.

Fitzgerald-Bocarsly, P. (2002). Natural interferon-alpha producing cells: the plasmacytoid dendritic cells. Biotechniques*Suppl*, 16–20, 22, 24–29.

Fitzgerald-Bocarsly, P., Dai, J., and Singh, S. (2008). Plasmacytoid dendritic cells and type I IFN: 50 years of convergent history. Cytokine Growth Factor Rev. *19*, 3–19.

Gonzalez-Rey, E., and Delgado, M. (2008). Vasoactive intestinal peptide inhibits cycloxygenase-2 expression in activated macrophages , microglia , and dendritic cells. Brain, Behav. Immun. *22*, 35–41.

Harmar, A.J., Fahrenkrug, J., Gozes, I., Laburthe, M., May, V., Pisegna, J.R., Vaudry, D., Vaudry, H., Waschek, J.A., and Said, S.I. (2012). Pharmacology and functions of receptors for vasoactive intestinal peptide and pituitary adenylate cyclase-activating polypeptide: IUPHAR review 1. Br. J. Pharmacol. *166*, 4–17.

Isaacs, A., and Lindenmann, J. (1957).Virus Interference. I. The Interferon. Proc. R. Soc. London *147*, 258–267.

Iwasaki, A., and Medzhitov, R. (2004).Toll-like receptor control of the adaptive immune responses. Nat. Immunol. *5*, 987–995.

Lehmann, C., Harper, J.M., Taubert, D., Hartmann, P., Fätkenheuer, G., Jung, N., van Lunzen, J., Stellbrink, H.-J., Gallo, R.C., and Romerio, F. (2008). Increased interferon alpha expression in circulating plasmacytoid dendritic cells of HIV-1-infected patients. J. Acquir. Immune Defic.Syndr.*48*, 522–530.

Liu, K.-J.(2006). Dendritic cell, Toll-like receptor, and the immune system. J. Cancer Mol. *2*, 213–215.

Martinson, J.A., Roman-Gonzalez, A., Tenorio, A.R., Montoya, C.J., Gichinga, C.N., Rugeles, M.T., Tomai, M., Krieg, A.M., Ghanekar, S., Baum, L.L., *et al*. (2007). Dendritic cells from HIV-1 infected individuals are less responsive to toll-like receptor (TLR) ligands. Cell.Immunol.*250*, 75–84.

Mckenna, K., Beignon, A.-S., and Bhardwaj, N. (2005).Plasmacytoid Dendritic Cells : Linking Innate and Adaptive Immunity. J. Virol. *79*, 17–27.

Miller, E., and Bhardwaj, N. (2013).Dendritic cell dysregulation during HIV-1 infection.Immunol. Rev. *254*, 170–189.

Miller, E.A., Spadaccia, M.R., O'Brien, M.P., Rolnitzky, L., Sabado, R., Manches, O., Frleta, D., and Bhardwaj, N. (2012). Plasma factors during chronic HIV-1 infection impair IL-12 secretion by myeloid dendritic cells via a virus-independent pathway. J. Acquir. Immune Defic.Syndr.*61*, 535–544.

Petrovsky, N., and Harrison, L.C. (1995).Cytokine-based human whole blood assay for the detection of antigen-reactive T cells. J. Immunol. Methods *186*, 37–46.

Sabado, R.L., O'Brien, M., Subedi, A., Qin, L., Hu, N., Taylor, E., Dibben, O., Stacey, A., Fellay, J., Shianna, K. V, et al. (2010).Evidence of dysregulation of dendritic cells in primary HIV infection.Blood *116*, 3839–3852.

Sedger, L.M., and McDermott, M.F. (2014). TNF and TNF-receptors: From mediators of cell death and inflammation to therapeutic giants – past, present and future. Cytokine Growth Factor Rev. 25, 453–472.

Chapter 6

Distribution of $CD8^+CD38^+$, $CD8^+PD\text{-}1^+$ and $CD8^+CD38^+PD\text{-}1^+$ T lymphocyte subsets and relationship to apoptosis and activation markers expressing DCs during HIV-1 infection

6.1 Introduction

In addition to the gradual depletion of CD4 T lymphocytes, untreated HIV-1 infection is also characterised by aberrant immune activation. The latter phenomenon, however, is currently not assessed together with the standard HIV-1 clinical tests that quantify viral load and CD4 T lymphocyte numbers. Immune activation during HIV-1 infection has been assessed via expression of CD38 (T lymphocyte activation associated antigen) on CD8 T lymphocytes. Related studies strongly suggest the inclusion of this assay in ongoing clinical assessment of the disease. It was shown to have the potential in predicting disease progression to AIDS (Mahnke YD, *et al*. 2013; Liu Z, *et al.* 1997) as well as ARV therapy failure in vertically HIV-1 infected children (Resino S, *et al.* 2004). It might also prove to be an imperative test during HIV-1/TB co-infection where disease progression is more rapid.

Many have investigated the distribution of $CD8^+CD38^+$ T lymphocyte subset during untreated HIV-1 infection and reported significantly higher frequency distribution of this subset compared to healthy individuals (Sharada RS, *et al*. 2012; Shi W, *et al.* 2009; Tuaillon E, *et al.* 2009; Hunt PW, *et al.* 2008; Almeida M, *et al.* 2007; Hazenberg MD, *et al*. 2003; Sousa AE, *et al.* 2002). According to Chun T-W, *et al.* (2004), this subset was more prone to spontaneous and FAS mediated apoptosis and showed a distribution frequency that directly correlated with viral load. Others have shown the direct relationship between a related phenotype ($CD8^+CD45RO^+CD38^+$ T lymphocyte) and plasma IFN-α (Hardy GAD, *et al*. 2013) and that prolonged ARV treatment seemed to induce a decline in frequency distribution of these cells (Resino S, *et al.* 2004; Tilling R, *et al*. 2002).

In addition to altered $CD8^+CD38^+$ T lymphocyte subset frequencies during HIV-1 infection, also higher numbers of $CD8^+$ T lymphocyte subsets expressing Programmed Death 1 (PD-1/CD279) have been observed. Its association with disease progression has also been reported (as reviewed by Keir ME, *et al.* 2008; Day CL, *et al*. 2006; Trautmann L, *et al.* 2006). PD-1 is a member of the CD28/CTLA-4 family of negative (inhibitory) regulators of T lymphocyte activation. Studies using a lymphocytic choriomeningitis virus (LCMV) infected mouse model have illuminated the role of PD-1 as a marker of immune exhaustion. Barber DL, *et al.* (2006) introduced the Armstrong and clone 13 LCMV strain into adult mice which produced an acute (cleared within 7 days) and chronic infection, respectively. Acute LCMV infection is characteristic of robust LCMV-specific CD8 T cell responses, while the functionality of these subsets wanes during chronic LCMV infection. Accordingly, post infection *in vitro* cultures showed CD8 T lymphocytes from chronically infected mice weakly responding to stimulation with LCMV peptide, displaying a significantly lower expression of CD44 (marker of proliferation) and IFN-γ (effector cytokine). In parallel, steady up-regulation (at mRNA as well as protein level) of PD-1 was observed in these mice during consecutive days of infection. The authors also observed an up-regulated expression of PD-1 on virus specific CD8 T lymphocyte during acute LCMV infection (6 days post infection), however, expression levels returned to a basal state upon clearance of the virus. The inhibitory effect associated with PD-1 is induced upon interaction with its natural

ligand, PD-1L. Notably, in employing *in vivo* anti-PD-L1 blocking treatment the authors observed improved antigen-specific CD8 T cell responses viz. higher expression of IFN-γ and TNF-α. This was also accompanied by effective reduction of viral titers in serum and various organs. However, contrary to expectations, PD-L1 knock-out mice infected with Armstrong clone 13 LCMV strain succumbed to immune associated damage. This was indicative of the essential role that PD-1 plays in protecting immune responses from going into lethal "overdrive".

Main research interest

Literature describes HIV-1 associated changes with regard to immune activation and exhaustion via the expression of CD38 and PD-1 on CD8 T lymphocyte subsets, respectively (Tuaillon E, et al. 2009; Zhang J-Y, et al. 2007; Day CL, et al. 2006;Petrovas C, et al. 2006; Trautmann L, et al. 2006; Hazenberg MD, et al. 2003; Sousa AE, et al. 2002). We wished to evaluate mono and dual CD38 and PD-1 expression on CD8 T lymphocytes in ARV untreated and treated patients with or without TB co-infection and relate the distribution of these CD8 T lymphocyte subsets to DCs positively expressing markers of apoptosis, activation and migration.

Study aim:

The present study aimed to profile CD38 and PD-1 (mono and dual) expression on CD8 T lymphocytes to investigate immune activation and exhaustion during HIV-1 infection and HIV-1/TB co-infection with or without ARV therapy.

Study objectives

- ***to determine the frequency distribution of the percentage CD8 T lymphocyte subsets as well as the CD4 and CD8 T lymphocyte count and CD4:CD8 ratio in HIV-1 and HIV-1/TB co-infected patients on or naïve for ARV therapy.***
- ***to determine the relationship of the CD8 T lymphocyte subsets to CD4 T lymphocyte counts and viral load***
- ***to determine the relationship of DC subsets positively expressing markers of apoptosis, activation and migration to each of the CD8 T lymphocyte subsets during untreated and ARV treated HIV-1 and HIV-1/TB co-infection.It is believed that the current study is first to report on these relationships.***

6.2 Outline of the study

Refer to sections 6.3.1 - 6.3.6 for a detailed description on sample collection and processing

SAMPLE COLLECTION
Patient recruitment, blood collection by venesection at various clinics in the Western Cape, South Africa

↓

STUDY GROUPS
5 Study groups: Control, ARV$^-$HIV-1, ARV$^-$HIV-1/TB, ARV$^+$HIV-1 and ARV$^+$HIV-1/TB

↓

WHOLE BLOOD (EDTA)		PLASMA (EDTA)
50µl	100µl	1ml
↓	↓	↓
4-COLOUR FLOW CYTOMETRY		**REAL TIME PCR**
CD4 and CD8 T cell quantification. **ASSAY:** Staining with BD MultiTEST™ mAbs: CD3 FITC, CD8 PE, CD45 PerCP, CD4 APC in BD TruCOUNT™ tube	**CD8 T lymphocyte profiling** **ASSAY:** Staining with mAbs: CD3 FITC, CD8 PerCP, CD38 APC, PD-1 PE	**Viral load quantification** **ASSAY:** ABBOTT Real Time HIV-1 PCR assay (ABBOTT m2000rt)/bioMérieuxNucliSensEasyQ® HIV-1, v1.2 test
↓	↓	↓
DATA COLLECTED		
CD4 and CD8 T cells - cells/µl	**CD8 T lymphocytes** - % CD8$^+$CD38$^+$T lymphocytes - % CD8$^+$PD-1$^+$ T lymphocytes - % CD8$^+$CD38$^+$PD-1$^+$ T lymphocytes	**Viral load** - RNA copies/ml

6.3 Material and methods

6.3.1 Study groups and clinical data

A subset of participants (enrolled between Sept 2011 and Mar 2012) of the 5 study groups described within the broader project (chapters 4 and 5) were concurrently also used in this part of the study. Table 6.1 summarises the demographic and clinical data of the participants of the 5 study groups (Controls (n=16), ARV^-HIV-1 (n=13), ARV^-HIV-1/TB (n=12), ARV^+HIV-1 (n=12) and ARV^+HIV-1/TB (n=16)). Refer to Table 3.1 for a detailed description on the criteria for participant enrolment relevant to these study groups. Recruited patients on ARVs were using one of the following treatment regimens: TDF, Lamivudine, EFV (57% of the total ARV users); Stavudine, Lamivudine, EFV (17%) and less than 7% were using different combination of ARV therapy. TB co-infected patients were either using Pyridoxine or Rifafour (Combination of four agents: Rifampicin, Isoniazid, Pyrazinamide and Ethambutol) drugs.Participants were from state clinics in a peri-urban area of Cape Town, South Africa, which included Tygerberg (1% of the total recruits), Idasvalley (12%), Durbanville (66%), Kuilsriver (5%) as well as the Desmond Tutu Emavundleni Clinic Site in Khayelitsha (16%). Participants from the latter site were predominantly enlistees of the ARV^-HIV-1 study groups.Note that this assay was initiated on a later stage during the study due to an emerging interest to examine the relationship of HIV-1 associated immune activation and exhaustion to DCs positively expressing markers of apoptosis, activation and migration. Accordingly, this part of the study comprised of a smaller sample size per study group.

Table 6.1: Demographic and clinical data of participants in the study groups analysed to examine CD38 and PD-1 (mono and dual) expression by CD8 T lymphocytes

	Study Groups				
	Control	ARV^-		ARV^+	
		HIV-1	HIV-1/TB	HIV-1	HIV-1/TB
Total (n)	16	13	12	12	16
Male: Female					
nr	5:7	2:10	6:6	5:7	10:6
%	42:58	17:83	50:50	42:58	63:38
Age[a]					
Median	29	30	34	42	38
Range	21-58	22-50	23-69	23-55	26-50
Time on ARV therapy[b]					
Median	N/A	N/A	N/A	16	5
Range				<1 - 49	2 - 69
Time on anti-TB therapy[b]					
Median	N/A	N/A	0	N/A	3
Range			0-8		0-8

[a] *Age median and range expressed in years*
[b] *Time on treatment median and range expressed in months*

6.3.2 General specimen processing

Specimens were processed as described in section 4.3.2. Briefly, the blood sample that was collected in EDTA vacutainer tubes (BD Biosciences, San Jose, CA) for CD4 and CD8 T lymphocyte absolute number (refer to section 3.3.6) and HIV viral load (refer to section 3.3.7) quantification was also used for whole blood staining with markers to examine immune activation and exhaustion.

6.3.3 mAbs used to investigate signature markers of immune activation and exhaustion on CD8 T lymphocytes in peripheral whole blood

Mouse anti-human mAbs used in this part of the study included CD3 FITC (expressed on T lymphocytes); CD8 PerCP (expressed on cytotoxic T lymphocytes); CD38 APC (expressed on activated T lymphocytes) and PD-1 PE (expressed on activated T and B lymphocytes). These mAbs were purchased from either Biolegend[1] (San Diego, CA), BD Biosciences[2] (San Jose, CA) or e-Bioscience[3] (San Diego, CA). Refer to Table 6.2 for mAb clone and isotype information.

Table 6.2: Clone , isotype and reactivity information on the mAbs used to detect immune activation and exhaustion

mAb	Clone	Isotype	Reactivity
CD3 FITC[1]	OKT3	Mouse IgG_{2a}, κ	Human
CD8 PerCP[2]	SK1	Mouse IgG_1, κ	Human
CD38 APC[2]	HB7	mouse IgG_1, κ	Human
PD-1 PE [3]	MIH4	Mouse IgG_1, κ	Human

6.3.4 Whole blood staining procedure to detect CD38 and PD-1 expressing CD8 T lymphocytes

Staining of EDTA whole blood (100 µl) was performed as outlined in section 4.3.5. Briefly, the mAb cocktail used consisted of 5µl of each of the CD8 PerCP, CD38 APC,CD3 FITC and PD-1 PE mAbs as well as 50µl staining buffer (titration was not required as a standardised in-house assay was followed). After lysing and washing, the sample was resuspended in 500µl staining buffer and immediately acquired on a BD FACSCalibur™ 4-colour flow cytometer utilizing the BD CellQuest™ Pro software (BD Biosciences, San Jose, CA). The BD FACSDiva™ software v6.1.3 (BD Biosciences, San Jose, CA) was used to analyze the acquired events. The gating strategy is displayed in Figure 6.1. During event acquisition, the general lymphocyte population was identified in a SSC-A vs. FSC-A density plot and a stopping gate set to collect a total of a 100 000 gated lymphocyte events (Figure 6.1 B). A specific threshold was set on the FSC parameter to exclude debris.

6.3.5 Flow cytometric analyses: Gating strategy to define the CD38 and PD-1 expressing CD8 T lymphocytes from total acquired events

In analyses, total acquired events was displayed in a SSC vs. CD3 dot plot and a polygon gate, P1, used to select CD3 positive events with low SSC properties (Figure 6.1 A). In parallel, these events were also identified in a SSC vs. FSC density plot displaying total acquired events. P1 was then displayed in a CD3 vs. CD8 density plot (Figure 6.1 C) and a P2 polygon gate collected the dual CD3 and CD8 expressing T lymphocyte population. The latter was displayed in a CD38 vs. CD8 (Figure 6.1D), PD-1 vs. CD8 (Figure 6.1

E) and CD38 vs. PD-1 (Figure 6.1 F) density plot and events analysed using a quadrant (Q) gating. Q2, Q2-1 and Q2-2 defines the CD8 T lymphocytes expressing CD38, PD-1 and dual CD38 PD-1, respectively. These populations were also referred to as $CD8^{+}CD38^{+}$, $CD8^{+}PD\text{-}1^{+}$ and $CD8^{+}CD38^{+}PD\text{-}1^{+}$T lymphocyte subsets. The position of the polygon and quadrant gates to distinguish between positive and negative events was determined via the procedure of FMO controls as previously described (Section 4.3.7.2).

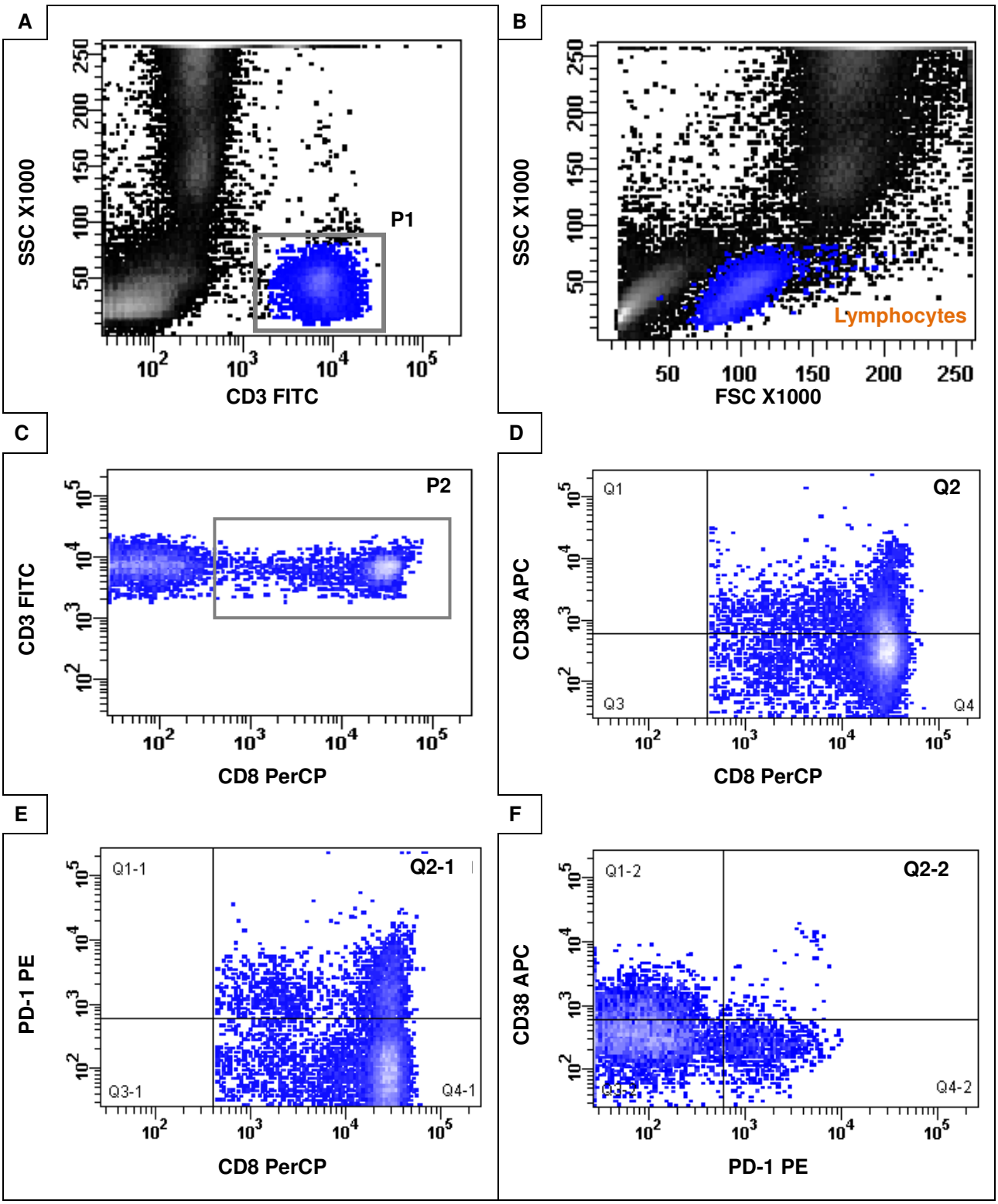

Figure 6.1: Identifying $CD8^+CD38^+$, $CD8^+PD\text{-}1^+$ and $CD8^+CD38^+PD\text{-}1^+$T lymphocyte subsets from total acquired events

Total acquired events were displayed in a SSC vs. CD3 dot plot and $CD3^+$ events collected in a P1 polygon gate (A) which corresponded to the lymphocyte population identified in SSC-A vs. FSC-A density plot showing total acquired events (B). The P1 events were further analysed in CD3 vs.CD8 dot plot and P2 collected the $CD3^+CD8^+$ events. These were further analysed in appropriate density plots to acquire the percentage $CD8^+CD38^+$ (D, Q2), $CD8^+PD\text{-}1^+$ (E, Q2-1) and $CD8^+CD38^+PD\text{-}1^+$*(F, Q2-2) events.*

6.3.6 Statistical analyses

Comparative statistical analyses of the percentage $CD8^+CD38^+$, $CD8^+PD\text{-}1^+$ and $CD8^+CD38^+PD\text{-}1^+$ T lymphocytes; CD4 and CD8 T lymphocytes absolute counts and CD4:CD8 ratio was primarily performed as described in section 3.3.8. Correlation analyses were performed using the test as described in section 3.3.8 and the following was of interest: the relationships of the percentage $CD8^+CD38^+$, $CD8^+PD\text{-}1^+$ and $CD8^+CD38^+PD\text{-}1^+$ T lymphocyte subsets to a) CD4 T lymphocyte counts of the control, HIV-1 and HIV-1-related study groups, b) viral load of the ARV^-HIV-1 and ARV^-HIV-1/TB study groups and c) percentage DCs positively expressing markers related to apoptosis (these include TNFR-2^+pDCs, TNFR-2^+mDCs, FAS^+mDCs) and activation ($CD62L^+$pDCs, $CD62L^+$mDCs and $CD86^+$mDCs) of the control, HIV-1 and HIV-1-related study groups. Statistical analysis was performed using the Graphpad Prism version 5.00 software (San Diego, California, USA)**.** Refer to Table 3.4for the summary of the method used to report significant and non-significant data as well as the corresponding p value range.

6.4 Results and Discussion

6.4.1 Frequency distribution of the percentage $CD8^+CD38^+$, $CD8^+PD\text{-}1^+$and $CD8^+CD38^+PD\text{-}1^+$ T lymphocytes of the control and HIV-1-related study groups

Significantly higher levels of $CD8^+CD38^+$, $CD8^+PD\text{-}1^+$and dual expressing $CD8^+CD38^+PD\text{-}1^+$ T lymphocytes circulate during ARV^-HIV-1 infection.

The current study observed marked changes in the distribution of $CD8^+CD38^+$, $CD8^+PD\text{-}1^+$ and, in particular, $CD8^+CD38^+PD\text{-}1^+$T lymphocytes during ARV untreated HIV-1 infection and HIV-1/TB co-infection. Compared to the control study group, the frequency distribution of the median percentage $CD8^+CD38^+PD\text{-}1^+$T lymphocytes showed a significant increase of 3.85 fold and 4.62 fold in the ARV^-HIV-1 study group ($p \leq 0.001$) andARV^-HIV-1/TB study group ($p \leq 0.001$), respectively(Table 6.3; Figure 6.2C). These study groups also showed significantly higher frequencies of the CD38and PD-1 mono expressing CD8 T lymphocytes subsets, however, to a lesser degree of intensity when compared to the dual expressing subset.In relation to the control study group, the median percentage$CD8^+CD38^+$and $CD8^+PD\text{-}1^+$T lymphocyte subsets was significantly higher in the ARV^-HIV-1 study group at a degree of 82% ($p \leq 0.05$) and 81% ($p \leq 0.01$), respectively, as well as in the ARV^-HIV-1/TB study group at a degree of 112% ($p \leq 0.001$) and 73% ($p \leq 0.01$), respectively (Table 6.3; Figure 6.2: A and B). These changes observed clearly show the impact of an HIV-1 infection on immune activation and exhaustion. However, not much has been reported on the specific process that triggers these changes. A report by Hunt PW, *et al*. (2008) proposed microbial leakage to play a role as the authors were able to correlate plasma LPS levels with enhanced $CD38^+$HLA-DR^+CD8^+ T lymphocyte frequency during HIV infection. In view of a report by Peretz Y, *et al*. (2012), it was proposed that studies on T cell exhaustion should also investigate the frequency distribution of CD8 T lymphocyte subsets expressing CD160 (a negative regulator of T lymphocyte activation) together with PD-1 and CD38 as this may represent a phenotype with suboptimal functional abilities. The authors showed that $CD160^+CD8^+PD\text{-}1^+$T lymphocytes were indicative of a functionally exhausted phenotype compared to subsets of T lymphocytes mono expressing CD160/PD-1.

Similar distribution of CD8 T lymphocytes with mono and dual expressing CD38 and PD-1 markers observed during ARV^-HIV-1 infection and ARV^-HIV-1/TB co-infection

Contrary to expectations, a significant change in the frequency distribution of the median percentage $CD8^+CD38^+$, $CD8^+PD\text{-}1^+$ and $CD8^+CD38^+PD\text{-}1^+$T lymphocytes between the ARV^-HIV-1 and ARV^-HIV-1/TB study groups was not observed (Table 6.3; Figure 6.2: A, B and C, respectively). This finding indicated that a TB co-infection does not alter the distribution of these subsets more significantly than an HIV-1 infection. Similar findings were reported by Sunder SR, *et al*. (2012) with regard to the $CD8^+CD38^+$and $CD8^+PD\text{-}1^+$ T lymphocyte subsets. In contrast to our findings, however, the authors did observe a significantly higher distribution of $CD8^+CD38^+PD\text{-}1^+$T lymphocytes during HIV-1/TB co-infection compared to HIV-1 infection. As little information was available on the study cohort investigated we proposed several factors for the discrepancy between the studies, namely, difference in sample size as well as cohort specific factors such as stage of HIV and TB disease, viral load, CD4 T lymphocyte count and immunological status (CD4:CD8 ratio) at the time of data collection.

Reduced frequency of$CD8^+CD38^+$, $CD8^+PD\text{-}1^+$ and dual expressing $CD8^+CD38^+PD\text{-}1^+$ T lymphocytes circulate during ARV treatment > 12 months.

Untreated HIV-1 infection allows unrestrained replication of the HIV-1and drastically impacts on various aspects of the immune system. However, ARV treatment (in most cases) has proven effective in controlling HIV-1 replication and reducing viral load to undetectable plasma levels (Almeida M, *et al.* 2006). Similarly, ARV therapy seemed to have a strong restorative impact on circulating $CD8^+CD38^+$, $CD8^+PD\text{-}1^+$ and $CD8^+CD38^+PD\text{-}1^+$T lymphocyte subsets during HIV-1 infection as a clear trend towards normalisation was observed. In comparing the percentage CD8 T lymphocyte subsets of the ARV^+HIV-1 study group to the ARV^-HIV-1 study group, the $CD8^+CD38^+$, $CD8^+PD\text{-}1^+$ and $CD8^+CD38^+PD\text{-}1^+$ T lymphocyte subsets seemed to circulate at a reduced median frequency of 37% ($p = 0.087$), 27% ($p = 0.054$) and 60% ($p = 0.054$), respectively. Notably, the indicated p values strongly curved towards significance (Table 6.3; Figure 6.2: A, B and C). However, the propensity of ARV therapy to reduce immune activation and exhaustion was not observed in the ARV^+HIV-1/TB study group. In comparing the CD8 T lymphocyte subsets of the latter study group to the corresponding ARV^-HIV-1/TB study group the study observed a minor decline of 11%, 10% and 33%in the median percentage $CD8^+CD38^+$, $CD8^+PD\text{-}1^+$ and $CD8^+CD38^+PD\text{-}1^+$T lymphocytes, respectively. Notably, comparative statistics for the latter CD8 T lymphocyte subset trended towards significance ($p=0.1$). The insignificant reduction in these subsets was, as expected, mirrored by the lack of immune recovery. Compared to the control study group, the ARV^+HIV-1/TB study group showed a significantly higher median distribution to a degree of 87% ($p \leq 0.01$), 56% ($p \leq 0.05$) and 274% ($p \leq 0.001$) in the $CD8^+CD38^+$, $CD8^+PD\text{-}1^+$ and $CD8^+CD38^+PD\text{-}1^+$T lymphocyte subsets, respectively (Table 6.3; Figure 6.2: A, B and C). It was proposed that the lack of decline in frequency distribution of the CD8 T lymphocyte subsets of the ARV^+HIV-1/TB study group was most probably due to an insufficient time on ARV therapy. The median time on ARV therapy for the ARV^+HIV-1/TB study group was 5 months, vastly different to the 16 months of the ARV^+HIV-1 study group, which, as reported previously, showed a significant decline in the distribution of the CD8 T lymphocyte subsets. Hence, these findings suggest that prolonged treatment (> 12 months) is required to reduce the CD8 T lymphocyte subset levels. A longitudinal study conducted by Tilling R, *et al.* (2002), following the $CD8^+CD38^+$T lymphocytes over a 7 month period of HAART treatment, also showed the frequency of these cells to decline during treatment. Noteworthy is the fact that the besides ARV therapy (> 12 month) influencing immunological recovery (to a certain degree) with 1) immune activation and exhaustion levels normalizing and 2) CD4 T lymphocyte numbers and CD4:CD8 ratio improving (partially) (chapter 3) it does not induce DC number recovery (chapter 3).

Table 6.3: Summary of the CD4 and CD8 T lymphocyte absolute number and percentage; CD4:CD8 ratio; viral load (as applicable) as well as the percentage distribution of the $CD8^+CD38^+$, $CD8^+PD\text{-}1^+$ and $CD8^+CD38^+PD\text{-}1^+$ T lymphocyte of the control, HIV-1 and HIV-1-related study groups.

Study groups						
		Control	**ARV^-HIV-1**	**ARV^-HIV-1 /TB**	**ARV^+HIV-1**	**ARV^+HIV-1 /TB**
CD4 T cells	**Me^a**	960	369	200	388	243
	R^a	412-1694	14-909	51-598	143-1072	52-840
	Me^b	44	22	15	20.5	14
	R^b	31-67	4-31	11-30	11-31	4-47
CD8 T cells	**Me^a**	582	1045	816	1058	818
	R^a	205 - 1132	187 - 1667	229 - 3106	477 - 1789	306 - 2738
	Me^b	28.5	51	56.5	48	61.5
	R^b	15 - 40	38 - 77	45 - 76	34 - 73	34 - 85
CD4:CD8 ratio	**Me^c**	1.44	0.43***	0.26***	0.49**	0.25***
	R^c	0.81 - 2.8	0.07 - 0.66	0.16 - 0.6	0.15 - 0.72	0.08 - 0.39
$CD38^+$ $CD8^+$T cells	**Me^b**	31.35	56.95	66.33	36.05	58.75
	R^b	11.86 - 67.27	8.98 - 97.54	33.98 - 89.74	4.46 - 70.05	13.16 - 92.59
$PD\text{-}1^+$ $CD8^+$T cells	**Me^b**	28.84	52.17	50	37.83	44.91
	R^b	6.8 - 48.44	19.10 - 80.85	29.11 - 76.09	14.04 - 61.72	15.98 - 80.94
$CD38^+$ $PD\text{-}1^+$ $CD8^+$ T cells	**Me^b**	6.19	30.02	34.81	12	23.17
	R^b	1.14 - 24.89	4.37 - 76.12	21.37 - 57.52	1.42 - 32.05	9.01 - 77.09
Viral load	**Me^d**	N/A	$2.7x10^3$	$7.2x10^4$	LOD	LOD
	R^d		LOD - $3.5x10^6$	340-$3.3x10^6$	LOD-310	LOD–$1.3x10^3$

Data indicated as:

Me^a *= Median cells/µl,*
R^a *= Range cells/µl,*
Me^b *= Median % of CD8 T lymphocytes,*
R^b *= Range % of CD8 T lymphoctes,*
Me^c *= Median ratio of CD4 Lymphocyte absolute number to CD8 T lymphocyte absolute number*
R^c *= Range of CD4:CD8 ratio*
Me^d *= Median RNA copies/ml,*
R^d *= Range RNA copies/ml*

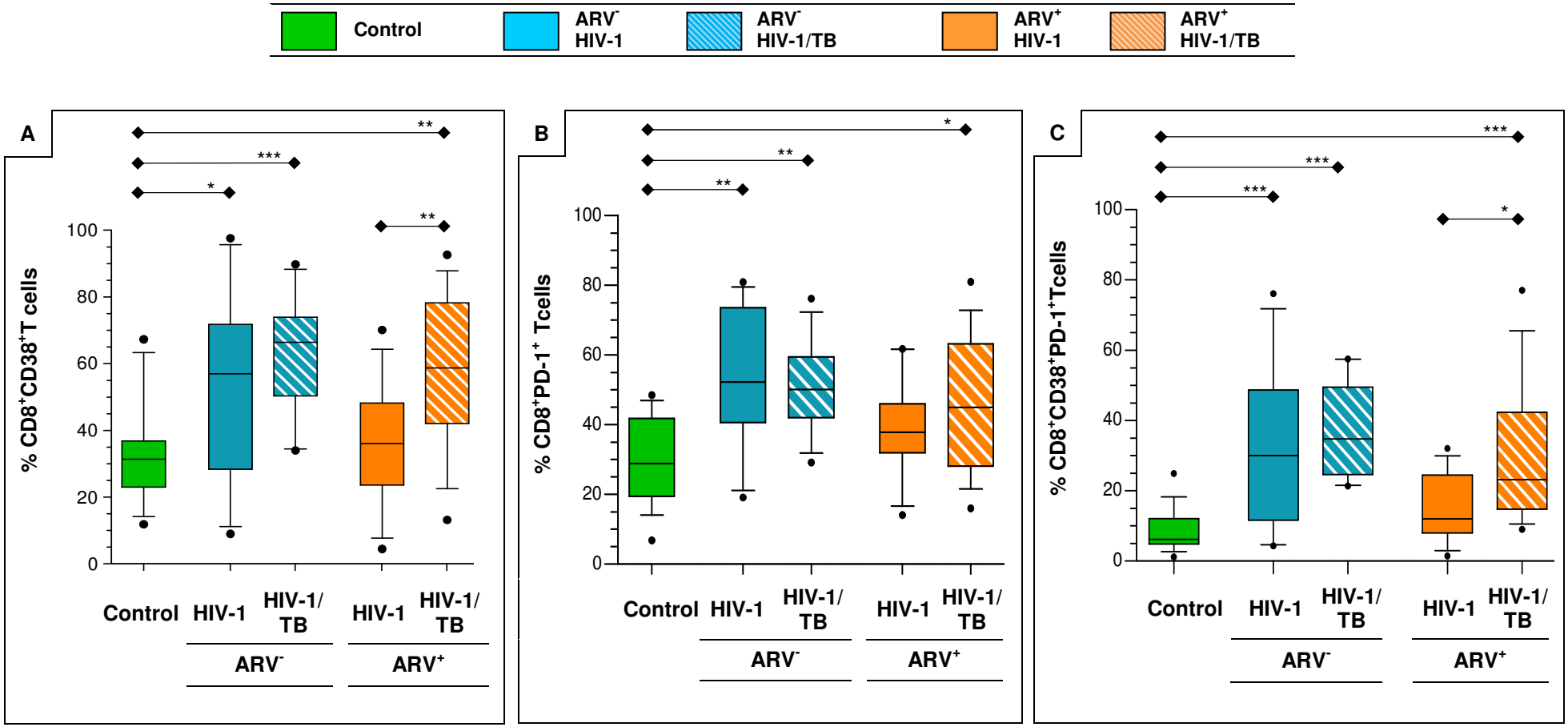

Figure 6.2: **Changes in percentage $CD8^+CD38^+$, $CD8^+PD\text{-}1^+$ and dual expressing $CD8^+CD38^+PD\text{-}1^+$T lymphocytes during ARV untreated and treated HIV-1 mono and HIV-1/TB co-infection**

Peripheral whole blood was appropriately stained to examine the expression (mono and dual) of CD38 and PD-1 on CD8 T lymphocytes using 4- colour flow cytometry. The box and whiskers plot graph represent the percentage $CD8^+CD38^+$ T lymphocytes(A), $CD8^+PD\text{-}1^+$ T lymphocytes (B) and $CD8^+CD38^+PD\text{-}1^+$ T lymphocytes (C) of the control, untreated and ARV treatedHIV-1 and HIV-1/TB study groups. Each boxplot shows the 10-90 percentile range of data (whiskers) and horizontal line the median value. Outliers are represented by a black enclosed circle. Horizontal lines with diamond arrows indicate the specific study group comparison of interest and an asterisk(s) the significance. Refer to Table 3.4 for a description of the method used to indicate the level of statistical significance.

6.4.2 Absolute numbers of CD4 and CD8 T lymphocyte counts and CD4:CD8 ratio in the control and HIV-1-related study groups

Additionally, the CD4 and CD8 T lymphocyte counts of the participants enrolled were also determined. Compared to the control study group, the decline in the median CD4 T lymphocyte count of the HIV-1 and HIV-1-related study groups was significant and, notably, similar between the ARV untreated and treated study groups. Also, the same profile was observed upon evaluation of the CD4:CD8 ratio across the different study groups. The median CD4 T lymphocytes counts in both the ARV^{-}HIV-1 and ARV^{+}HIV-1 study groups were observed at a 60% lower frequency (ARV^{-}HIV-1: $p \leq 0.01$; ARV^{+}HIV-1: $p \leq 0.05$) while in the ARV^{-}HIV-1/TB and ARV^{+}HIV-1/TB study group a 79% ($p \leq 0.001$) and 75% ($p \leq 0.001$) lower frequency was observed compared to the control study group, respectively (Table 6.3, Figure 6.3 A and B). As the median CD4 T lymphocyte absolute number as well as CD4:CD8 ratio distribution of the untreated study groups was analogous to the ARV treated study groups, we were unable to show in this part of the study the ARV-associated (partial) recovery as reported in chapter 3. This contrasting finding was attributed to various factors such as the small sample size of the study groups as well as enrolment of individuals regardless of their CD4 T lymphocyte count. Hence, it is most likely that the study groups included participants at various stages of HIV-1 disease progression which may influence the statistical outcome. The median CD8 T lymphocyte counts were higher in both the ARV treated and untreated study groups, however the change when compared to the control study group was only significant in the ARV^{+}HIV-1 study group ($p \leq 0.05$).

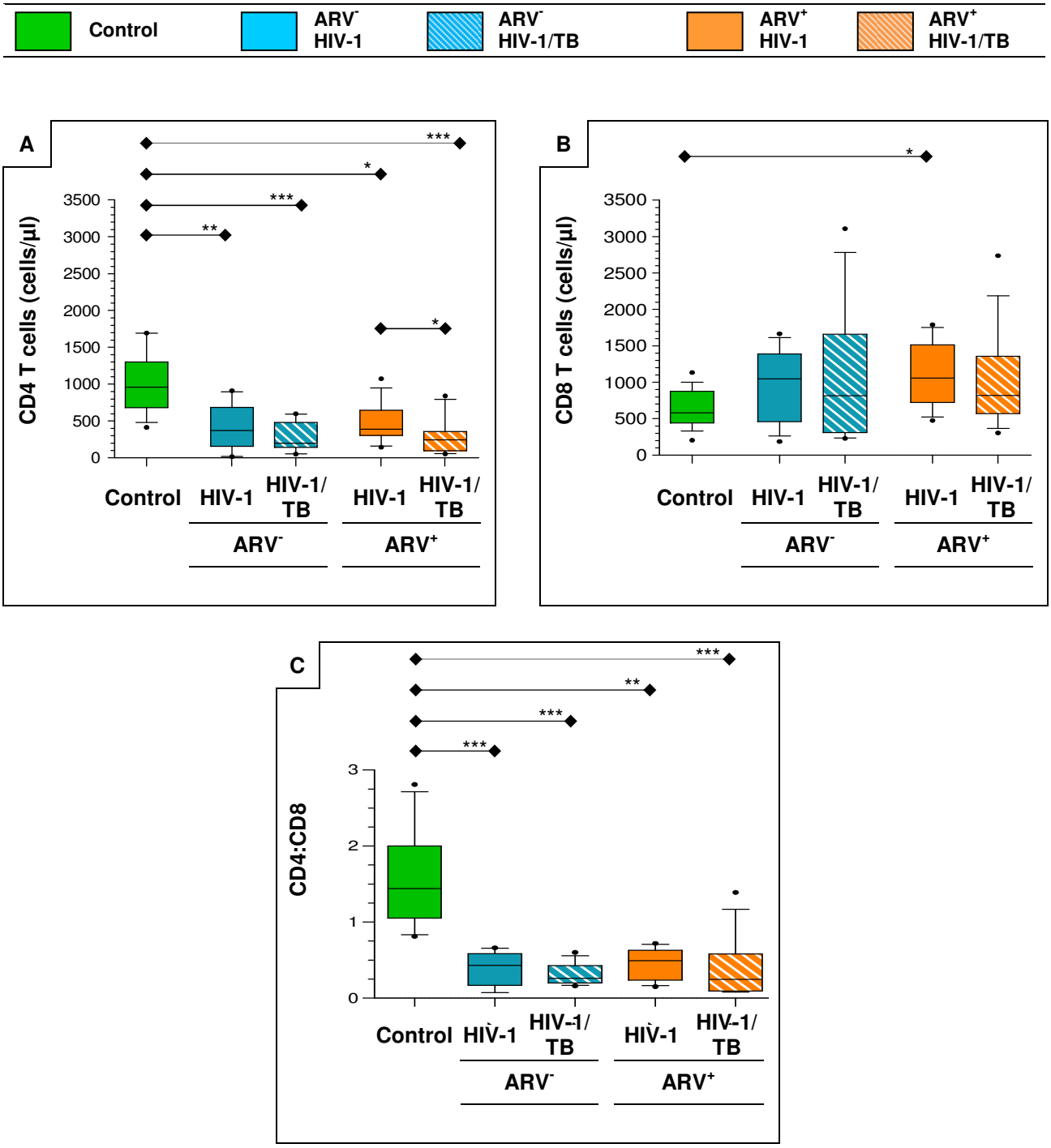

Figure 6.3: Changes in CD4 T lymphocyte and CD8 T lymphocyte absolute number as well as CD4:CD8 ratio during ARV untreated and treated HIV-1 mono and HIV-1/TB co-infection

Peripheral whole blood was stained with the BD MultiTEST™ reagent (CD3, CD8, CD45, CD4 mAb cocktail) using the BD TruCOUNT™ assay and analysed using 4 - colour flow cytometry to determine the absolute count (cells/µl) of CD4 and CD8 T lymphocytes and CD4:CD8 ratio. The box and whiskers graph represents the absolute number of CD4 T lymphocytes (A), CD8 T lymphocytes (B) and CD4:CD8 ratio (C) of the control, untreated and ARV treated HIV-1 and HIV-1/TB study groups. Each boxplot shows the 10-90 percentile range of data (whiskers) and horizontal line the median value. Outliers are represented by black enclosed circles. Horizontal lines with diamond arrows indicate the specific study group comparison of interest and an asterisk(s) the significance. Refer to Table 3.4 for a description of the method used to indicate the level of statistical significance.

6.4.3 Correlating $CD8^+CD38^+$, $CD8^+PD\text{-}1^+$ and $CD8^+CD38^+PD\text{-}1^+$ T lymphocytes frequency to CD4 T lymphocyte count and viral load

Immune activation and exhaustion levels indirectly correlate with CD4 T lymphocyte count and directly with viral load during HIV-1 infection

Distinctively different profiles were obtained in the control and ARV^-HIV-1 study group when correlating the percentage $CD8^+CD38^+$, $CD8^+PD\text{-}1^+$ and $CD8^+CD38^+PD\text{-}1^+$ T lymphocytes with median CD4 T lymphocyte counts. In the control study group no correlation was found, hence, constant frequencies of the CD8 T lymphocyte subsets was observed across the CD4 T lymphocyte count range ($CD8^+CD38^+$ T lymphocytes ($r = 0.04$, $p = 0.74$), $CD8^+PD\text{-}1^+$ T lymphocytes ($r = -0.02$, $p = 0.96$), $CD8^+CD38^+PD\text{-}1^+$ lymphocytes ($r = 0.009$, $p = 0.86$) (Figure 6.4). However, this profile was mostly altered in the ARV^-HIV-1 study group. A strong indirect correlation was observed between median CD4 T lymphocyte counts and the percentage $CD8^+CD38^+$ ($r = -0.85$, $p = 0.0002$) as well as the percentage $CD8^+CD38^+PD\text{-}1^+$ ($r = -0.8$, $p = 0.004$) T lymphocytes. The percentage $CD8^+PD\text{-}1^+$ T lymphocytes ($r = -0.44$, $p = 0.15$) showed a weak indirect correlation (Figure 6.5 A). Clearly, this finding suggests that concurrent to the higher frequencies of CD8 T lymphocyte subsets associated with immune activation and/or exhaustion, lower CD4 T lymphocyte numbers circulate during untreated HIV-1 infection. In addition, raised activation levels were also associated with increasing viral load. In the ARV^-HIV-1 study group we observed a significant direct association between viral load and the percentage $CD8^+CD38^+$ T lymphocytes ($r = 0.54$, $p = 0.01$), a weak direct association with the percentage $CD8^+CD38^+PD\text{-}1^+$ T lymphocytes ($r = 0.32$, $p = 0.1$) and no correlation with the percentage $CD8^+PD\text{-}1^+$ lymphocytes ($r = -0.07$, $p = 0.73$) (Figure 6.6 A). Clearly, CD38 expression, but less to that of PD-1 is influenced by viral load.

In assessment of the percentage CD8 T lymphocyte subsets vs. CD4 T lymphocyte count of the ARV^-HIV-1/TB study group, we observed a correlation profile different to the ARV^-HIV-1 study group (Figure 6.5 B). One would have expected the correlation profile of the two study groups to be similar as these groups manifested with similar 1) frequencies of circulating CD8 T lymphocyte subsets (Table 6.3) and 2) CD8 T lymphocyte subsets vs. viral load correlation profiles. As with the ARV^-HIV-1 study group, the viral load of the ARV^-HIV-1/TB study group showed a strong direct correlation with the percentage $CD38^+8^+$ T lymphocytes ($r = 0.78$, $p = 0.003$), weak direct correlation with percentage $CD8^+CD38^+PD\text{-}1^+$ lymphocytes ($r = 0.43$, $p = 0.13$) and no correlation with the percentage $CD8^+PD\text{-}1^+$ T lymphocytes ($r = -0.22$, $p = 0.79$) (Figure 6.6 B). However, a pertinent difference between the two study groups was the median CD4 T lymphocyte counts. The ARV^-HIV-1 and ARV^-HIV-1/TB study group had a median CD4 T lymphocyte count of 369 cells/µl, ranging from 14 – 909 cells/µl and 200 cells/µl, ranging from 51 - 598 cells/µl, respectively. Accordingly, the former study group included participants from early to late stage of disease progression, while the latter group mostly represent participants in intermediate to late state of disease progression. Hence, it was proposed that the dissimilar correlation pattern between the ARV^-HIV-1 and ARV^-HIV-1/TB study group might be due to the inadvertent exclusion of participants with a CD4 T lymphocyte count suggestive of early stage of disease. Hence, we propose that future studies aiming to define or monitor the relationship between the CD8 T lymphocyte subsets and CD4 T lymphocyte count during HIV-1 infection, includes participants with disease status ranging from early to late stage.

Prolonged ARV therapy contributes to reduced immune activation and exhaustion

A clear indirect correlation profile was observed when comparing the percentage $CD8^+CD38^+$ T lymphocytes ($r = -0.67$, $p = 0.05$), $CD8^+CD38^+PD\text{-}1^+$ T lymphocytes ($r = -0.62$, $p = 0.08$) and $CD8^+PD\text{-}1^+$ T lymphocytes ($r = -0.48$, $p = 0.11$) to the CD4 T lymphocyte count of the ARV^+HIV-1/TB study group (Figure 6.5 D). The former two subsets showed a mostly strong, while the latter a weak relationship. The correlation profile of this ARV treated HIV-1/TB study group was comparable to that of the untreated HIV-1 study group and attributed to the short and ineffective median ARV treatment time (5 months) associated with the former group. In contrast, the CD4 T lymphocyte count of the ARV^+HIV-1 study group did not correlate with any of the CD8 T lymphocytes subsets ($CD8^+CD38^+$ T lymphocytes ($r = -0.09$, $p = 0.85$), $CD8^+PD\text{-}1^+$ ($r = -0.42$, $p = 0.26$) and $CD8^+CD38^+PD\text{-}1^+$ T lymphocytes ($r = -0.32$, $p = 0.36$)) (Figure 6.5 C) and produced a correlation profile closely related to the control study group (Figure 6.4). This study group had a median time on ARV therapy of more than 12 months and clearly showed that prolonged ARV control over HIV-1 replication effectively reduced immune activation and exhaustion. However, as the median CD4 T lymphocyte counts of the ARV^+HIV-1 study group (median: 369 cells/µl, range: 14-949 cells/µl) after 16 months of ARV therapy was similar to that of the untreated HIV-1 study group (median 388 cells/µl, range143-1072 cells/µl) it seems that an ARV treatment period greater than 1 year does not exert a similar remedial effect on CD4 T lymphocyte numbers as observed with the CD8 T lymphocyte subsets. This, however, needs to be confirmed upon analyses of a bigger sample cohort.

Correlation between the CD8 T lymphocyte subsets and viral load was not determine for the ARV^+HIV-1 and ARV^+HIV-1/TB study group as the median viral load for both groups was LOD.

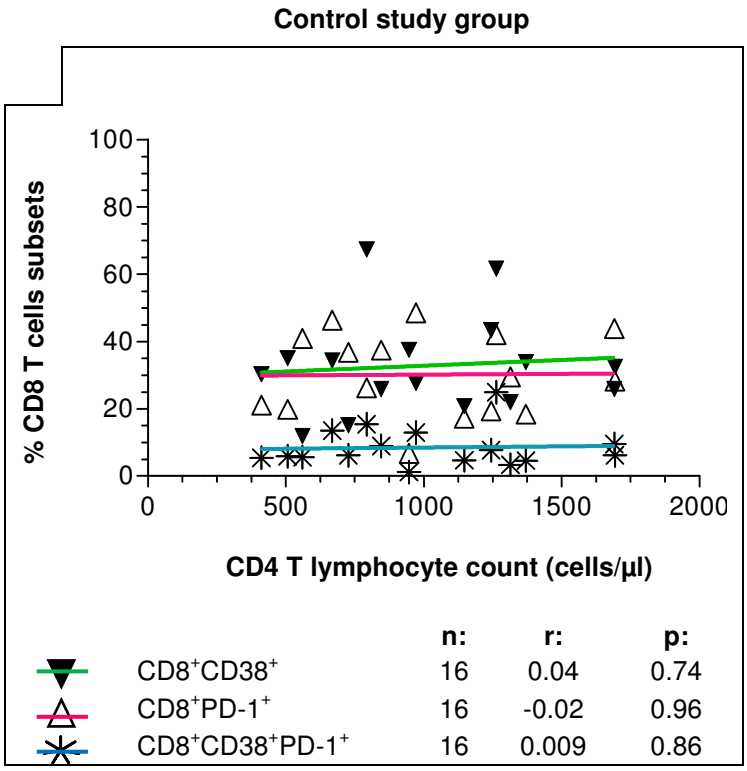

Figure 6.4: Correlating percentage CD8 T lymphocyte subsets and CD4 T lymphocyte counts in the control study group.

The percentage$CD8^+CD38^+$, $CD8^+PD\text{-}1^+$ and $CD8^+CD38^+PD\text{-}1^+$ T lymphocytes was determined for each of the participants of the control study group and plotted together with corresponding CD4 T lymphocyte count on a line graph. The percentage $CD8^+CD38^+$, $CD8^+PD\text{-}1^+$ and $CD8^+CD38^+PD\text{-}1^+$ T lymphocyte subsets were 1) represented by the symbols ▼, △ and ✳, and 2) relationship to CD4 T lymphocyte count illustrated by a green, pink and blue-coloured linear regression line, respectively. The non-parametric Spearman test was use to correlate the percentage CD8 T lymphocyte subsets to CD4 T lymphocyte counts.

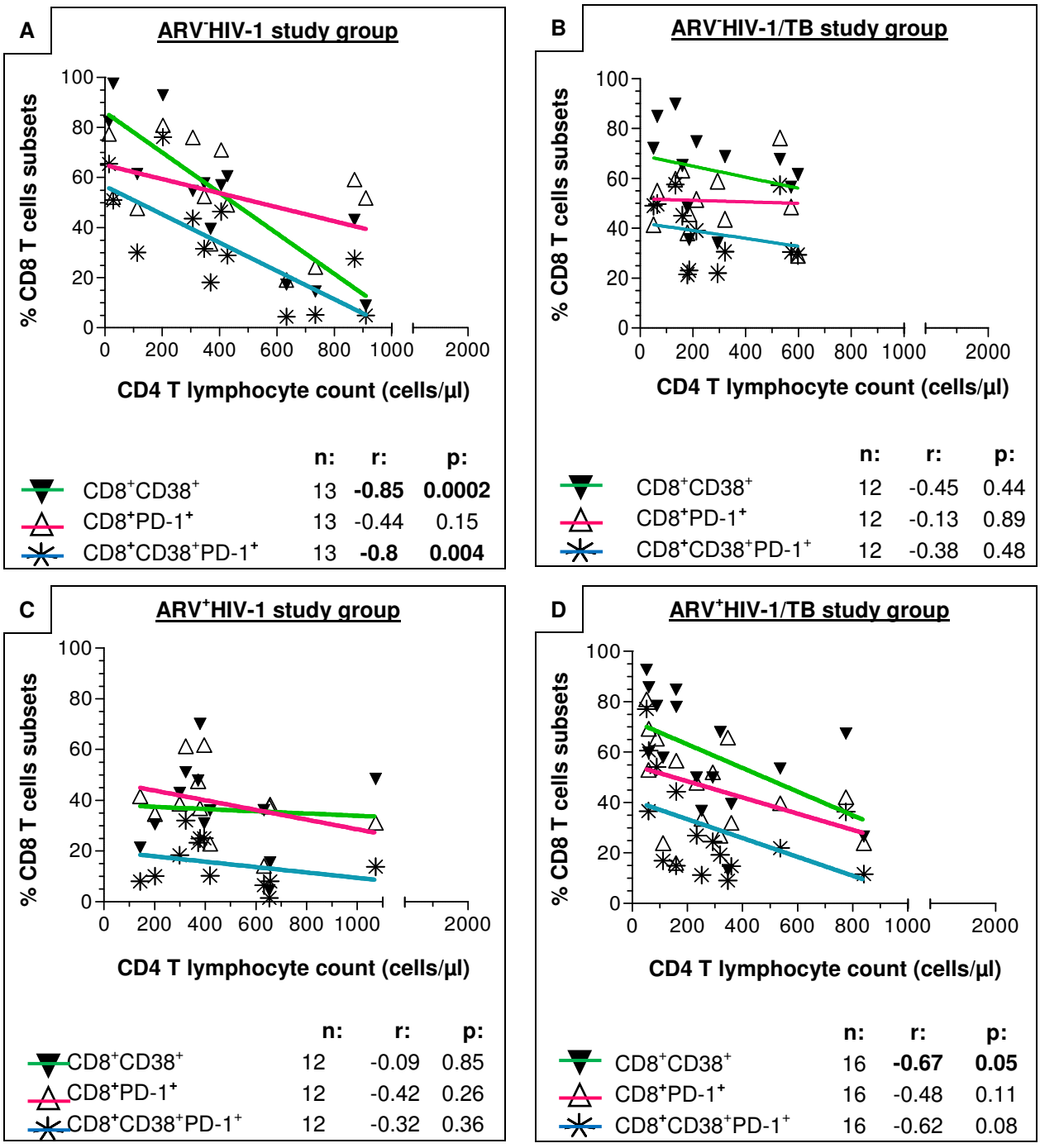

Figure 6.5: Correlating the percentage CD8T lymphocyte subsets to CD4 T lymphocyte counts during ARV untreated and treated HIV-1 mono and HIV-1/TB co-infection

The percentage$CD8^+CD38^+$, $CD8^+PD\text{-}1^+$ and $CD8^+CD38^+PD\text{-}1^+$ T lymphocytes was determined for each of the participants of the HIV-1-related study groups and plotted together with corresponding CD4 T lymphocyte count on a line graph. The percentage $CD8^+CD38^+$, $CD8^+PD\text{-}1^+$ and $CD8^+CD38^+PD\text{-}1^+$ T lymphocyte subsets were 1) represented by the symbols ▼, △ and ✳, and 2) relationship to CD4 T lymphocyte count illustrated by a green, pink and blue-coloured linear regression line, respectively. The non-parametric Spearman test was use to correlate the percentage CD8 T lymphocyte subsets to CD4 T lymphocyte counts. Statistically significant data are highlighted in bold.

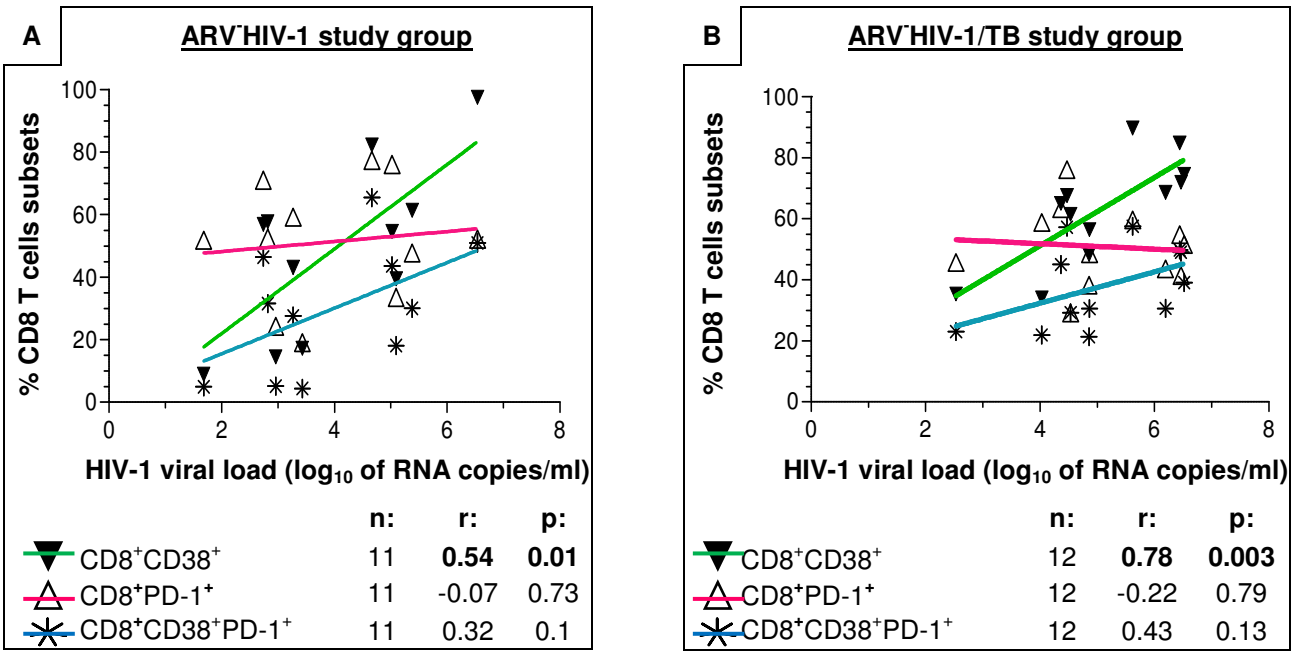

Figure 6.6: Correlating the percentage CD8 T lymphocytes to viral load during ARV untreated HIV-1 mono and HIV-1/TB co-infection

The percentage$CD8^+CD38^+$, $CD8^+PD\text{-}1^+$ and $CD8^+CD38^+PD\text{-}1^+$ T lymphocytes was determined for each of the participants of the control and HIV-1-related study groups and plotted together with corresponding HIV-1 viral load on a line graph. The percentage $CD8^+CD38^+$, $CD8^+PD\text{-}1^+$ and $CD8^+CD38^+PD\text{-}1^+$ T lymphocyte subsets were 1) represented by the symbols ▼, △ and ✳, and 2) relationship to viral load illustrated by a green, pink and blue-coloured linear regression line, respectively. The non-parametric Spearman test was use to correlate the percentage CD8 T lymphocyte subsets to CD4 T lymphocyte counts. Statistically significant data are highlighted in bold.

6.4.4 Correlating $CD8^+CD38^+$, $CD8^+PD\text{-}1^+$ and $CD8^+CD38^+PD\text{-}1^+$ T lymphocytes to DC subsets positively expressing markers of apoptosis, migration and activation

As described previously, TNF-R2 and FAS play a role in apoptosis, CD62L is a marker related to cell activation and CD86 is a characteristic DC activation marker. These markers were investigated in accordance with the current study's hypothesis proposing cell death, migration and activation to play a role in the decline of DCs numbers during HIV-1 infection. As described in Chapter 4 these markers were found positively expressed by either both or one of the DC subsets. Furthermore, comparative analysis found no significant change in the frequency distribution of mDCs expressing TNF-R2, FAS, CD62L and CD86 and pDCs expressing CD62L. However, a significant change in distribution of TNF-R2 expressing pDCs during HIV-1 infection was observed. It was of great interested to determine the relationship of DCs positively expressing these markers of apoptosis, migration and activation to signature markers of exhaustion and activation during HIV-1 infection. Hence, this part of the study focused on correlating the $CD8^+CD38^+$, $CD8^+PD\text{-}1^+$ and $CD8^+CD38^+PD\text{-}1^+$ T lymphocytes subsets to $TNF\text{-}R2^+$pDCs, $TNF\text{-}R2^+$mDCs, FAS^+mDCs, $CD62L^+$pDCs,$CD62L^+$mDCs and $CD86^+$mDCs of the control, HIV-1 and HIV-1-related study groups.

$TNF\text{-}R2^+$pDCs did not significantly correlate with the CD8 T lymphocyte subsets during HIV-1 infection

In evaluating the relationship of the percentage $CD8^+CD38^+$T lymphocytes ($r = 0.16$, $p = 0.17$) and $CD8^+PD\text{-}1^+$ T lymphocytes ($r = 0.18$, $p = 0.38$) to the percentage $TNF\text{-}R2^+$pDCs of the control study group, no significant correlation was observed. However, the percentage dual CD38 and PD-1 expressing CD8 T lymphocytes($r = 0.44$, $p = 0.10$) showed a weak tendency to directly correlate with the percentage $TNF\text{-}R2^+$pDCs (Figure 6.7). Furthermore, no significant relationship was observed between the percentage $TNF\text{-}R2^+$pDCs and percentage $CD8^+CD38^+$ T lymphocytes, $CD8^+PD\text{-}1^+$ T lymphocytes and $CD8^+CD38^+PD\text{-}1^+$ T lymphocytes of the ARV^-HIV-1 study group ($r = 0.28$, $p = 0.20$; $r = 0.22$, $p = 0.51$; $r = 0.21$, $p = 0.42$, respectively, Figure 6.8A), ARV^-HIV-1/TB study group ($r = 0.25$, $p = 0.33$; $r = -0.13$, $p = 0.8$; $r = 0.18$, $p = 0.46$, respectively, Figure 6.8B) as well as the ARV^+HIV-1/TB study group ($r = 0.24$, $p = 0.26$; $r = 0.23$, $p = 60$; $r = 0.38$, $p = 0.20$, respectively, Figure 6.8D). Notably, as the relationship between $TNF\text{-}R2^+$pDCs and the CD8 T lymphocytes of the control study group steered towards a direct correlation, an inverse relationship was observed with the ARV^+HIV-1 study group ($r = -0.18$, $p = 0.57$; $r = -0.22$, $p = 0.25$; $r = -0.37$, $p = 0.42$) (Figure 6.8C). However, these relationships were not significant.

Prolonged ARV therapy (>1year) results in higher percentage $TNF\text{-}R2^+$mDCs to circulate with declining levels of the CD8 T lymphocyte subsets

The control study group showed a strong direct and significant relationship upon correlating the percentage $TNF\text{-}R2^+$mDCs to the percentage $CD8^+PD\text{-}1^+$ T lymphocyte subsets which was accompanied by a strong tendency of this mDC subset to indirectly correlate with $CD8^+CD38^+$T lymphocytes ($r = -0.42$, $p = 0.06$). Also in this study group the $CD8^+CD38^+PD\text{-}1^+$ T lymphocyte population ($r = 0.42$, $p = 0.09$) showed a weak but insignificant direct relationship with $TNF\text{-}R2^+$mDCs. Hence, it seems that higher frequency of $TNF\text{-}R2^+$mDCs tends to associate with increasing apoptotic and declining activation activity in HIV-1 uninfected individuals (Figure 6.9). However, in the ARV^-HIV-1 study group the percentage $CD8^+CD38^+$T lymphocytes ($r = 0.21$, $p = 0.53$), $CD8^+PD\text{-}1^+$T lymphocytes ($r = 0.22$, $p = 0.51$) and $CD8^+CD38^+PD\text{-}1^+$ ($r = 0.51$, $p = 0.88$) of the ARV^-

HIV-1 study group showed a positive, but insignificant, relationship with TNF-R2$^+$mDCs (Figure 6.10A). An interesting observation was the significant correlation between the percentage TNF-R2$^+$mDCs and percentage CD8 T lymphocyte subsets of the ARV$^+$HIV-1 study group. Here the study observed a strong indirect correlation between the percentage TNF-R2$^+$mDCs and 1) the percentage CD8$^+$CD38$^+$ T lymphocytes (r = -0.84, P = 0.06), 2) CD8$^+$PD-1$^+$ lymphocytes (r = -0.56, p = 0.01) and 3) CD8$^+$CD38$^+$PD-1$^+$ T lymphocytes (r = -0.88, p = 0). It seems that ARV therapy reduces the distribution of the CD8 T phenotype subsets together with TNF-R2$^+$mDCs (Figure 6.10C). In contrast to the profile observed with the ARV$^+$HIV-1 study group, the percentage CD8$^+$CD38$^+$T lymphocytes (r = 0.51, p = 0.05), CD8$^+$PD-1$^+$ T lymphocyte (r = 0.2, p = 0.48) and CD8$^+$CD38$^+$PD-1$^+$ T lymphocytes (r = 0.37, p = 0.18) of the ARV$^+$HIV-1/TB study group showed a direct correlation with TNF-R2$^+$mDCs of which the former subset correlated significantly (Figure 6.10D). It was proposed that the contrasting profile observed between the ARV$^+$HIV-1 and ARV$^+$HIV-1/TB study groupsmaybe the effect of prolonged ARV therapy as the median time on therapy of the former study group was 16 months and that of latter study group 5 months. Its debated, whether this association that develops upon the use of ARV therapy would be beneficial to the host as the relationship of CD8$^+$PD-1$^+$ T lymphocytes and CD8$^+$CD38$^+$PD-1$^+$ T lymphocytes to TNF-R2$^+$mDCs did not revert to that of the control study group during ARV therapy, in fact, a direct contrasting profile was observed.

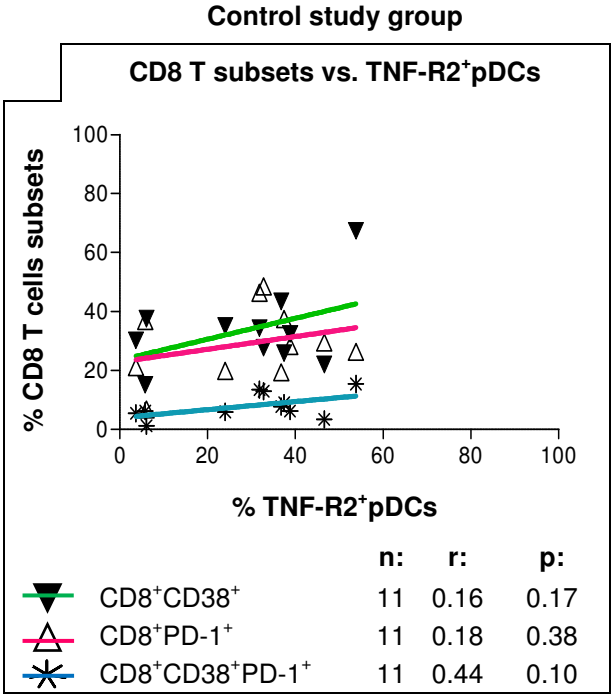

Figure 6.7: Correlating TNF-R2$^+$pDCs to percentageCD8 T lymphocyte subsets in the control study group.

The percentageCD8$^+$CD38$^+$, CD8$^+$PD-1$^+$ and CD8$^+$CD38$^+$PD-1$^+$ T lymphocytes was determined for each of the participants of the control study groups and plotted together with corresponding percentage TNF-R2 pDCs on a line graph. The CD8$^+$CD38$^+$, CD8$^+$PD-1$^+$ and CD8$^+$CD38$^+$PD-1$^+$ T lymphocyte subsets were 1) represented by the symbols ▼, △ and ✳, and 2) relationship to percentage TNF-R2 pDCs illustrated by a green, pink and blue-coloured linear regression line, respectively. The non-parametric Spearman test was use to correlate the percentage CD8 T lymphocyte subsets to percentage TNF-R2$^+$pDCs.

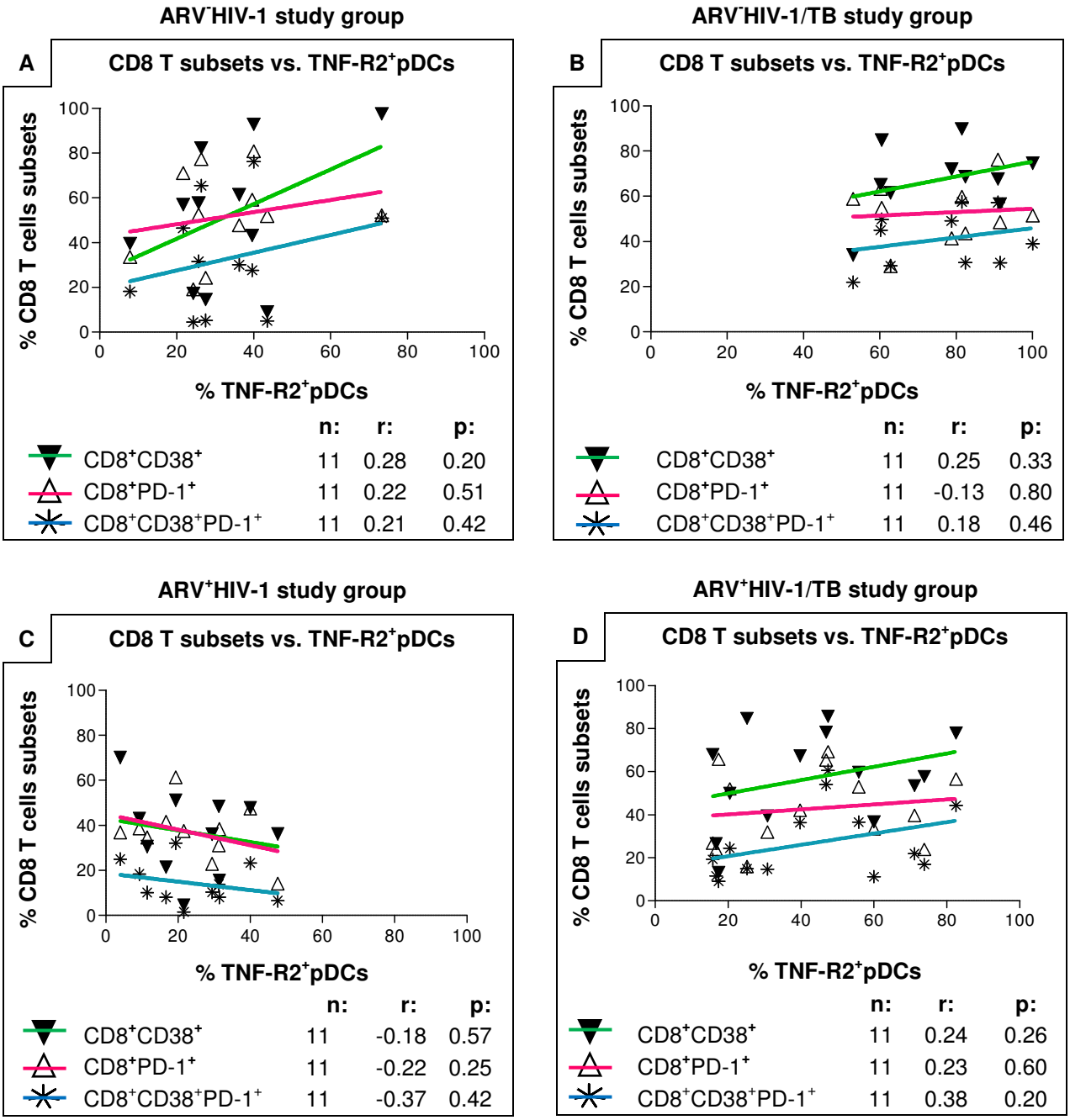

Figure 6.8: Correlating TNF-R2$^+$pDCs to percentage CD8 T lymphocyte subsets in ARV untreated and treated HIV-1 mono and HIV-1/TB co-infection

The percentage$CD8^+CD38^+$, $CD8^+PD\text{-}1^+$ and $CD8^+CD38^+PD\text{-}1^+$ T lymphocytes was determined for each of the participants of the HIV-1-related study groups and plotted together with corresponding percentage TNF-R2 pDCs on a line graph. The percentage $CD8^+CD38^+$, $CD8^+PD\text{-}1^+$ and $CD8^+CD38^+PD\text{-}1^+$ T lymphocyte subsets were 1) represented by the symbols ▼, △ and ✳, and 2) relationship to percentage TNF-R2$^+$pDCs illustrated by a green, pink and blue-coloured linear regression line, respectively. The non-parametric Spearman test was use to correlate the percentage CD8 T lymphocyte subsets to percentage TNF-R2$^+$pDCs.

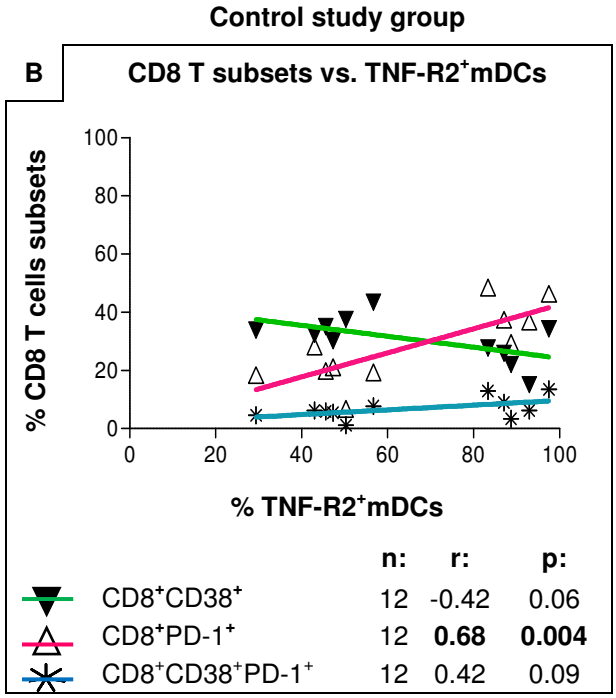

Figure 6.9: Correlating TNF-R2$^+$mDCs to percentage CD8 T lymphocyte subsets of the control study group.

The percentage$CD8^+CD38^+$, $CD8^+PD\text{-}1^+$ and $CD8^+CD38^+PD\text{-}1^+$ T lymphocytes was determined for each of the participants of the control study group and plotted together with corresponding percentage TNF-$R2^+$mDCs on a line graph. The $CD8^+CD38^+$, $CD8^+PD\text{-}1^+$ and $CD8^+CD38^+PD\text{-}1^+$ T lymphocyte subsets were 1) represented by the symbols ▼, △ and ✳, and 2) relationship to percentage TNF-R2 mDCs illustrated by a green, pink and blue-coloured linear regression line, respectively. The non-parametric Spearman test was use to correlate the percentage CD8 T lymphocyte subsets to percentage TNF-$R2^+$mDCs. Statistically significant data are highlighted in bold.

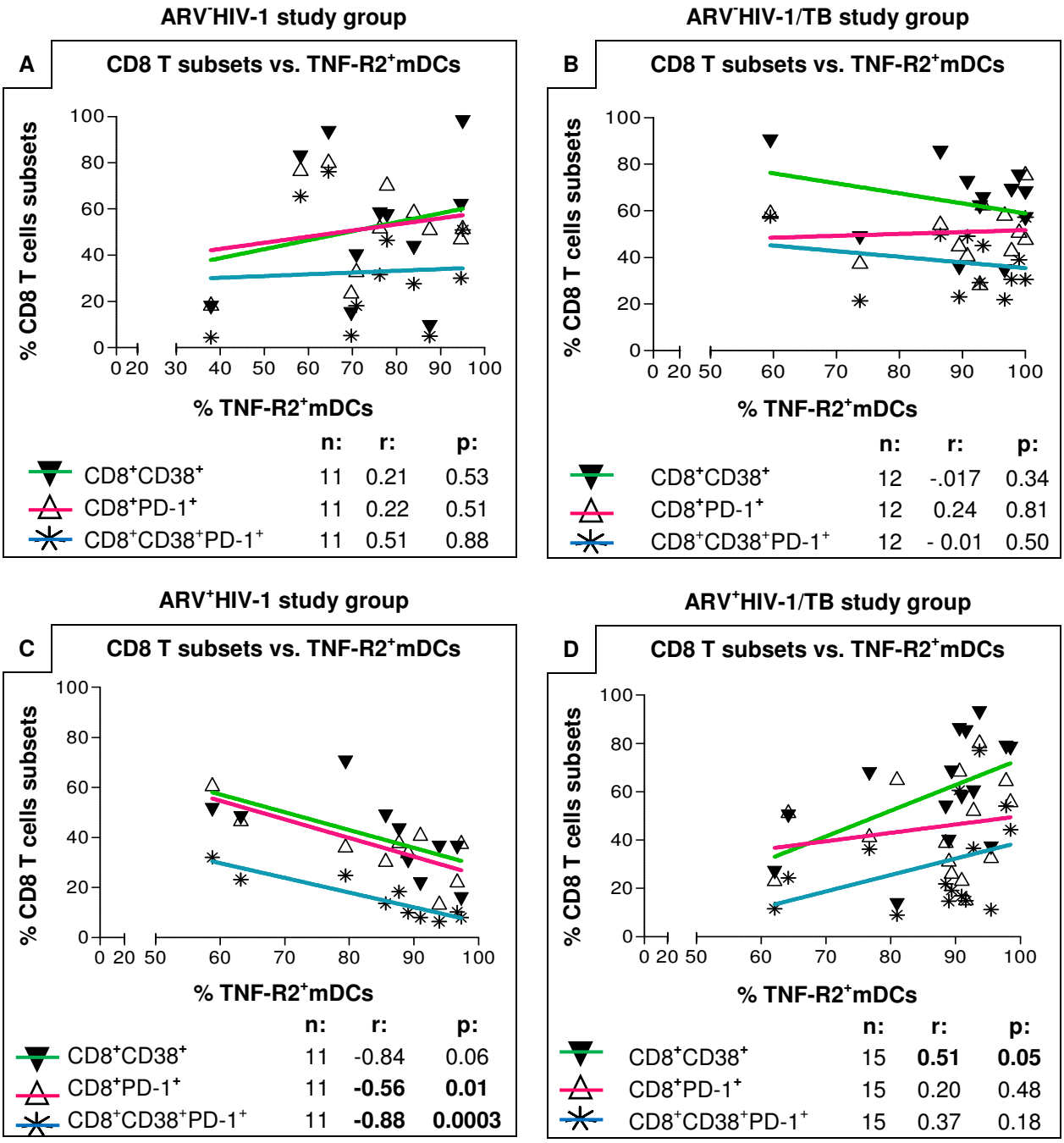

Figure 6.10: Correlating TNF-R2$^+$mDCs to percentage CD8 T lymphocyte subsets in ARV untreated and treated HIV-1 mono and HIV-1/TB co-infection

The percentage$CD8^+CD38^+$, $CD8^+PD\text{-}1^+$ and $CD8^+CD38^+PD\text{-}1^+$ T lymphocytes was determined for each of the participants of the HIV-1-related study groups and plotted together with corresponding percentage TNF-R2$^+$mDCs on a line graph. The percentage $CD8^+CD38^+$,$CD8^+PD\text{-}1^+$and $CD8^+CD38^+PD\text{-}1^+$T lymphocyte subsets were 1) represented by the symbols ▼, △ and ✳, and 2) relationship to percentage TNF-R2$^+$mDCs illustrated by a green, pink and blue-coloured linear regression line, respectively. The non-parametric Spearman test was use to correlate the percentage CD8 T lymphocyte subsets to percentage TNF-R2$^+$mDCs. Statistically significant data are highlighted in bold.

No correlation between the CD8 T lymphocyte subsets and FAS$^+$mDCs during HIV-1 infection

No signicant relationship was observed in relating the percentage CD8$^+$CD38$^+$, CD8$^+$PD-1$^+$, CD8$^+$CD38$^+$PD-1$^+$ T lymphocyte subsets to the percentage FAS$^+$mDCs of the control study group (r = 0.14, p = 0.73; r = -0.16, p = 0.49; r = -0.10, p = 0.68, respectively, Figure 6.11), ARV$^-$HIV-1 study group (r = 0.10, p = 0.91; r = -0.44, p = 0.26; r = -0.23, p = 0.49, respectively; Figure 6.12A), ARV$^-$HIV-1/TB study group (r = 0.31, p = 0.52; r = -0.21, p = 0.68; r = 0.12, p = 0.51, respectively, Figure 6.12B), ARV$^+$HIV-1 study group (r = -0.36, p = 0.35; r = 0.17, p = 63; r = 0.06, p = 0.94, respectively, Figure 6.12C) and ARV$^+$HIV-1/TB study group (r = 0.38, p = 0.21; r = 0.09, p = 0.43; r = 0.40, p = 0.16, respectively, Figure 6.12D)..

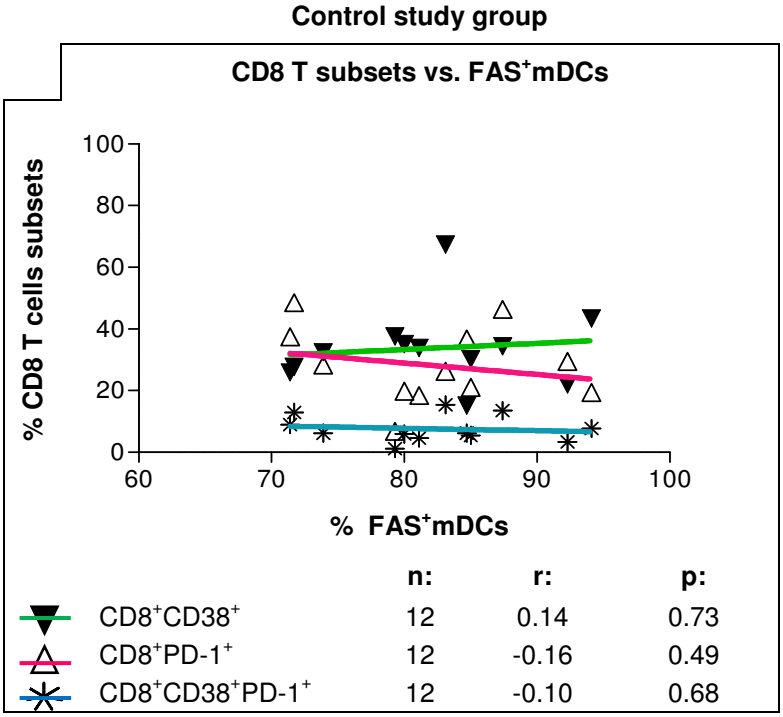

Figure 6.11: Correlation FAS$^+$mDCs to percentage CD8 T lymphocyte subsets of the control study group.

The percentageCD8$^+$CD38$^+$, CD8$^+$PD-1$^+$ and CD8$^+$CD38$^+$PD-1$^+$ T lymphocytes was determined for each of the participants of the control study group and plotted together with corresponding percentage FAS$^+$mDCs on a line graph. The CD8$^+$CD38$^+$, CD8$^+$PD-1$^+$ and CD8$^+$CD38$^+$PD-1$^+$ T lymphocyte subsets were 1) represented by the symbols ▼, △ and ✳, and 2) relationship to percentage FAS$^+$mDCs illustrated by a green, pink and blue-coloured linear regression line, respectively. The non-parametric Spearman test was use to correlate the percentage CD8 T lymphocyte subsets to percentage FAS$^+$mDCs.

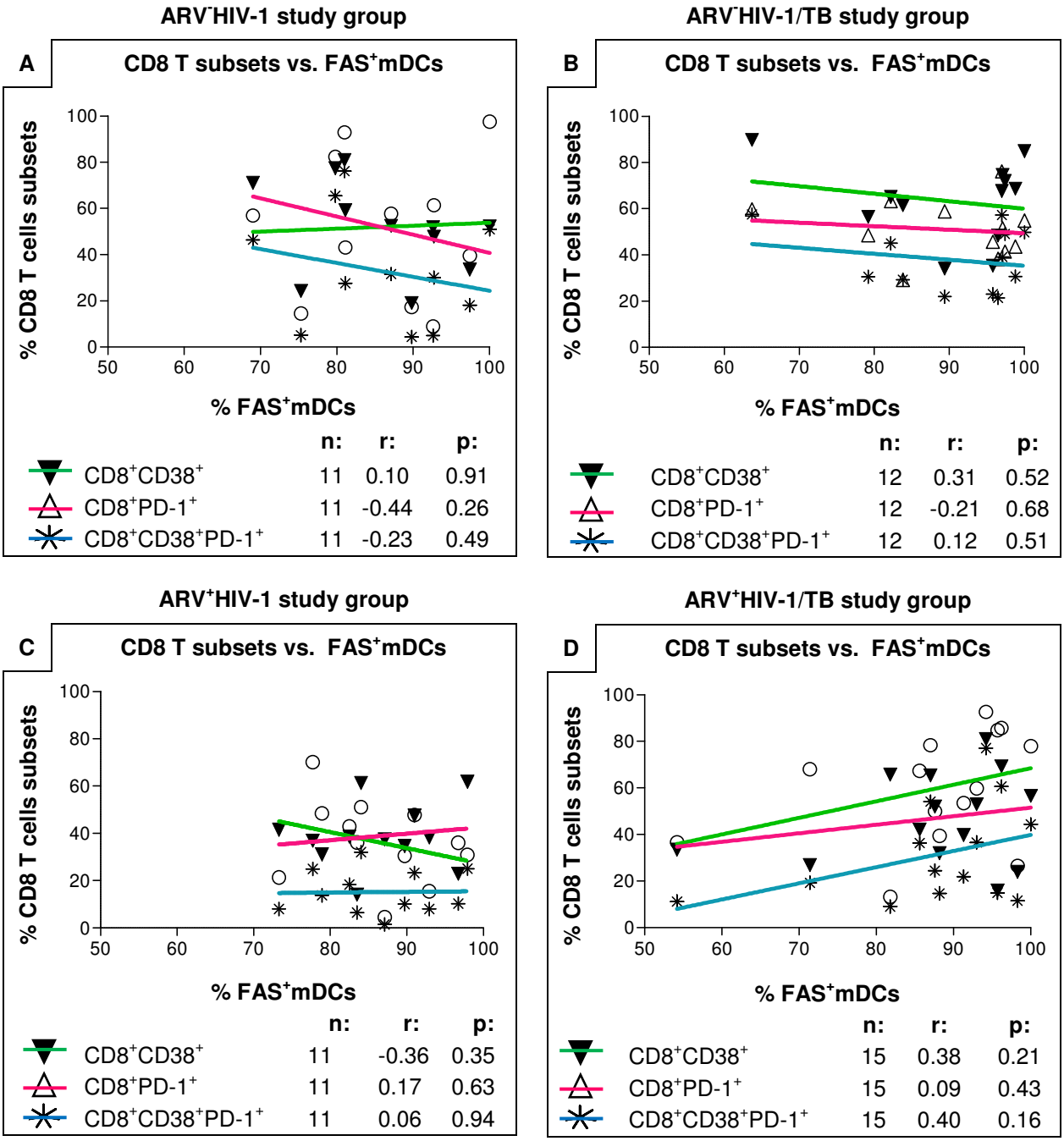

Figure 6.12: Correlating FAS$^+$mDCs to % CD8 T lymphocyte subsets in ARV untreated and treated HIV-1 mono and HIV-1/TB co-infection

The percentageCD8$^+$CD38$^+$, CD8$^+$PD-1$^+$ and CD8$^+$CD38$^+$PD-1$^+$ T lymphocytes was determined for each of the participants of the HIV-1-related study groups and plotted together with corresponding percentage FAS$^+$mDCs on a line graph. The CD8$^+$CD38$^+$, CD8$^+$PD-1$^+$ and CD8$^+$CD38$^+$PD-1$^+$ T lymphocyte subsets were 1) represented by the symbols ▼, △ and ✳, and 2) relationship to percentage FAS$^+$mDCs illustrated by a green, pink and blue-coloured linear regression line, respectively. The non-parametric Spearman test was use to correlate the percentage CD8 T lymphocyte subsets to percentage FAS$^+$mDCs.

No correlation between the CD8 T lymphocyte subsets and CD62L$^+$pDCs and mDCs during HIV-1 infection

In correlating the percentage CD62L$^+$pDCs to the percentage CD8$^+$CD38$^+$ T lymphocytes(r = 0.12, p = 0.63), CD8$^+$PD-1$^+$ T lymphocytes (r = -0.27, p = 0.76) and CD8$^+$CD38$^+$PD-1$^+$ T lymphocytes subsets (r = 0.02, p= 0.92) of the control study group (Figure 6.13) no significant correlation was found. Also, no significant relationship was found between the percentage CD62L$^+$pDCs and percentage CD8$^+$CD38$^+$, CD8$^+$PD-1$^+$, CD8$^+$CD38$^+$PD-1$^+$ T lymphocyte subsets of the ARV$^-$HIV-1 study group (r = -0.36, p = 0.31; r = -0.45, p = 0.22; r = -0.60, p = 0.14, respectively, Figure 6.14 A), ARV$^-$HIV-1/TB study group (r = 0.28, p = 0.61; r = 0.25, p = 0.26; r = 0.39, p = 0.62, respectively; Figure 6.14 B), ARV$^+$HIV-1 study group (r = 0.01, p = 0.18; r = 0.26, p = 0.86; r = 0.25, p = 0.39, respectively, Figure 6.14 C) and ARV$^+$HIV-1/TB study group (r = 0.33, p = 0.32; r = -0.06, p = 78; r = 0.13, p = 0.65, respectively, Figure 6.14 D).

A similar profile, as observed with CD62L$^+$pDCs, was found when correlating the CD8 T lymphocyte subsets with CD62L$^+$mDCs. No significant relationship was detected upon correlating the percentage CD62L$^+$mDCs to the percentage CD8$^+$CD38$^+$ T lymphocytes(r = -0.08, p = 0.45), CD8$^+$PD-1$^+$ T lymphocytes (r = -0.02, p = 0.77) and CD8$^+$CD38$^+$PD-1$^+$ T lymphocytes subsets (r = 0.07, p = 0.46) of the control study group (Figure 6.15). Also no correlation was observed when relating the CD8$^+$CD38$^+$, CD8$^+$PD-1$^+$, CD8$^+$CD38$^+$PD-1$^+$ T lymphocyte subsets of the ARV$^-$HIV-1 (r = -0.16, p = 0.45; r = -0.34, p = 0.23; r = -0.39, p = 0.13, respectively, Figure 6.16A), ARV$^-$HIV-1/TB (r = -0.08, p = 0.85; r =0.24, p = 0.47; r = 0.02, p = 0.84, respectively; Figure 6.16B), ARV$^+$HIV-1 (r = 0.01, p = 0.53; r = -0.20, p = 0.35; r = 0.15, p = 0.99, respectively, Figure 6.16 C) and ARV$^+$HIV-1/TB study groups (r = 0.43, p = 0.14; r = 0, p = 0.75; r = 0.17, p = 0.71, respectively, Figure 6.16 D) to CD62L$^+$mDCs.

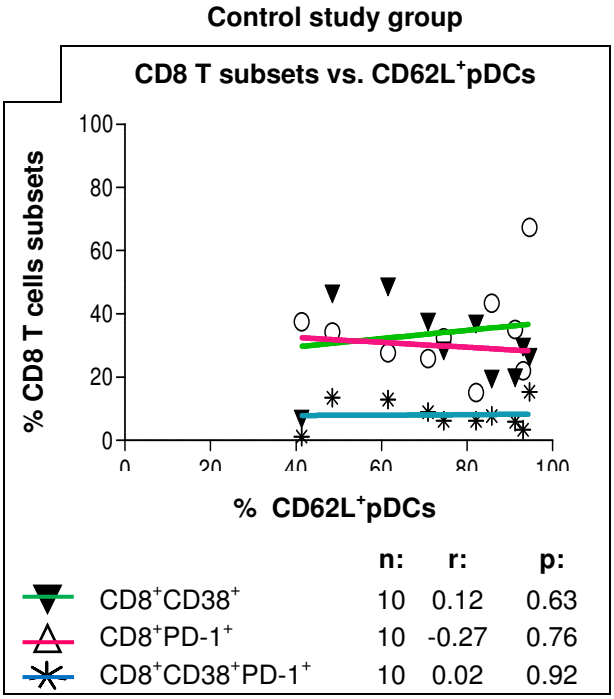

Figure 6.13: Correlating CD62L$^+$pDCs to percentageCD8 T lymphocyte subsets of the control study group.

The percentageCD8$^+$CD38$^+$, CD8$^+$PD-1$^+$ and CD8$^+$CD38$^+$PD-1$^+$ T lymphocytes was determined for each of the participants of the control study group and plotted together with corresponding percentage CD62L$^+$pDCs on a line graph. The CD8$^+$CD38$^+$, CD8$^+$PD-1$^+$ and CD8$^+$CD38$^+$PD-1+ T lymphocyte subsets were 1) represented by the symbols ▼, △ and ✳, and 2) relationship to percentage CD62L$^+$pDCs illustrated by a green, pink and blue-coloured linear regression line, respectively. The non-parametric Spearman test was use to correlate the percentage CD8 T lymphocyte subsets to percentageCD62L$^+$pDCs.

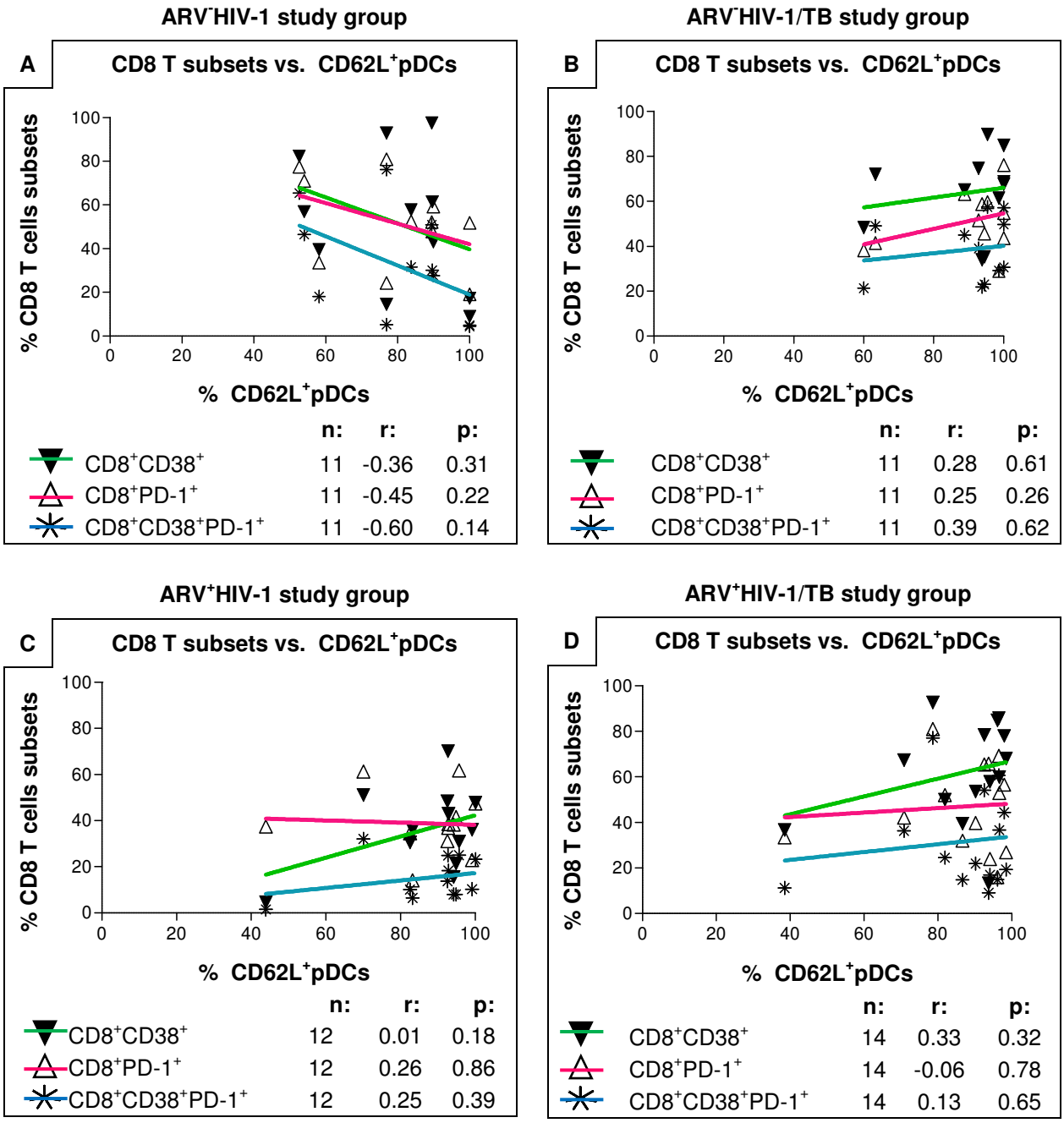

Figure 6.14: Correlating CD62L$^+$pDCs to percentage CD8 T lymphocyte subsets in ARV untreated and treated HIV-1 mono and HIV-1/TB co-infection

The percentageCD8$^+$CD38$^+$, CD8$^+$PD-1$^+$ and CD8$^+$CD38$^+$PD-1$^+$ T lymphocytes was determined for each of the participants of the HIV-1-related study groups and plotted together with corresponding percentageCD62L$^+$pDCs on a line graph. The percentage CD8$^+$CD38$^+$, CD8$^+$PD-1$^+$ and CD8$^+$CD38$^+$PD-1$^+$ T lymphocyte subsets were 1) represented by the symbols ▼, △ and ✳, and 2) relationship to percentageCD62L$^+$pDCs illustrated by a green, pink and blue-coloured linear regression line, respectively. The non-parametric Spearman test was use to correlate the percentage CD8 T lymphocyte subsets to percentageCD62L$^+$pDCs.

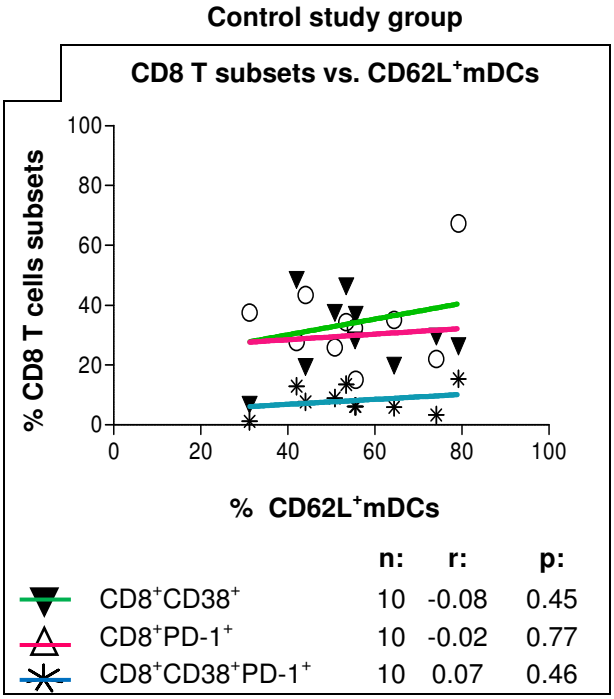

Figure 6.15: Correlating CD62L$^+$mDCs to percentage CD8 T lymphocyte subsets of the control study group.

The percentage$CD8^+CD38^+$, $CD8^+PD\text{-}1^+$ and $CD8^+CD38^+PD\text{-}1^+$ T lymphocytes was determined for each of the participants of the control study group and plotted together with corresponding percentage $CD62L^+$mDCs on a line graph. The $CD8^+CD38^+$, $CD8^+PD\text{-}1^+$ and $CD8^+CD38^+PD\text{-}1^+$ T lymphocyte subsets were 1) represented by the symbols ▼, △ and ✳, and 2) relationship to percentage $CD62L^+$mDCs illustrated by a green, pink and blue-coloured linear regression line, respectively. The non-parametric Spearman test was use to correlate the percentage CD8 T lymphocyte subsets to percentage $CD62L^+$mDCs.

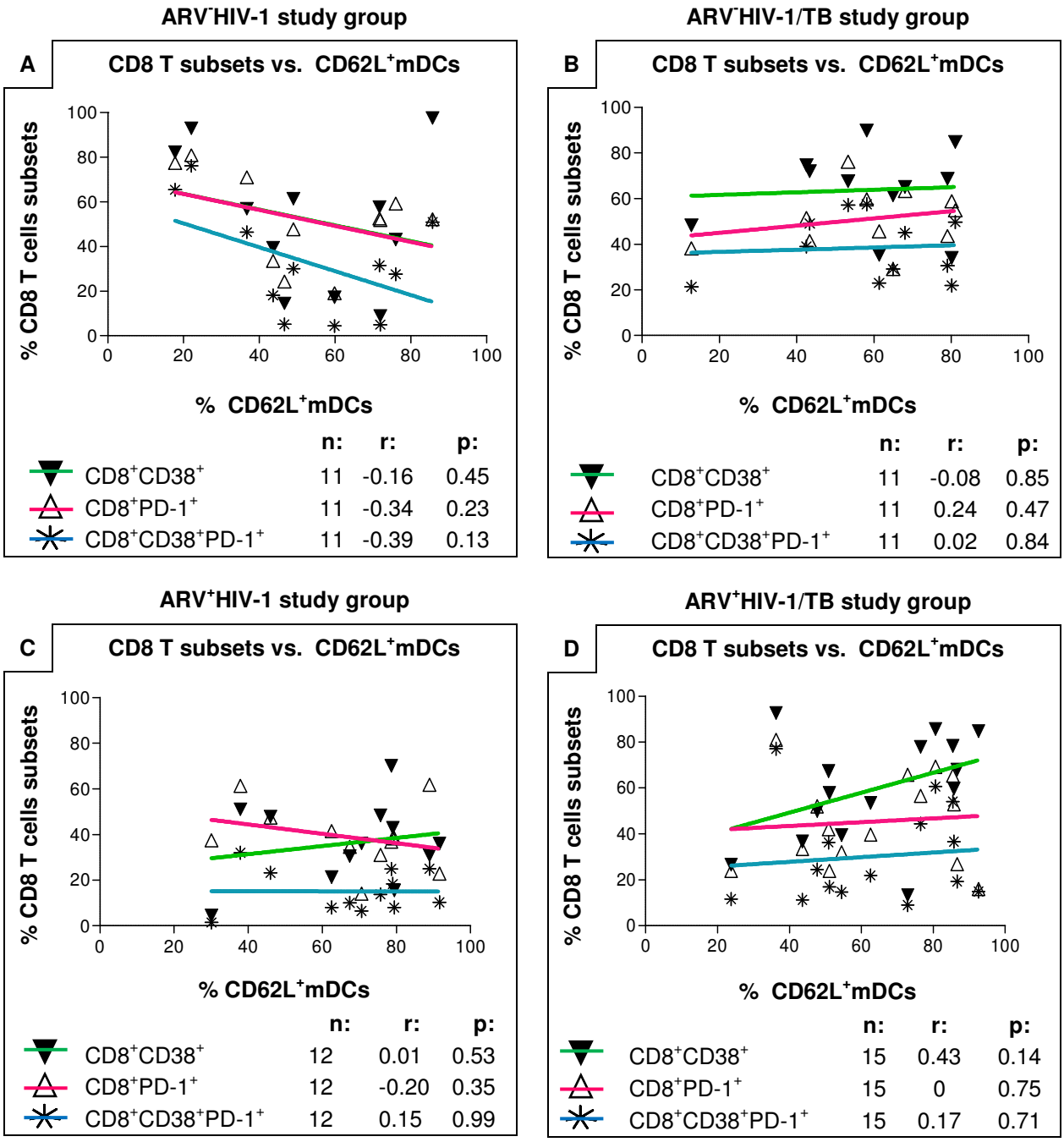

Figure 6.16: Correlation between CD62L$^+$mDCs to percentage CD8 T lymphocyte subsets during ARV untreated and treated HIV-1 mono and HIV-1/TB co-infection

The percentageCD8$^+$CD38$^+$, CD8$^+$PD-1$^+$ and CD8$^+$CD38$^+$PD-1$^+$ T lymphocytes was determined for each of the participants of the HIV-1-related study groups and plotted together with corresponding percentageCD62L$^+$mDCs on a line graph. The percentageCD8$^+$CD38$^+$, CD8$^+$PD-1$^+$ and CD8$^+$CD38$^+$PD-1$^+$ T lymphocyte subsets were 1) represented by the symbols ▼, △ and ✳, and 2) relationship to percentageCD62L$^+$mDCs illustrated by a green, pink and blue-coloured linear regression line, respectively. The non-parametric Spearman test was use to correlate the percentage CD8 T lymphocyte subsets to percentageCD62L$^+$mDCs.

CD86$^+$mDCs tend to weakly correlate with the CD8 T lymphocyte subsets during HIV-1 infection

CD86$^+$mDC of the control study group showed an overall low indirect correlation with the CD8 T lymphocyte subsets. Specifically, the relationship of CD86$^+$mDC to 1) the percentage CD8$^+$CD38$^+$PD-1+ T lymphocytes (r = -0.51, p = 0.02) was significant, 2) the percentage CD8$^+$CD38$^+$T lymphocytes (r = -0.16, p = 0.10) weakly significant and 3) the percentage CD8$^+$PD-1$^+$ T lymphocytes (r = -0.36, P = 0.27) not significant (Figure 6.17). Similar to the control study group an indirect correlation was observed in the ARV$^-$HIV-1 study group. In this group the relationship of the percentage CD8$^+$CD38$^+$ T lymphocytes (r = -0.68, p = 0.13), CD8$^+$PD-1$^+$ T lymphocytes (r = -0.69, p = 0.1) and CD8$^+$CD38$^+$PD-1$^+$ T lymphocytes (r = -0.67, p = 0.11) to CD86$^+$mDCs was weakly significant (Figure 6.18A). In clear contrast, a positive correlation was observed between CD86$^+$mDCs and CD8$^+$CD38$^+$ T lymphocytes (r = 0.85, p = 0.01) as well as the percentage CD8$^+$CD38$^+$PD-1$^+$ T lymphocytes (r = 0.61, p =0.11) in the ARV$^-$HIV-1/TB study of which the former was significant and the latter weakly significant. The percentage CD8$^+$PD-1$^+$ T lymphocytes (r = 0.13, p = 0.98) of this study group did not correlate with the CD86$^+$mDCs (Figure 6.18B). In the ARV$^+$HIV-1/TB study group a direct but insignificant relationship was observed between the CD86$^+$mDCs and 1) CD8$^+$CD38$^+$ T lymphocyte subset (r = 0.26, p = 0.31), 2) percentage CD8$^+$PD-1$^+$ T lymphocytes (r = 0.29, p = 0.33) and 3) CD8$^+$CD38$^+$PD-1$^+$ (r = 0.19, p = 0.39) (Figure 6.18D). Notably, in the ARV$^+$HIV-1 study group a significant and strong direct relationship was observed between CD86$^+$mDCs and both the percentage CD8$^+$PD-1$^+$ T lymphocytes (r = 0.63, p = 0.01) and the percentage CD8$^+$CD38$^+$PD-1$^+$ T lymphocyte (r = 0.78, p = 0.01). In this group the percentage CD8$^+$CD38$^+$T lymphocytes showed no significant correlation with the percentage CD86$^+$mDCs (Figure 6.18C).

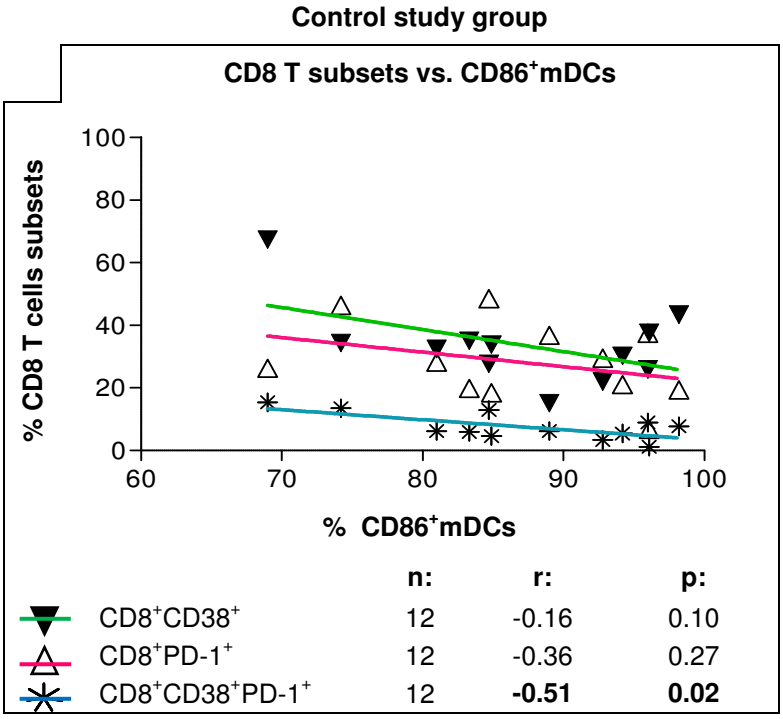

Figure 6.17: Correlating CD86$^+$mDCs to percentage CD8 T lymphocyte subsets of the control study group.

The percentageCD8$^+$CD38$^+$, CD8$^+$PD-1$^+$ and CD8$^+$CD38$^+$PD-1$^+$ T lymphocytes was determined for each of the participants of the control study group and plotted together with corresponding percentageCD86$^+$mDCs on a line graph. The CD8$^+$CD38$^+$, CD8$^+$PD-1$^+$ and CD8$^+$CD38$^+$PD-1$^+$ T lymphocyte subsets were 1) represented by the symbols ▼, △ and ✳, and 2) relationship to percentageCD86$^+$mDCs illustrated by a green, pink and blue-coloured linear regression line, respectively. The non-parametric Spearman test was use to correlate the percentage CD8 T lymphocyte subsets to percentage CD86$^+$mDCs. Statistically significant data are highlighted in bold.

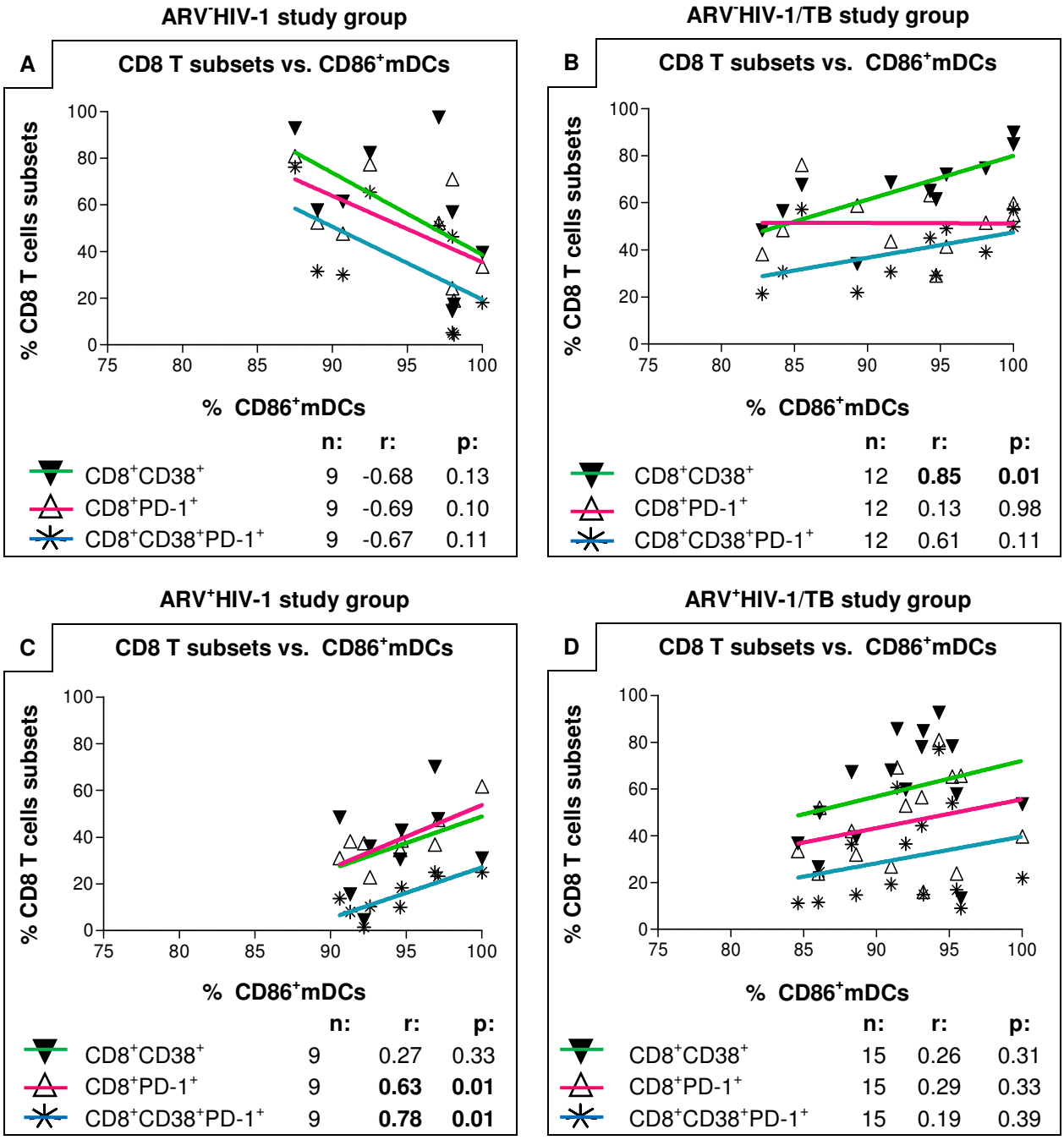

Figure 6.18: Correlating CD86$^+$mDCs to percentage CD8 T lymphocyte subsets during ARV untreated and treated HIV-1 mono and HIV-1/TB co-infection

The percentageCD8$^+$CD38$^+$, CD8$^+$PD-1$^+$ and CD8$^+$CD38$^+$PD-1$^+$ T lymphocytes was determined for each of the participants of the HIV-1-related study groups and plotted together with corresponding percentageCD86$^+$mDCs on a line graph. The CD8$^+$CD38$^+$, CD8$^+$PD-1$^+$ and CD8$^+$CD38$^+$PD-1$^+$T lymphocyte subsets were 1) represented by the symbols ▼, △ and ✳, and 2) relationship to percentageCD86$^+$mDCs illustrated by a green, pink and blue-coloured linear regression line, respectively. The non-parametric Spearman test was use to correlate the percentage CD8 T lymphocyte subsets to percentage CD86$^+$mDCs. Statistically significant data are highlighted in bold.

6.5 Conclusion

In addition to the characteristic decline of CD4 T lymphocytes during HIV-1 infection, persistent immune activation with consequent exhaustion is also a well-described feature of this disease. Immune activation and exhaustion during HIV-1 infection is examined via the expression of CD38 and PD-1 on CD8 T lymphocytes, respectively. The current study was interested in evaluating the frequency distribution of these CD8 T lymphocyte subsets during HIV-1/TB co-infection, anticipating significantly altered frequencies in dual infection. Briefly, the study investigated the 1) frequency distribution of the $CD8^+CD38^+$, $CD8^+PD\text{-}1^+$, $CD8^+CD38^+PD\text{-}1^+$ T lymphocyte subset in chronically HIV-1 infected and HIV-1/TB co-infected patients on or naïve for ARV therapy and 2) relationship of the percentage CD8 T lymphocyte subsets to CD4 T lymphocytes counts and viral load. The study found the $CD8^+CD38^+$, $CD8^+PD\text{-}1^+$ and $CD8^+CD38^+PD\text{-}1^+$ T lymphocytes subsets to:

1) circulate in significantly higher frequencies in peripheral blood during ARV^-HIV-1 infection.
2) have a similar distribution profile during HIV-1 and HIV-1/TB co-infection - contrary to expectations.
3) normalise upon ARV treatment of more than 1 year, opposed to CD4 T lymphocyte number and CD4:CD8 ratio which showed no recovery
4) indirectly correlate with CD4 T lymphocytes during ARV^-HIV-1 infection
5) directly correlate with viral load, although, PD-1expression did not seem affected by HIV-1 infection

Additionally, the relationship of the CD8 T lymphocyte subsets to $TNF\text{-}R2^+$pDCs, $TNF\text{-}R2^+$mDCs, FAS^+mDCs, $CD62L^+$pDCs, $CD62L^+$mDCs and $CD86^+$mDCs was also determined. In summary the study found

1) No correlation between the $TNF\text{-}R2^+$pDCs and CD8 T lymphocyte subsets during HIV-1 infection
2) Prolonged ARV therapy (>1year) resulted in higher percentage $TNFR\text{-}2^+$mDCs to circulate with declining levels of the CD8 T lymphocyte subsets
3) FAS^+mDC, $CD62L^+$pDCs and $CD62L^+$mDCs did not correlate with the CD8 T lymphocyte subsets
4) $CD86^+$mDCs indirectly but weakly correlated with the CD8 T lymphocyte subsets during HIV-1 infection while with ARV therapy a significant direct relationship was observed with the $CD8^+PD\text{-}1^+$ and $CD8^+CD38^+PD\text{-}1^+$ T lymphocytes.

Parallel to the increase in immune activation observed in untreated HIV-1 infection is the fact that the HIV-1 virus causes a chronic infection; hence, immune activation is a persistent phenomenon in the disease. It is proposed to have major damaging effects (e.g. tissue damage, immune exhaustion). Importantly, ARV therapy has the ability to optimally manage chronic immune activation (alleviating immune pressure) whilst the impact on recovery of DC and CD4 T cell numbers is limited. This is indicative of other factors that need to be targeted so to correct waning cellular numbers during untreated HIV-1 infection.

6.6 References

Almeida, M., Cordero, M., Almeida, J., and Orfao, A. (2006).Persistent abnormalities in peripheral blood dendritic cells and monocytes from HIV-1 positive patients after 1 year of antiretroviral therapy. J. Acquir. Immune Defic.Syndr.*41*, 405–415.

Almeida, M., Cordero, M., Almeida, J., and Orfao, A. (2007). Relationship between CD38 expression on peripheral blood T-cells and monocytes , and response to antiretroviral therapy: A one-year longitudinal study of a cohort of chronically infected ART-Naive HIV-1+ patients. Cytom.Part B Clin.Cytom.*72B*, 22–33.

Barber, D.L., Wherry, E.J., Masopust, D., Zhu, B., Allison, J.P., Sharpe, A.H., Freeman, G.J., and Ahmed, R. (2006). Restoring function in exhausted CD8 T cells during chronic viral infection. Nature *439*, 682–687.

Chun, T.-W., Justement, J.S., Sanford, C., Hallahan, C.W., Planta, M. a, Loutfy, M., Kottilil, S., Moir, S., Kovacs, C., and Fauci, A.S. (2004). Relationship between the frequency of HIV-specific CD8+ T cells and the level of CD38+CD8+ T cells in untreated HIV-infected individuals. Proc. Natl. Acad. Sci. U. S. A. *101*, 2464–2469.

Day, C.L., Kaufmann, D.E., Kiepiela, P., Brown, J.A., Moodley, E.S., Reddy, S., Mackey, E.W., Miller, J.D., Leslie, A.J., Depierres, C., *et al*. (2006). PD-1 expression on HIV-specific T cells is associated with T-cell exhaustion and disease progression. Nature *443*, 350–354.

Hardy, G.A.D., Sieg, S., Rodriguez, B., Anthony, D., Asaad, R., Jiang, W., Mudd, J., Schacker, T., Funderburg, N.T., Pilch-Cooper, H.A., *et al*. (2013). Interferon-α is the primary plasma type-I IFN in HIV-1 infection and correlates with immune activation and disease markers. PLoS One *8*, 1–9.

Hazenberg, M.D., Otto, S. aA, van Benthem, B.H.B., Roos, M.T.L., Coutinho, R.A., Lange, J.M.A., Hamann, D., Prins, M., and Miedema, F. (2003). Persistent immune activation in HIV-1 infection is associated with progression to AIDS. AIDS *17*, 1881–1888.

Hunt, P.W., Brenchley, J., Sinclair, E., Mccune, J.M., Roland, M., Page-Shafer, K., Hsue, P., Emu, B., Krone, M., Lampiris, H., *et al*. (2008). Relationship between T cell activation and CD4+T cell count in HIV-seropositive individuals with undetectable plasma HIV RNA levels in the absence of therapy. J. Infect. Dis. *197*, 126–133.

Keir, M.E., Butte, M.J., Freeman, G.J., and Sharpe, A.H. (2008).PD-1 and its ligands in tolerance and immunity.Annu. Rev. Immunol. *26*, 677–704.

Liu, Z., Cumberland, W., Hultin, L., Prince, H.E., Detels, R., and Giorgi, J. V (1997). Elevated CD38 antigen expression on CD8+ T cells is a stronger marker for the risk of chronic HIV disease progression to AIDS and death in the multicenter AIDS cohort study than CD4+ cell count, soluble immune activation markers or combinations of HLA-DR. J. Acquir. Immune Defic.Syndr. Hum. Retrovirology*16*, 83–92.

Mahnke, Y.D., Song, K., Sauer, M.M., Nason, M.C., Giret, M.T.M., Carvalho, K.I., Costa, P.R., Roederer, M., and Kallás, E.G. (2013).Early immunologic and virologic predictors of clinical HIV-1 disease progression.AIDS *27*, 697–706.

Peretz, Y., He, Z., Shi, Y., Yassine-Diab, B., Goulet, J.-P., Bordi, R., Filali-Mouhim, A., Loubert, J.-B., El-Far, M., Dupuy, F.P., *et al*. (2012). CD160 and PD-1 co-expression on HIV-specific CD8 T cells defines a subset with advanced dysfunction. PLoSPathog. *8*, 1–13.

Petrovas, C., Casazza, J.P., Brenchley, J.M., Price, D. a, Gostick, E., Adams, W.C., Precopio, M.L., Schacker, T., Roederer, M., Douek, D.C., *et al*. (2006). PD-1 is a regulator of virus-specific CD8+ T cell survival in HIV infection. J. Exp. Med. *203*, 2281–2292.

Resino, S., Bellón, J.M., Gurbindo, M.D., and Muñoz-Fernández, M.A. (2004). CD38 expression in CD8+ T cells predicts virological failure in HIV type 1-infected children receiving antiretroviral therapy. Clin. Infect. Dis. *38*, 412–417.

Sharada, R.S., Rani, H.S., Pydi, S.S., Subbanna, J., and Valluri, V.L. (2012). CD38 expression on CD8+ cells—Its influence on development of tuberculosis in HIV positive individuals. Open J. Immunol. *02*, 65–71.

Shi, W., Zhang, Z., Zhang, M., Liu, J., Jiang, Y., Wang, Y., Jin, X., Han, X., and Shang, H. (2009). The frequency, activation, and coreceptor expression of lymphocytes in human immunodeficiency virus/hepatitis C virus co-infected patients in China. Jpn. J. Infect. Dis. *62*, 284–2888.

Sousa, A.E., Carneiro, J., Meier-Schellersheim, M., Grossman, Z., and Victorino, R.M.M. (2002). CD4 T cell depletion is linked directly to immune activation in the pathogenesis of HIV-1 and HIV-2 but only indirectly to the viral load. J. Immunol. *169*, 3400–3406.

Sunder, S.R., Hanumanth, S., Bandaru, A., Pydi, S., Gaddam, S., Jonnalagada, S., and Valluri, V. (2012). Influence of CD38/PD1 co-expression on T cell subsets in HIV-TB co-infection. BMC Infect. Dis. *12 (Suppl*, O4.

Tilling, R., Kinloch, S., Goh, L.-E., Cooper, D., Perrin, L., Lampe, F., Zaunders, J., Hoen, B., Tsoukas, C., Andersson, J., *et al*. (2002). Parallel decline of CD8+/CD38++ T cells and viraemia in response to quadruple highly active antiretroviral therapy in primary HIV infection.AIDS *16*, 589–596.

Trautmann, L., Janbazian, L., Chomont, N., Said, E.A., Gimmig, S., Bessette, B., Boulassel, M.-R., Delwart, E., Sepulveda, H., Balderas, R.S., *et al*. (2006). Upregulation of PD-1 expression on HIV-specific CD8+ T cells leads to reversible immune dysfunction. Nat. Med. *12*, 1198–1202.

Tuaillon, E., Al Tabaa, Y., Baillat, V., Segondy, M., Picot, M.-C., Reynes, J., and Vendrell, J.-P. (2009). Close association of CD8+/CD38 bright with HIV-1 replication and complex relationship with CD4+ T-cell count.Cytom. Part B *76B*, 249–260.

Zhang, J.-Y., Zhang, Z., Wang, X., Fu, J.-L., Yao, J., Jiao, Y., Chen, L., Zhang, H., Wei, J., Jin, L., *et al*. (2007). PD-1 up-regulation is correlated with HIV-specific memory CD8+ T-cell exhaustion in typical progressors but not in long-term nonprogressors. Blood *109*, 4671–4678.

Chapter 7

Concluding remarks

Challenges of the study: Analysis of rare cellular events and the dark art of flow cytometry

The study encountered and overcame many technical challenges. Primarily, the naturally low number distribution of blood pDCs and mDCs in circulation made flow cytometric analyses of marker expression complex, even more so in an HIV-1 infection setting of reduced numbers. It may be beneficial that future blood DC studies investigate the use of a concentrated leukocyte suspension (buffy coat) as substitute to whole blood analyses of pDCs and mDCs. Furthermore, accurate data reporting required optimization on various levels viz. gating strategy for collecting pDCs and mDCs from acquired events (refer to 4.3.9), acquiring mDC specific events from occasional non-DC events contaminating the HLA-DR^{+}LIN1^{DIM} gate (possibly a result of cellular change due to HIV-1 infection, refer to 4.3.10), adjustment of compensation to remove fluorescence overlap (refer to section 4.3.7.1), identification of true positive events and false positive events (as a result of autofluorescence(refer to 5.3.2.4), direct and/or indirect non-specific binding and undercompensated data (refer to 4.3.7.1 and Figure 4.1)), identification of internal controls to determine the negative staining border and guide the identification of true positive events in the absence of daily experimental controls (refer to 4.3.8, Figure 4.3, the daily use of FMO controls was excluded from this study due to this technique being a prohibitory expensive routine) and general analyses of marker expression by rare events (refer to 4.3.8).

Population cohort

The enrollment of HIV-1 infected patients regardless of CD4 T lymphocyte count and disease status throughout this cross-sectional study resulted in blood analyses of participants at various 1) stages of disease progression and 2) periods of ARV therapy.Accordingly, the CD4 T lymphocyte count data summarised in chapter 3 showed number recovery during ARV therapy, whereas in Chapters 4-6 the CD4 T lymphocyte counts were similar between the ARV naïve and treated study groups. This raised the question whether the impact of ARV therapy was actually captured per the objectives of the particular chapters. However, Chapter 6 showed normalisation of the CD8 T subsets in parallel to no CD4 T cell number recovery of the HIV-1 study cohort on ARV therapy. This finding showed that recovery time while on ARV therapy varies between the different affected compartments of the host and that additional to incrementing CD4 T lymphocyte numbers, other factors should also be monitor to determine the impact of ARV therapy and resulting recovery. A longitudinal study is proposed for future work in this field.

Proposed future of therapeutic interventions

It remains a mystery why the relationship of the (genetically related) viruses, HIV-1 and SIV, to their respective (also related) hosts is so vastly different. Contrary to SIV infection of the natural host, which seems not to harm the natural primate host, HIV-1 infection induces a high rate of morbidity and mortality in the human species. In view of this it seems that the immune system of the non-human primate has the ability to exert a level of immune control over SIV infection. It is proposed that upon defining the exact mechanism underlying SIV immune control, so to manipulate the human immune system to exert a similar control over

HIV-1 infection, would drastically transform the life expectancy of millions of people currently living with the virus.

Narrowing the scope

HIV is a formidable virus as demonstrated by an extensive database on the complex viral-host interaction and a, yet, undefined intervention. This may indicate suboptimal strategies in the fight against HIV, warranting a radical paradigm change so that in the near future signs of a previous HIV-1 infection would be reflected by only the “footprint” of remnant antibodies in the human system.